The interaction of acidification and warming on the South African abalone, *Haliotis midae*, and the potential for mitigation in aquaculture

By

Nina Catherine Lester

Submitted in fulfilment of the requirements for a Doctor of Philosophy in the

Faculty of Science at the University of Cape Town

March 2021

Supervisor:

Prof. John J. Bolton, University of Cape Town

A.Prof Mike Lucas, University of Cape Town

Co-supervisor:

Prof. Lutz Auerswald, Department of Environment, Forestry and Fisheries of South Africa, Stellenbosch University

UNIVERSITY OF CAPE TOWN
IYUNIVESITHI YASEKAPA • UNIVERSITEIT VAN KAAPSTAD

DECLARATION

I declare that this thesis is my own, unaided work, except for x-ray diffraction (XRD) analysis which was performed by Nico Fischer, Department of Chemical Engineering, University of Cape Town. Some shells were crushed for XRD analysis and compressed by an honour's student, Michaela Martins, as part of her honour's project. This thesis has not been submitted in this or any form to another University. Where use has been made of the research of others, it has been duly acknowledged in the text. Experimental work discussed in this thesis was carried out under the supervision of Prof. J. J. Bolton of the Department of Biological Sciences, University of Cape Town and A. Prof. Mike Lucas of the Department of Biological Sciences, University of Cape Town.

Signed by candidate

Nina Catherine Lester

Department of Biological Sciences, University of Cape Town

Special Note

This thesis was written in memory of A. Prof. Mike Lucas who introduced me to the wonderful world of abalone and global change science; the spark.

ACKNOWLEDGEMENTS

First and foremost, I would like to extend every ounce of gratitude to my wonderful supervisor John Bolton. Your patience has never worn thin and your wisdom is a perennial fountain. To my co-supervisor, Lutz Auerswald, thank you for sticking with me and helping me achieve this enormous task.

I would like to extend my thanks to the Abalone Farmers Association of South Africa (AFASA) for sponsoring this research – without your help this project would just be a dream.

A special thank you to the team at Aqunion. I am forever grateful for providing a location for this project, but I am more so thankful for your full support and for accepting me into your family as a hatchery manager. My understanding and passion for abalone will remain strong with the memories of the Aqunion team.

To Bruce Spolander and MetOcean Services International, thank you for creating the data-logger-relay system. I am forever grateful for your services and the hours spent creating this device.

Lutz Auerswald and Jarred Knapp, you have helped enormously by running the haemolymph samples for me and for providing a much needed beer at the end of a long day of sampling.

Thank you Nico Fischer, Department of Chemical Engineering, University of Cape Town, for analysing the powdered shell samples. It must have seemed like a strange request at the time, but I hope that you enjoyed the challenge as much as I did.

ABSTRACT

The South African abalone, *Haliotis midae*, is an economically important species. *H. midae* is the largest of the five endemic abalone species in South Africa and is especially valuable in Asian markets. Over-fishing, increased predation (due a geographical shift in lobster populations), and prolific poaching of this commercially valuable species have depleted natural populations. Commercial abalone aquaculture began as a means to meet the market demand for *H. midae* and currently accounts for 77 % of South Africa's aquaculture revenue. Despite marked growth in this industry over the past decade, further increases will be challenged by the predicted threat of climate change, particularly ocean acidification. Calcifying organisms, such as abalone, are particularly susceptible to the impacts of ocean acidification and its resultant alteration in seawater carbonate chemistry. Most calcifying organisms display reduced calcification and growth in response to ocean acidification, with possible alterations to acid-base regulation, development, gonadal maturation and behaviour, as well as reduced larval and gamete survival. A further potential challenge to abalone aquaculture is global warming. The effects of temperature change depend on the organism's level of sensitivity, taxonomy, distribution and life history. The distribution of *H. midae* ranges from Saldanha Bay (cool-temperate) to Riet Point (warm-temperate), with the majority of commercial aquaculture production occurring in Hermanus (cool-temperate). Abalone aquaculture facilities will need to adapt to these environmental changes and assess potential mitigation strategies.

This study investigated the long-term (12 months) impact that ocean acidification and warming will have on the South African abalone, *Haliotis midae,* by incorporating the natural variability of seawater pH and temperature in Hermanus. Ambient seawater retained natural pH and temperature variability and acidified seawater was offset to natural pH variability using CO_2/O_2 diffusion and a data-logger-relay system to incorporate local-scale variability of seawater in the abalone farm, where this experiment was based. A multi-parameter approach was used to investigate the effects of reduced pH (- 0.4 from ambient) and warming (+ 1.5 °C from ambient) on abalone growth, spawning patterns, acid-base regulation, shell growth, morphology, shell strength and mineralogy over 12 months. This study also investigated the potential use of *Ulva* (Chlorophyta) as a mitigational tool to ameliorate acidified seawater, by photosynthetic carbon dioxide uptake, in a flow-through aquaculture system on a South African abalone farm. This study assessed the effects of seaweed-treated seawater on abalone growth, spawning patterns, acid-base regulation, shell growth, morphology, shell strength and mineralogy over 12 months in comparison to ambient and acidified seawater.

Ocean acidification conditions resulted in a decrease in *H. midae* haemolymph pH and an increase in pCO_2 (indicative of uncompensated respiratory acidosis), which resulted in reduced growth (whole-, muscle-, and shell-mass) and an alteration in spawning patterns. Acidification conditions also altered shell shape (smaller area with a wider shape) and significantly reduced shell strength. Warming conditions were within the thermal optimum ranges for *H. midae* and did not significantly affect abalone growth; however warming did bring about significant changes in Condition Factor, shell shape, and strength over time and shifted acid-base regulation towards a more stable status. The combined impact of warming and acidification were similar to the effects of reduced pH alone, with the exception of effects on acid-base regulation (severe uncompensated respiratory acidosis) and

shell shape (lengths and widths were moderately increased). Ocean acidification and warming conditions, singularly and in combination, had no significant impact on shell mineralogy (percentage weight of aragonite, and aragonite and calcite crystal diameter).

Bio-mitigation of acidified seawater by *Ulva* increased abalone wet weight, GBI, shell length, shell width and shell area in comparison to acidified conditions. Warming, caused by *Ulva* cultivation, resulted in similar effects on abalone shell growth and acid-base regulation as those exposed to warmed conditions alone. However, ambient and acidified seaweed-treated seawater caused a significant reduction in abalone muscle mass during summer months in comparison to abalone grown in ambient seawater. This decrease in muscle mass occurred concurrently with a decline in *Ulva* yield (due to photoinhibition), suggesting an interactive effect of *Ulva* (under stressor conditions) and abalone which needs to be studied further.

The findings of this thesis are of particular concern for the South African abalone industry as ocean acidification conditions are likely to result in slower abalone growth, increased cultivation time to reach market-size, and reduction in quality of abalone (as the shells are more easily damaged). This study highlights the importance of incorporating local-scale, natural variability into ocean acidification and warming studies to guide management practices for cultivation and protection of this valuable species. The incorporation of natural seawater variability highlights an over-exaggerated effect of warming on abalone exposed to constant-temperature experiments. Although predicted increases in seawater temperature (+ 1.5 °C) are within the optimal thermal ranges for *H. midae* in Hermanus, warming could pose a risk for aquaculture sites in warm-temperate areas of the South African coast. This thesis provides feedback on a potential mitigation strategy for abalone farms, with options for improvements in design as well as further mitigational options in the face of climate change. This is the first study to assess the effects of long-term elevated CO_2 and warming on *H. midae*, and the first to incorporate long-term, natural variability into climate change research for any species outside of a laboratory.

Table of Contents

CHAPTER 1

GENERAL INTRODUCTION

1.1. Abalone Biology

1.1.1. Classification of abalone

Abalone are members of the phylum Mollusca, which includes mussels, clams, sea slugs, and octopuses, and fall under the class *Gastropoda* with whelks, conches and limpets. Their taxonomy puts them in the family *Haliotidae* which contains only one genus, *Haliotis* (Linneaus 1758). The most comprehensive assessment of the family considers 56 species valid, with 18 additional subspecies (Geiger & Owen 2012).

The South African *perlemoen* abalone, *Haliotis midae*, is the largest of the five endemic South African abalone, reaching a shell length of approximately 200mm (Newman 1969, Geiger 1999). Previous descriptions of endemic abalone to South Africa include *Haliotis pustulata* (1969) although this species was rejected by Geiger (1999) upon genetic analysis of world-wide Haliotidae.Other endemic abalone species in order of maximum shell length include: Quekett's abalone (*H. queketti;* 45mm), spiral-ridged siffie (*H. parva*; 50mm), venus ear siffie (*H. spadicea*; 70mm), and beautiful ear-shell (*H. speciosa*; 80mm) (Figure 1.1). The local name perlemoen comes from the Dutch word 'perlemoer', which translates to 'mother of pearl', referring to the pearlescent inner layer of the abalone shells.

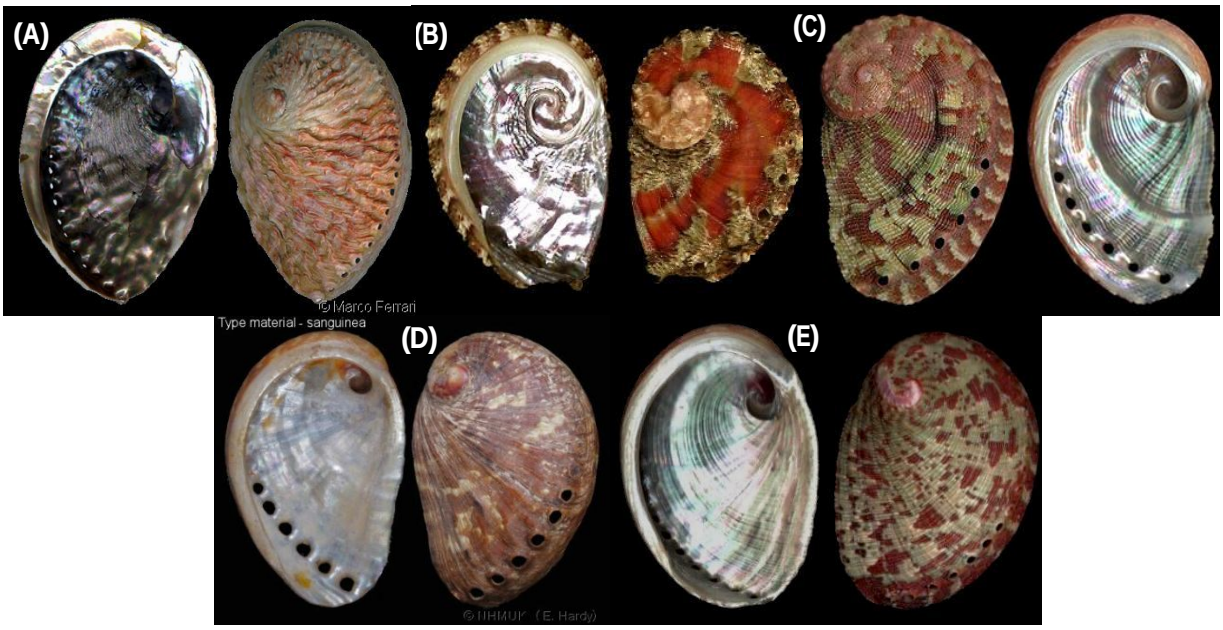

Figure 1.1. The six endemic abalone of South Africa including **(A)** *Haliotis midae* (150 mm), **(B)** *H. queketti* (30 mm), **(C)** *H. parva* (33-34 mm), **(D)** *H. spadicae* (52-67 mm), and **(E)** *H. speciosa* (50-80 mm). Photos were taken from the Worldwide Seashell Collection (http://www.idscaro.net/sci/01_coll/index.htm).

1.1.2 Appearance and anatomy of H. midae

The outer skeleton of *H. midae*, the shell, is whorled at the apex and flattened. The shell has strong wave-like corrugations parallel to the growing edge, which is thinner and fairly sharp (Figure 1.2).

The rounded edge of the shell is thicker and has several open pores used for respiration, egestion and excretion, as well as reproduction. The shell ranges in colour from white and blue to a brick-red depending mostly on diet (Gallardo et. al. 2003, Qi et. al. 2010, Hoang et. al. 2016, Marchais et. al. 2017, Hoang et. al. 2017), genetics and water quality (White 2011, Avignon et. al. 2020). The foot of the abalone is a smooth muscle with a fringe of densely packed, branched projections interspersed with long unbranched tentacles (epipodium). The foot ranges in colour from grey to yellow-green. The head of the abalone is located on the opposite end of the shell to the apex and is viewed externally as a tubular mouth surrounded by two cephalic tentacles with two eye stalks containing light receptors.

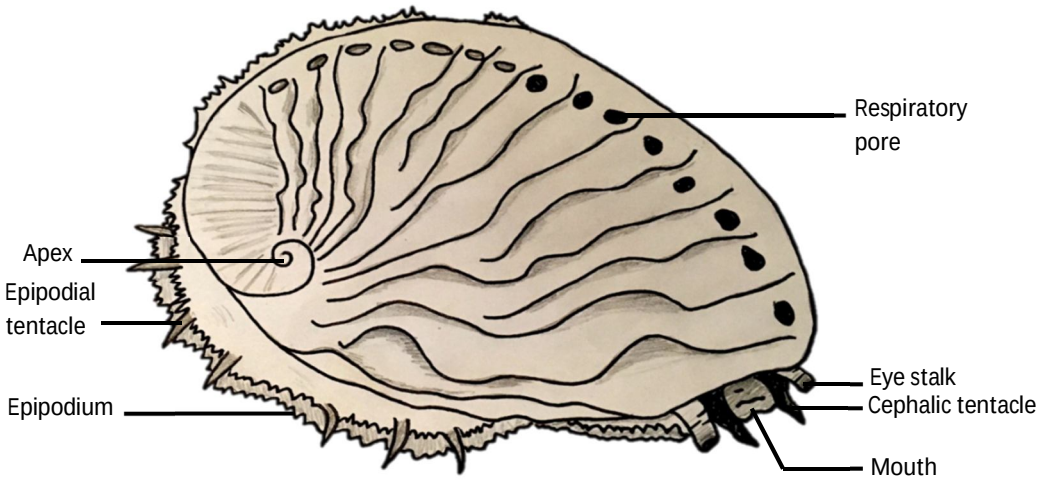

Figure 1.2. External appearance of the South African abalone, *Haliotis midae*. Graphical representation of abalone (ca. 15 cm).

Figure 1.3. Peripheral view of the internal anatomy of the South African abalone, *Haliotis midae*. Graphical representation of abalone (ca. 15 cm).

The epipodium is connected to the shell by a strong adductor muscle (Figure 1.3). The vital organs are protected between the shell and epipodium by a smooth mantle, which has two openings beneath the shell pores, to allow for respiration and excretory functions. The gills, gut and heart and located beneath the shell pores and the gonad is located on the growing-edge side of the animal.

1.1.3. Distribution and movement

The distribution of *H. midae* ranges from Saldanha Bay on the West Coast of South Africa to Riet Point on the East coast (Figure 1.4, Rhode et. al. 2017). Abalone are generally found on rocky substrate between the low water mark and approximately 10m depth, although they have been sighted at a depth of 36m (Newman 1969, Barkai & Griffiths 1986). Abalone in optimal habitats tend to remain quiescent, but when they need to move, they can move at a mean rate of 274.34 meters over 104-558 days over a variety of substrates (Newman 1969, Tarr 1995).

Figure 1.4. Distribution of the South African abalone *H. midae* along the South African coastline (red).

1.1.4. Life cycle

Haliotis midae are dioecious, asynchronous broadcast spawners with a high fecundity (Newman 1968; Wood & Buxton 1996). Breeding season extends from March to October with spawning peaking between April and June; although spawning can be induced in captivity on a more regular basis (Wood & Buxton 1996). Sexual maturity is first attained at approximately 20-25mm shell width (Wood & Buxton 1996). Fertilization of gametes produces free-swimming lecithotrophic, trocophore larvae within approximately 22 hours (Genade et. al 1988). Abalone continue to develop as free-swimming larvae for approximately seven days before settling onto hard substrates, using chemical settlement cues from benthic diatoms or the mucous from other abalone (Alfaro et. al. 2014; Figure 1.5). Post-settlement larvae undergo torsion to develop a flattened appearance and graze on diatom biofilms until they are large enough to graze on macroalgae (Matthews & Cook 1995). Abalone recruits and juveniles (approx. 3-35mm in length) shelter beneath sea urchins (*Parechinus angulosus*) for protection and access to food captured by the urchins; without this protection, abalone populations dwindle and disappear (Day 1998, Day & Branch 2000).

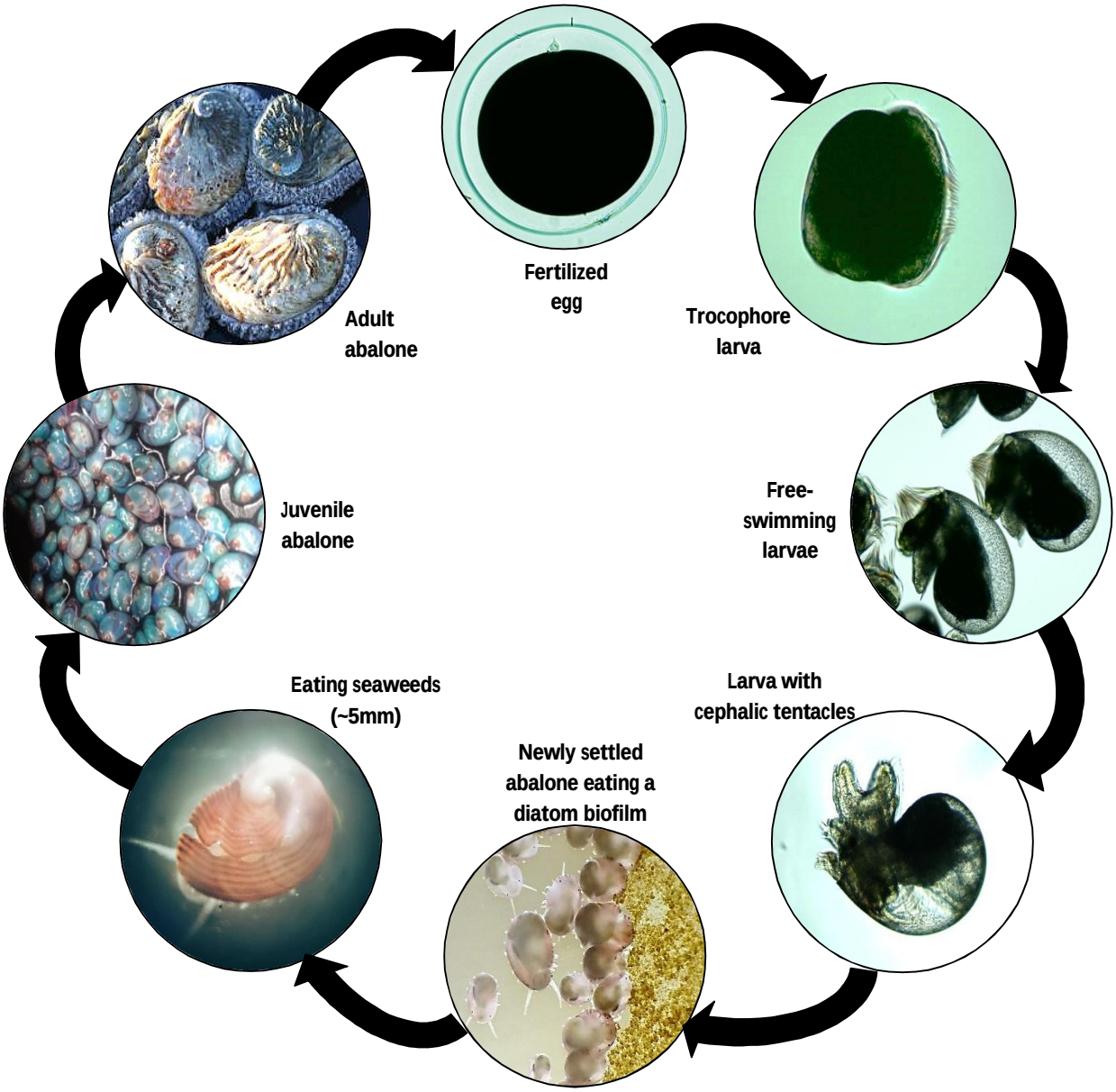

Figure 1.5. Life cycle of the South African abalone, *Haliotis midae*.

1.1.5. Food and growth

The perlemoen abalone are predominantly herbivorous, with most of their diet consisting of kelp (56% *Ecklonia maxima*) and red algae (21% *Plocamium spp*.) on the west and south-west coast; smaller abalone (75-85mm) were recorded to consume a larger proportion of *Ulva spp.* (45%) than larger abalone (<5%) (Barkai & Griffiths 1986).

H. midae has been recorded to reach a maximum size of approximately 200mm at an age of over 30 years in its natural habitat (Newman 1968), and growth rates around the coast can range from 5-33mm.year^{-1} (Tarr 1995).

1.2 The South African Abalone Fishery

1.2.1. The demand for abalone

H. midae is considered to be one of the world's most premium abalone species, with a larger size, white flesh and unique taste preferred by Asian importers (Figure 1.6). Abalone is used in traditional Asian dishes and is seen as a delicacy, fetching a high market price (Raemaekers & Britz 2009, Cook 2016). The market value of abalone depends on the processing of the product (e.g. dried, canned, live) and demand for the product. For example, in 2000, the price of live abalone was approximately $45 per kilogram and dried abalone were sold for $700-2000 a kilogram (Gordon 2000). This extraordinary profit margin for an abalone that can be plucked from the bottom of the ocean has created a demand for abalone that has led to prolific poaching.

Figure 1.6. Processed abalone, *Haliotis midae*, meat with creamy white flesh (ca. 8cm).

1.2.2 History of South African abalone fishery

The Asian demand for abalone became known in South Africa in 1949 and spurred on the start of the South African abalone fishery (Newman 1964). This started as a period of unregulated fisheries where abalone were overharvested and beds of abalone were depleted (Figure 1.7). The first quota of 385 tonnes production mass was implemented in 1968 (Newman 1964, Tarr 1993, Raemaekers et. al. 2011). This led to a relatively stable capture of abalone from the 1970's through to the 1990's, during which time total allowable catch (TAC) regulations were implemented in 1983 (Tarr et. al. 1996, Tarr 2000, Gordon & Cook 2004, Raemaekers et. al. 2011; Figure 1.7). The stability of the abalone fishery began to weaken in the 1990's when a combination of factors caused wild abalone stocks to plummet. The elimination of restrictive Apartheid laws in the early 1990's resulted in weakened border control systems and weakened South African Rand in comparison to the U.S. dollar, which made export, including illegal export, very lucrative (Hauck & Sweijd 1999, Tarr 2000, Steinberg 2005). These factors, in combination with the presence of a well-established crime network in South Africa, promoted the bartering of drugs for abalone and spurred the illegal trade of abalone into fruition (Raemakers & Britz 2009). Recruitment surveys were taken annually from 1988

to 1993 in main fishing zones and discovered an additional negative impact on abalone stocks. Juvenile abalone, as well as sea urchin, populations were declining due to an unprecedented southward migration of predatory rock lobsters (*Jasus lalandii*) into commercial abalone fishing areas (Tarr et. al. 1996, Mayfield & Branch 2000, Cockroft et. al. 2008, Blamey et. al. 2010). Recreational abalone fisheries were closed in 2003 due to the radical decline in recreational TAC, which was followed by a reduction in commercial TAC (DEAT 2003). There was an 88% stepwise decrease in commercial TAC between 1995/6 and 2007/8 fishing seasons, which resulted in the temporary closure of the commercial fishery in 2008 (DEAT 2007). In May 2007, the South African abalone, *H.midae,* was listed on Appendix III of CITES (the Convention on International Trade in Endangered Species of Wild Fauna and Flora) as a means to incorporate international trade and market controls (Raemakers 2011). In 2007/8 75 tons of abalone TAC was caught legally and more than 2000 tons was caught illegally, only 14% of which was confiscated by law enforcement (Raemakers & Britz 2009, Plagányi et. al. 2011). At this point abalone populations were estimated to be at less than 18% of pre-exploitation spawning biomass; one of the four major fishing zones was estimated to be at 4% (Plagányi & Butterworth 2010). Only two of the fishing zones were reopened to legal fisheries. Unfortunately, South Africa withdrew the listing on CITES on 25 May 2010 under the claim that recent changes to CITES legislation made it too difficult to receive permit endorsement for international trade (Bürgener 2010, Raemakers et. al. 2011). Abalone populations collapsed in lobster-invaded areas due to the pressures of illegal fishing and increased predation (Blamey et. al 2013). Abalone populations were modelled and it was determined that the abalone population collapse in lobster-invaded areas would persist even if lobsters were absent from the area for the next 50 years due to abalone recruitment failure (Blamey et. al. 2013).

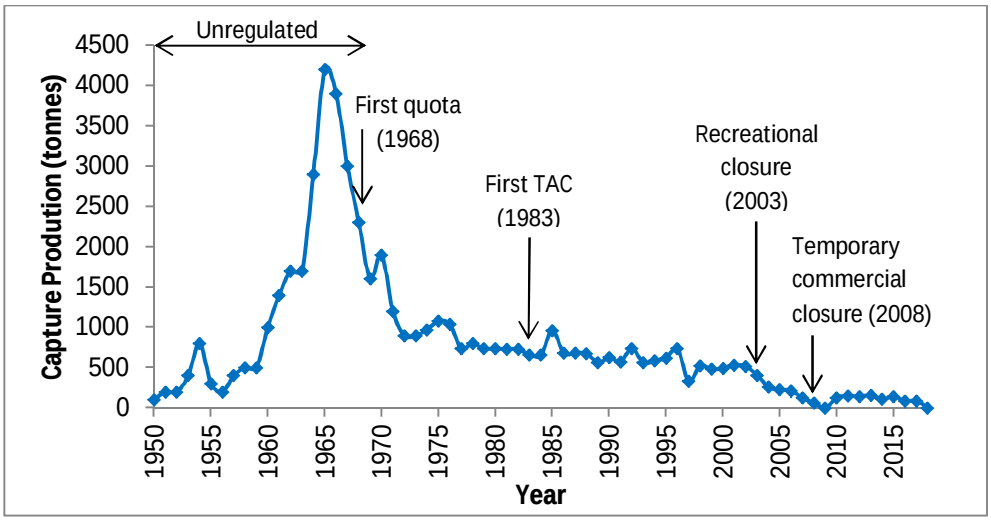

Figure 1.7. South African abalone, *Haliotis midae*, legal capture production from 1950 – 2018. Data accessed from FAO on 5 December 2020 on http://www.fao.org/fishery/statistics/en.

Abalone are slow-growing, long-lived, and have a high economic value which makes them particularly susceptible to the effects of a rising illegal fishery (Plagányi et. al. 2011). Illegal and unregulated fishing of abalone trade was estimated by South Africa's Department of Agriculture Forestry and Fisheries to be R440 mill (US$ 33 mill) in 2016, roughly 50% of South Africa's total

abalone export value for the year (FAO 2017b). Today the demand for abalone is largely met through aquaculture (FAO 2018b) as capture production was halted in 2018.

1.2.3 Abalone aquaculture

Cultivation and spawning of abalone, *H. midae* began in 1981, but only began to fully develop as commercial aquaculture in the 1990's alongside the development of international aquaculture systems (Sales & Britz 2001). Currently over 95 % of world abalone production comes from aquaculture and is dominated by China and Korea, followed by South Africa (FAO 2018b). In 2018, abalone aquaculture accounted for 24.6 % of the total animal aquaculture production from South Africa (FAO 2018b; Figure 1.8) and 77 % of South Africa's aquaculture revenue in 2019 (Parliamentary Monitoring Group 2020).

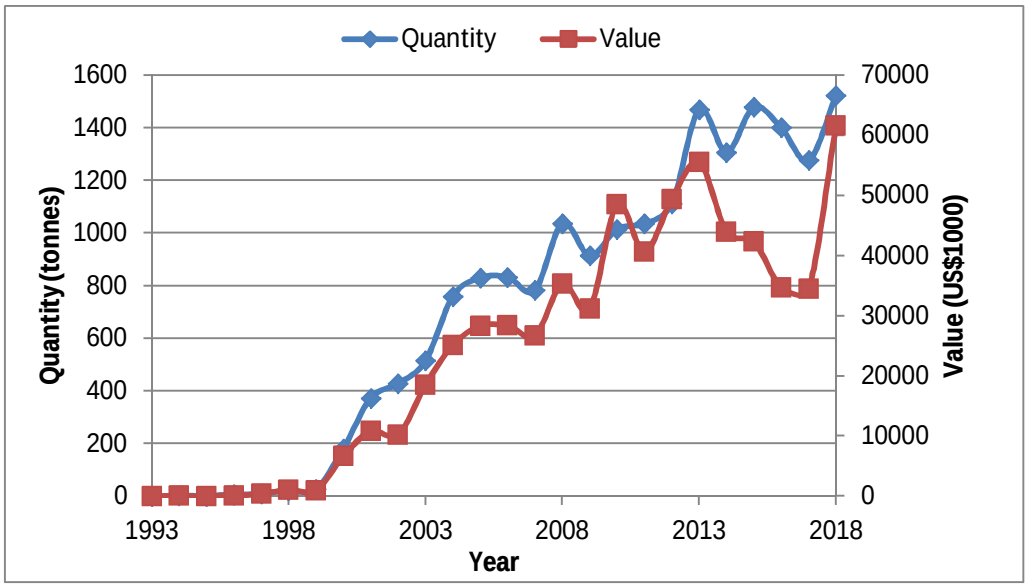

Figure 1.8. South African abalone, *Haliotis midae*, aquaculture production and production value from 1993-2018. Data accessed from FAO on 5 January 2020 on http://www.fao.org/fishery/statistics/en.

There are currently 14 commercially operational abalone aquaculture farms in South Africa (Parliamentary Monitoring Group 2020). Abalone are cultivated in land-based tank systems on farms that are situated very close to the shore line. Large quantities of seawater are actively pumped ashore into a main header tank where it is filtered before being gravity-fed to commercial abalone tanks. In most cases effluent is released directly into the environment, although some farms are able to partially recirculate the water, via appropriate filtration and water treatment systems, to avoid unfavourable ocean conditions. Commercial abalone are typically fed a formulated diet, although some farms incorporate seaweeds into the diet. Farms characteristically consist of a hatchery area and a 'grow-out' area where adult abalone are cultivated (Figure 1.9). The aquaculture process of *H. midae* can take approximately 45 months from spawning to harvesting. This thesis will focus on abalone in the grow-out section of the farm.

The primary goal in aquaculture is to produce quality, harvest-sized product using minimal costs in as short a time as possible in order to maximise profits. Due to the large volume of seawater that is constantly pumped onshore in land-based aquaculture, pre-treatment of the water is limited and farms can be vulnerable to negative ocean conditions, such as harmful algal blooms (Bothes et. al. 2003), ocean temperature changes and toxic spills.

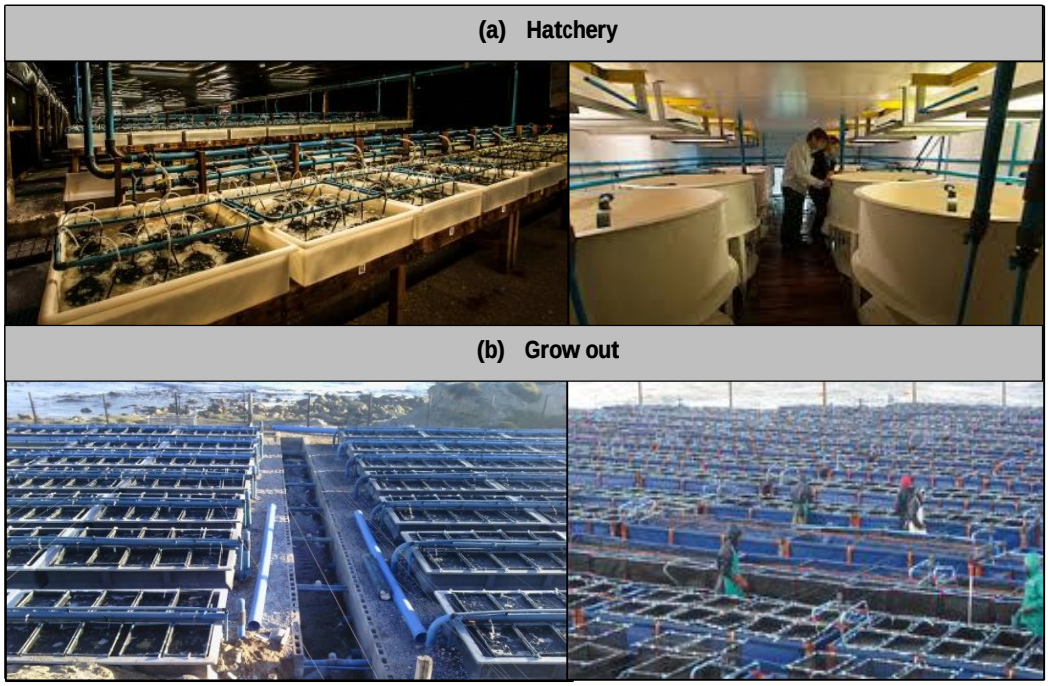

Figure 1.9. Abalone, *Haliotis midae*, aquaculture farms in South Africa are typically divided into two sections: (a) hatchery and (b) grow-out. Hatcheries contain broodstock and larval/juvenile developing abalone, and "grow-out sections" contain adult abalone.

1.3 Global Warming

1.3.1. Evidence of global warming

Global warming is the currently increasing temperature of the Earth's surface, land and water, as well as its atmosphere (Cubasch et. al. 2013, Table 1.1, Figure 1.10). The Earth's temperature has fluctuated throughout its existence, with maximum temperatures of above 32°C in the Neoproterozoic period between 600 and 800 million years ago (McInerney & Wing 2011, Masson-Delmott et. al. 2013); however the current rate of warming is unprecedented (Petit et. al. 1999). Two thirds of the increase in surface temperatures has been attributed to an increase in anthropogenic greenhouse gases (Hartmann et. al. 2013).

Table 1.1. Trend estimates and 90% confidence intervals for land-surface air temperatures (LSAT) global average values over five common periods from four data sets (Table from Hartmann et. al 2013).

Data Set	Trends in °C per decade				
	1880-2012	1901-2012	1901-1950	1951-2012	1979-2012
CRUTEM4.1.1.0 (Jones et. al. 2012)	0.086 ± 0.015	0.095 ± 0.020	0.097 ±0.029	0.175 ± 0.037	0.254 ± 0.050
GHCNv3.2.0 (Lawrimore et. al. 2011)	0.094 ± 0.016	0.107 ± 0.020	0.100 ± 0.033	0.197 ± 0.031	0.273 ± 0.047
GISS (Hansen et. al. 2010)	0.095 ± 0.015	0.099 ±0.020	0.098 ± 0.032	0.188 ± 0.032	0.267 ± 0.054
Berkeley (Rohde et. al. 2013)	0.094 ± 0.013	0.101 ± 0.017	0.111 ± 0.034	0.175 ± 0.029	0.254 ± 0.049

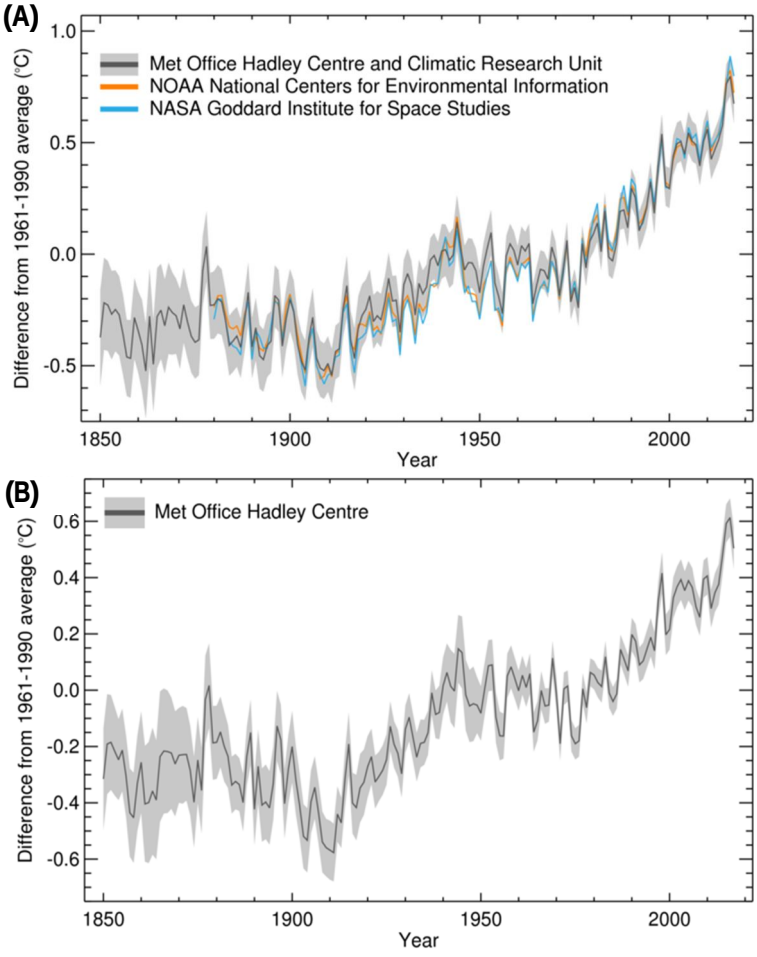

Figure 1.10. Global annual average temperature anomaly for (A) surface temperature (HadCRUT4) and (B) sea-surface temperature from 1850-2017. Data is depicted as annual average temperature anomaly times series (black lines) and the 95% confidence ranges in the values (gray areas; in the long-run the true value will fall within this range in 19 out of 20 cases). Sea surface temperature (SST) observations come from buoys deployed across the world's oceans and ships in the Voluntary Observing Ship Programme. Together they take around 1.5 million observations each month. These readings are checked by a computer and any obviously inaccurate readings are excluded.: https://www.metoffice.gov.uk/research monitoring/climate/surface-temperature.

1.3.2. The greenhouse effect

A greenhouse gas is a gas present in the atmosphere, which absorbs and emits radiant energy within the thermal infrared range (Hartmann et. al. 2013). Primary greenhouse gases include water vapour, methane (CH_4), carbon dioxide (CO_2), nitrous oxide (N_2O) and ozone (O_3). Without greenhouse gases the Earth's temperature would be approximately -18°C rather than the present average of approximately 15°C (Karl & Trenberth 2003).

CO_2 has contributed, more than any other greenhouse gas, to global warming between 1750 and 2012 due to its high concentration in the atmosphere (Hartmann et. al. 2013). Since the start of the industrial revolution (~1750) the concentration of CO_2 in the atmosphere has increased by over 47 % from 280 ppm to 412 ppm in November 2020 (NOAA, Figure 1.11). This increase has occurred despite natural carbon sinks involved in the carbon cycle; such as plants, soils and the ocean (Hartmann et. al. 2013). The majority of anthropogenic emissions come from the combustion of fossil fuels and land use change (Hartmann et. al. 2013). Precise and accurate measurements of atmospheric CO_2 concentrations are taken at Moana Loa, Hawai'i and the South Pole and were started by C.D. Keeling of the Scripps Institute of Oceanography in the 1950's (Keeling et. al. 1976a, Keeling et. al. 1976b).

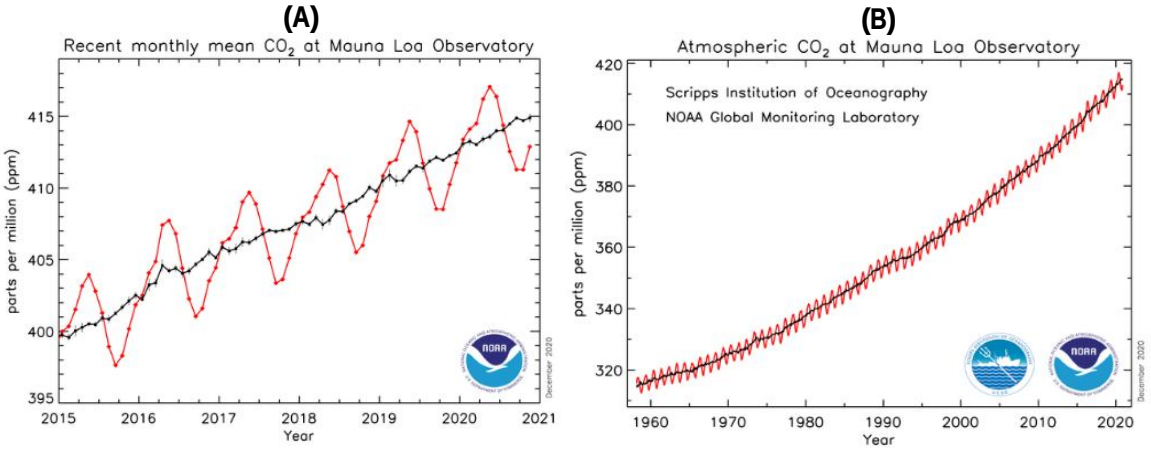

Figure 1.11. Mean atmospheric carbon dioxide (CO_2) concentration (red curve) measured as the mole fraction in dry air at **(A)** Mauna Loa Observatory, Hawai'i, from 1958-2020 and **(B)** global monthly mean from 1974-2018. The **black** curve represents the seasonally corrected data. Data are reported as a dry mole fraction defined as the number of molecules of carbon dioxide divided by the number of molecules of dry air multiplied by one million (ppm). Graphs supplied by the Global monitoring division, Earth system research laboratory, National Oceanic and Atmospheric Administration on 10 January 2020 (NOAA).

Projected changes in temperatures for the year 2100 according to the IPCC 5th assessment report show increases in temperature, with the highest temperature increase projected for Arctic regions (Collins et. al. 2013, Table 1.2). The ocean has absorbed 93% of the excess heat produced by greenhouse gases between 1971-2010, with most (64%) of the warming occurring in the upper 700m of the ocean (Gleckler et. al. 2010, Pierce et. al. 2012, Rhein et. al. 2013, Hoegh-Guldberg 2014). Global sea surface temperatures (SST) have increased at a rate of 0.121°C (Kennedy et. al. 2011) to 0.124°C (Rayner et. al. 2006) per decade based on in situ measurements from 1979-2012 (Hansen et. al. 2006) and temperature measurements show a continuing increase in heat content of the oceans (Hartmann et. al. 2013, Rhein et. al. 2013; Figure 1.10).

Table 1.2. Coupled Model Intercomparison Project Phase 5 (ICMP5) annual mean surface air temperature anomalies (°C) from the 1986–2005 reference period for selected regions under the RCP4.5 emissions scenario for the year 2100. The mean ±1 standard deviation ranges are listed and the 5-95% ranges from the model's distribution (based on a Gaussian assumption and obtained by multiplying the CMIP5 ensemble standard deviation by 1.64) are given in brackets. Values from Collins et. al. 2013.

	RCP 4.5 (ΔT in °C)
Land	2.4 ± 0.6 (1.3, 3.4)
Ocean	1.5 ± 0.4 (0.9, 2.2)
Tropics	1.6 ± 0.4 (0.9, 2.3)
Polar - Arctic	4.2 ± 1.6 (1.6, 6.9)
Polar - Antarctic	1.5 ± 0.7 (0.3, 2.7)

1.3.4. Local temperature changes

South Africa is bordered by two oceans, the Indian and Atlantic. The Indian Ocean has warmed at a rate of 0.11°C per decade and the Atlantic has warmed by 0.08°C per decade in the top 700m of the oceans (Hoegh-Guldberg et. al. 2014). The study site is mostly influenced by the Benguela current, which is an eastern boundary upwelling current that flows northward in the South Atlantic Ocean. Most research on the Benguela current has focused on fisheries and oceanography, with minimal attention to climate change due to stong inter-annual and interdecadal variability in physical oceanography, which makes the detection and designation of biophysical trends to climate change difficult (Hoegh-Guldberg et. al. 2014). Despite this, the physical conditions of the Benguela Current are highly sensitive to climate variability over a range of magnitudes (Hutchings et. al. 2009, Leduc et. al. 2010, Richter et. al. 2010, Rouault et. al., 2010). Therefore, there is medium scientific agreement within the intergovernmental panel on climate change (IPCC) in the 5th assessment report that upwelling intensity and associated variables, such as temperature, from the Benguela system will change as a result of climate change (Demarq 2009, Hoegh-Guldberg et. al. 2014).

The temperature of the surface waters of the Benguela Current did not increase from 1950 to 2009, and short-term records show a temperature decrease of 0.35-0.55°C per decade in the south-central Benguela Current between 1982 to 2009 (Rouault et. al. 2010) and an increase of 0.24°C in temperature for the whole Benguela region between 1982 to 2006 (Belkin, 2009). The differences in small- and large-scale data sets and short- versus long-term records indicate a substantial influence of long-term variability (Belkin 2009, Hoegh-Guldberg et. al. 2014, Schlegel & Smit 2016). Thus, a confident projection of seawater temperature for the ocean surrounding the study site for the end of the 21st century is not possible.

1.3.5. Biological effects of warming

Temperature influences the rate of fundamental biochemical and metabolic processes (Hochachka & Somero 2002, O'Connor et. al. 2007, Strotz et. al. 2018). Warming therefore has the ability to regulate organismal attributes such as developmental rates, growth, and survival (O'Connor et. al. 2007, Byrne & Przeslawski 2013, Harvey et. al. 2013, Przeslawski et. al. 2015). A disturbance in

organismal developmental rates can influence larval dispersion, local adaptation and speciation (Durant et. al. 2007, O'Connor et. al. 2007, Harley et. al. 2012, Przeslawski et. al. 2015, Boyd et. al. 2018). Temperature is one of the main triggers for processes such as spore production, flowering and seed germination in marine macrophytes and changes in temperatures can therefore disrupt these ontogenetic processes (Diaz-Almela et. al. 2007, Waycott et. al. 2007, Mohring et. al. 2013, Wernberg et. al. 2016). In marine macrophytes, respiration is typically more sensitive than photosynthesis to temperature increases and would create a larger energetic cost than primary production (Stæhr & Wernberg 2009). Where organisms live close to their thermal limits, small increases in temperature could have profound effects on physiological processes such as metabolic rates, cell protein damage, reduction in membrane fluidity and respiratory stress (Eggert 2012), and disruption of nutrient intake and photosynthetic inhibition in macrophytes (Davison & Pearson 1996, Foden et. al. 2013, Wernberg et. al. 2013). Prolonged exposure to increased temperatures can result in reallocation of resources for protection and repair and eventually mortality (Hawkins 1981, Harley et. al 2012, Wernberg et. al. 2013)

The effects of temperature change depend on the organisms level of sensitivity, taxonomy, distribution and life history (López-Urrutia et. al. 2006, Vázquez-Domínguez et. al. 2007, Pörtner et. al. 2008, Hoegh-Guldberg & Bruno 2010, Polovina et. al. 2011, Przeslawski et. al. 2015). Assessing a species vulnerability to climate change can be difficult, especially when applying projected temperatures for the end of the 21st century; however there are some traits which make animals more or less vulnerable to projected changes. Some studies suggest that life history traits might be more important than taxonomy and distribution in determining species vulnerability to climate change (Foden et. al. 2013; Pacifici et. al. 2015), but further traits that can increase the vulnerability of a species include limited dispersal abilities, slow reproductive rates, specialized habitats and dietary requirements (Przeslawski et. al. 2015). *H. midae* have slow reproductive rates, reaching 50% sexual maturity at an age of approximately 3-5 years (Newman 1968; Wood & Buxton 2008; Proudfoot et. al. 2008), and require sea urchins to be present in nursery areas (Day 1998, Day & Branch 2000). This could make them at risk of ocean surface warming from an ecosystem perspective.

Warming can also influence the geographical distribution of species with an enhanced risk of local extinction if the organism is unable to move away from unfavourable temperatures (Hochachka & Somero 2002, Parmesan & Yohe 2003, Thomas et. al. 2004, Hoegh-Guldberg et. al. 2005; Perry et. al. 2005, Poloczanska et.al. 2013; Hoegh-Guldberg et. al. 2014). Poloczanska et. al. (2013) determined in a meta-analysis of 1735 biological responses that the rates of distributional shifts in marine species, across regional and taxonomic groups, were consistent with those required to track temperature changes in the ocean surface. Distributional shifts can have profound impacts on ecosystem functioning and configuration, ocean primary productivity, carbon sinks and biochemistry of the Earth (Gregg et. al. 2003, Wiltshire & Manly 2004, Behrenfeld et. al. 2006, Polovina et. al. 2008, Pörtner & Farrell 2008, Doney et. al. 2009, Riebesell et. al. 2009, Hoegh-Guldberg & Bruno 2010, Poloczanska et. al.2013). Distributional shifts have already been observed in intertidal and shallow subtidal macrophytes communities with broad and vertical expansions into deeper water where fluctuations in temperature are less pronounced (Lima et. al. 2007, Fernandez 2011, Wernberg et. al. 2011, Martinez et. al. 2012, Tanaka et. al. 2012, Smale & Wernberg et. al. 2013).

In the coastal waters of South Africa, the Cape anchovy, *Engraulis encrasicolus*, made an eastward distributional shift in the Southern Benguela in 1996, which corresponded with an abrupt decrease in SST on the Agulhas Bank by 0.5 °C (Roy et. al. 2007). The West Coast rock lobster, *Jasus lalandii*, displayed a southward distributional shift from the west coast to the south-west coast in the 1980's which has been attributed to changes in environmental conditions (Cockroft et. al. 2008). Long-term data sets are insufficient for use in determining the exact changes in environmental conditions; however coastal water cooling was observed between 1982 and 2010 (Rouault et. al. 2010). This particular distributional shift transformed a kelp forest system, that was dominated by *H. midae*, urchins (*P. angulosus*), and winkles (*Oxystele* and *Turbo* spp.), into a system that is now dominated by *J. lalandii* and foliar algae (Blamey et al. 2010). Bank Cormorants, *Phalacrocorax neglectus*, also displayed a distributional shift consistent with the distribution shifts of their primary food source, *J. lalandii* (Crawford et. al. 2008). This demonstrates that seemingly small changes in SST can have large implications on the coastal ecosystems surrounding South Africa.

Similar to range expansions, range reductions are also possible if the organism is unable to expand its distribution in the face of climate change. The Northern abalone, *H. kamtschatkana*, population numbers are dwindling in the southern portion of their distribution range on the west coast of North America. These population declines are thought to be due to warming oceans in combination with predation by sea otters and commercial fishing pressure (Rogers-Bennett 2007).

1.4. Ocean Acidification

1.4.1. The chemistry of acidification

When anthropogenic CO_2 is released into the atmosphere it integrates into the Earth's carbon cycle. The oceans are the largest active carbon sinks on Earth, absorbing more than a quarter of anthropogenic CO_2 in the last 20 years (Mikaloff-Fletcher et. al. 2006, Hartmann et. al. 2013, Wanninkhof et. al. 2013, Le Quére et. al. 2014, Schmitt 2018). The absorption of CO_2 by the ocean has resulted in the decrease of the oceans' average pH; this is known as ocean acidification.

An increase in carbon dioxide in the atmosphere drives CO_2 to dissolve in and react with seawater to form carbonic acid (H_2CO_3) through the following chemical reaction (Ciais et. al. 2013):

$$CO_2 + H_2O \leftrightarrow H_2CO_3$$

Carbonic acid is unstable and mostly dissociates to form bicarbonate (HCO_3^-) and hydrogen (H^+) ions:

$$H_2CO_3 \leftrightarrow H^+ + HCO_3^-$$

The production of H^+ results in an increase of the H^+ concentration ($[H^+]$) and a decrease of seawater pH, which is the negative logarithm of the H^+ concentration (pH =-log10 $[H^+]$) (Wolf-Gladrow & Rost 2014).

Fortunately, the ocean is saturated with carbonate ions (CO_3^{2-}) that act as a buffer by reacting with CO_2 and excess hydrogen ions to form bicarbonate ions, reducing the concentration of hydrogen ions in the seawater slightly:

$$CO_2 + H_2O + CO_3^{2-} \leftrightarrow 2HCO_3^-$$

A reduction in the amount of carbonate ions in the oceans causes an imbalance in the following chemical reaction. These imbalances and reactions are displayed in the Bjerrum plot (Figure 4.1.2; Wolf-Gladrow et. al. 2007):

$$Ca^{2+} + CO_3^{2-} \leftrightarrow CaCO_3$$

This causes a decline in the saturation state (Ω) of $CaCO_3$, which affects the ability of calcifying organisms such as corals, coccolithiphores and molluscs to produce their calicified shells or skeletons (Hoegh-Guldberg et. al. 2007, Doney et. al. 2009, Feely et. al. 20009, Hoegh-Guldberg et. al. 2014).

The ocean is supersaturated with a $CaCO_3$ mineral (eg. aragonite, calcite, high-Mg calcite) when the saturation state of that mineral is larger than 1 (Ω>1); calcification is favoured more than dissolution (Feely et. al. 2009, Adkins et. al. 2021). Dissolution occurs despite the oceans being supersaturated with $CaCO_3$ because of the slow abiotic precipitation rates for $CaCO_3$ minerals (Feely et. al. 2009, Adkins et. al. 2021). The saturation states of $CaCO_3$ minerals declines with ocean depth as total dissolved CO_2 increases. The saturation horizon of $CaCO_3$ minerals is the depth where Ω=1, below which dissolution is favoured over calcification. The Ω=1 threshold is a useful indicator for biomineralisation and dissolution, but is not a strict criterion (Feely et. al. 2009). Biomineralization differs between organisms, where some might require a Ω well above 1 and others may be able to build/maintain calcified structures in undersaturated conditions (Przeslawski et. al. 2015)).

As more CO_2 is absorbed by the ocean the depth of these saturation horizons shallows (Feely et. al. 2004, Feely et. al. 2009, Adkins et. al. 2021).

1.4.2. Ocean acidification predictions

Uptake of atmospheric CO_2 by the oceans has decreased ocean pH by approximately 0.1 units over the past 100 years, which equates to a 30% increase in hydrogen ion concentration (Hoegh-Guldberg et. al. 2014). According to the IPCC 5th assessment report, projected changes in the open ocean range from a decline in pH by 0.14 units with Representative Concentration Pathway (RCP) 2.6 (GHG peak between 2010-2020 and decline substantially thereafter) to 0.43 units with RCP 8.5 (Hoegh-Gulberg et. al. 2014; Figure 1.12).

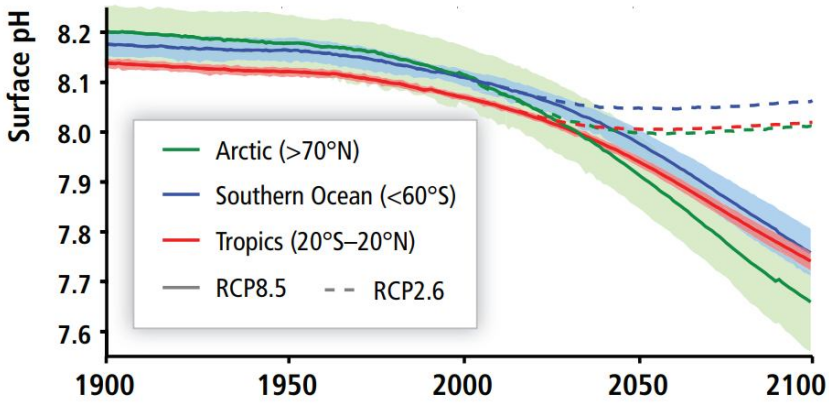

Figure 1.12. Projected ocean acidification from 11 Coupled Model Intercomparison Project Phase 5 (CMIP5) Earth System models under RCP8.5 and RCP 2.6 (other Representative Concentration Pathway (RCP) scenarios have also been run with the CMIP5 Models): Time series of surface pH shown as the mean (solid line) and range of models (shaded area), given as area-weighted averages over the Arctic Ocean (green), the tropical oceans (red), and the Southern Ocean (blue). From Hoegh-Guldberg et. al. 2014.

Saturation horizons for aragonite and calcite will become significantly shallower in all oceans, with aragonite saturations between 0-1500m in the Atlantic Ocean (Sabine et. al. 2004, Orr et. al. 2005; Figure 1.13). Aragonite is the primary $CaCO_3$ mineral in abalone shells, putting them at risk of shell dissolution. The increase in dissolved CO_2 in the oceans will ultimately affect the entire carbonate chemistry of the ocean (Figure 1.14).

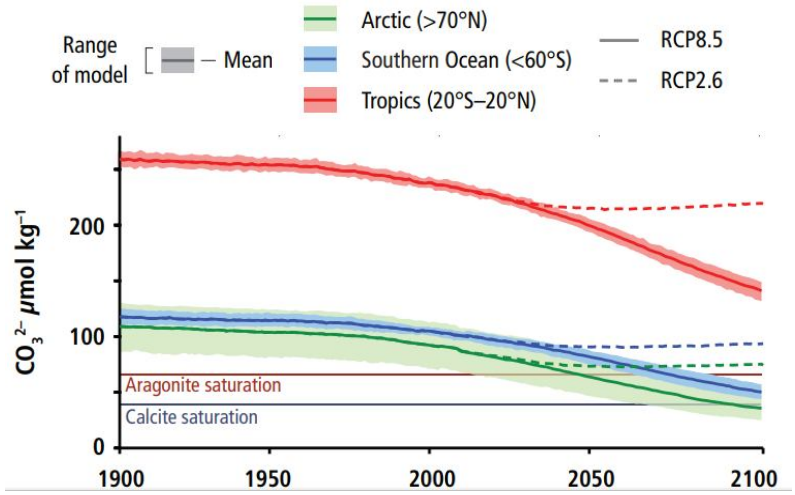

Figure 1.13. Projected aragonite saturation state from 11 Coupled Model Intercomparison Project Phase 5 (CMIP5) Earth System Models under Representative Concentration Pathway 8.5 (RCP8.5) scenario. Time series of surface carbonate ion (CO_3^{2-})concentration shown as the mean (solid line) and range of models (shaded area), given as area-weighted averages over the Arctic Ocean (green), the tropical oceans (red), and the Southern Ocean (blue).

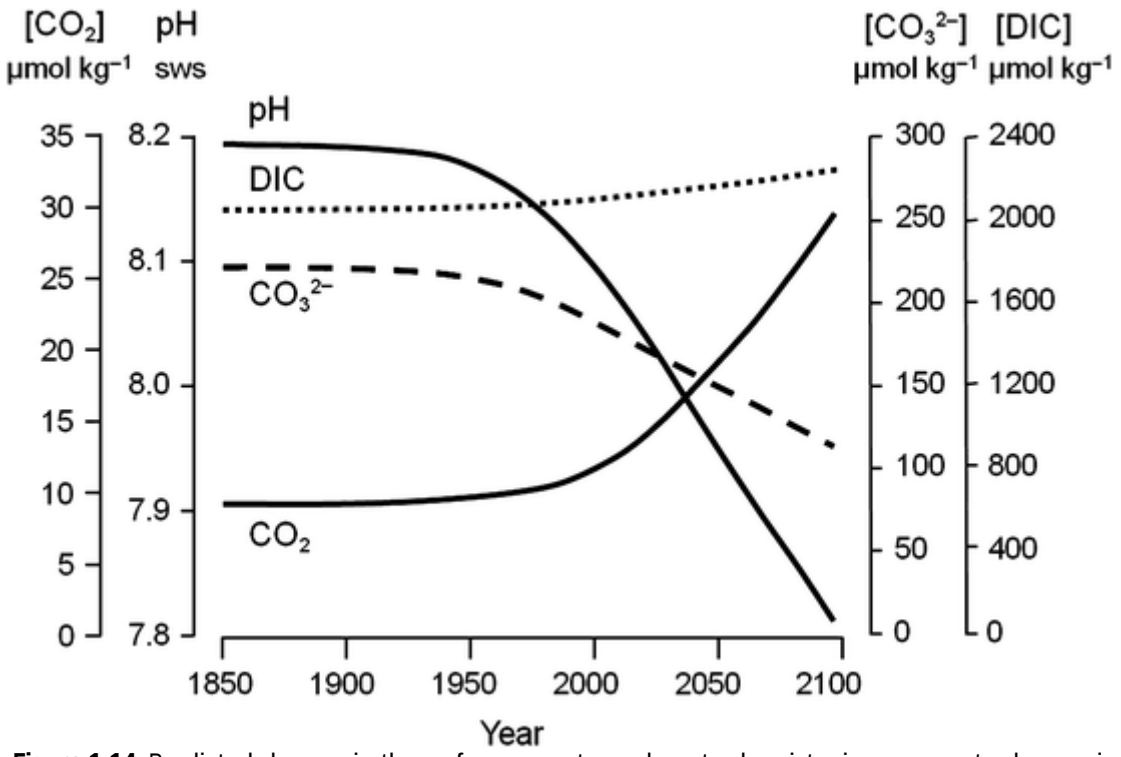

Figure 1.14. Predicted changes in the surface seawater carbonate chemistry in response to changes in atmospheric pCO_2 assuming the IS92a scenario (After Wolf-Gladrow & Rost 2014; modified from Wolf-Gladrow et. al. 1999).

Upwelling regions, that have naturally high CO_2 concentrations and low pH, are potentially vulnerable to ocean warming and acidification according to the 5th assessment report of the IPCC (Hoegh-Guldberg et. al. 2014). There is limited evidence and minimal scientific agreement as to how upwelling systems are likely to change; however ocean acidification will result in upwelling waters being CO_2-rich, with impacts on coastal ecosystems and fisheries already evident in areas such as the California Current (Hauri et. al. 2009). These risks pose a significant challenge for fisheries and associated livelihoods along the west coasts of Africa, South America, and North America where upwelling is predominant (Ciais et. al. 2013,Hoegh-Guldberg et. al. 2014, Ahmed et. al. 2018).

Upwelling in the southern Benguela displays low partial pressure of CO_2 (Santana-Casiano et. al. 2009, Arnone et. al. 2017); however the consequences of changing upwelling intensity remain poorly explored with respect to ocean acidification (Hoegh-Guldberg et. al. 2014).

1.4.3. Biological effect of ocean acidification

Ocean acidification affects organisms in a variety of ways, not all of which are negative. Macrophytes that rely solely on CO_2 diffusion may stand to benefit from a high-CO_2 environment in terms of photosynthetic performance and growth (Gao et. al. 1999, Gao 2002, Harley et. al. 2012, Wernberg et. al. 2013). Ocean acidification has been shown to cause an increase in carbon fixation rates in some calcifying and non-calcifying photosynthetic organisms, but can be limited by a variety of other environmental factors, such as nutrients and sunlight (Tortell et. al. 2008, Doney et. al. 2009, Ciais et. al. 2013, Dhir et. al. 2015). Most brown and green algae utilize bicarbonate in seawater by

converting it into CO_2 intracellularly using CO_2 concentrating mechanisms (CCM). When exposed to high CO_2 concentrations, macrophytes with CCM's will not benefit as much as macrophytes without CCM's (Hepburn et. al. 2011, Mackey et. al. 2015). When macrophytes with CCM's are exposed to high CO_2 environments they do not show an increase in photosynthetic rate, but there is a shift towards an increase in the utilization of CO_2 diffusion over CCM's (Harley et. al. 2012, Raven et. al. 2012, Wernberg et. al. 2013). A decrease in growth has only been observed in calcifying macrophytes and the observations have been consistent (Kroeker et. al. 2010, Mackey et. al. 2015).

Most calcifying organisms demonstrate reduced calcification in response to ocean acidification (Fabry et. al. 2008, Ries et. al. 2009, Kroeker et. al. 2010, Byrne et. al. 2011a, Przeslawski et. al. 2015, Pfister et. al. 2016, Cattano et. al. 2018, Hurd et. al. 2019). Ecosystems that are characterized by high rates of calcium carbonate deposition, such as coral reefs and calcareous plankton communities, are sensitive to the decrease in the saturation states of calcite and aragonite caused by ocean acidification (Fabry et. al. 2008, Munday et. al. 2009, Kroeker et. al. 2013, Hoegh-Guldberg et. al. 2014, Pfister et. al. 2016). Projected changes are very likely to result in a loss of three-dimensional coral reef frameworks (Hoegh-Guldberg et. al. 2007, Manzello et. al. 2008, Fabricius et. al. 2011, Andersson & Gledhill 2013, Dove et. al. 2013, Ciais et. al. 2013, Hurd et. al. 2019). Varying responses by organisms to carbonate dissolution reflects differences in the ability to regulate pH at the site of calcification and the extent to which their outer shell layers are protected by an organic layer (Ries et. al. 2009, Pfister et. al. 2016, Avignon et. al. 2020).

Ocean acidification can further influence the physiology of marine organisms through acid-base imbalance and reduced oxygen transport capacity (Fabry et. al. 2008, Hendriks et. al. 2010, Byrne et. al. 2011a, Heuer & Grosell 2016, Knapp et. al. 2015). Fish and non-calcifying organisms display a lower sensitivity to ocean acidification than calcifying organisms due to a steep outwards-directed CO_2 gradient during respiration (Heuer and Grosell 2014, Wolf-Gradrow & Rost 2014). There are however, significant impacts on neurosensory and behavioural activities, otolith growth, olfactory detection, mitochondrial function, and metabolic rate, which relate to acid-base regulatory functions and an increased cost on respiratory functioning (Munday et. al. 2009, Dixson et. al. 2010, Cripps et. al. 2011, Heuer & Grosell 2014, Cattano et. al. 2018).

The combined effect of increased CO_2, lower carbonate ion concentrations and warming is a multi-stressor scenario. These stressors can be antagonistic and mitigate the effects of increased CO_2 or synergistic, compounding the negative effects of acidification (Baumann 2019). Meta-analysis by Harvey et. al. (2013) and Byrne and Przeslawski (2013)revealed that the interactive effects of warming and CO_2 had no interaction on early life survival in crustaceans, but had compounding negative impact on calcification, reproduction, size of larvae, and survival of mollusc species, greater than the observed responses for the stressors in isolation. Although these analyses found predominantly synergistic effects of warming and CO2, a more recent meta-analysis revealed predominantly more antagonistic or mitigatory interactions than synergistic interactions (Przeslawski et. al. 2015). Thus, it is imperative that more research is focused towards the interactions of multi-stressors on marine organisms to obtain a clearer projection for predicted climate scenarios as the biological effects vary depending on species, environment, and life history of the organism (Fabry 2008, Byrne & Przeslawski 2013, Harvey et. al. 2013, Breitburg et. al. 2015, Baumann 2019).

Because both warming and ocean acidification will be occurring simultaneously, there is a strong need to move away from single-stressor studies and focus on more ecologically relevant responses (Harvey et. al. 2013, Hoegh-Guldberg et. al. 2014, Baumann 2019). The vast majority of research on ocean acidification and warming use constant or controlled seawater pH or temperatures with no inclusion of the natural variability of the seawater pH in the organism's environment. Incorporating natural variability into climate change studies can be particularly important for organisms that live in a highly variable environment such as one dominated by photosynthesising organisms (Frieder et. al. 2012) and/or an upwelling environment (Hoffman et. al. 2011). It is understandable that there is a trade-off between fully controlled experimental designs in laboratory settings and environmental realism. It is also important to realise that the choice to incorporate environmental realism will result in the inability to determine exact mechanistic responses, but it will allow for the incorporation indirect environmental effects and provide better insight into ecosystem responses which controlled settings are unable to obtain (Baumann 2019). In addition, most climate change studies have short-term experimental results, which make the data more likely to overestimate the impacts of acidification and warming rates on marine organisms (Hoegh-Guldberg et. al. 2014). There is a strong need for longer-term studies, especially for longer living organisms (Baumann 2019). Overall, there is a strong need to develop adaptation strategies to mitigate rapidly growing risks and uncertainties to the coastal and oceanic industries (Hoegh-Guldberg et. al. 2014).

The South African abalone is a calcifying mollusc with little to no published research carried out with regards to climate change responses. Some aquaculture farms have noted a general shiny appearance of abalone shells in abalone tanks with low pH (Figure 1.15), but no further impacts have been assessed as yet for climate change related scenarios. The 5th assessment report of the IPCC states that there is a strong need for adaptation and mitigation strategies for coastal communities that may be affected by CO_2-induced stressors (Ciais et. al. 2013, Hoegh-Guldberg et. al. 2014, Ahmed et. al. 2019). Aquaculture facilities have the potential to mitigate low pH seawater through seaweed bioremediation, but the methods to do so require thorough testing for efficacy.

Figure 1.15. Eroded abalone shell (ca. 23cm) from an abalone aquaculture facility. Photo curtesy of Heart of Abalone, Abagold, South Africa.

1.5 Thesis aims and objectives

This experiment aims to meet the climate change research demands by applying climate change projections to *H. midae* in an aquaculture facility and incorporating a multi-stressor environment of reduced pH (-0.4 from ambient) and increased temperature (+1.5 °C from ambient), alone and in combination, including natural variability of seawater over 12 months, longer than other climate change studies on marine calcifiers. A reduction in seawater pH of 0.4 units below ambient was chosen based on IPCC's 4th assessment report for projected pH declines by the year 2100 (IS92a, Meehl et. al. 2007), which was the most recent global assessment at the time of the experimental design process. However, this decrease in ocean pH has since been projected by a more pessimistic global change scenario model for the year 2100 (RCP 8.5, Hoegh-Gulberg et. al. 2014). The decrease in seawater pH of 0.4 units was retained for the following reasons:

1) Changes/declines in ocean pH are expected to be largest at the surface of the ocean (Meehl et. al. 2007) where water is withdrawn to be pumped ashore by abalone farms

2) The Benguela Current system is characterized by frequent upwelling events (Bakun 1990, Hoegh-Guldberg et. al. 2014) and periods of low oxygen due to algal decay and bacterial respiration (Pitcher et. al. 2010) , which have been predicted to increase in frequency and severity due to climate change.

An experimental elevation of seawater temperature by 1.5 °C above ambient was chosen based on an optimistic global change scenario for the year 2100 (RCP 4.5, Collins et. al. 2013) due to conflicting projections of local seawater temperature changes (Belkin 2009, Rouault et. al. 2010).

The project objectives will be to, firstly, determine whether the pH and temperature projections for the year 2100 will affect the abalone growth, physiology and spawning by measurement of whole weight, meat quantity, Condition Factor (CF), Gonadal Bulk Index (GBI) and acid-base regulation. The second objective will be to determine the potential impacts that reduced pH and increased temperature, alone and in combination, will have on abalone shell growth, shape, compressive shell strength and shell mineralogy.

Lastly, this project aims to test the viability of a pH mitigation strategy in an aquaculture system. This will be determined through the use of commercially farmed seaweed, *Ulva rigida* (Chlorophyta), as a biomitigation tool in series with experimental abalone tanks to ameliorate reduced pH seawater (-0.4 from ambient), by photosynthetic carbon uptake, prior to the seawater entering experimental abalone tanks. *Ulva* is currently used as an aquacultural feed supplement and in some cases as a bioremediation tool to remove ammonia in recirculation systems on abalone farms. This multi-parameter study will determine the impacts of ambient and acidified seaweed-treated seawater on abalone growth (body- , meat- , and shell- mass), acid-base regulation, shell growth and morphology, shell strength and shell mineralogy using repeated measures of wet weight, condition factor (CF), muscle mass, haemolymph samples, shell weight, shell morphometrics, shell strength and shell mineralogy.

The experimental tanks were built outside, without shelter, alongside commercial abalone tanks to provide environmental realism and realistic feedback for commercial abalone aquaculture production.

CHAPTER 2

EXPERIMENTAL DESIGN AND GENERAL METHODS

2.1 History of experimental animals

South African abalone, *Haliotis midae* (weight: 40.59 ± 4.27 g ; shell length: 60.70 ± 2.88 mm; n=720), were provided by Aqunion© Whale Rock farm (Hermanus, Figure 2.1.). The sex of the animals was not able to be determined for all abalone as the gonads of the abalone were not fully mature in all individuals at the start of the experiment. All experimental abalone were spawned by the same group of commercially-spawning, wild-collected broodstock abalone in the Aqunion Whale Rock hatchery on 21 December 2012 as abalone from the same batch have been shown to have a heterogenous growth rate (Lee 2004). The abalone were reared on the land-based seawater farm in a flow-through seawater system. They were reared on a natural biofilm composed mostly of diatoms, followed by seaweed for approximately three months before being weaned onto a commercial diet, fed ad libitum for approximately three more months in the hatchery. The abalone were then transferred into commercial tanks (Table 2.2.1) where they were fed a commercial diet of compound feed ad libitum (Abfeed® S34 Prime leaf pellet; Marifeed (Pty) Ltd., Hermanus, South Africa) until being transferred into the experimental system. Abfeed® is a compound, formulated feed containing fishmeal, starch, spirulina, vitamins and minerals with 34 % protein content. The commercial tanks contained 6-8 baskets within each tank. Each basket contained a black PVC rack to increase surface area in the basket as well as a cover plate which floated above the rack to limit sunlight exposure and further increase the useable surface area within the tank. Stocking of abalone in the commercial tanks was controlled by size-grading procedures which occurred once every four months in order to maintain the tanks at a stocking density of 18% of the surface area within each basket. The commercial method for determining available surface area (m^2) within the basket (SA) is the sum of the surface area of the rack and underside of the feeder plate, not including the surface area of the basket. The surface area of each experimental basket was 1.18 m^2. Commercial calculations for determining the number of abalone per basket at an 18% stocking density are as follows:

$$Abalone\ Length\ (AL) = 18.435 \times (avg.weight^{0.3215})$$

$$Abalone\ Width\ (AW) = AL \times 0.64$$

$$Abalone\ per\ Basket = \left(\frac{SA \times 18}{100}\right) \div \left(\frac{AL}{1000} \times \frac{AW}{1000}\right)$$

Average weight (g) of abalone is determined during size-grading. Abalone length and width are calculated in millimetres.

Experimental abalone were size-graded on the 16th February 2015 (Chapter 3.3.3) and placed into the experimental seawater system. In this study, individual abalone were used as evaluation units.

Figure 2.1. Location of experimental site. White scale bars (bottom left corner of maps) show (A) South Africa at 200 km, (B) south-west Cape Peninsula 20 km, and (C) Hermanus at 1 km, and an aerial image of (D) the abalone farm, Aqunion Whale Rock.

2.2 Experimental Tank Design

The experimental system was installed on the farm along-side commercial abalone tanks in order to achieve comparable water conditions with abalone grown on the farm. The commercial and experimental tanks were aerated using horizontal, polyvinyl chloride (PVC) airlines at the base of the tank (Figure 2.2). The airlines contained pin holes in the pipes to release air and a valve to turn the airflow on/off. The commercial and experimental tanks were designed as seawater flow-through systems whereby seawater was supplied to the tank at an exchange rate of 2 exchanges per hour, which resulted in a flow index of 15 $L.kg^{-1}.h^{-1}$ (Naylor et al. 2011), and removed from the tank via a vertical drain pipe (Figure 2.2). Commercial tanks contained 6 oyster mesh baskets and the experimental system contained one oyster mesh basket per tank (Table 2.1). Each experimental basket contained four polyvinyl plates, which were linked together to create a rack to increase the surface area within the basket (Figure 2.2). The commercial and experimental baskets each contained a corrugated plate which covered the area above the rack to provide protection from light as well as a surface for feeding at night (Figure 2.2). The experimental tanks were made from a thinner plastic than the commercial tanks, and thus the outside of the experimental tanks were painted black to prevent light exposure inside the tank.

The experimental system consisted of thirty-six experimental abalone tanks (Figure 2.3 and Figure 2.5); the tanks were split into six groups of six tanks per experimental treatment. Five replicate tanks of each treatment group were stocked with animals, which left one basket open for use during cleaning. Cleaning of the abalone tanks occurred once a week and involved scraping of the sides of the tanks to reduce biological fouling. The animals were stocked at 18% of the available surface area with 90.3 ± 4.3 abalone basket^{-1} initially, in accordance with farm procedures. There was no significant difference in abalone wet weight between treatments at the start of the experiment (df=5, F=1.293, p=0.264). A stocking density of 18% was maintained for 12 months by following standard farm size-grading procedures every four months on the 16th February 2015, 16th June 2015, 14th October 2015 and 16th February 2016.

Table 2.1. Comparison of commercial abalone tanks with experimental abalone tanks.

	Commercial system	**Experimental system**
Tank length (cm)	390	60
Tank width (cm)	85	40
Tank depth (cm)	100	35
Tank volume (L)	3315	84
Number of baskets	6	1
Basket length (cm)	70	56
Basket width (cm)	51	38
Basket depth (cm)	60	33
Number of polyvinyl plates	6	4
Total surface area of basket/rack (m^2)	3.03	1.18

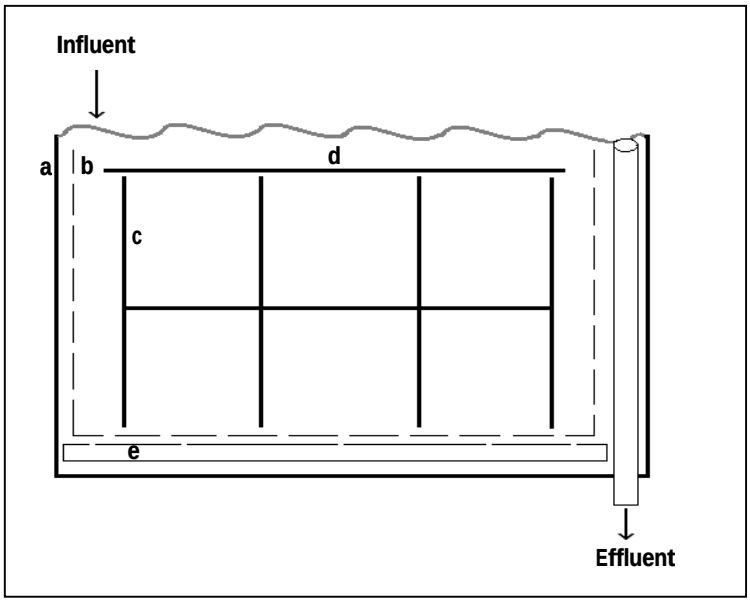

Figure 2.2. Experimental abalone (**a**) tank design. Influent seawater entered the tank at the water surface at one end and effluent left the tank via an outlet situated at the water surface at the opposite end. Each tank contained one (**b**) oyster-mesh basket. The baskets contained a (**c**) rack with vertical polyvinyl plates; a (**d**) horizontal plate covered the surface of the rack. Aeration was supplied beneath the baskets via (**e**) a perforated PVC pipe.

The experimental treatments were labelled and grouped as follows:

C – The control group for pH and temperature manipulation,

T – Temperature-manipulated seawater,

P – pH-manipulated seawater,

PT – pH- and temperature-manipulated seawater,

CM – Control group for pH mitigation using *Ulva for* photosynthetic carbon uptake in ambient seawater ,

PM– pH mitigation using *Ulva for* photosynthetic carbon uptake in pH-manipulated seawater

These treatments were achieved through a series of header tanks. Seawater, which was also supplied to commercial abalone tanks, was pumped into a 370 L header tank in order to obtain constant measurements of incoming seawater pH and temperature (Figure 2.3). Water was channelled from this first header tank into the control tanks (C, CM), towards the heated seawater treatment (T), and into a second 370 L header tank through a non-return valve (Figures 2.3, 2.4). The second header tank was used to alter the pH of the seawater (Section 2.3). Water was channelled out of the second header tank to the pH-manipulated treatments (P, PT, PM; Figures 2.3, 2.4). All header tanks and pipes were cleaned once a week with fresh water to prevent biological fouling.

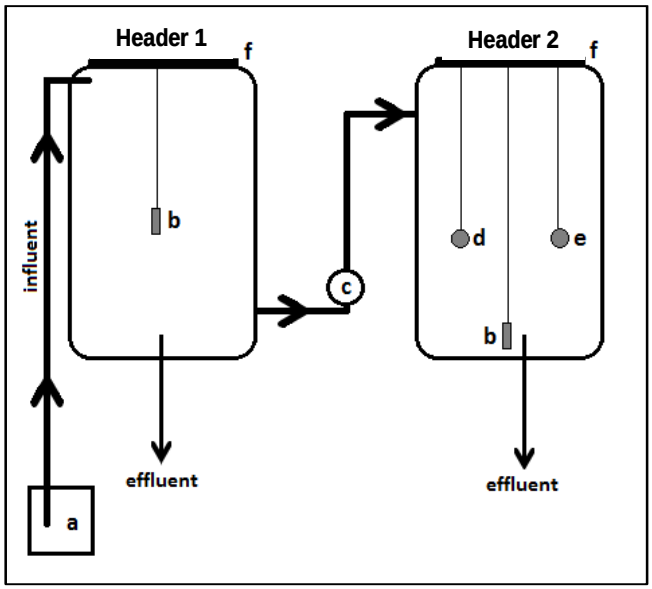

Figure 2.3. Schematic diagram of experimental header tanks. Seawater was pumped (**a**) into the first header tank (**Header 1**) which contained (**b**) pH and temperature probes. Seawater flowed from the first header tank into the second header tank via (**c**) a non-return valve. The second header tank contained (**b**) pH and temperature probes, (**d**) an air-stone which intermittently bubbled CO_2 and (**e**) an air-stone which continuously bubbled pumped air. Both header tanks had (**f**) sealed lids.

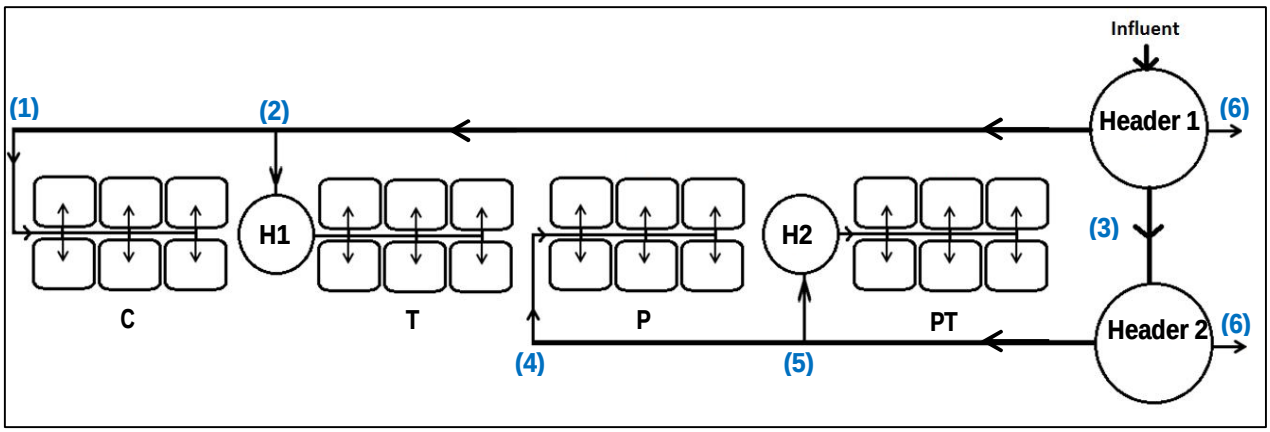

Figure 2.4. Schematic diagram of the temperature and pH manipulated portion of the experimental tank layout. Arrows show direction of water movement. Influent seawater was pumped into the first header tank (**Header 1**) where pH and temperature were measured. Seawater was distributed from the first header tank into **(1)** the control group of abalone tanks (**C**), and into **(2)** the heating chamber (**H1**) for the temperature manipulated treatment tanks (**T**). Seawater was also channelled from the first header tank via a non-return valve into **(3)** the second header tank (**Header 2**) where pH was manipulated. Seawater was distributed from the second header tank into **(4)** the pH manipulated treatment tanks (**P**) and into **(5)** the heating chamber (**H2**) for the pH and temperature manipulated treatment tanks (**PT**). Seawater was distributed from the first and second header tanks into **(6)** the biomitigation section of the experimental system (Figure 2.5).

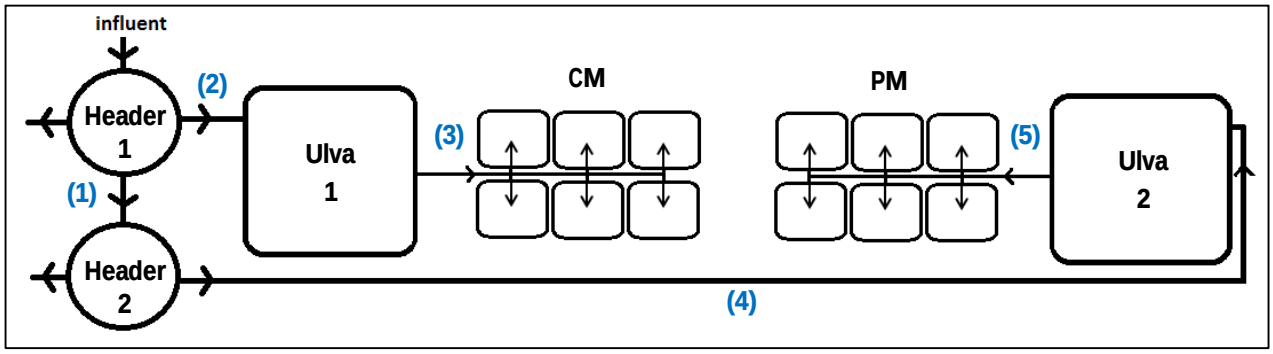

Figure 2.5. Schematic diagram of the bioremediation portion of the experimental tank layout. Arrows show direction of water movement. Seawater influent was pumped into the first header tank (**Header 1**) where pH and temperature were measured, then into **(1)** the second header tank (**Header 2**) where pH was manipulated. Seawater was distributed from the first header tank into **(2)** a 480L tank stocked with 4 kg of *Ulva* (**Ulva 1**). Seawater from the Ulva 1 tank was distributed to **(3)** the control mitigation treatment tanks (**CM**). Seawater from the second header tank was channelled into **(4)** a second 480L tank stocked with 4 kg of *Ulva* (**Ulva 2**). Seawater from the Ulva 2 tank was distributed to **(5)** the pH mitigation treatment tanks (**PM**).

2.3 Statistical analysis

Best practice for climate change research calls for true replication at the system (ie. Header tank) level (Cornwall & Hurd 2016). Due to limitations on physical space available for the experimental system on the farm and the costs associated with individual CO_2 and temperature monitoring systems for each required system, replication at the system level was unable to be achieved despite best intentions. Hurlbert (1984) defines this study's experimental system as "B4 –Clumped segregation and interdependent replicates within treatments" which is an inappropriate design. However, the variation from non-treatment effects was controlled for by treating these as random factors in the statistical analysis as recommended by Hurd & Cornwall (2016). Abalone that were measured during size-grading procedures were not placed back into the experimental system after being measured in order to eliminate re-sampling of the same animal.

To determine whether the linear variables changed as a function of time within individual treatment groups, the *lme* function from the *nlme* package (Pinheiro et. al. 2016) in R (The R Core Team, 2012) was used to create linear mixed effects models. Normality was determined by visual interpretation of histograms and the function *skewness* from the *e1071* package, although several authors argue that the violation of normality is not a serious problem as a consequence of the central limit theory (Sokal and Rohlf 1995, Zar 1999, Zuur et al. 2012) and some argue that it is not necessary at all provided that the sample size is large enough (Fitzmaurice et al 2004). The response variable was transformed in the case of non-normal data distribution. Residual spread and homogeneity of variances was tested by applying a Bartlett test to each model. Temporal autocorrelation was determined by means of autocorrelation function (ACF) plots and model comparison. Model selection was determined using AIC values for each response variable. The *emmeans* package (Lenth 2018), which uses the Tukey method, was used for all post-hoc comparisons between treatments. Significance was assigned to p-values < 0.05 for all analyses.

To determine whether non-linear data changed as a function of time within individual treatment groups, the *gam* function from the *mgcv* package (Wood 2003, Wood 2011, Wood et. al. 2016) in R (The R Core Team, 2012) was used to create a generalized additive mixed effects models. Normality was determined by visual interpretation of histograms and the function *skewness* from the *e1071* package. The response variable was transformed in the case of non-normal data distribution. Model selection was based on model fit (R^2-values) and the generalized cross-validation statistic (GCV) of GAM models. An AR1 structure was applied to each model. The general formula used for each response variable was:

$$y \sim Treatment + s(Time, by=Treatment, k=3) + s(Tank, Time, bs="re")$$

Residual spread and homogeneity of variances was determined by residual plots of the response and fitted values of the model. Model comparison using the *compareML* function from the *itsadug* package (van Rij et. al. 2020) was used to determine the effect of treatment over time. Post-hoc comparisons of treatments were performed using ordered factor contrasts of the smooth term for treatment over time, which allowed the control treatment to be contrasted against the other treatments. Ordered factor contrasts were not able to be used as a pairwise comparison between all treatments because a change in the order of the contrasts resulted in a comparison of different models with different smoothers and provided conflicting results. Significance was assigned to p-values < 0.05 for all analyses.

2.4 Electrical Relay System

2.4.1 pH manipulation

Seawater pH was measured continuously using two pH probes (Milwaukee MA913B/3 combined epoxy pH electrode) which were placed in the first and second header tanks. Seawater pH was continuously monitored using a data logger (CR1000, Campbell Scientific) which averaged and recorded the incoming millivolt readings from the probes every 60 seconds and translated the readings to pH. A 5 volt control relay system was connected to the data logger which closed/opened a solenoid valve connected to the CO_2 gas cylinder when the pH of the second header tank was below/above 0.4 respectively. The data logger and relay system were housed within an outdoor electrical box and two 50 g silicone dehydrant bags were placed within the box to prevent moisture build up and rusting. Air was bubbled into the second header tank to increase seawater pH when bubbled CO_2 was halted. The pH probes were cleaned daily using a soft sponge and calibrated twice a week using NBS buffer solutions of pH 7.00 and 10.01. Calibration of the probes was achieved by visual inspection of the millivolt readings on LoggerNet (version 4.2.0.22, Campbell Scientific, Inc. 2013) to ensure that the probes delivered a millivolt reading of 0 ± 30 mV when placed in pH 7.00 buffer and -178 ± 30 mV when placed in pH 10.01 buffer. The slope of the millivolt readings achieved when the probes were placed in each buffer solution was also compared to the Nernstian response (N_R) using the following formulas:

$$N_R = RT/nF$$

Where *R* is the universal gas constant, *T* is the temperature (Kelvin), *n* is the ionic charge (+1 for hydrogen ions), and *F* is the Faraday constant.

$$Slope = (mV_{pH7.00} - mV_{pH10.01}) / ((10.01\text{-}7.00) \times N_R)$$

The programming code for the data logger was adjusted using CRBasic Editor (version 3.4.0.31, Campbell Scientific, Inc. 2013) to ensure a Nernstian slope or nearly so (>99 %) when the slope was >95 %. If the slope was between 92-95 %, the probes were rinsed with distilled water, cleaned with dish detergent and recalibrated. If the slope was calculated <92 %, the probes were replaced and recalibrated. The pH probes were routinely replaced every 3 months, but two probes needed to be replaced within that time frame after a wind-storm blew the lids of the header tanks and the probes out of the tanks. Recorded data during calibration or replacement of the probes was removed from the data set in order to avoid skewing the results. This system resulted in an adjustment of the seawater pH in the second header tank to 0.44±0.03 (mean ± standard deviation) below the ambient seawater pH in the first header tank over the course of the study (t-test: $p<0.01$; Figure 2.6). Seawater pH in the control abalone tanks was significantly different from the seawater pH treatment abalone tanks (t-test: $p<0.01$) and the pH x temperature (PT) treatment abalone tanks (t-test: $p<0.01$; Figure 2.7).

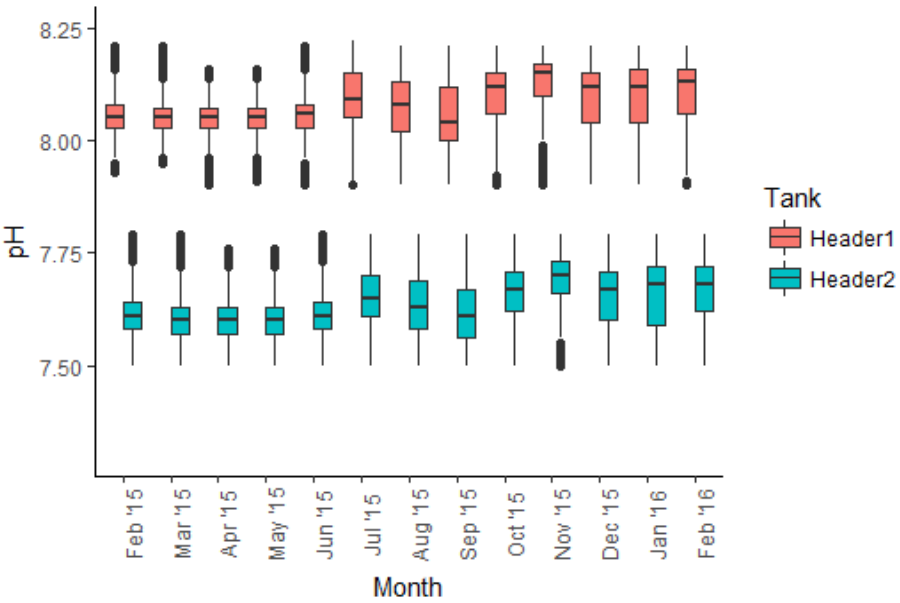

Figure 2.6. Boxplots of ambient seawater pH within Header 1 (red) and manipulated seawater pH within Header 2 (blue) for each month over the course of the study. Seawater pH was measured continuously and recorded every 60 seconds over the course of the study.

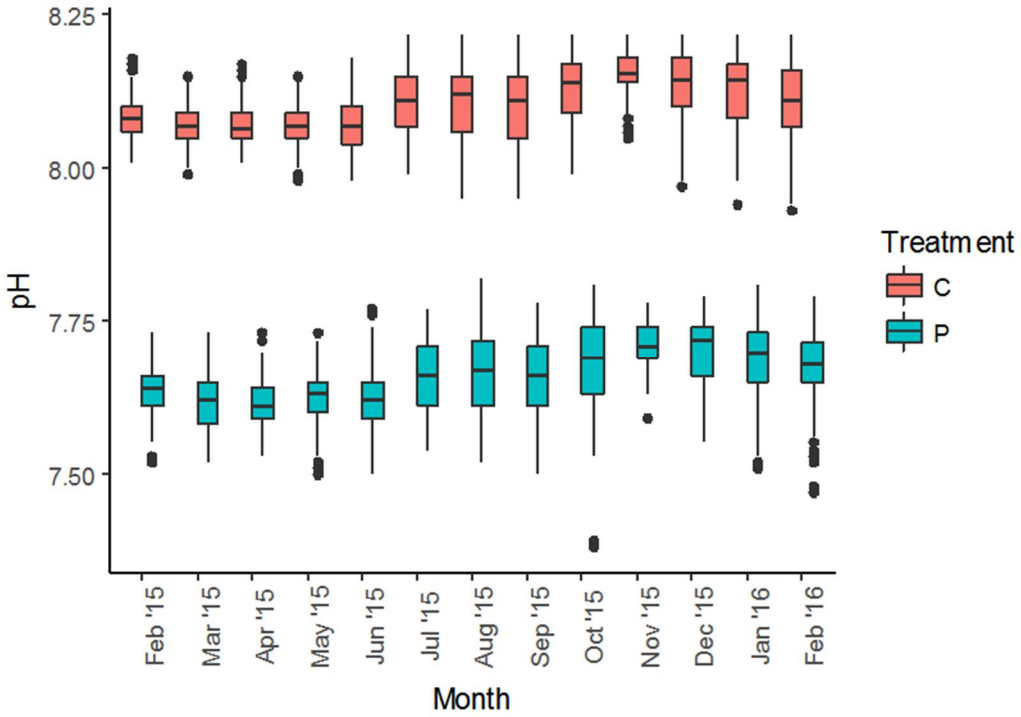

Figure 2.7. Ambient seawater pH within the control (C) treatment abalone tanks (red) and manipulated seawater pH within the pH (P) treatment abalone tanks (blue) for each month over the course of the study. Seawater pH was measured twice daily within each of the five abalone tanks per treatment. The pH outliers in October were the result of a water-off event due to cleaning of the farms tanks, which damaged the pH probes.

2.4.2 Temperature manipulation

Seawater temperature was measured continuously using four stainless steel 2-wire termination probes (Milwaukee MA913B/3 combined epoxy pH electrode) which were placed in the first and second header tanks as well as in the two heating chambers. The probes were cleaned daily using a soft sponge and calibrated once a week using a multimeter (YSI ProPlus; Yellow Springs, OH, USA). Each heating chamber consisted of an airtight, insulated 101L PVC cylinder with valves on either end to retain water within the chambers before the seawater was released into the temperature manipulated treatments' (T, PT) abalone tanks. Each cylinder contained four 300W aquarium heaters (model number VAH300, ViaAqua) which were triggered by the data logger and 5 volt control relay system to turn on/off when the seawater inside the cylinder was below/above 1.5°C respectively. This system resulted in a significant temperature increase of 1.51±0.02 °C in the first heating chamber (H1) and 1.50±0.01°C in the second heating chamber (H2) compared to the first header tank (paired t-test: $p<0.01$; Figure 2.8) and second header tank (paired t-test: $p<0.01$; Figure 2.9) respectively over the course of the study . The adjustment in temperature in the heating chambers resulted in a significant increase in seawater temperatures of 1.51±0.02 °C between the control (C) treatment abalone tanks and the temperature (T) treatment (paired t-test: $p<0.01$; Figure 2.10) and an increase of 1.50±0.02 °C between the pH (P) treatment abalone tanks and the pH x temperature (PT) treatment abalone tanks (paired t-test: $p<0.01$; Figure 2.11).

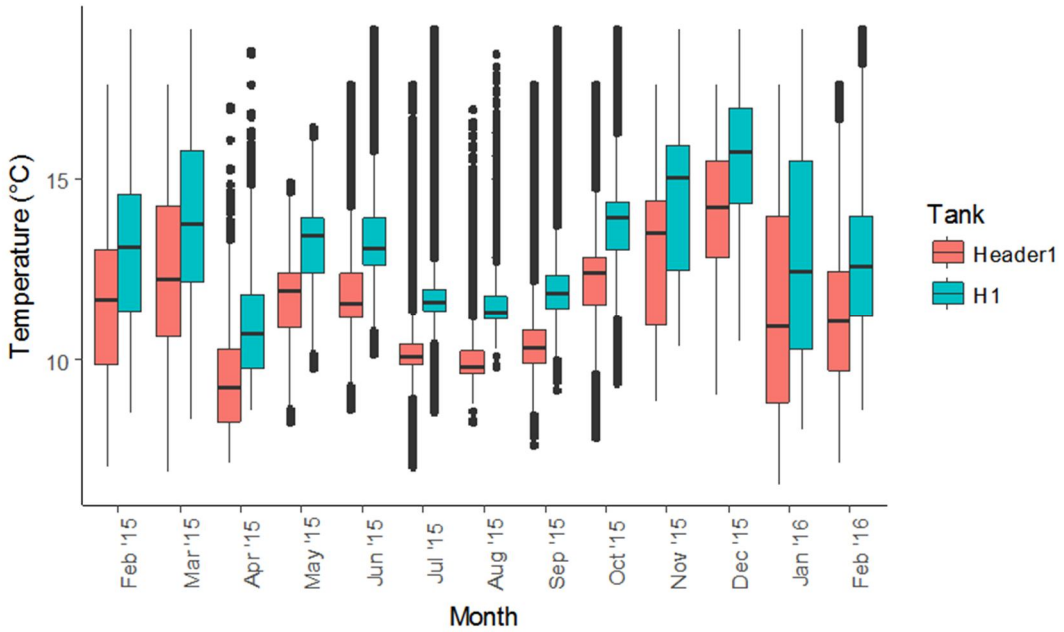

Figure 2.8. Ambient seawater temperature within Header 1 (red) and manipulated seawater temperature within the first heating chamber (H1, blue) for each month over the course of the study. Seawater temperature was measured continuously and recorded every 60 seconds over the course of the study.

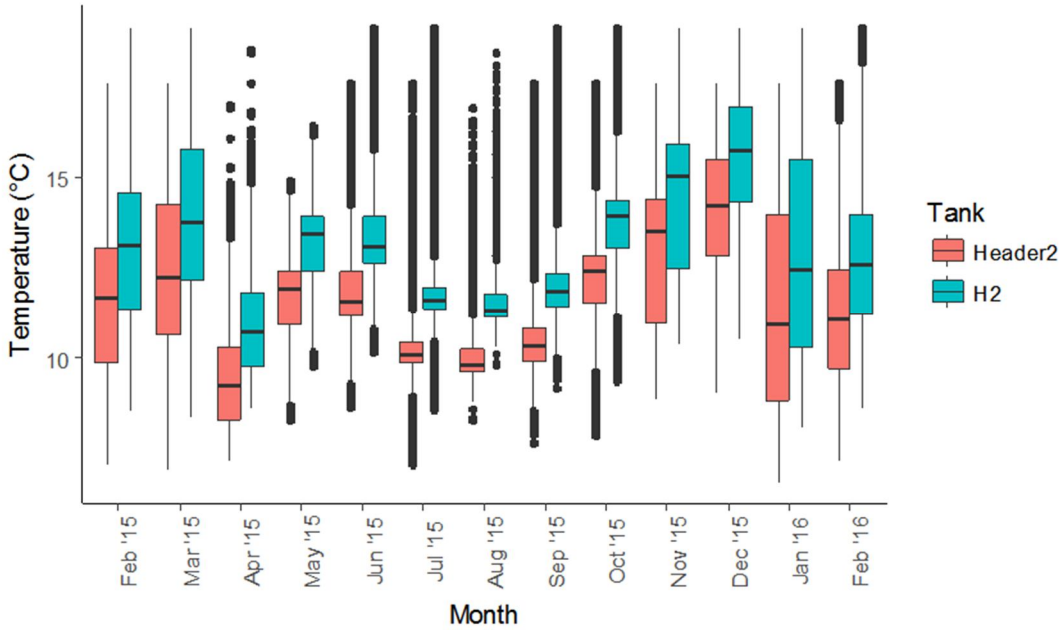

Figure 2.9. Ambient seawater temperature within Header 2 (red) and manipulated seawater temperature within the second heating chamber (H2, blue) for each month over the course of the study. Seawater temperature was measured continuously and recorded every 60 seconds over the course of the study.

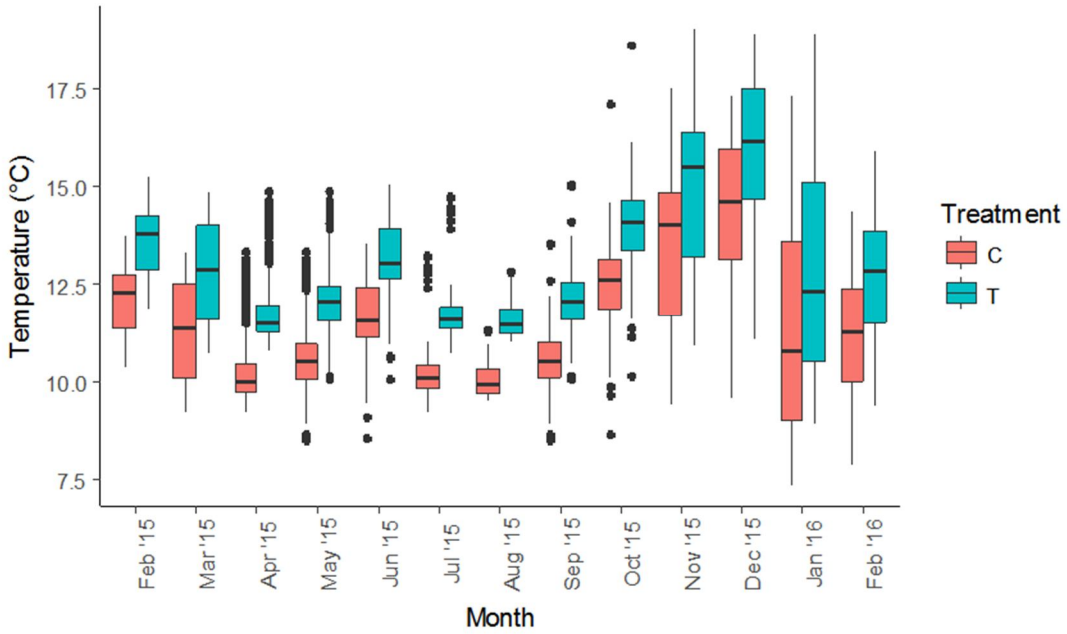

Figure 2.10. Ambient seawater temperature within abalone tanks from the control (C) treatment (red) and manipulated seawater temperature within abalone tanks from the temperature (T) treatment (blue) for each month over the course of the study. Seawater temperature was measured twice daily within each of the five abalone tanks per treatment.

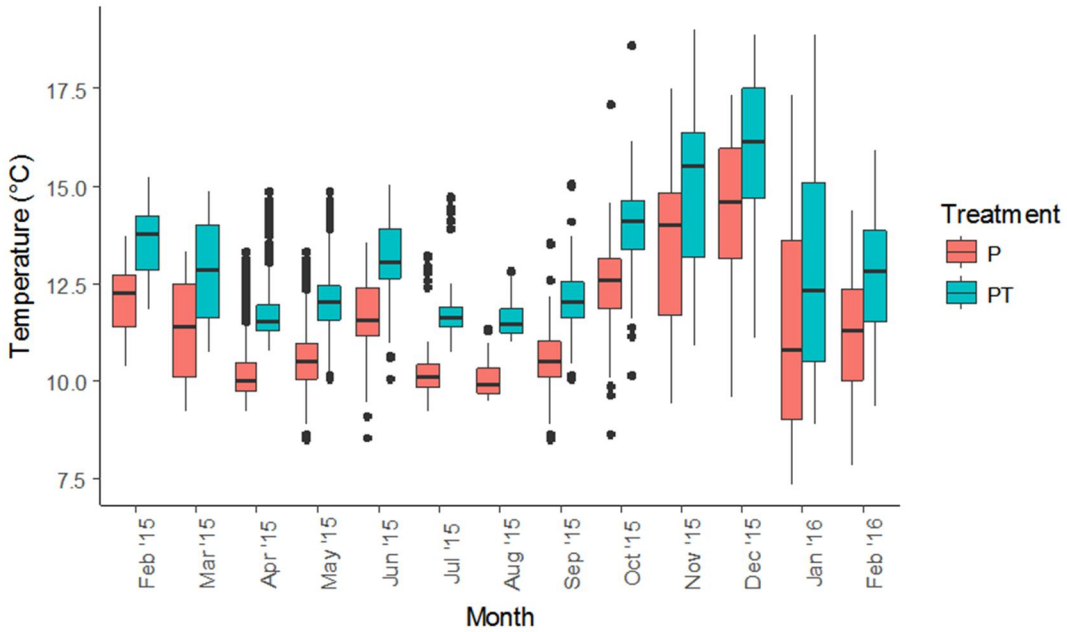

Figure 2.11. Ambient seawater temperature within abalone tanks from the pH (P) treatment (red) and manipulated seawater temperature within abalone tanks from the pH x temperature (PT) treatment (blue) for each month over the course of the study. Seawater temperature was measured twice daily within each of the five abalone tanks per treatment.

2.5 Water quality

Temperature, pH, dissolved oxygen (DO) concentration, total alkalinity (TA) and the concentration of total ammonia nitrogen (TAN) were monitored daily at the outflow of each animal holding tank between 09:00 and 10:00 every morning and in the evenings between 15:00 and16:00 (Table 2.2). Samples were taken in the morning between 09:00 and 10:00 in order to achieve the most reliable estimate of daily means (Yearsley 2008) and in the evening to increase water quality monitoring.

Temperature, pH and DO measurements were obtained using a multimeter (YSI ProPlus; Yellow Springs, OH, USA). DO measurements were taken to monitor for hypoxic and hyperoxic conditions which can cause DNA damage. DO measurements remained within the range that is considered healthy for South African abalone (>83 %, <115 %; Vosloo et. al. 2013).

TAN was measured using a portable photometer (Mi407, Milwaukee low range photometer) to prevent the risk of ammonia toxicity in the tanks (Reddy-Lopata et. al. 2006). TAN values never exceeded 0.1 $mg.L^{-1}$; an acceptable level for a healthy flow-through system (Reddy-Lopata et. al. 2006).

TA measurement of the seawater followed the methods described by Sarazin et al. (1999). 50 mL of the tank water from each animal holding tank was collected in sealable plastic tubes. 25 µL of saturated mercuric chloride ($HgCl_2$) was added to each tube as a bactericide immediately after sampling. TA samples were stored in these tubes for a maximum of 23 days. 50mM bicarbonate (HCO_3^-) stock solution was prepared and diluted into standard solutions (6.25, 4.5, 3.13, 1.56, 0.78 mM) using artificial seawater, prepared as described by Sarazin et. al. (1999). 500µL of each stock solution and each TA sample was pipetted into Eppendorf tubes (max. vol. 2 mL). To each tube, 500 µL of dye reagent, containing known concentrations of methanoic acid, bromophenol-blue and ionic strength buffer (NaCl 0.7M), was added. The tubes were shaken vigorously after the dye reagent was added in order to release CO_2 (gas) from solution. The standards and experimental samples were analysed at 590 nm in a spectrophotometer (U-1900, Hitachi).

Salinity was assessed using a salinity refractometer (Red Sea, Reef-Spec). Salinity averaged 35.5 ± 0.3 for all tanks over the course of the experiment. Aragonite (Ω_{ar}) and calcite (Ω_{ca}) saturation values for each temperature–pH combination (Table 2.4.1) were determined from TA, pH and salinity data using CO2SYS (version 2.1, 2012). Water flow into each of the holding tanks was monitored/corrected daily at 08:00 and 16:30.

Table 2.2. Water quality and experimental conditions of abalone, *H. midae*, tanks in a flow-through seawater system. Seawater samples were collected from each tank twice daily for the 12-month experimental duration. Values are represented as the mean ± standard deviation for each of the six experimental treatment groups of tanks.

	Treatment	pH	Temperature (°C)	Dissolved oxygen (mg/L)	Salinity	TAN (mg/L)	TA (µM/L)	*Ωar*	*Ωca*
Feb 2015-Feb 2016	Ambient (A)	8.10±0.06	15.64±2.16	8.14±0.04	35.5±0.3	0.070±0.029	2341.5±17.9	2.87±0.42	4.46±0.64
	Temp (AT)	8.11±0.06	17.16±2.16	8.12±0.04	35.5±0.3	0.071±0.029	2338.5±18.4	3.05±0.48	4.72±0.72
	pH (P)	7.66±0.07	15.66±2.17	8.14±0.04	35.5±0.3	0.070±0.029	2341.5±18.3	1.19±0.23	1.85±0.35
	pHxtemp (PT)	7.66±0.08	17.19±2.17	8.12±0.04	35.5±0.3	0.067±0.027	2339.1±18.5	1.28±0.24	1.98±0.37
	*Ulva*xAmbient (CM)	8.41±0.09	16.60±2.18	8.15±0.03	35.5±0.3	0.053±0.028	2340.4±17.8	4.88±0.68	7.58±1.06
	*Ulva*xpH (PM)	7.95±0.07	16.62±2.18	8.15±0.04	35.5±0.3	0.044±0.024	2340.9±18.1	2.17±0.33	3.37±0.51
Feb 2015-Jun 2015	Ambient (A)	8.06±0.03	15.40±2.05	8.13±0.03	35.5±0.3	0.073±0.029	2341.9±17.5	2.65±0.24	4.13±0.36
	Temp (AT)	8.07±0.03	16.94±2.04	8.12±0.03	35.5±0.3	0.072±0.029	2339.2±18.8	2.81±0.25	4.35±0.37
	pH (P)	7.61±0.04	15.42±2.05	8.14±0.01	35.5±0.3	0.070±0.029	2341.5±18.3	1.07±0.12	1.66±0.19
	pHxtemp (PT)	7.62±0.04	16.98±2.05	8.11±0.02	35.5±0.3	0.073±0.029	2340.1±18.1	1.15±0.13	1.77±0.20
	*Ulva*xAmbient (CM)	8.41±0.03	16.98±2.05	8.14±0.01	35.5±0.3	0.059±0.029	2341.4±17.7	4.86±0.36	7.55±0.53
	*Ulva*xpH (PM)	7.96±0.04	16.97±2.05	8.14±0.02	35.5±0.3	0.034±0.015	2341.2±17.9	2.20±0.24	3.41±0.36
Jun 2015-Oct 2015	Ambient (A)	8.10±0.06	14.71±1.11	8.19±0.02	35.5±0.3	0.070±0.030	2342.5±17.8	2.76±0.30	4.30±0.47
	Temp (AT)	8.11±0.06	16.23±1.11	8.17±0.01	35.5±0.3	0.071±0.029	2339.3±18.2	2.98±0.33	4.62±0.51
	pH (P)	7.66±0.06	14.71±1.10	8.18±0.02	35.5±0.3	0.071±0.029	2342.7±17.8	1.17±0.16	1.81±0.25
	pHxtemp (PT)	7.67±0.06	16.23±1.10	8.17±0.03	35.5±0.3	0.072±0.029	2340.3±18.3	1.25±0.17	1.94±0.27
	*Ulva*xAmbient (CM)	8.5±0.06	15.57±1.11	8.19±0.01	35.5±0.3	0.040±0.020	2341.8±17.9	5.42±0.47	8.43±0.73
	*Ulva*xpH (PM)	7.99±0.06	15.57±1.10	8.20±0.01	35.5±0.3	0.056±0.029	2341.8±17.7	2.29±0.29	3.56±0.46
Oct 2015-Feb 2016	Ambient (A)	8.13±0.06	16.77±2.52	8.11±0.03	35.5±0.3	0.068±0.029	2340.0±18.4	3.19±0.47	4.94±0.71
	Temp (AT)	8.14±0.06	18.29±2.51	8.08±0.02	35.5±0.3	0.071±0.029	2337.1±18.3	3.38±0.50	5.22±0.74
	pH (P)	7.70±0.06	16.81±2.52	8.11±0.02	35.5±0.3	0.069±0.029	2338.6±18.0	1.36±0.24	2.10±0.36
	pHxtemp (PT)	7.70±0.06	18.33±2.52	8.08±0.01	35.5±0.3	0.057±0.019	2337.0±18.8	1.45±0.26	2.24±0.38
	*Ulva*xAmbient (CM)	8.33±0.06	17.34±2.51	8.11±0.01	35.5±0.3	0.059±0.030	2338.0±17.6	4.42±0.59	6.85±0.88
	*Ulva*xpH (PM)	7.90±0.06	17.39±2.52	8.11±0.01	35.5±0.3	0.043±0.020	2339.8±18.4	2.05±0.34	3.81±0.51

CHAPTER 3:
Growth of the South African Abalone, *Haliotis midae*, Under the Influence of Seawater Acidification and Warming, and Their Interaction

3.1 Introduction

CO_2 induced global warming and ocean acidification is predicted to cause ocean temperatures to warm by 1.5±0.4 °C and ocean pH to decline by 0.43 units as a global average by the end of the 21st century according to the RCP8.5 models generated for the 5th assessment report of the IPCC (Collins et. al. 2013, Hoegh-Guldberg et. al. 2014, Gattuso et. al. 2015). These stressors will exert varying effects on marine organisms, with most negative effects experienced by marine calcifiers (Hoegh-Guldberg et. al. 2014).

The South African abalone, H*aliotis midae*, is of particular importance to the South African economy because it is a main aquaculture product and holds a high export value (See Chapter 1). *H. midae* may be at risk of the negative impacts of ocean acidification due to its mostly aragonitic shell (Lester 2012), but the effects of predicted increased ocean temperatures are mostly unknown, particularly in combination with ocean acidification.

The possible effects of predicted temperature increase on *H. midae* can be inferred from various studies aimed at determining temperature preference and thermal tolerance of *H. midae*. Tarr (1995) noted that *H. midae* grew faster in the warm-temperate waters on the south-east coast of South Africa than on the cool-temperate west coast. In a study by Britz et. al. (1997), *H. midae* growth and food consumption was significantly greater with increased treatment temperatures from 12 °C to 20 °C and declined at temperatures between 20 °C and 24 °C after 3 months. Britz et. al. (1997) concluded that temperatures between 12 °C to 20 °C were physiologically optimal for *H. midae,* although the largest weight gain was experienced at a constant temperature of 20 °C. Lyon (1996) noticed a physiological maximum in *H. midae* exposed to at 23°C seawater by noting that oxygen consumption and ammonia excretion of *H. midae* increased proportionally with an increase in temperature from 16 °C to 23 °C after 24 hours of exposure to three temperature treatments of 16, 20, and 23 °C. Physiological maxima of abalone have been reported to peak at higher temperatures than the growth maxima (Díaz et. al. 2000), therefore placing Lyon's results within the scope of the results seen by Britz et. al. (1997) when *H. midae* is exposed to warmer, constant temperatures.

Exposure time and temperature stability play a key role in abalone response to increased temperatures. In a short-term (24 hour) experiment on the effects of stable temperature (16 °C, 19 °C and 22 °C) on *H. midae* physiology, it was noted that the specific rates of oxygen consumption increased with an increase in temperature and *H. midae* showed a higher reliance on proteins to fuel metabolism with an increase in temperature (Vosloo & Vosloo 2010). However, after 1 month of exposure to constant temperatures there was a decrease in specific rates of oxygen consumption, a higher reliance on carbohydrates as a food source, and an increase in total muscle proteins with increasing temperatures (Vosloo & Vosloo 2010). Vosloo and Vosloo (2010) suggested that *H. midae* has the ability to acclimatise to higher temperatures within its natural temperature range of 12 °C to

20 °C provided that temperatures are stable and no short-term spikes in temperature occur. However, when given the choice of environmental temperature in experimental conditions, *H. midae* show a behavioural preference for 24.1 – 24.5 °C seawater (Hecht 1994), much warmer than the temperate waters that the majority of *H. midae* inhabit (Chapter 1, Section 1.1.3).

Abalone response to warming is species dependant. Two southern Californian abalone species, *Haliotis rufescens* and *Haliotis fulgens*, were exposed to seawater that was warmed to 2.5 °C above variable ambient temperatures (14-18 °C) in La Jolla, California for 49 weeks (Vilchis et. al. 2013). Although the methods used to warm the seawater in this experiment were not explained, it was noted that warming increased the onset of withering syndrome in red abalone, *H. rufescens*, halting growth and reproduction; whereas the green abalone, *H. fulgens*, showed no change in growth or reproduction. This difference in response to warming could be due to a difference in optimum growth temperatures between species. *H. fulgens* exhibits optimum growth in a temperature range of 24-28 °C (Leighton et. al. 1981) and *H. rufescens* exhibits optimum growth between 14-17.8 °C (Steinarsson & Imsland 2003). Boch et. al. (2018) noted that oxidative stress rather than temperature increases had a greater negative effect on growth of *H. fulgens* juveniles when abalone were exposed to the oceanographic conditions of field experiments in two different localities, Morro Prieto and Punta Prieta. In lab experiments it was noted that *H. fulgens* juveniles incurred the physiological stress of decreased haemocyte viability during 5 °C warming (22.9 – 27.5 °C) over short time periods, but were able to rapidly acclimate to warming through inactivity.

García-Esquivel et. al. (2007) investigated the effect of two seawater temperatures (20 and 25 °C) on *H. fulgens* and reported that there was a difference in the ratio of dry flesh weight to shell weight, with the higher ratio occurring at 20 °C. The black abalone, *Haliotis cacherodii*, displayed a similar increase in susceptibility to withering syndrome with an increase in temperature linked to intertidal variability (Ben-Horin et. al. 2013). Cheng et. al. (2004) also noted a decrease in immune response to injected Tryptic-soy-broth-grown *Vibrio parahaemolyticus,* as measured by total haemocyte count, phenoloxidase activity, respiratory burst, and phagocytic activity to *V. parahaemolyticus* after 24, 72 and 120 hours, in the Taiwan abalone, *Haliotis diversicolor supertexta*, with an increase in temperature above 24°C.

There are no published studies of the effects of ocean acidification on *H. midae*; however a study that used a recirculated seawater system noted that growth in terms of whole wet weight was negatively correlated with H^+ concentration (Yearsley 2007; pH: 8.3 - 5.9). When combined with growth-limiting levels of free ammonia nitrogen (2.38 ± 1.21 $\mu g.L^{-1}$), reduced pH was a limiting variable on *H. midae* growth (Naylor et. al. 2011; pH: 7.79 – 7.6).

Studies on the effects of ocean acidification on abalone growth and development in other species have been mostly focused on larval and juvenile abalone growth in terms of shell development. Shell development will be discussed in Chapter 4. A study by Avignon et. al. (2020) used a multifactorial approach to investigate the effects of constant, lowered pH (-0.3; ambient: 8.0) on adult European abalone, *Haliotis tuberculata*, for 2 months and noted no significant differences in haemolymph pH or muscle mass between treatments. Li et. al. (2018) exposed juvenile *Haliotis discus hannai* to three constant pH treatments of 8.1, 7.9, and 7.7 for three months and noticed a reduction in growth rates in term of body weight. It was also noted that the allocation of energy storage was

altered by chronic acidification as observed by a reduction in glycogen and lipid content in the muscle tissues. In a study on the juvenile (7-13mm) red abalone, *H. rufescens*, exposed to seawater with raised pCO_2 (1120 µatm vs. ambient 485 µatm) for 4 weeks, White (2011) recorded reduced body weights and reduced tissue weights in constant, low pH seawater in comparison to abalone in ambient seawater conditions. Most studies on acidification of abalone larvae noted a decrease in shell growth (Byrne et. al. 2011, Crim et. al. 2011, Kimura et. al. 2011, Kim et. al. 2013, Li et. al. 2013). In general, skeletal growth of calcifying invertebrates decreases with a decrease in seawater pH (Hoegh-Guldberg et. al. 2014).

The interactive effects of warming and acidification are only documented for a few species of invertebrates and the majority of these are focused on corals and early life history stages (Byrne & Przeslawski 2013, Harvey et. al 2013, Hoegh-Guldberg et. al. 2014, Przeslawski et. al. 2015). The development of invertebrates under multi-stressor conditions is poorly understood and varies greatly between species. To compound matters further, there is no evidence of whether warming and acidification will act synergistically to cause extreme negative effects in adult abalone or whether they will act antagonistically, mitigating the overall negative effects (Reynaud et. al. 2003, Byrne et. al. 2011b). Extensive meta-analyses on interactive effects of CO_2 and temperature have focused on molluscs, crustaceans, echinoderms, and corals, but have provided contradicting results. Earlier meta-analyses concluded that synergistic effects of co-stressors are less frequent than antagonistic effects (Byrne & Przeslawski 2013, Harvey et. al 2013), and a later meta-analysis concluded the opposite for early life stages (Przeslawski et. al. 2015). Ocean acidification is expected to be a greater stressor for calcifying organisms by impairing calcification and supressing metabolism, whereas warming is expected to enhance developmental processes within optimal temperature ranges (Byrne 2011, Byrne & Przeslawski 2013, Przeslawski et. al. 2015).

In a similarly designed study to the current experiment, which incorporated the natural variability of ambient seawater, the community effects of warming and ocean acidification on several intertidal species, including *H. rufescens,* were assessed (Lord et. al. 2017). After 10 weeks (~2 months) of exposure to lowered seawater pH (-0.3) and warming (+2 °C) it was noted that elevated CO_2 was the only factor that had a significant effect on abalone shell weight (40 % reduction), resulting in a reduced shell:tissue ratio, although tissue growth was non-significantly reduced. The increase in temperature only had a significant effect on abalone feeding rates. It was concluded that *H. rufescens* was more robust to changes in temperature rather than pH and that the increase in temperature was not a stressor as no stress response was exhibited by the abalone (Lord et. al. 2017). *Haliotis coccoradiata* larvae hatched in multi-stressor conditions of constant warming (ambient: 20 °C; warmed: 22 °C, 24 °C) and acidification (ambient pH: 8.18; reduced pH: 7.8, 7.6) experienced complete developmental failure of reduced calcification and abnormal phenotypes (Byrne et. al. 2011b). At present there are no long-term (> 10 weeks) studies on multi-stressor effects on invertebrates (or *H. midae*) that incorporate natural variability of pH and temperature.

3.1.1 Aims and objectives

This study aims to assess the impacts of variably warmed (+1.5 °C) and reduced pH (-0.4 units) seawater in comparison to ambient, variable seawater, in isolation and combination, on *H. midae*

growth (wet weight, muscle mass, and proportion of muscle to body mass), spawning patterns (condition factor (CF), and Gonadal Bulk Index (GBI)), and maintenance of acid-base regulation.

The objectives of this study were to expose abalone to warmed- (+1.5 °C) and reduced pH (-0.4 units) seawater, compared to ambient, for 12 months using a data-logger-relay system to offset the ambient pH and temperature and incorporate the natural variability of incoming seawater in the abalone aquaculture facility, where this experiment was based. The experimental tanks were built outside, without shelter, alongside production tanks to provide environmental realism and realistic feedback for commercial abalone aquaculture production. Abalone tanks were smaller than those used in commercial aquaculture production, but were stocked in accordance with the facility's commercial stocking density per tank. Food and feeding regimes were maintained in accordance with the facility's regimes. Repeated measurements of wet weight, CF, muscle mass, and haemolymph samples were collected every 4 months when the abalone were size-graded and tanks were re-stocked, in keeping with commercial aquacultural timeframes for size-grading. GBI was analysed once, after 12 months of exposure to experimental conditions when all abalone were able to be harvested.

This study hypothesises that growth, in terms of wet weight and muscle mass, will be different between treatment groups and that these differences will be amplified the longer the experiment continues. I hypothesise that abalone exposed to warmed seawater within optimal growth temperatures will display increased growth and that abalone exposed to reduced pH seawater and multi-stressor conditions will display reduced growth.

Muscle mass is hypothesised to be higher in *H. midae* exposed to warmer seawater because abalone exposed to warmed seawater for an extended time have been shown to have an increase in total muscle proteins, although no studies have shown the effects on muscle mass after 1 year of exposure and no studies have specifically researched the difference between the whole muscle mass of abalone in environments with differing seawater temperatures. Abalone exposed to reduced pH seawater and multi-stressor conditions are hypothesised to have lower muscle mass due to a diversion in energy usage from somatic growth towards repair and maintenance.

The proportion of muscle to body mass (PMB) is hypothesised to be higher in abalone exposed to warmed seawater provided that muscle mass increases substantially over time. PMB is hypothesised to be lower in abalone exposed to reduced pH seawater and multi-stressor conditions due to a decrease in meat mass. PMB is expected to be different between groups and these differences are expected to be amplified over the duration of the experiment.

Condition factor (CF) is a method of quantitatively measuring the condition of individuals by taking into account the length and weight of the abalone and is commonly used in South African abalone aquaculture studies and commercial operations. An abalone with a CF of over 1 is considered to be in good condition and a higher value represents more weight per unit of length. CF can be influenced by the age of the abalone, season, feed type (Britz 1996a, Britz 1996b, Britz & Hecht 1997, Dlaza et. al. 2008), fullness of gut, parasite load (Simon et. al. 2006), stage of maturation and degree of muscular development. Britz et. al. (1997) observed a decrease in abalone condition factor with increasing temperature from 12 °C to 24 °C with the poorest condition observed for abalone in

temperatures between 22 °C and 24 °C. Condition factor is expected to vary on a seasonal basis. Abalone age and food supply were controlled in this experiment so it is expected that abalone CF would be most influenced by changes in muscular development and gonadal maturation. This experiment will use CF as an estimation of spawning events during the course of the experiment; declines in CF can be linked to spawning events (Wood & Buxton 1996). I hypothesise that these declines in CF related to spawning events will occur sooner for abalone in warmed seawater treatments due to the effect of temperature on spawning, and that these spawning events will occur in a similar pattern to those seen in natural populations by Wood & Buxton (1996; Figure 3.1).

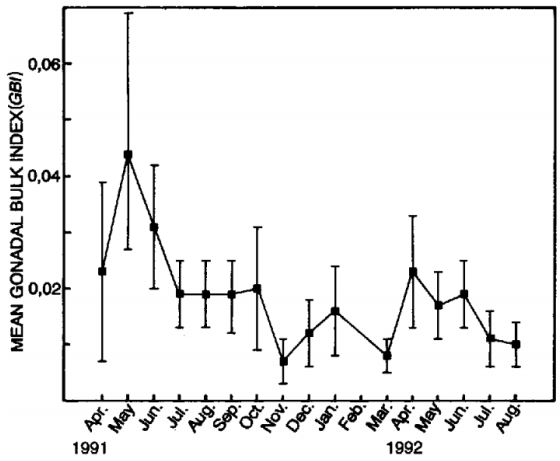

Figure 3.1. Spawning events of abalone in Port Alfred, South Africa, from April 1991 to August 1992 from Wood & Buxton (1996). Declines in mean Gonadal Bulk Index relate to spawning events.

Abalone gonadal bulk index (GBI) allows for the detection of reduction in gonad size due to spawning events. *H. midae* along the coast of South Africa usually have a peak GBI in April and May followed by a gradual decline throughout the year with the lowest GBI occurring in November and March (Wood & Buxton 1996). Because abalone are broadcast spawners, spawning cycles are synchronised in a population to maximise fertilization success (Hahn 1988). Gonad maturation and spawning in *H. midae* is initiated earlier in warmer regions of South Africa (Port Alfred, Southeast coast) than in cooler regions on the West coast of South Africa (Wood & Buxton 1996). Newman (1967) described *H. midae* reproduction biology of abalone on the west coast of South Africa (Dassen Island, Sea Point, Stony Point) and noted that temperature was an important stimulus, but cautioned that other factors might be involved. Newman (1967) also ascertained an approximate spawning period for abalone on the west coast of South Africa to be between October and December based on gamete maturation. Abalone aquaculture facilities use warmed seawater (approximately 18°C) for their broodstock abalone as a means to improve sperm and egg production. Studies on the spawning of other abalone species have shown reproduction to be largely influenced by water temperature (Litaay & De Silva 2003, Awaji & Hamano 2004, Grubert & Ritar 2004). It is expected that the GBI of abalone from the temperature treatment will be lower than for those in ambient conditions due to earlier spawning times accelerated by temperature. There have been no studies looking at the effect of reduced pH seawater on the ability of *H. midae* to spawn or mature reproductive organs, however gonad weight was observed to be significantly reduced in *H. tuberculata* individuals exposed to pH 7.7 seawater compared to those exposed to pH 8.0 seawater

after 4 months (Avignon et. al. 2020). I hypothesise that *H. midae* exposed to reduced pH seawater and multi-stressor conditions will also exhibit reduced gonadal weight reflected in a reduced GBI due to a shift in energy use from reproduction to repair and maintenance of the shell and acid-base regulation.

Haemolymph analysis of pH, partial pressure of CO_2 (pCO_2) and bicarbonate concentration will be used to assess the sensitivity of *H. midae* acid-base regulation over 12 months. For adequate calcification to occur, acid-base regulation and ion exchange need to be maintained (Pörtner 2008). Maintenance of extracellular pH seems to be the first line of defence against hypercapnia in both calcifying and non-calcifying organisms (Pörtner 2008). An acute exposure experiment by Novak (2012) showed that adult *H. midae* were only capable of partial acid-base regulation when exposed to reduced pH seawater (7.33 vs 8.03 normocapnic) for 24 hours. During the first three hours of exposure, haemolymph bicarbonate concentration increased by approximately 20 % and haemolymph pH declined from 7.4 to 7.2. Thereafter, haemolymph bicarbonate concentrations returned to pre-experimental conditions, however haemolymph pH continued to decline to 7.10 (vs 7.51 in control). Abalone were then placed in normocapnic seawater for 8 hours to recover from experimental conditions and haemolymph pH increased to 7.55. When juvenile *H. midae* were exposed to acute hypercapnia (-0.4) for two weeks (Lester 2012), metabolic alkalosis of the haemolymph was observed as a response mechanism; haemolymph pH was elevated beyond normal range as a direct result of an increase in bicarbonate concentrations. Chronic exposure of adult *H. midae* to reduced pH seawater (7.3 vs 8.07 in normocapnic) for 18 months revealed non-compensated respiratory acidosis; no relevant elevation of haemolymph bicarbonate concentration to retain haemolymph pH at pre-incubation/normocapnic levels (Haupt et. al. unpublished). Chronic exposure to reduced pH seawater showed a decline in haemolymph pH (7.05 vs 7.29 in normocapnia), however the reduced haemolymph pH levels were still sufficient to ensure an outward pCO_2 gradient was maintained at a level higher than found in normocapnia (Haupt et. al. unpublished). I hypothesise that adult *H. midae* exposed to hypercapnic conditions in this study will follow similar acid-base regulation to the observations in Haupt et. al. (unpublished), and will vary seasonally. There are no published studies on the physiological effects of hypercapnia and warming on *H. midae* acid-base regulation, but it is expected that levels of pH, bicarbonate concentration and pCO_2 will vary seasonally, and will differ between treatments, and that these differences will be amplified as the experiment progresses.

3.2 Materials and Methods

See Chapter 2 for experimental design and general methods.

3.2.1 Size-grading

H. midae were deprived of food one day prior to size-grading. At each size-grading (June 2015, October 2015 and February 2016), baskets from each tank were put into a CO_2 bath for 5 minutes to anaesthetize the animals before removing them from the basket by hand, following standard farm procedure (van der Merwe 2009). The CO_2 bath consisted of a commercial abalone tank which was filled with seawater and connected to a CO_2 gas cylinder which released CO_2 into the tank. Seawater pH in CO_2 baths has been recorded to be between 4.8 and 5.4 during these size-grading procedures (van der Merwe 2009). Seawater inside the CO_2 tank was recirculated within the tank through a fine mesh sieve to collect dirt and debris. The CO_2 bath was flushed and refilled between each treatment. Twenty-four abalone from each basket were put aside randomly for sampling once all the abalone were removed from the basket. The twenty-four, sample abalone from each basket were weighed (to 0.01 g) using an electronic scale (Kern PLS 4200-2F), shell length was measured (0.01 mm) along the longest length of the shell using Vernier callipers, and photos were taken of each animal (Sony Z3 2014). While the sample abalone were measured, the baskets and racks were left in HCl (30-33% concentration) for 5 minutes and sprayed off with pressurised, fresh water. Clean baskets were restocked with randomly selected abalone from the same treatment in order to reduce a tank effect. Restocking of the baskets with abalone was determined by the average weight of the sample abalone for the entire treatment (AW), basket surface area (BA = 1.18m^2) and stocking density (SD=18 %) using the following calculations:

$$Length = Abalone\ length\ (mm) = \left[\left(\frac{AW}{0.0002}\right)^{\frac{1}{2.9909}}\right]$$

$$AoA\ (m^2) = Area\ of\ abalone = \frac{22}{7} \times \left(\frac{Length/1000}{2}\right)^2$$

$$Weight\ in\ basket\ (g) = \frac{SD \times BA}{AoA} \times AW$$

Each basket for that treatment was then filled with abalone to the ``Weight in basket`` weight. These calculations were according to farm protocol for size-grading procedures. Abalone were size-graded by staff from the aquaculture facility to avoid selection bias by the author. Length and weight measurements were measured recorded by the author. Abalone that were sampled in the size-grading process were not replaced back into the experimental system to avoid repeated measurements of the same abalone in future sampling periods. Sampled abalone and excess abalone from each treatment that were not used to fill the baskets were labelled and placed into oyster bags and left in a holding tank until all the tanks from that treatment had been sampled (approximately 1.5 hours). Once the tanks from a treatment were sampled, the excess animals were taken to an abalone processing facility (<1 km drive). Abalone condition factor (CF) was calculated for all abalone according to the formula in Britz et. al. (1996):

$$CF\ (g.mm^{-1}) = \left(\frac{Weight\ (g)}{Length\ (mm)^{2.99}}\right) \times 5575$$

3.2.2 Factory Processing

Excess abalone (n=20 per experimental abalone tank) were shucked and put into sample dishes at Aqunion: Processing Facility (Hermanus, South Africa). The unshucked -, shucked -, visceral - and muscle mass was weighed (to 0.01 g) using an electronic scale (Kern PLS 4200-2F). The heads of the abalone were not removed for muscle mass weights and haemolymph was allowed to drain from the shucked animals for 30 minutes - 1 hour during sampling whilst the meat was in the dishes. The proportion of muscle to body mass (PMB) was determined using the individuals' muscle mass (MM) as a proportion of the total unshucked body mass BM) in the following equation:

$$PMB = MM/BM$$

The viscera of 10 males and 10 females from each experimental abalone tank in the final sampling period were placed in plastic, airtight jars containing ethanol. The viscera were transferred into a 10% formalin preservative in freshwater after five days for determination of gonad bulk index.

3.2.3 Gonadal Bulk Index (GBI)

The mean GBI was determined using the methods of Tutschulte and Connell (1988) and Wood and Buxton (1996). Arc length and linear dimensions of the conical appendage (CA) and the digestive gland (DG) of each preserved visceral sample was measured using Vernier callipers (0.01mm) and a section was removed from the midpoint of each CA was removed. Photographs (Sony Z3 2014) of each CA section alongside Vernier callipers were taken from 100mm above the section. Measurements of the linear dimensions of the digestive gland (A and B) and the entire section (X and Y) from the transverse section through BD (Figure 3.2.b) were determined using the software, ImageJ (Schneider et. al. 2012, Figure 3.1). These measurements were used to estimate the effective gonad volume (EGV) from the following calculation:

$$EGV\ (mm^3) = \frac{AS\pi}{96}\left\{8(X+Y)^2 - \frac{(X+Y+A+B)^3}{(X+Y)}\right\}$$

An estimate of GBI was obtained by dividing EGV by the shucked mass of the animal (g).

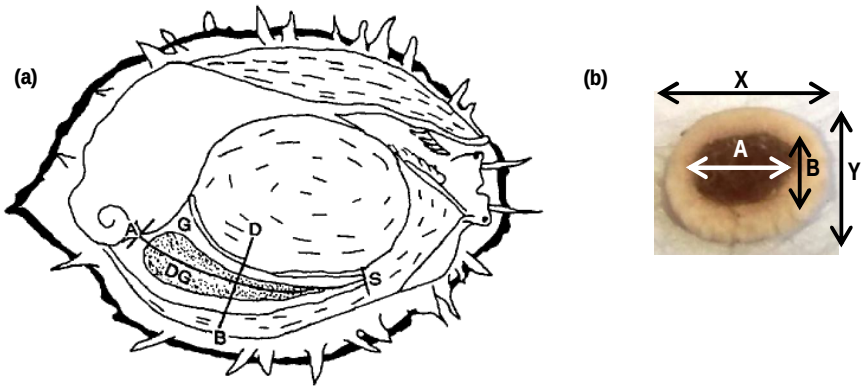

Figure 3.2. Internal structure of *H. midae*, showing (a) the position of the section (**BD**), which is halfway along the measured cone length (**AS**), and part of the gonad (**G**), which has been cut away to reveal the digestive gland (**DG**) (Source: Wood & Buxton 1996); (b) transverse section through **BD**, showing the linear dimensions of the digestive gland (**A** and **B**) and the entire section (**X** and **Y**), used for calculating EGV.

3.2.4 Total CO_2 content, pH and bicarbonate concentration in abalone haemolymph

Haemolymph samples (500 µL) were withdrawn from abalone (n=8 per treatment) one-two days prior to each size-grading. The samples were taken between the mouth and the anterior portion of the foot using a 0.90x38 mm needle and 1 mL syringe (Figure 3.3). Environmental conditions were recorded prior to sampling (Table 3.2.1). Samples were refrigerated overnight and analysed the following day at DEFF Research Aquarium (Sea Point, South Africa). Samples were allowed to acclimatise to 18 °C before the pH of each sample was measured using a microelectrode (Micro pH meter, ThermoScientific, USA) calibrated with NBS-precision calibration solution (pH 7.413). The temperatures of the samples were recorded as 18.1 °C, 18.5 °C, and 18.7 °C for each sampling period respectively. Total haemolymph CO_2 (cCO_2) was determined using infrared analysis (Cameron 1986) by means of a CO_2 analyser (SBA4, PP-Systems, USA). A 50 mM standard stock solution of sodium bicarbonate ($NaHCO_3$) was diluted to create solutions with concentrations of 12.50 mM, 6.25 mM, 3.13 mM, 1.56 mM, and 0.78 mM. These known concentrations of stock solution (500µL) were injected into an acrylic glass acidification chamber, which contained 0.1M sulphuric acid (H_2SO_4) and mixed by a magnetic stirrer bar. The acid reverts the various CO_2 forms within the injected solution to soluble CO_2 that is bound by the nitrogen carrier gas (N_2) pumped into the chamber via silicon tubing at 50 $mL.min^{-1}$. The dissolved CO_2 and inert N_2 were then carried to the CO_2 sensor via silicon tubes where the infrared absorption of CO_2 was detected in millivolts (mV). The signal was received and transferred to a PC using PP Systems transfer software. Once the mV signal of cCO_2 for each known solution was determined, a standard curve was created for each size grading (R^2=0.9992, R^2=0.9994, R^2=0.9992). Each haemolymph sample was injected into the infrared CO_2 analyser using the same procedure and the mV signal of cCO_2 for each sample was obtained. Total CO_2 content (mM) was calculated using the standard curve. None of the other atmospheric gases have any infrared absorption, so there are no interferences to be concerned with (Cameron 1986).

The indirect (calculation) method was used for determination of the partial pressure of CO_2 (pCO_2; Cameron 1971, Cameron 1986). This involves the application of the Henderson-Hasselbalch equation (eqn. 1) into a readjusted form (eqn. 2):

$$pH = pK_1' + log\left[\left(\frac{cCO_2}{\propto pCO_2}\right) - 1\right] \qquad \textbf{(eqn. 1)}$$

$$pCO_2 = \frac{cCO_2}{\propto\left[\left(10^{pH-pK_1'}\right)+1\right]} \qquad \textbf{(eqn. 2)}$$

pH – measurement taken before infrared gas analysis

cCO_2 - total CO_2 content from standard curve in millimolar

α - Solubility constant of CO_2

pK_1' - The first apparent dissociation constant

pCO_2 – Partial pressure of CO_2 in torr (1 torr = 133.3224 Pa)

The solubility constant of CO_2 and the first apparent dissociation constant values were estimated from the nomograms designed by Truchot (1976) for the shore crab, *Carcinus maenas*. To the

author's knowledge, no nomograms have been created for *H. midae*. The solubility constant (α) values for June 2015, October 2015 and February 2016 were 0.0455 (*t*=18.1°C and *S*=35‰), 0.045 (*t*=18.5°C and *S*=35‰) and 0.0445 (*t*=16.4°C and *S*=35‰) respectively. The pK_1' values for June 2015, October 2015 and February 2016 were 6.01 (*t*=18.1°C and *S*=35‰), 6.008 (*t*=18.5°C and *S*=35‰) and 6.005 (*t*=16.4°C and *S*=35‰) respectively.

Haemolymph bicarbonate (HCO_3^- + CO_3^{2-}) was calculated using a further readjustment (eqn. 3) of the Henderson-Hasselbalch equation:

$$[HCO_3^-] = cCO_2 - (\propto \times pCO_2) \qquad \textbf{(eqn. 3)}$$

Davenport diagrams were created using for each time period. Isobars for pCO_2 were generated by inserting set pCO_2 values into equation 1 for set pH values (pH 6.85-8, increasing by 0.1 units) to calculate cCO_2 values. Generated cCO_2 values were inserted into equation 3 to determine HCO_3^- concentrations for each individual. Bicarbonate concentrations and pH values for each treatment were averaged and the standard errors calculated for each time period.

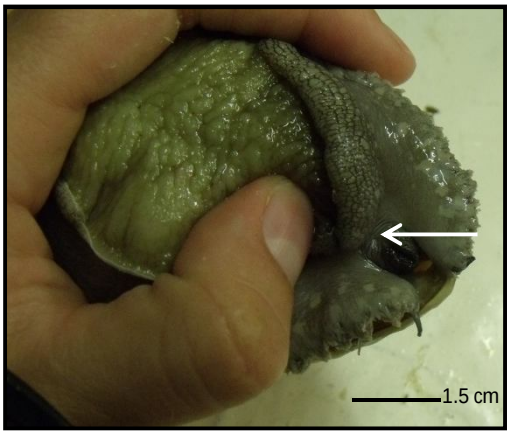

Figure 3.3. Withdrawal site of haemolymph (white arrow) from *H. midae*.

Table 3.2.1. Environmental conditions (± standard deviation) of experimental tanks from four treatments (C=control, T=temperature, P=pH, PT=pH x temperature) at time of haemolymph sampling.

Sample date	Treatment	Tank pH	Tank temperature (°C)
June '15	C	8.07 ± 0.00	11.19 ± 0.01
	T	8.09 ± 0.01	12.72 ± 0.01
	P	7.63 ± 0.00	11.23 ± 0.02
	PT	7.64 ± 0.01	12.75 ± 0.01
Oct '15	C	8.15 ± 0.00	12.76 ± 0.01
	T	8.15 ± 0.01	14.27 ± 0.01
	P	7.73 ± 0.00	12.76 ± 0.01
	PT	7.74 ± 0.01	14.29 ± 0.01
Feb '16	C	8.09 ± 0.01	8.07 ± 0.01
	T	8.09 ± 0.01	9.61 ± 0.01
	P	7.65 ± 0.02	8.10 ± 0.01
	PT	7.66 ± 0.01	9.64 ± 0.01

3.2.5. Statistical Analysis

To determine whether whole wet weight, muscle mass, and GBI changed as a function of time within individual treatment groups, the *lme* function from the *nlme* package (Pinheiro et. al. 2016) in R (The R Core Team, 2012) was used to create linear mixed effects models. The response variable was transformed in the case of non-normal data distribution (Table 3.2.2). Residual spread and homogeneity of variances was tested by applying a Bartlett test to each model (Table 3.2.2). Temporal autocorrelation was determined by means of autocorrelation function (ACF) plots and model comparison (Table 3.2.2). Model selection was determined using AIC values for each response variable (Table 3.2.3).

Table 3.2.2. Transformations and model assumption tests for linear mixed effects models.

Response Variable	Data Transformation	Bartlett Test	Variance structure	Autocorrelation Structure	Rho
Whole wet weight	Log	K^2=6.212, df=3, p=0.10	None	None	0.28
Muscle mass	None	K^2=6.252, df=3, p=0.10	None	None	0.08
GBI	Square Root	K^2=2.806, df=3, p=0.42	None	N/A	N/A

Table 3.2.3. Linear mixed effects models used to determine the effect of treatment over time for *H. midae* exposed to four treatments over a 12 month period.

Response Variable	Formula	Random Effect	AIC
Whole wet weight	y ~ Treatment * Time	1+Time|Tank	1862.58
Muscle mass	y ~ Treatment * Time	1+Time|Tank	6778.55
GBI	y ~ Treatment	1|Tank	185.96

To determine whether non-linear data such as: abalone PMB, condition factor, haemolymph pH, and haemolymph bicarbonate changed as a function of time within individual treatment groups, the *gam* function from the *mgcv* package (Wood 2003, Wood 2011, Wood et. al. 2016) in R (The R Core Team, 2012) was used to create a generalized additive mixed effects models. The response variable was transformed in the case of non-normal data distribution (Table 3.2.4). The general formula used for each response variable was:

$$y \sim Treatment + s(Time, by=Treatment, k=3) + s(Tank, Time, bs="re")$$

with the exception of CF (the number of knots (k) was extended to 4) to improve model fit.

Residual spread and homogeneity of variances was determined by residual plots of the response and fitted values of the model (Table 3.2.5).

Table 3.2.4. Transformations and model assumption tests for generalized additive mixed effects models.

Response Variable	Transformation	Residual Plot
PMB	Logit transformation and scale distributed	Homogenous
CF	None	Homogenous
Haemolymph pH	Logit transformation and scale distributed	Homogenous
Haemolymph bicarbonate	None	Homogenous

Table 3.2.5. Model fit statistics for generalized additive mixed effects models.

Response Variable	GCV	R 2
PMB	0.0012187	0.206
CF	0.010923	0.12
Haemolymph pH	0.0064792	0.753
Haemolymph bicarbonate	0.13994	0.325

3.3 Results

3.3.1. Seawater Parameters

Mean seawater carbonate chemistry parameters are presented in Chapter 2. Ambient seawater temperature was 15.6±2.2 °C for the duration of the experiment and followed natural environmental variations. Average heated seawater temperature was 17.2±2.2 °C in the temperature treatment tanks and 17.2±2.2 °C in the pH *x* temperature treatment tanks, offset to natural environmental temperature variations. Ambient seawater pH was 8.10±0.06 for the duration of the experiment and followed natural environmental variations. Average CO_2-diffused seawater pH was 7.66±0.07 in the pH treatment tanks and 7.66±0.08 °C in the pH *x* temperature treatment tanks, offset to natural environmental pH variations. Salinity was 35.5±0.03 in all experimental tanks and remained fairly stable for the duration of the experiment.

3.3.2. Abalone growth

Abalone growth was measured in terms of wet weight (Figure 3.3.1, Table 3.5.1). Treatment had a significant effect on abalone wet weight over the course of the study (df=16, F=10.6, p<0.01). Abalone from the control treatment (112.2±14.3 g) and temperature treatment (113.6±14.5 g) were significantly heavier than abalone from the pH (102.6±14.7 g) and pH *x* temperature treatments (105.0±13.8 g) after 12 months (Table 3.3.1). There was no significant difference between abalone from the control and temperature treatments or between abalone from the pH and pH x temperature treatments (Table 3.3.1).

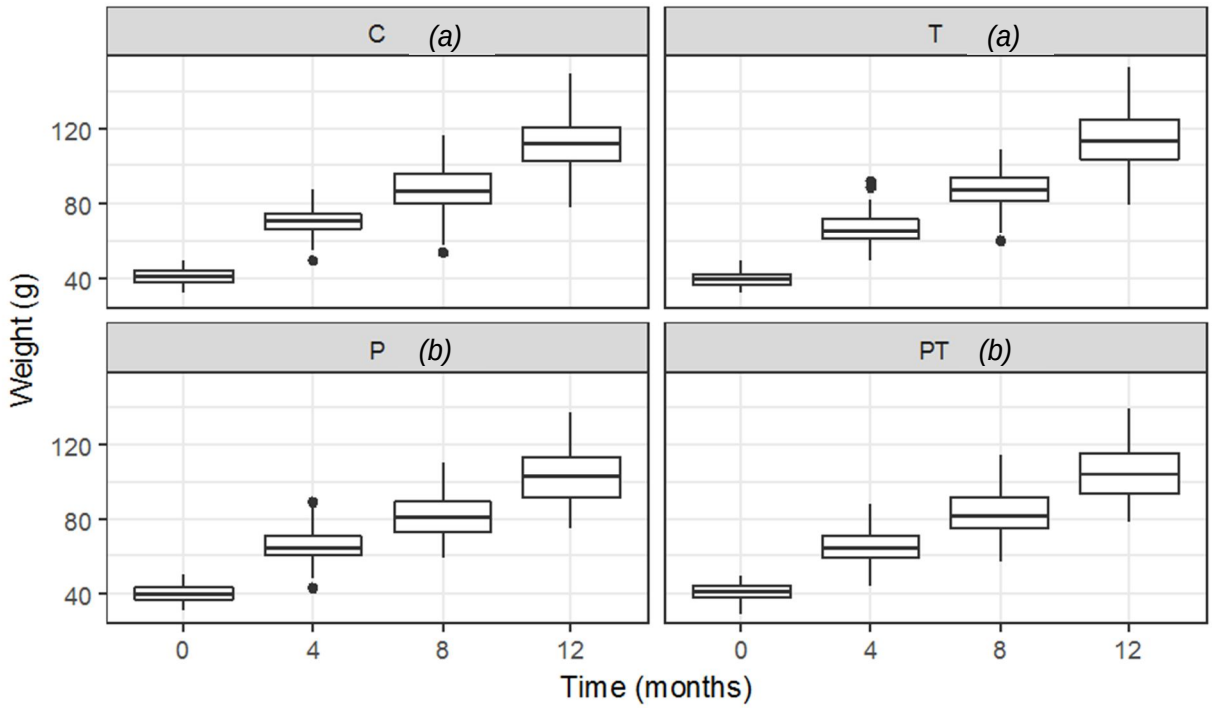

Figure 3.3.1. Boxplots of the wet weights (± standard deviation) of abalone, *H. midae*, exposed to four treatments (C=control, T=temperature, P=pH, PT=pH x temperature) over a 12-month experimental period in a flow-through seawater system. Each treatment group contains repeated measurements at 0-, 4-, 8-, and 12-month sampling times. Same letters in italics between treatments denote no statistical difference between treatments (alpha = 0.05).

Table 3.3.1. Pairwise differences of abalone wet weights between treatments (C=control, T=temperature, P=pH, PT=pH x temperature) using the Tukey method to compare family estimates. Significant values are taken at the 5% level and shaded in grey.

Contrast Treatments	Comparison (g)	Comparison (%)	Degrees of Freedom	t-ratio	p-value
C - T	-1.4	-1.2%	16	1.495	0.46
C - P	9.6	8.9%	16	5.628	<0.01
C - PT	7.2	6.6%	16	4.255	<0.01
T - P	11.0	10.2%	16	4.133	<0.01
T - PT	8.6	7.9%	16	3.760	0.04
P - PT	-2.4	-2.3%	16	-1.373	0.53

3.3.3. Abalone Muscle Mass

Abalone muscle tissue growth was represented by abalone muscle mass (Figure 3.3.2, Table 3.5.1). Treatment had a significant effect on abalone muscle mass over the course of the study (df=16, F=17.212, p<0.01). Abalone from the control (66.14±9.64 g) and temperature treatments (68.41±10.11 g) had significantly heavier muscle mass in comparison to abalone from the pH (59.97±10.15 g) and pH x temperature treatments (62.56±10.06 g) after 12 months (Table 3.3.2). There was no significant difference between the muscle mass of abalone from the control and temperature treatments nor between abalone from the pH and pH x temperature treatments (Table 3.3.2).

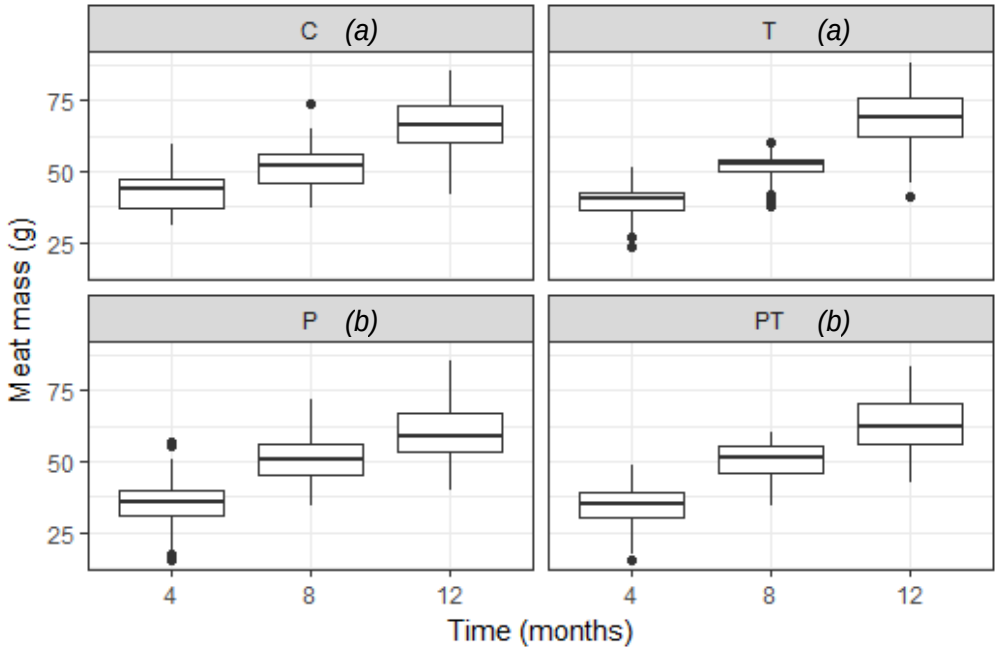

Figure 3.3.2. Muscle mass (± standard deviation) of abalone, *Haliotis midae*, exposed to four seawater treatments (C=control, T=temperature, P=pH, PT=pH x temperature) over a 12-month experimental period in a flow-through seawater system. Each treatment group contains repeated measurements at 4-, 8-, and 12-month sampling times. Same letters in italics between treatments denotes no statistical difference between treatments (alpha = 0.05).

Table 3.3.2. Pairwise differences in abalone muscle mass between treatments (C=control, T=temperature, P=pH, PT=pH x temperature) using the Tukey method to compare family estimates. Significant values are taken at the 5% level and shaded in grey.

Contrast Treatments	Comparison (g)	Comparison (%)	Degrees of Freedom	t-ratio	p-value
C - T	-2.27	-3.4%	16	0.409	0.98
C - P	6.17	9.8%	16	5.55	<0.01
C - PT	3.58	5.6%	16	4.686	<0.01
T - P	8.44	13.1%	16	5.141	<0.01
T - PT	5.85	8.9%	16	4.77	<0.01
P - PT	-2.59	-4.2%	16	-0.864	0.82

3.3.4. Proportion muscle to whole body mass (PMB)

The proportion of meat to whole body mass was represented as PMB (Figure 3.3.3). Treatment had a significant effect on abalone PMB over the course of the study (df=2.3, χ^2=0.049, p<0.01). Abalone from the control treatment had a significantly different PMB from all other treatments (Table 3.3.3, Figure 3.3.4). Abalone in ambient conditions displayed a linear decrease in PMB over time (edf=1.005); whereas abalone responded to the temperature treatment with a rapid decline in PMB for 8 months, followed by a period of stabilization until the end of the experiment. Abalone responded to the pH and pH x temperature treatments with a peak in PMB after 8 months, followed by a gradual decline in PMB until the end of the experiment (Figure 3.3.5).

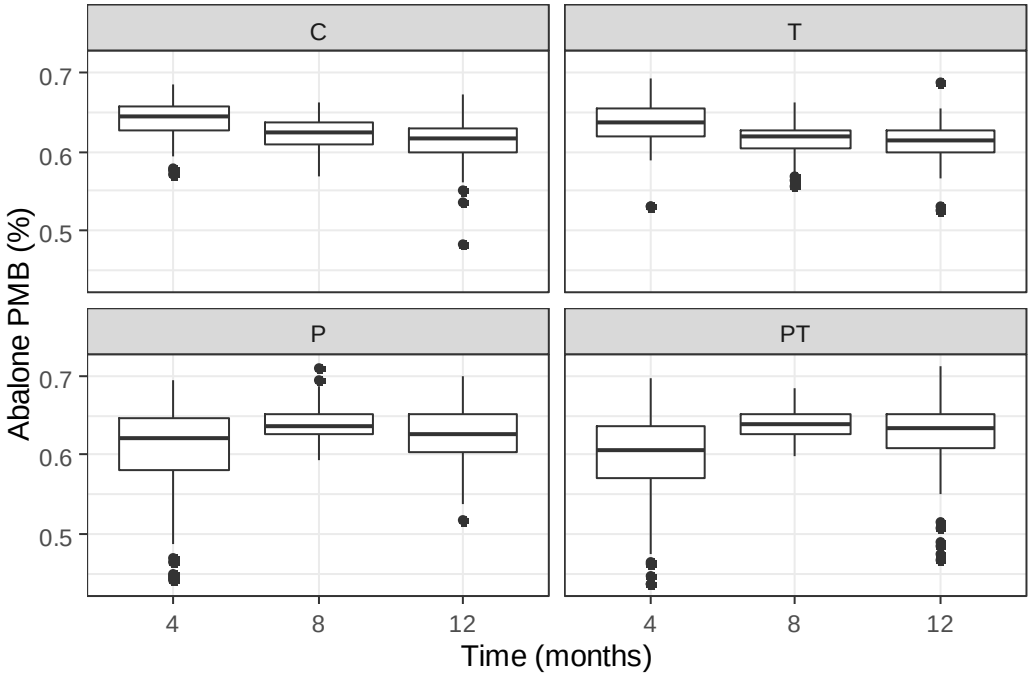

Figure 3.3.3. PMB (± standard deviation) of abalone, *Haliotis midae*, exposed to four seawater treatments (C=control, T=temperature, P=pH, PT=pH x temperature) over a 12-month experimental period in a flow-through seawater system. Each treatment group contains repeated measurements at 4-, 8-, and 12-month sampling times.

Table 3.3.3. Ordered factor contrasts of smoothing terms for abalone PMB between treatments (C=control, T=temperature, P=pH, PT=pH x temperature) over the 12-month study. Significant values are taken at the 5% level and shaded in grey.

Contrast Treatments	Comparison (%)	Estimated Degrees of Freedom	F-value	p-value
C - T	-2.27	1.741	8.339	<0.01
C - P	6.17	1.947	11.927	<0.01
C - PT	3.58	1.936	13.815	<0.01

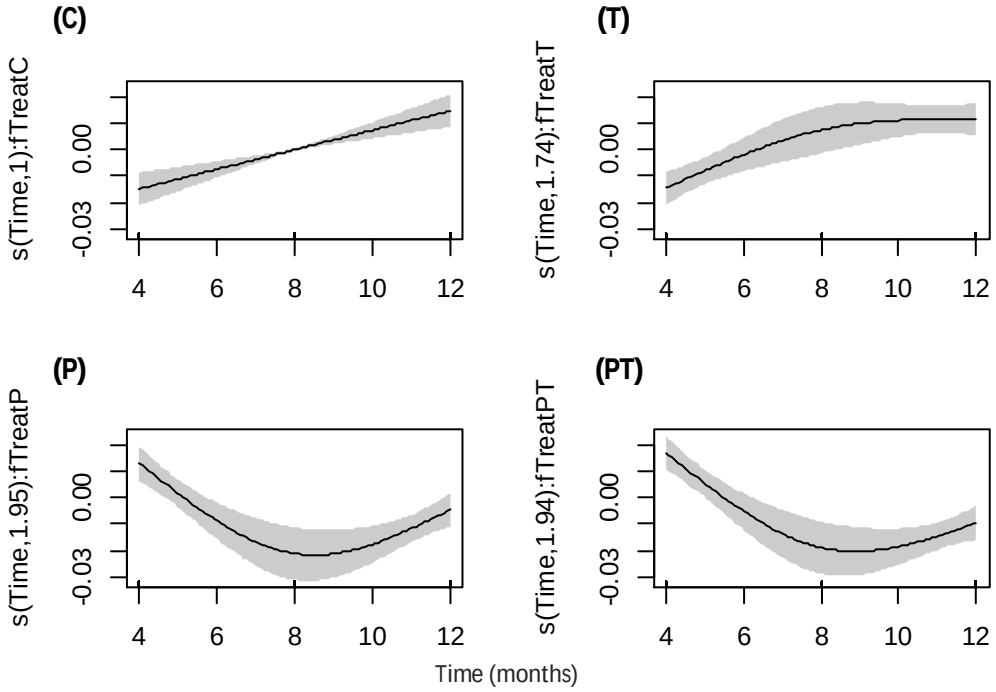

Figure 3.3.4. Smoothing function (logit and square root transformed) of abalone PMB response to four treatments (C=control, T=temperature, P=pH, PT=pH x temperature) over a 12-month experimental period in the optimal generalized additive mixed model. The estimated degrees of freedom (EDF) for each treatment are listed on the y-axis for each treatment.

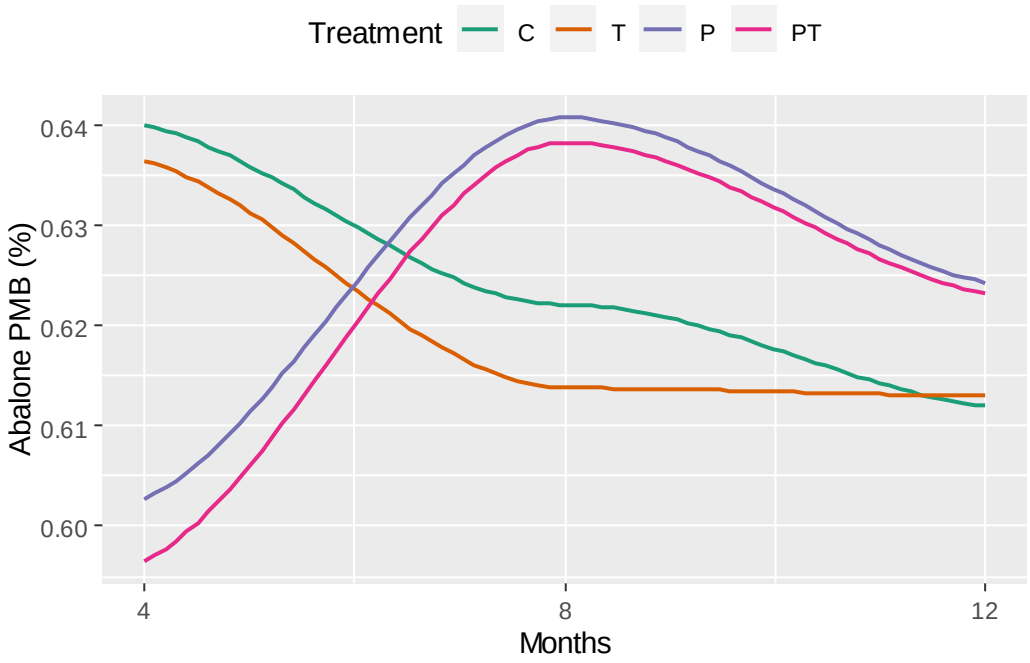

Figure 3.3.5. Abalone PMB response to four treatments (C=control, T=temperature, P=pH, PT=pH x temperature) over a 12-month experimental period using LOESS smoothers. Each treatment group contains repeated measurements at 4-, 8-, and 12-month sampling times.

3.3.5. Condition Factor

Abalone from all treatments had a condition factor (CF) greater than 1, indicating that all abalone were in good condition during the experimental period. Treatment had a significant effect (df=5.6, χ^2=2.4099, p<0.01) on abalone condition factor over the course of the study (Figure 3.3.6). Abalone in ambient conditions had a significantly different response in CF over 12 months in comparison to the other treatments (Table 3.3.4). Abalone from the control treatment displayed a peak CF in June 2015 (4 months) and a trough in October-November 2015 (8 months, Figure 3.3.7). The same peak and trough were seen in abalone exposed to the temperature treatment; however abalone from the temperature treatment had a poorer CF (Figure 3.3.7). Abalone exposed to low pH and pH x temperature treatments also displayed a peak CF in June 2015, but did not display an obvious trough in October-November 2015; instead there was a continuous and gradual decline in abalone condition until the end of the experimental period (Figure 3.3.7).

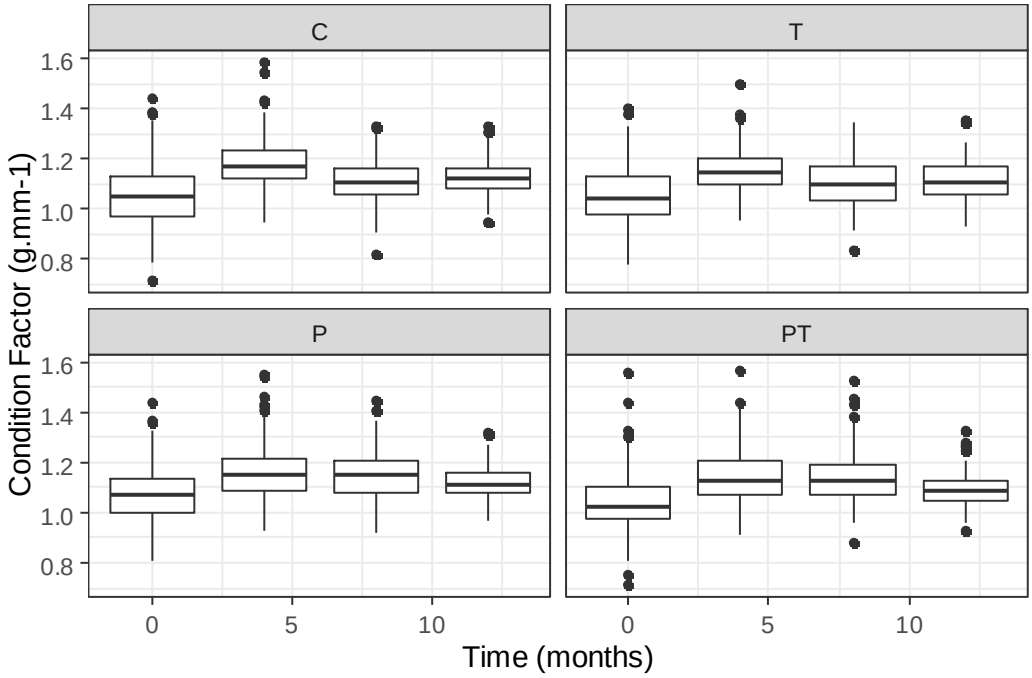

Figure 3.3.6. Boxplots of Condition Factor (± standard deviation) of abalone, *H. midae*, exposed to four treatments (C=control, T=temperature, P=pH, PT=pH x temperature) over a 12-month experimental period in a flow-through seawater system. Each treatment group contains repeated measurements at 0-, 4-, 8-, and 12-month sampling times.

Table 3.3.4. Ordered factor contrasts of smoothing terms for abalone condition factor between treatments (C=control, T=temperature, P=pH, PT=pH x temperature) over the 12-month study. Significant values are taken at the 5% level and shaded in grey.

Contrast Treatments	Comparison ($g.mm^{-1}$)	Comparison (%)	Estimated Degrees of Freedom	F-value	p-value
C - T	0.013	0.9%	2.912	16.189	<0.01
C - P	0.004	0.0%	2.794	17.378	<0.01
C - PT	0.030	2.7%	2.824	25.567	<0.01

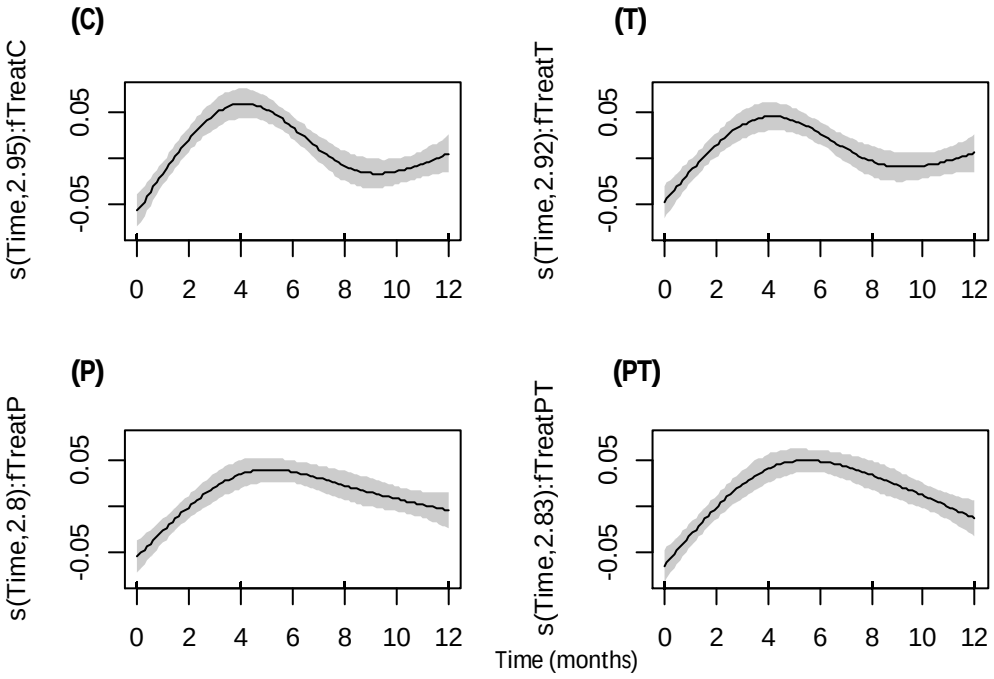

Figure 3.3.7. Smoothing function of abalone condition factor (CF) response to four treatments (C=control, T=temperature, P=pH, PT=pH x temperature) over a 12-month experimental period in the optimal generalized additive mixed model. The estimated degrees of freedom (EDF) for each treatment are listed on the y-axis for each treatment.

3.3.6. Gonad Development

Abalone gonadal bulk index (GBI) differed significantly (df=3, F=6.479, p<0.01) between treatments after 12 months of exposure to experimental conditions (Figure 3.3.8). GBI of abalone from ambient conditions (0.833±0.285 g.mm^{-1}) was significantly greater than abalone from the low pH (0.551±0.196 g.mm^{-1}) and pH x temperature treatments (0.665±0.226 g.mm^{-1}) after 12 months of exposure to experimental conditions (Table 3.3.5). Abalone exposed to the temperature treatment (0.734±0.231 g.mm^{-1}) had significantly greater GBI than abalone from the low pH treatment (Table 3.3.5).

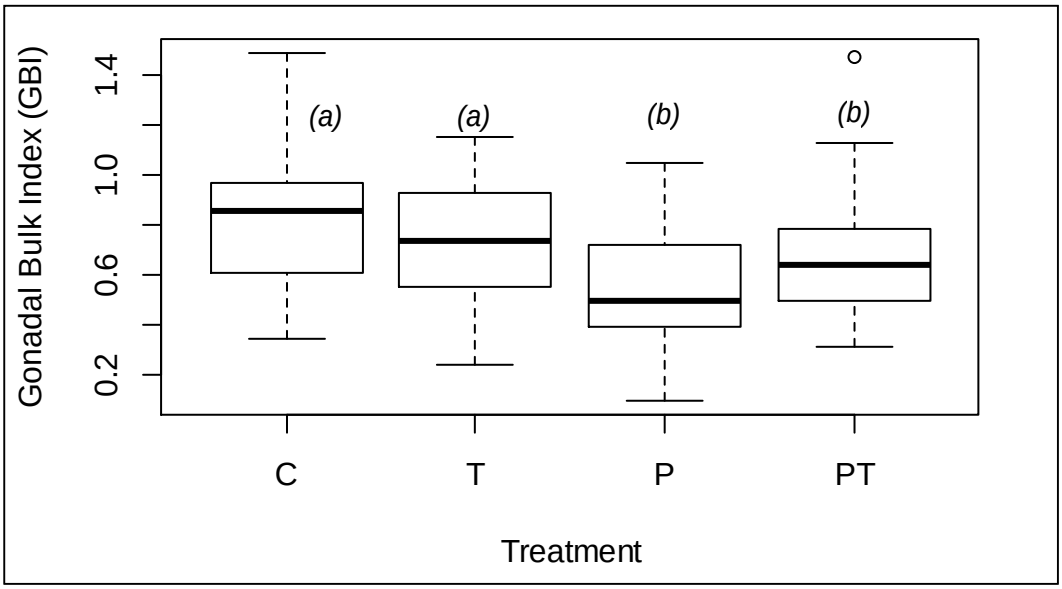

Figure 3.3.8. Boxplot of *H. midae* gonadal bulk indices (± standard deviation) after 12 months of exposure to four seawater treatments (C=control, T=temperature, P=pH, PT=pH x temperature). Same letters in italics between treatments denotes no statistical difference between treatments (alpha = 0.05).

Table 3.3.5. Pairwise differences in abalone gonadal bulk index (GBI) between treatments (C=control, T=temperature, P=pH, PT=pH x temperature) over the course of the study using the Tukey method to compare family estimates. Significant values are taken at the 5% level and shaded in grey.

Contrast Treatments	Comparison (mm3.g-1)	Comparison (%)	Degrees of Freedom	t-ratio	p-value
C - T	0.10	12.6%	16	1.362	0.54
C - P	0.28	40.8%	16	4.271	0.00
C - PT	0.17	22.4%	16	2.394	0.12
T - P	0.18	28.5%	16	2.909	0.05
T - PT	0.07	9.9%	16	1.032	0.73
P - PT	-0.11	-18.8%	16	-1.877	0.28

3.3.7. Haemolymph pH and bicarbonate

In vivo haemolymph parameters of abalone are presented in Table 3.3.6. Haemolymph pH and bicarbonate concentration were analysed for statistical differences and patterns over time.

Table 3.3.6. *In vivo* haemolymph parameters of *H. midae* exposed to four seawater treatments (C=control, T=temperature, P=pH, PT=pH x temperature) for 12 months (Feb 2015 - Feb 2016), sampled every 4 months.

Sample date	Treatment	pH	cCO_2 (mM)	pCO_2 (Torr)	pCO_2 (kPa)	$[HCO_3^-]$ (mM)
June '15	C	7.24 ± 0.02	1.96 ± 0.11	2.41 ± 0.13	0.32 ± 0.02	1.85 ± 0.11
	T	7.30 ± 0.02	2.16 ± 0.10	2.33 ± 0.14	0.31 ± 0.02	2.05 ± 0.10
	P	7.28 ± 0.03	2.19 ± 0.17	2.45 ± 0.21	0.33 ± 0.03	2.08 ± 0.16
	PT	7.32 ± 0.02	2.39 ± 0.08	2.46 ± 0.14	0.33 ± 0.02	2.28 ± 0.08
Oct '15	C	7.42 ± 0.02	2.83 ± 0.09	2.33 ± 0.11	0.31 ± 0.02	2.73 ± 0.09
	T	7.40 ± 0.02	2.45 ± 0.13	2.10 ± 0.10	0.28 ± 0.01	2.36 ± 0.13
	P	7.29 ± 0.02	2.83 ± 0.10	3.14 ± 0.13	0.42 ± 0.02	2.69 ± 0.10
	PT	7.28 ± 0.03	2.46 ± 0.2	2.86 ± 0.30	0.38 ± 0.04	2.34 ± 0.19
Feb '16	C	7.15 ± 0.03	2.38 ± 0.09	3.63 ± 0.23	0.48 ± 0.03	2.22 ± 0.09
	T	7.27 ± 0.03	2.66 ± 0.11	3.15 ± 0.25	0.42 ± 0.03	2.52 ± 0.10
	P	7.02 ± 0.02	2.33 ± 0.07	4.68 ± 0.24	0.62 ± 0.03	2.12 ± 0.07
	PT	6.91 ± 0.02	2.71 ± 0.10	5.44 ± 0.38	0.73 ± 0.05	1.93 ± 0.09

There was a significant difference (df=8.2, χ^2=0.397, p<0.01) in the response of abalone haemolymph pH to the treatments over time (Figure 3.3.9). Abalone in ambient conditions displayed a significantly different response in haemolymph pH to the other treatments (Table 3.3.7). Haemolymph pH in ambient conditions peaked after 8 months (October 2015) then declined until the end of the experimental period. Abalone from the temperature treatment displayed a similar response in haemolymph pH, but had a more alkaline pH after 12 months in comparison to the control (Figure 3.3.10, Table 3.5.1). Abalone from the low pH and pH x temperature treatments did not follow the same response as abalone in ambient conditions; both treatments remained fairly stable for 8 months of exposure to experimental conditions and declined thereafter (Figure 3.3.11).

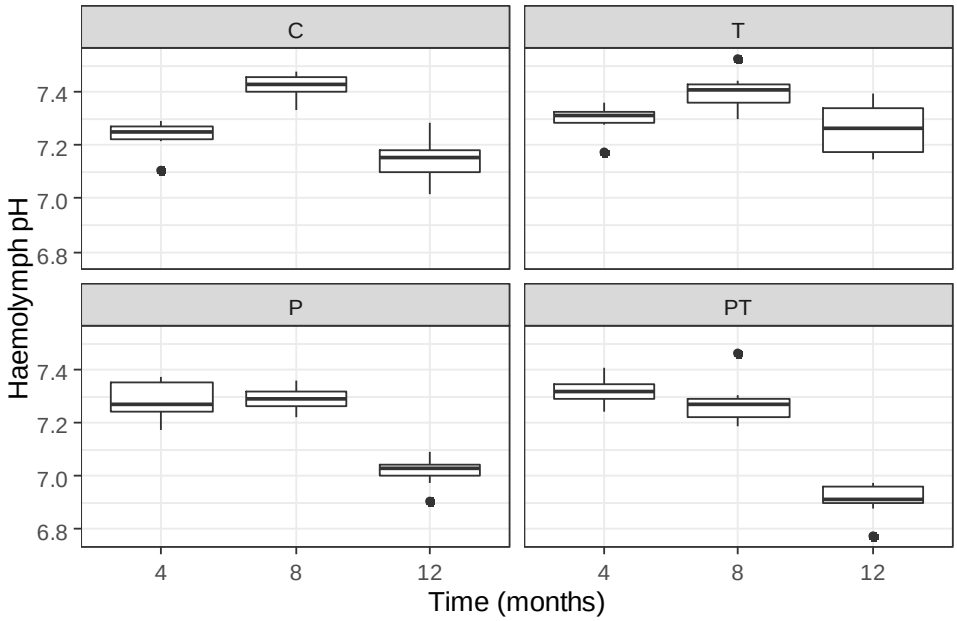

Figure 3.3.9. Haemolymph pH (± standard deviation) of abalone, *Haliotis midae*, exposed to four seawater treatments (C=control, T=temperature, P=pH, PT=pH x temperature) over a 12-month experimental period in a

flow-through seawater system. Each treatment group contains repeated measurements at 4-, 8-, and 12-month sampling times.

Table 3.3.7. Ordered factor contrasts of smoothing terms for abalone haemolymph pH between treatments (C=control, T=temperature, P=pH, PT=pH x temperature) over the 12 month study. Significant values are taken at the 5% level and shaded in grey.

Contrast Treatments	Comparison (units)	Comparison (%)	Estimated Degrees of Freedom	F-value	p-value
C - T	-0.120	-1.7%	1.933	6.997	0.001
C - P	0.130	1.8%	1.969	9.647	<0.01
C - PT	0.240	3.4%	1.978	19.308	<0.01

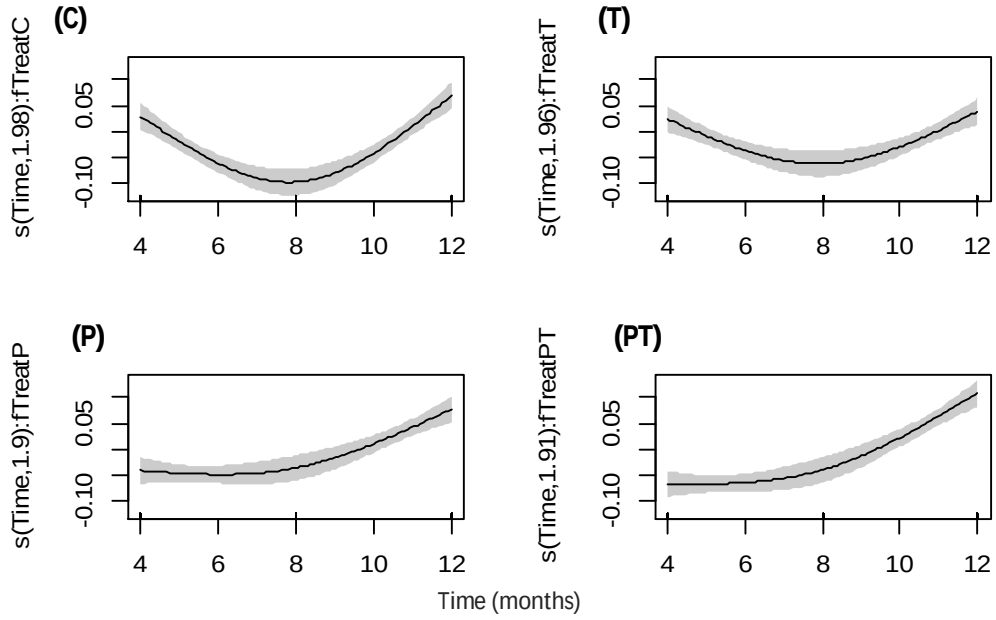

Figure 3.3.10. Smoothing function (logit and square root transformed) of abalone haemolymph pH for four treatments (C=control, T=temperature, P=pH, PT=pH x temperature) over a 12-month experimental period in the optimal generalized additive mixed model. The estimated degrees of freedom (EDF) for each treatment is listed on the y-axis for each treatment.

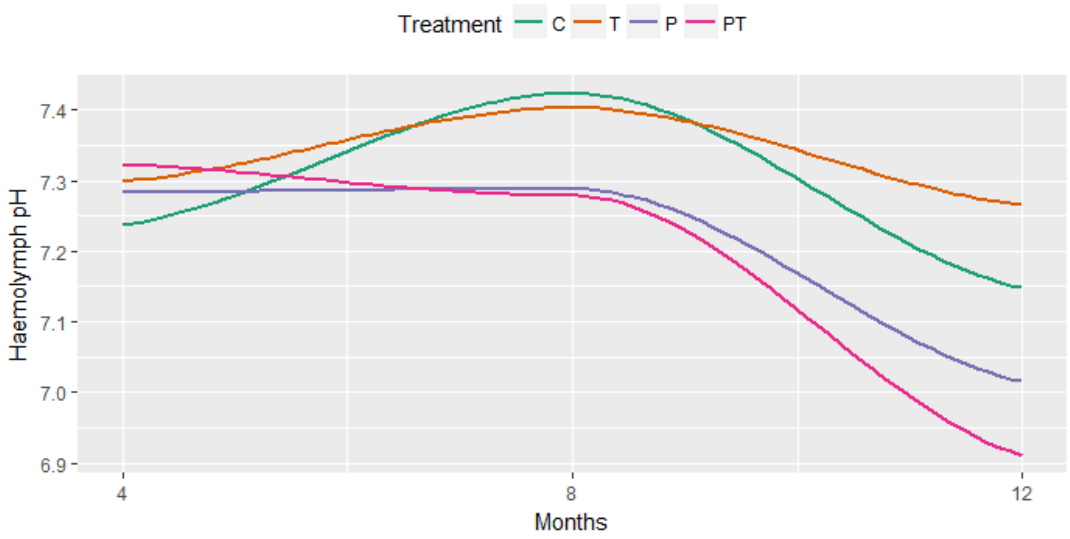

Figure 3.3.11. Abalone haemolymph pH response to four treatments (C = control, T = temperature, P = pH, PT = pH x temperature) over a 12-month experimental period using LOESS smoothers. Each treatment group contains repeated measurements at 4-, 8-, and 12-month sampling times.

Treatment had a significant effect (df=7.2, χ^2=6.541, p<0.01) on the response of haemolymph bicarbonate concentrations [HCO_3^-] over the course of the study (Figure 3.3.11). Abalone in ambient conditions displayed a significantly different response in haemolymph [HCO_3^-] to the other treatments over the course of the experiment (Table 3.3.8). Haemolymph [HCO_3^-] in ambient conditions peaked after 8 months (October 2015) then declined until the end of the experimental period. Abalone from the reduced pH treatment displayed a similar response in haemolymph pH, but had a lower [HCO_3^-] after 12 months in comparison to the control. Abalone from the temperature treatment had a linear (edf=1.00), gradual increase in [HCO_3^-] over 12 months (Figure 3.3.12). Abalone from the pH x temperature treatment remained fairly stable during the first 8 months of exposure to experimental conditions and declined thereafter (Figure 3.3.12).

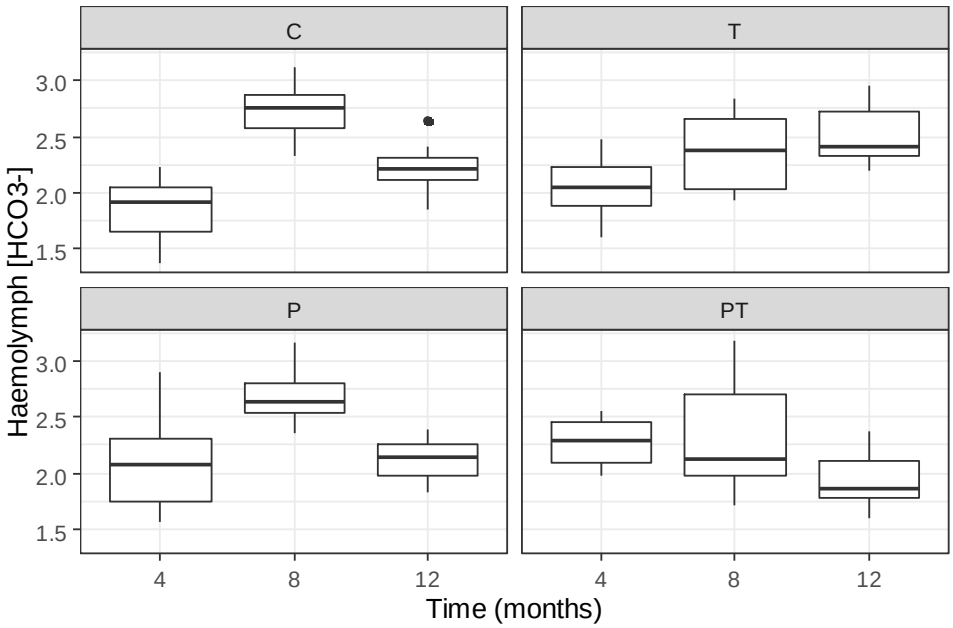

Figure 3.3.11. Haemolymph bicarbonate concentrations [HCO_3^-](± standard deviation) of abalone, *Haliotis midae*, exposed to four seawater treatments (C=control, T=temperature, P=pH, PT=pH x temperature) over a 12-month experimental period in a flow-through seawater system. Each treatment group contains repeated measurements at 4-, 8-, and 12-month sampling times.

Table 3.3.8. Ordered factor contrasts of smoothing terms for abalone haemolymph bicarbonate concentrations between treatments (C=control, T=temperature, P=pH, PT=pH x temperature) over the 12-month study. Significant values are taken at the 5% level and shaded in grey

Contrast Treatments	Comparison (units)	Comparison (%)	Estimated Degrees of Freedom	F-value	p-value
C - T	-0.300	-12.7%	1.000	6.411	0.01
C - P	0.100	4.6%	1.928	6.454	<0.01
C - PT	0.290	14.0%	1.526	19.308	<0.01

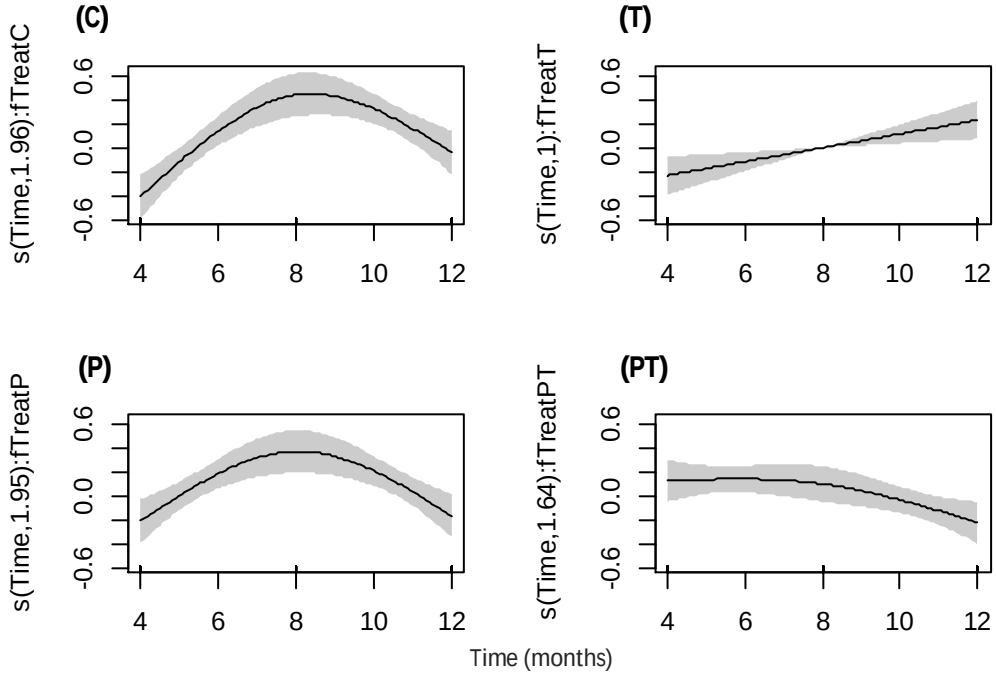

Figure 3.3.14. Smoothing function of abalone haemolymph bicarbonate concentrations for four treatments (C=control, T=temperature, P=pH, PT=pH x temperature) over a 12-month experimental period in the optimal generalized additive mixed model. The estimated degrees of freedom (EDF) for each treatment are listed on the y-axis for each treatment.

Abalone haemolymph from the control treatment ranged in pH from 7.15-7.42, in [HCO_3^- + CO_3^{2-}] from 1.85-2.73 mM, and in pCO_2 from 1.96-2.83 Torr over the course of the study. The Henderson-Hasselbalch diagram displayed a similar status of [HCO_3^- + CO_3^{2-}], pCO_2 and pH for all treatments in comparison to the control treatment after 4 months of exposure to experimental conditions. Contrasting treatments had slightly higher haemolymph pH and [HCO_3^- + CO_3^{2-}] in comparison to the control treatment (Figure 3.3.15 A).

After 8 months, haemolymph pH from the low pH and pH x temperature treatments were 0.13 units (1.8 %) and 0.14 units (1.9 %) lower and pCO_2 was 0.81 Torr (29.6 %) and 0.53 Torr (20.4 %) higher, respectively, than haemolymph from the control treatment. Haemolymph [HCO_3^- + CO_3^{2-}] from the pH x temperature treatment was 0.39 mM (15.4 %) less than haemolymph from the control treatment; however haemolymph [HCO_3^- + CO_3^{2-}] from the pH treatment was similar to the control treatment (Figure 3.3.15 B). Abalone haemolymph from the temperature treatment displayed a similar status of pH and pCO_2 in comparison to the control treatment, but haemolymph [HCO_3^- + CO_3^{2-}] were 0.37 mM (14.5 %) less than individuals from the control treatment.

After 12 months, haemolymph pH from the pH x temperature treatment had decreased throughout the study and was 0.24 units (3.4 %) less than the control treatment with a 1.81 Torr (39.9 %) higher haemolymph pCO_2 (Figure 3.3.15 C). Haemolymph [HCO_3^- + CO_3^{2-}] from the pH x temperature treatment was 0.29 mM (14.0 %) less than the control treatment, but was within the range of [HCO_3^- + CO_3^{2-}] experienced by abalone from the control treatment, indicating that abalone from the pH x temperature treatment experienced uncompensated respiratory acidosis; there was no relevant

increase in [HCO_3^- + CO_3^{2-}] to retain internal pH at normocapnic levels. Haemolymph from the low pH treatment also indicated uncompensated respiratory acidosis in comparison to the control treatment, but to a lesser extent. Haemolymph $pCO_2$from the pH treatment was 1.05 Torr (25.3 %) more than the control treatment and haemolymph pH was 0.13 units (1.8 %) less than the control group, however [HCO_3^- + CO_3^{2-}] was within the range of [HCO_3^- + CO_3^{2-}] experienced by abalone from the control treatment. Haemolymph from the temperature treatment displayed a smaller range of [HCO_3^- + CO_3^{2-}], pCO_2 and pH as the control treatment over the course of the study (Figure 3.3.15 C)**.**

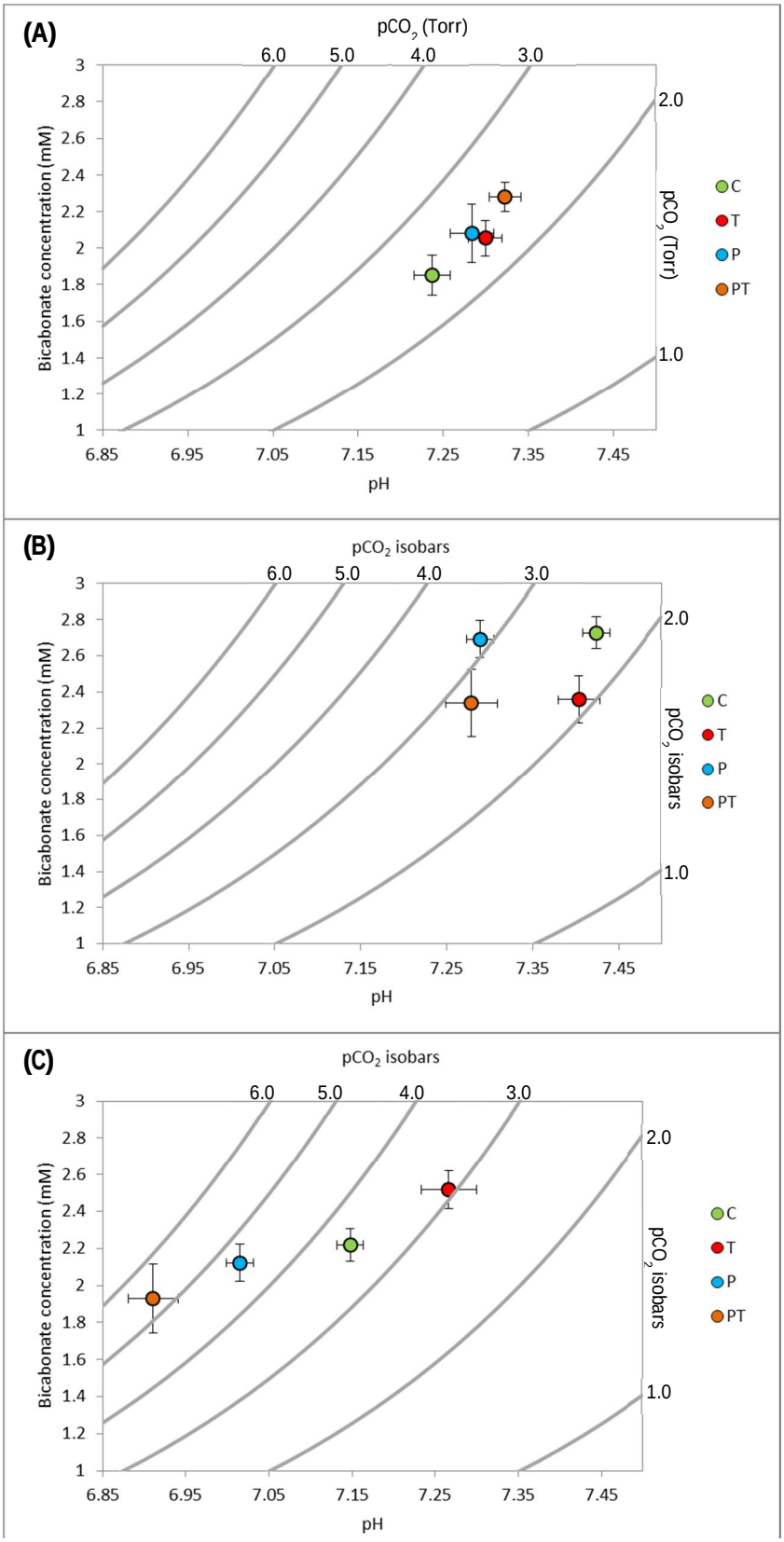

Figure 3.3.15. Davenport diagrams for haemolymph samples of adult *H. midae*, exposed to four seawater treatments (C=control, T=temperature, P=pH, PT=pH x temperature) for **(A)** 4-, **(B)** 8- , and **(C)** 12- months in a flow-through seawater system. The pCO_2 isopleths (grey lines) were derived from the Henderson–Hasselbalch equation. Appropriate values for the first dissociation constant (pK'1) and solubility coefficient (α) were derived from Truchot (1976). Values are means ± S.E. (1 Torr = 0.133 kPa).

3.4 Discussion

This experiment exposed abalone to four variable seawater conditions: ambient, increased temperature, lowered pH and the combination of increased temperature and lowered pH. The manipulated seawater parameters were applied to the natural variability within ambient seawater and maintained for 12 months. This experiment was conducted on an abalone aquaculture facility to provide realistic feedback for the South African abalone aquaculture industry. To the author's knowledge, this is the first study that will assess the effects of these treatments on *H. midae* growth, spawning pattern, and acid-base regulation.

Table 3.4.1. Summary of results reported as mean ± standard deviation for *H. midae* exposed to four treatments (C=control, T=temperature, P=pH, PT=pH x temperature) for 12 months. Means followed by the same letter(s) within a column are not significantly different ($p<0.05$).

Treatment	Wet Weight (g)	Muscle Mass (g)	PMB (%)	CF ($g.mm^{-1}$)	GBI ($g.mm^{-1}$)	Haemolymph pH	Haemolymph HCO_3^- ($mmol^{-1}$)
C	112.2 ± 14.3^{c}	66.14 ± 9.64^{a}	0.612 ± 0.028^{a}	1.12 ± 0.08	0.833 ± 0.285^{a}	7.15 ± 0.08^{a}	2.22 ± 0.24^{a}
T	113.6 ± 14.5^{b}	68.41 ± 10.11^{a}	0.613 ± 0.024^{b}	1.11 ± 0.08	0.734 ± 0.231^{ac}	7.27 ± 0.09^{b}	2.52 ± 0.31^{b}
P	102.6 ± 14.7^{b}	59.97 ± 10.15^{b}	0.624 ± 0.035^{b}	1.12 ± 0.07	0.551 ± 0.196^{b}	7.02 ± 0.06^{b}	2.12 ± 0.19^{b}
PT	105.0 ± 13.8^{b}	62.56 ± 10.06^{b}	0.623 ± 0.047^{b}	1.09 ± 0.07	0.665 ± 0.226^{bc}	6.91 ± 0.07^{b}	1.93 ± 0.26^{b}

Reduced seawater pH had the most pronounced effect on abalone growth in this study (Table 3.4.1). Abalone grown in variable, reduced pH conditions weighed 4.4 % less and had 4.9 % less muscle growth than abalone raised in ambient conditions after 12 months. *H. midae* grown in reduced seawater pH conditions displayed reduced PMB after 8 months but were able to recover to a similar PMB as abalone in the control treatment after 12 months, albeit with lower wet- and muscle mass. Reduction in weight is an indication of stress and was reflected in a lower GBI (- 20.3 %), absence/delay of spawning (as indicated by CF), and respiratory acidosis.

These findings concur with previous research on *H. midae* in reduced seawater pH in aquaculture facilities, which noted reduced growth as a result of reduced seawater pH. Naylor et. al. (2011) raised *H. midae* in a serial-use raceway where the pH of the seawater decreased in stages from 7.79 to 7.6 and observed a significant reduction in weight gain at reduced pH after 3 months. Similarly, Yearsley (2007) raised *H. midae* in a serial-use raceway with a serial decrease in pH from 8.3 to 5.9 over 104 days and noted a significant reduction in weight gain at lower seawater pH. These observations in serial-use raceways observed changes in multiple water parameters, such as pH, ammonia and temperature, but pH was still found to be the most significant contributor to observed reductions in weight.

A similar reduction in weight due to lowered seawater pH was also noted in the red abalone, *H. rufescens*. White (2011) reported a 9% lower wet weight in *H. rufescens* juveniles exposed to extended upwelling conditions (pH: 7.62 vs. 7.97) for 4 weeks. Research on *H. fulgens* and *H. tuberculata* response to lowered seawater pH do not correspond to the findings in this study. *H. fulgens* exposed to a reduced seawater pH (-0.3), offset to the variability of ambient seawater, had no significant decrease in tissue weight after 10 weeks (~2 months) of exposure to experimental

conditions (Lord et. al. 2017), although a meaningful change in weight would require a longer experimental period for a slow-growing species such as *H. tuberculata* (Forster 1967).

Reduced pH in isolation affected abalone acid-base regulation, indicating uncompensated respiratory acidosis after 12 months. Future studies could elaborate on the physiological processes that occur within *H. midae* during hypercapnia by monitoring haemolymph oxygen levels to substantiate these findings. The acid-base regulation of *H. midae* in this study concurs with the findings of Haupt et. al. (unpublished), which also noted uncompensated respiratory acidosis after 18 months of exposure to non-variable, reduced seawater pH (7.3). Novak (2012) has shown that *H. midae* are able to survive and recover from acute (24 hour) hypercapnic events by increasing haemolymph bicarbonate concentrations. Venter et. al. (2018) studied the metabolic response of *H. midae* to hypoxic conditions and noted that *H. midae also* have well developed metabolic mechanisms for surviving short-term (6 hours) hypoxic events. *H. midae* metabolism shifted to catabolic processes in order to maintain cell homeostasis, resulting in amino acid metabolism, most predominantly in the adductor muscle (Venter et. al. 2018). Presumably, *H. midae* were initially able to maintain acid-base regulation during exposure to lowered seawater pH due to this well-developed metabolic response, but were not able to maintain homeostasis over longer periods. Amino acid metabolism as a homeostatic response to hypoxia and presumably hypercapnia, would explain the significant reduction in muscle mass when *H. midae* were exposed to hypercapnic conditions. Reduced seawater pH (pH =7.3, as opposed to ambient conditions of 8.05) caused a similar response in the growth of Mediterranean mussels, *Mytilus galloprovincialis* (Michaelidis et. al. 2005). *M. galloprovincialis* juveniles displayed reduced soft tissue growth when exposed to hypercapnic conditions for 3 months. *M. galloprovincialis* also displayed an increase in haemolymph bicarbonate concentrations and permanent reduction in haemolymph pH after 3 months of exposure to hypercapnic conditions. The majority of calcifying invertebrates respond to acidic conditions with a decrease in shell and wet weight (Byrne & Przeslawski 2013, Hoegh-Guldberg et. al. 2014, Przeslawski et. al. 2015).

Further investigation into the metabolic changes that occur in *H. midae* during long-term hypercapnia would help predict metabolic responses and make it possible for aquaculture facilities to intervene accordingly with recovery diets and supplements during low pH events, as can be accomplished during hypoxic events (Venter et. al. 2018). During stressful events, metabolism shifts from anabolic activity towards catabolic processes to uphold adenosine triphosphate (ATP) supply to living cells for growth, reproduction and metabolic regulation (Salway 2004, Garrett & Grisham 2010, Sokolova et. al. 2012, Venter et. al. 2018). Knowledge on holistic metabolic responses of abalone during long-term, variable, hypercapnic conditions is scarce. An investigation into the metabolite and oxygen profiles of *H. midae* during long-term hypercapnia can provide insight into the energy sources used and required during these conditions and a recovery diet can be formulated using this information (Venter et. al. 2018).

Prolonged metabolic stress and reduced growth may have resulted in reduced GBI after 12 months of exposure to low pH conditions. It is highly plausible that energy may have been diverted from gonad development and growth towards homeostasis. Aalto et. al. (2020) noted that *H. fulgens* fecundity scaled with abalone size, revealing that a decrease in growth rate or maximum size due to environmental stressors had disproportionate effects on larval production in adult *H. fulgens* populations. This study has interpretational limitations on GBI analysis as the data was only obtained

at the end of the experimental period, February 2016, where GBI has been shown to be lower than most months (Wood & Buxton 1996). It is recommended that future studies increase the number of GBI assessments or, if samples can only be obtained at a singular time period, to assess GBI in May as Wood & Buxton (1996) have shown that GBI tends to peak in May.

This study concluded that the combination of two seawater parameters, increased temperature and reduced pH, resulted in similar findings to the reduced pH treatment with significant reductions in *H. midae* wet- and muscle- mass (and CF), PMB, GBI, and induced severe respiratory acidosis in comparison to those in ambient conditions. The observed metabolic stress suggests that limited energy may remain for other metabolic demands such as growth, reproduction and/or behaviour (Sokolova 2013) and may explain the reduced growth observed in this study. An increase in seawater temperature did not act antagonistically or synergistically with the stress of reduced seawater pH as none of the effects on growth and haemolymph parameters were significantly different to the effects of lowered seawater pH alone. This concurs with the observed effects of increased temperature on *H. midae*. The increase in seawater temperature was within *H. midae*'s thermal tolerance limits (elevation by 1.51±0.02 °C) and had no significant effect on abalone growth, although the increase in temperature did non-significantly improve wet weight and muscle mass by 1.2% and 3.4 % respectively in comparison to those in ambient conditions, and non-significantly improved wet weight and muscle mass of abalone exposed to the pH x temperature treatment by 2.4 % and 4.2 % respectively in contrast to the low pH treatment. Non-significant weight increases are not in accordance with previous research on *H. midae* exposed to constant elevated temperatures. Britz et. al. (1997) observed a significant increase in *H. midae* mass with an increase in constant temperatures between 12 and 20 °C after 3 months; a larger temperature differential and shorter experimental period than the current study. Britz et. al. (1997) also observed a decrease in growth rates and food consumption in abalone exposed to constant temperatures between 20 - 24°C. Vosloo & Vosloo (2010) observed a decrease in oxygen consumption, and reliance of carbohydrates as a food source with an increase in temperature from 16 - 22 °C after 3 months of exposure to constant temperatures. Vosloo & Vosloo (2010) reported an increase in muscle protein with an increase in stable temperatures between 19 and 22 °C after 1 month of exposure; however no significant increase in muscle mass was evident in the current study which had dynamic seawater temperatures and a longer experimental period.

The results of the current study concur with the effect of variable, increased temperature (+2 °C) on the green abalone *H. fulgens* (Lord et. al. 2017). Increased temperature did not significantly affect *H. fulgens* tissue weights or shell:tissue ratios after 2 months of exposure to experimental conditions. In an earlier study, the green abalone, *H. fulgens*, displayed increased growth when exposed to warmed effluent seawater within optimal growth range of 24-28 °C for 3 months (Leighton et. al. 1981) and in a 49-week (~11 month) study using variable water temperatures within optimum thermal conditions (2.5 °C above 4-18 °C) for *H. fulgens* (Vilchis et. al. 2013), the green abalone displayed similar responses to *H. midae*; green abalone were robust to changes in temperature and maintained growth. Constant temperature experiments contrast the findings of variable seawater parameters. When exposed to constant seawater temperatures of 25 °C in comparison to 20 °C, *H. fulgens* displayed a higher meat to body mass ratio after 2 weeks (Garcia-Esquivel et. al. 2007). These findings indicate a strong need for natural seawater pH and temperature variability to be

incorporated in future studies rather than the use of static systems. For more realistic representations on abalone responses to climate change, experimental changes to seawater chemistry would need to be incorporated into the natural variability of the environment that the subject inhabits, although this method reduces reproducibility of results and strict control over water parameters (Branch et. al. 2013, Baumann 2019). All previous thermal research on *H. midae* is based on constant thermal experiments, thus not entirely applicable to aquacultural practices or natural systems. Previous thermal research on *H. midae* growth in constant conditions reflects inflated growth over shorter periods of exposure time. Previous research on the effects of lowered pH seawater on *H. midae* (Naylor et. al. 2011, Yearsley 2007) have incorporated natural environmental variability to their experimental design, but did not incorporate or maintain a fixed pH parameter in the design to allow for further insight into the quantitative effects of reduced pH seawater on *H. midae*. The results still reflect a similar finding of reduced growth in abalone exposed to more acidic conditions.

H. midae did display a non-significant increase (2.27 %) in proportion of meat to body mass as a result of increased temperatures, however this increase was not seen in abalone exposed to the pH x temperature treatment in comparison to the low pH treatment, either due to dissolution of the aragonitic shell in low seawater pH (Chapter 4) or an increase in gut content as seen by an increase in feeding rate when *H. fulgens* is exposed to warmer seawater (Lord et. al. 2017). Increased seawater temperature non-significantly reduced abalone GBI (-12.6 %) in comparison to ambient conditions, however the addition of lowered pH in combination with increased temperature significantly increased GBI (+ 18.8 %) in comparison to the low pH treatment. Patterns in CF indicate that an increase in seawater temperature did not alter spawning period (October – November 2015). It is possible that GBI was affected by the imbalance in acid-base regulation and resulted in a divergence of energy from gonad development towards homeostasis. An increase in GBI when exposed to both low pH and increased temperature could be due to the lack of a spawning event as observed by CF patterns. This study looked at secondary indicators of spawning events, not direct observation of spawning events. Future studies will need to monitor egg and sperm releases to determine actual changes in spawning patterns and could benefit from including qualitative and quantitative measure of egg/sperm production. Abalone haemolymph analysis used small sample sizes due to time constraints on haemolymph viability. Haemolymph analyses were processed at a separate location and larger sample sizes would not have been able to be sampled in a timely manner before the haemolymph congealed, which would not have been viable for processing in the infrared-CO_2 analyser. Potential solutions to this may be duplicate machines set up closer to the experimental site. Despite smaller sample sizes, the results were still statistically significant.

In conclusion, it appears that under near-future climate change conditions, ocean acidification will pose a greater risk to *H. midae* growth, reproduction and acid-base regulation than warming, in the largest abalone aquaculture area of South Africa. Reduced pH seawater significantly reduced haemolymph pH, resulting in respiratory acidosis and a reduction in whole body- and muscle- mass (and PMB), and GBI of the commercially important South African abalone. Warming by 1.5 °C above ambient did not have any significant effects on abalone growth; however acid-base regulation was more stable over the course of the study. An increase in temperature acted synergistically with reduced pH seawater by significantly affecting acid base regulation, resulting in severe

uncompensated respiratory acidosis after 12 months of experimental conditions. Warming, in combination with reduced pH, increased *H. midae* GBI by 18.8 % in comparison to exposure to reduced pH alone. This indicates that natural populations will likely have a better reproductive output when incurring both ocean acidification and warming, however the survival of offspring may be severely affected, as seen in previous studies on abalone larvae under ocean acidification and warming conditions (Byrne et. al. 2011b, Crim et. al. 2011, Kimura et. al. 2011, Przeslawski et. al. 2015, Li et. al. 2018). An 8.9 % decrease in abalone growth and 9.8 % decrease in muscle growth under ocean acidification conditions are of particular concern for the South African abalone industry. Cultivated abalone will grow more slowly, increasing cultivation time and the costs associated with animal husbandry. The metabolic stress in *H. midae* associated with ocean acidification is also likely to increase abalone susceptibility to disease and parasite load (Cheng et. al. 2004).

CHAPTER 4:
The Influence of Warmed and Acidified Seawater on Abalone, *Haliotis midae*, Shell Morphology, Strength, and Mineralogy

4.1 Introduction

Mollusc shells offer vital protection from predators and environmental stressors (Lowenstam & Wiener 1989) and an impairment in the production of biomineral skeletons can also affect metamorphosis and growth (Byrne 2011, Byrne et. al. 2011b, Gazeau et al. 2013; Kroeker et al. 2013, Pzreslawski et. al. 2015, Fassbender et al. 2016). The influx of anthropogenic CO_2 into the atmosphere since the industrial era is being absorbed by the oceans, a natural carbon sink, with a resultant decline in the oceans' average pH (See chapter 1). This gradual decline in pH and continuing predicted decline by the year 2100 (-0.4) is known as ocean acidification (Hoegh-Guldberg et. al. 2014). Ocean acidification has the potential to negatively affect the biomineralisation of calcium carbonate skeletons and shells in most calcifying organisms due to lowered aragonite and calcite saturation states (Byrne 2011, Byrne et. al. 2011b, Byrne & Przeslawski 2013, Gazeau et al. 2013; Kroeker et al. 2013, Pzreslawski et. al. 2015, Fassbender et al. 2016, Kocot et. al. 2016). Bivalves and gastropods tend to have some regulatory control over biomineralisation by means of active and passive ion exchange from mineralization sites to deposition sites (either within or between cells) separate from ambient seawater (Wiener & Dove 2003). The energetic costs involved during metabolic regulation in stressor events, such as ocean acidification, and the duration for which they can be sustained before metabolic failure is species-specific and reliant on the environment that the organism is conditioned to (Vargas et. al. 2017). Organisms that reside in highly variable environments, such as intertidal and upwelling systems, are expected to be more metabolically robust to environmental stressors, such as ocean acidification (Duarte et. al. 2013, Vargas et. al. 2017, Cornwall et. al. 2018, Baumann 2019). However, with the sparse research on long term exposure to stressors and potential multi-generation adaptation/resilience of species it is hard to predict realistic responses of organisms to expected environmental challenges (Baumann 2019). Whilst ocean acidification is expected to have the largest influence on *Haliotis midae* shell growth, another factor to consider is gradual warming of the atmosphere and oceans. The changes in gastropod shell microstructure and mineralogy caused by thermal stress has been poorly investigated (Zheng et. al. 2020). To date, no studies have researched the effects of reduced pH or warmed seawater and the combination of these two factors on juvenile or adult *H. midae* shells either in a static system or a variable system.

4.1.1. Shell mineralogy and composition

Abalone shells are composed of intricate mixtures of calcium carbonate crystals in the form of calcite and aragonite bound together with proteins (Auzoux-Bordenave et. al. 2010, Marie et. al. 2010). A thin shell-forming tissue, the periostracum, is responsible for the extracellular production of the shell (Jackson et. al. 2006). The mantle margin of the shell secretes the periostracum and mineralises the prismatic layer at the shell margin (Figure 4.1, Jardillier et. al. 2008, Auzoux-Bordenave et. al. 2010). The mantle underlying the shell progressively accretes aragonitic nacreous shell across the entire inner shell, which therefore thickens over time (Menig et. al. 2000). Environment, behaviour

and nutritional status influence the rate of prismatic growth at the shell margin compared to nacreous thickening, in turn influencing shell morphology (Auzoux-Bordenave et. al. 2010). The proportion of aragonite in bulk shell mineralogy for the genus *Haliotis* ranges from 50-100 % (Lowentam 1954), indicating that abalone are potentially a monomineralic species (produce a predominant proportion of one calcium carbonate polymorph in comparison to another). This larger proportion of aragonite in comparison to calcite makes abalone potentially more susceptible to dissolution under ocean acidification conditions (Busenberg & Plummer 1986).

The shell acts as both a protective covering for the animal's soft tissues as well as a reservoir of calcium ions that can move from the shell to the circulatory system and back (Lowenstam & Wiener 1989). There are substantial uncertainties regarding the possible impacts of ocean acidification on shell polymorph mineralogy (Ries 2011). Ries (2011) investigated the effects of seawater bubbled with air-CO_2 mixtures of 409, 606, 903, and 2856 pCO_2 on 18 monomineralic and bimineralic calcifying species (species that produce comparable proportions of calcium carbonate polymorphs) for 60 days. They determined that calcite/aragonite ratios in bimineralic species increased significantly with increasing pCO_2, but were invariant in monomineralic species. Several species have displayed a reduction in calcification in response to ocean acidification scenarios (Fabry et. al. 2008) and some have been shown to upregulate calcification processes (Rodolfo-Metalpa et. al. 2010). Lowenstam (1954) showed that aragonite/calcite ratios increased with an increase in temperature in some species, but the effect varied by taxonomy, geographic- and climatic distribution.

A consistent change in shell appearance and mineralogy have been noted among various abalone species after exposure to reduced seawater pH. Avignon et. al. (2020) noted that *Haliotis tuberculata* adults exposed to a constant seawater pH of 7.7 (control: 8.0) for 5 months had a paler periostracum in comparison to individuals in the control treatment. Avignon et. al. (2020) also noted that the periostracum of individuals exposed to the reduced seawater pH treatment had an irregular and corroded surface which revealed biomineral characteristic of the underlying spherulitic layer and corroded aragonitic layers. Similarly, the shells of 1-year-old Pacific abalone, *Haliotis discus hannai*, displayed corroded aragonite plates with irregular structures after 9 days of exposure to constant, lowered (ambient: 8.1, reduced: 7.8 & 7.5) seawater pH (Zheng et. al. 2020). Zheng et. al. (2020) also determined that the gene expression of two nacre proteins (Hdh-AP7, Hdh-AP24), which directly affect shell crystal formation, were more sensitive to thermal stress (ambient: 20 °C, warmed: 24°C & 26 °C) than to acidification. Li et. al. (2018) noted that large areas of 5-month-old *Haliotis discus hannai* shells presented with large-scale exposure of the nacreous layer and large areas without a periostracum after 3 months of cultivation at a seawater pH of 7.7 (control: 8.1). White (2011) noted paler shells of *Haliotis rufescens* juveniles after 4 weeks of exposure to a static seawater pH of 7.62 (control: 7.97). No research has previously been conducted on the effects of ocean acidification and warming on *H. midae* shell mineralogy.

4.1.2. Shell growth and morphology

Shell morphology is defined as a result of a cumulative growth process of biomineral accretion (Réaumur 1716, Thompson 1942, Lowenstam & Wiener 1983). Béguinot (2014) explains the importance of animal adaptation and survival due to functionally relevant shell shape parameters, but notes that animals only have indirect control over these parameters via growth accretion. In an

aquaculture context, abalone shell morphology has little economic value except to influence the value of the abalone if sold live, but the shape of the pedal muscle can influence buyer preference for dried abalone. Assuming that the shape of the pedal muscle is influenced by the shape of the shell (e.g. an elongated shell will produce an elongated pedal muscle) a change in the shape of the animal could indirectly impact economic value of the meat. To date, no studies have researched the effects of seawater temperature and pH on abalone shell shape.

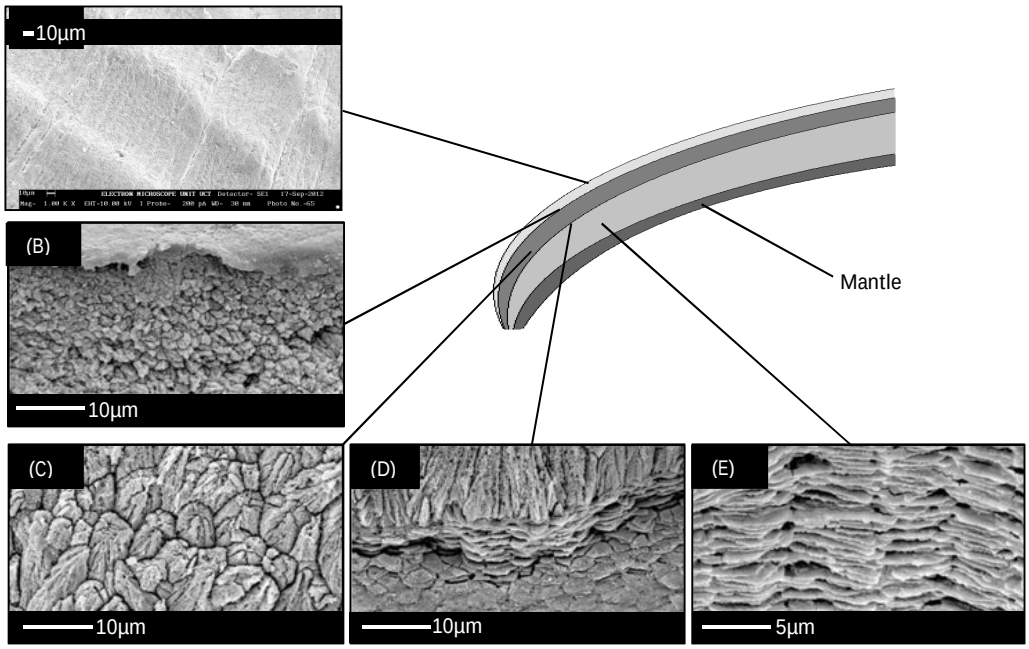

Figure 4.1. Simplified diagram of *H. midae* shell composition. SEM micrographs illustrate the: **(A)** periostracum in oblique view; **(B)** boundary between the periostracum (top) and prismatic calcite (bottom); **(C)** prismatic calcite layer; **(D)** boundary between calcite (top) and aragonite (bottom); and **(E)** the nacreous aragonitic layer. SEM micrographs B-E were modified from Marie et. al. (2010).

Shell growth is expected to be affected by ocean acidification as this is a common result in most studies on abalone and ocean acidification. Adult *H. tuberculata* display reduced shell length when exposed to 5 months of ocean acidification conditions (ambient: 8.0, reduced: 7.7), however acidification did not affect shell weight or thickness (Avignon et. al. 2020). Reddish-rayed abalone (*Haliotis coccoradiata*) larvae are highly sensitive to warming and acidification of the oceans (Figure 4.2). Larvae that were reared under static warmed (+ 2 °C, 4°C) and reduced pH (7.6, 7.8) conditions, and the combination of these two stressors exhibited the inability to form shells with the appearance of morphological abnormalities under severe conditions after 21 hours of exposure (Byrne et. al. 2011b). *Haliotis kamtschatkana* larvae exposed to static reduced pH conditions (1800 ppm vs 800 ppm CO_2) exhibited reduced shell sizes, shell abnormalities and formation without shells (Crim et. al. 2011). *H. rufescens* juveniles (4-5 months) that were exposed to static reduced pH conditions (pH 7.5 vs 8.0) twice for 24hours over 15 days exhibited negative shell growth and an increase in the variation of individual growth rates (Kim et. al. 2013). Larval *Haliotis diversicolor* and *H. discus hannai* showed a significant decrease in shell length with an increase in pCO_2 comparable with predicted ocean acidification conditions after 24 hours (Guo et. al. 2015). Similar findings were presented when juvenile *H. discus hannai* were exposed to static hypercapnic conditions (pH: 8.1 vs

7.9, 7.7) for 3 months and displayed reduced shell growth and eroded shell surfaces (Li et. al. 2018). These results are similar to the findings of Kimura et. al. (2011) in a study on the effects of ocean acidification conditions on *H. discus hannai* larvae, which noted smaller, malformed larvae after 15 hours of exposure to static hypercapnic conditions (450 vs 1650 and 2150 µatm pCO_2). Diurnal fluctuations in seawater pCO_2 from 800 to 1200 µatm resulted in greater negative impacts, in comparison to a constant pH, on the shell growth of *H. discus hannai* (Onitsuka et. al. 2018). Larval *H. tuberculata* exposed to lowered pH conditions (8.0 vs 7.8 , 7.7) for 5 days also displayed a reduced shell growth rate, an increase in developmental abnormalities and reduced survival (Wessel et. al. 2018).

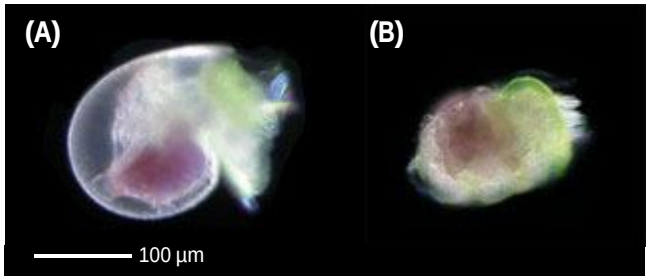

Figure 4.2. *H. coccoradiata* larvae under **(A)** ambient conditions and **(B)** warmed (+4 °C) and acidified (7.6) conditions after 21 hours (Byrne et. al. 2011b).

4.1.3. Shell Strength

Abalone shells consist primarily of aragonitic nacre, which is of particular interest due to its combination of strength and fracture toughness (Espinosa et. al. 2011). *H. rufescens*, shells have a mean compressive strength of between 300 – 500 $N.mm^{-2}$ (Meyers et. al. 2008) and the compressive strength is estimated to be 1.5 – 3 times the tensile strength of the shell (Menig et. al. 2000). The compressive strength of adult *H. tuberculata* shells, measured in a similar fashion to the current study, was significantly weaker (200 N vs 281 N) after 5 months of exposure to constant, reduced (-0.3) seawater pH (Avignon et. al. 2020).

Although no studies to date have assessed the effects of low pH and warming on *H. midae* shells, there have been reports on the strength of other marine calcified shells. A study on mussel, *Mytilus edulis*, shell strength noted that warming (+4°C) reduced shell strength more than acidification (-0.4 pH) after 6 months of exposure to experimental conditions (Mackenzie et. al. 2014). A study on the pteropod, *Limacina helicina antarctica*, noted that the mechanical properties of one species cannot be inferred from that of another species due to the possible difference in orientation of the calcitic structures (Tenniswood et. al. 2013) and comparisons between species could be insightful in species adaptation.

A reduction in shell strength can impact *H. midae* defence against predators in natural habitats and increase the risk of shell damage during handling on aquaculture facilities. Tarr (1995) noticed that shell growth in *H. midae* was abnormally slow in abalone that had experienced shell damage due to natural causes and parasitic boring by the sabellid polychaete, *Terebrasabella heterouncinata*. There

are no studies to date on the direct impact of shell damage on *H. midae* growth, however if shell damage is directly linked to retarded growth then aquaculture facilities could expect reduced growth rates in abalone with reduced shell strength, and an increase in poorer quality abalone due to broken shells.

4.1.4. Aims and objectives

This study aims to assess the impacts of variably warmed- (+1.5 °C above ambient) and acidified (-0.4 units below ambient) seawater in comparison to variable ambient seawater conditions, in isolation and combination, on *H. midae* shell morphology, integrity and mineralogy over 12 months with repeated measurements of shell length and width, and shell strength every four months. Mineralogical analyses were performed on shells that had been exposed to experimental conditions for 12 months. This study will provide valuable insight into how the predicted future changes in seawater, due to ocean acidification and seawater warming, will affect the formation and maintenance of *H. midae* shells. This study was conducted on an abalone aquaculture facility to provide realistic responses of *H. midae* to predicted global warming scenarios and to provide operational feedback for abalone aquaculture facilities.

This study hypothesises that shell length, and hence shell weight, will decrease when abalone are exposed to hypercapnic conditions due to multiple studies on abalone species that show a decrease in shell length when exposed to lowered seawater pH (Guo et. al. 2015, Kim et. al. 2013, Crim et. al 2011, Kimura et. al. 2011, Avignon et. al. 2020). *H. midae* shells are hypothesised to increase in length when abalone are exposed to warmed temperatures within their thermal optimum range (Vosloo & Vosloo 2010, Britz et. al. 1997, Tarr 1995), and an increase in precipitation rates of aragonite are expected with an increase in seawater temperature (Burton & Walter 1987). The exposure of abalone to warmed and acidified seawater is hypothesised to reduce shell length due to larger negative impacts by acidified seawater as the increased temperature is within the thermal optimum range for *H. midae*, assuming that warming does not act synergistically with reduced pH. The combined effects of acidification and warming on width and shape are largely uncertain as no studies to date have assessed these effects on abalone shell shape, although Melatunan et. al. (2013) did record a reduction in shell length and change in shape of predatory sea-snail *Limacina helicina* shells exposed to a static increase in seawater temperature (15 °C vs 20 °C) and decrease in seawater pH (7.7 vs 8.0) by means of bubbled CO_2 (1000 ppm vs 380 ppm). Thus, this study hypothesises a decrease in shell shape (length:width) when abalone are exposed to variable hypercapnic conditions, intrinsically and in conjunction with an increase in temperature, with no change in shell shape when abalone are exposed to an isolated increase in variable seawater temperature.

H. midae shell strength is hypothesised to decrease when abalone are exposed to hypercapnic conditions due to dissolution of the shell, similarly to *H. tuberculata* when exposed to ocean acidification conditions (Avignon et. al. 2020). The strength of the shell is not hypothesised to increase in warmer conditions as an increase in temperature increases the precipitation rates of aragonite and calcite (Burton & Walter 1987), possibly making the shells thicker, heavier and more resilient to compression. Zheng et. al. (2020) noticed that the genes responsible for aragonite crystal

formation in *H. discus hannai* were sensitive to increased temperatures, however the experimental temperatures used for their study were much greater than the 5th assessment IPCC report expects (Hoegh-Guldberg et. al. 2014). Following these hypotheses, shell strength is expected to decrease when abalone are exposed to multi-factor conditions due to a larger effect of dissolution on the shells in acidified conditions. Increased temperatures in conjunction with reduced pH conditions may partially mitigate the effects of dissolution under reduced pH conditions as the experimental temperatures are within the optimal thermal range of *H. midae* (Vosloo & Vosloo 2010, Britz et. al. 1997, Tarr 1995).

This study does not hypothesise a change in shell mineralogy in terms of calcite and aragonite concentrations due to the predominantly monomineralic structure of the abalone shell when abalone are exposed to warmed, hypercapnic or multi-factor conditions (Ries 2011). A change in calcite weight percentage was determined in a study on 14-month-old *H. iris* after exposing the abalone to reduced seawater pH (7.66) in contrast to local ambient seawater pH (8.00) for 4 months (Cummings et. al. 2019). This decline was attributed to the degree of exposure of calcitic layers of the shell to seawater. There was no significant change in aragonite weight percentage, contrary to expectations due to aragonite's higher solubility constant, but this was attributed to there being no direct contact between aragonitic layers and seawater. In a study by Auzoux-Bordenave et. al. (2020), 3-month-old *H. tuberculata* were exposed to stable pH treatments ranging from the global average seawater pH of 8.1 to 7.6, the extreme predicted decline in global ocean pH. After 3 months of exposure, *H. tuberculata* shells exposed to a pH of 7.6 displayed a significant decline in length, weight, and strength as well as a degradation of the inner aragonitic layer as identified by SEM photography. This potential degradation of the inner aragonitic layer could affect *H. midae* shells, although the abalone used in this study are more mature with thicker, more robust shells and less likely to experience changes to the inner layer of the shell.

4.2. Methods

See Chapter 2 for experimental design, animal husbandry and general methods.

4.2.1 Factory processing and shell measurements

Abalone were shucked and processed at the Aqunion Processing Facility (Hermanus, South Africa). Factory processing occurred every 4 months directly after size-grading on the aquaculture facility (See Chapter 3 for size-grading procedures). The shells assessed in this Chapter correspond to the individuals measured in Chapter 3. Abalone shells were weighed (to 0.01 g) using an electronic scale (Kern PLS 4200-2F). The shells were rinsed with seawater and placed in plastic bags prior to drying. The maximum width and length of the shells were measured using Vernier callipers (0.01 mm). Shell area was calculated as an approximate area using the formula: $Area = Length_{max} \times Width_{max}$. Shell shape was represented by the length:width ratio of the shells. Shells were laid out on a plastic sheet and dried at room temperature (16-21°C) in a dark room, without exposure to sunlight, for one week after shucking before being placed into individual bags and stored in a dark cupboard until shell compression tests were performed on them.

4.2.2 Shell Compression

An estimate of shell (compressive) strength for shells collected during factory processing was determined by measuring the maximum load, in Newtons (N), that each shell could endure during compression. This was assessed using a Zwick Universal testing machine (Model 1484, 100 kN load cell, Germany; Welladsen et al. 2010) at the University of Cape Town. Shells were individually placed on the flat, steel testing stage (1400 x 630 mm) with apex on the left and nacre facing the stage. The machine's steel piston, parallel to the stage descended at a rate of 2mm/min until the shell reached a failure point where a maximum force was applied. This force was recorded using Zwick/Roell TestXpert II (Germany) software.

4.2.3 Shell mineralogy

After compression, randomly chosen shells (n=20 per treatment) exposed to 12 months of experimental conditions were milled into a crystalline powder for quantitative mineral analysis by X-ray Diffraction (XRD) at the University of Cape Town. The shells did not undergo any form of pre-treatment prior to milling or XRD analysis (Smith et. al. 2016). Shells were individually broken into smaller fragments using a 2" x 6" BAER Sturtevant steel jaw crusher (Laboratory series, Christy Turner, UK) which ran at 120 cycles per minute for 5-10 seconds per shell. This was followed by further milling using a carbon steel Sieb mill which ran at 400 revolutions per minute for less than 10 seconds per shell until a fine crystalline powder was obtained. Milling times were kept to a minimum to prevent the inversion of aragonite to calcite by heat transfer (Davies & Hooper 1963, Smith et al. 2016, Lopičić et al. 2019). The powder was stored in airtight, plastic bottles to prevention absorption of moisture (Hoque et al. 2013). The steel jaw plates, collection containers, orbital discs and mill were cleaned thoroughly between shell samples using pressurized air and acetone to prevent cross-contamination of samples (Gray & Smith 2004).

XRD analysis was performed on the powder samples using a D8-Advance diffractometer (Bruker AXS) equipped with a cobalt source (λ = 1.789 Å) and position sensitive detector (LynxEye-XE Bruker AXS). Patterns were collected between 20 and 120˚ 2Θ with a step size of 0.037˚and a total scan time of 56 minutes and 19 seconds. To improve collection statistics the samples were rotated at 15 rpm during measurement. The obtained diffraction patterns were compared to entries in the ICDD PDF-2 2008 database. The diffractometer was able to queue 90 samples at any given time. Quantitative analysis of the composition as well as the crystallite sizes of the respective phases was obtained by a full pattern fitting using a Rietveld refinement methodology (software package Topas 5, Bruker AXS). From these measurements, XRD provided the percentage weight of calcite and aragonite relative to total calcium carbonate within the sample as well as average crystalline diameters of both calcite and aragonite in the sample.

4.2.4 Statistical analysis

To determine whether shell weight, shell length, shell width, shell area, percentage weight of aragonite, and diameter of aragonite and calcite crystals changed as a function of time within individual treatment groups, the *lme* function from the *nlme* package (Pinheiro et. al. 2016) in R (The R Core Team, 2012) was used to create linear mixed effects models. The response variable was transformed in the case of non-normal data distribution (Table 4.2.2). Residual spread and homogeneity of variances was tested by applying a Bartlett test to each model (Table 4.2.2). Temporal autocorrelation was determined by means of autocorrelation function (ACF) plots (Table 4.2.2). Model selection was determined using AIC values for each response variable (Table 4.2.3).

Table 4.2.2. Transformations and model assumption tests for linear mixed effects models.

Response Variable	Data Transformation	Bartlett Test	Variance structure	Autocorrelation Structure	Rho
Shell Weight	Logarithmic	K^2=1.862, df=3, p=0.60	None	CompSymm	0.84
Shell Length	None	K^2=2.899, df=3, p=0.41	None	AR1	0.35
Shell Width	None	K^2=1.156, df=3, p=0.76	None	AR1	0.28
Shell Area	Logarithmic	K^2=3.962, df=3, p=0.27	None	AR1	0.43
Percentage weight of aragonite	None	K^2=6.471, df=3, p=0.09	None	N/A	N/A
Diameter of aragonite crystals	None	K^2=0.776, df=3, p=0.86	None	N/A	N/A
Diameter of calcite crystals	None	K^2=2.393, df=3, p=0.50	None	N/A	N/A

Table 4.2.3. Linear mixed effects models used to determine the effect of treatment over time for *H. midae* exposed to four treatments over a 12 month period.

Response Variable	Formula	Random Effect	AIC
Shell Weight	y ~ Treatment * Time	1+Time|Tank	-1090.93
Shell Length	y ~ Treatment * Time	1+Time|Tank	5098.15
Shell Width	y ~ Treatment * Time	1+Time|Tank	4604.13
Shell Area	y ~ Treatment * Time	1+Time|Tank	-1944.95
Percentage weight of aragonite	y ~ Treatment	1|Tank	293.35
Diameter of aragonite crystals	y ~ Treatment	1|Tank	434.05
Diameter of calcite crystals	y ~ Treatment	1|Tank	530.34

To determine whether non-linear data such as: shell shape and compressive force changed as a function of time within individual treatment groups, the *gam* function from the *mgcv* package (Wood 2003, Wood 2011, Wood et. al. 2016) in R (The R Core Team, 2012) was used to create a generalized additive mixed effects models. The response variable was transformed in the case of non-normal data distribution (Table 4.2.4). Model selection was based on model fit (R^2-values) and the generalized cross-validation statistic (GCV) of GAM models (Table 4.2.5). Residual spread and homogeneity of variances was determined by residual plots of the response and fitted values of the model (Table 4.2.4).

Table 4.2.4. Transformations and model assumption tests for generalized additive mixed effects models.

Response Variable	Data Transformation	Residual Plot
Shell Shape	Logarithmic	Homogenous
Compressive Force	Logarithmic	Homogenous

Table 4.2.5. Model fit statistics for generalized additive mixed effects models.

Response Variable	GCV	R 2
Shell Shape	0.001838	0.036
Compressive Force	0.067665	0.276

4.3 Results

4.3.1 Seawater Parameters

Mean seawater carbonate chemistry parameters are presented in Chapter 2. Ambient seawater temperature was 15.64±2.16 °C for the duration of the experiment and followed natural environmental variations. Average heated seawater temperature was 17.16±2.16 °C in the temperature treatment tanks and 17.19±2.17 °C in the pH x temperature treatment tanks, offset to natural environmental temperature variations. Ambient seawater pH was 8.10±0.06 for the duration of the experiment and followed natural environmental variations. Average CO_2-diffused seawater pH was 7.66±0.07 in the pH treatment tanks and 7.66±0.08 °C in the pH x temperature treatment tanks, offset to natural environmental pH variations. Salinity was 35.5±0.03 in all experimental tanks and remained fairly stable for the duration of the experiment.

4.3.1. Shell Growth and Morphology

Abalone shell growth and morphology is represented by shell weight (Figure 4.3.1), length (Figure 4.3.2), width (Figure 4.3.3), shape (Figure 4.3.4), and area (Figure 4.3.6).

Treatment had a significant effect on abalone shell weight over the course of the study (df=16, F=21.2, p<0.01). Shells from the control treatment (28.43±3.74 g) and temperature treatment (29.27±4.04 g) were significantly heavier than shells from the pH (24.13±3.34 g) and pH x temperature treatments (25.26±3.24 g) after 12 months (Table 4.3.1). There was no significant difference between shells from the control and temperature treatments or between those from the pH and pH x temperature treatments (Table 4.3.1).

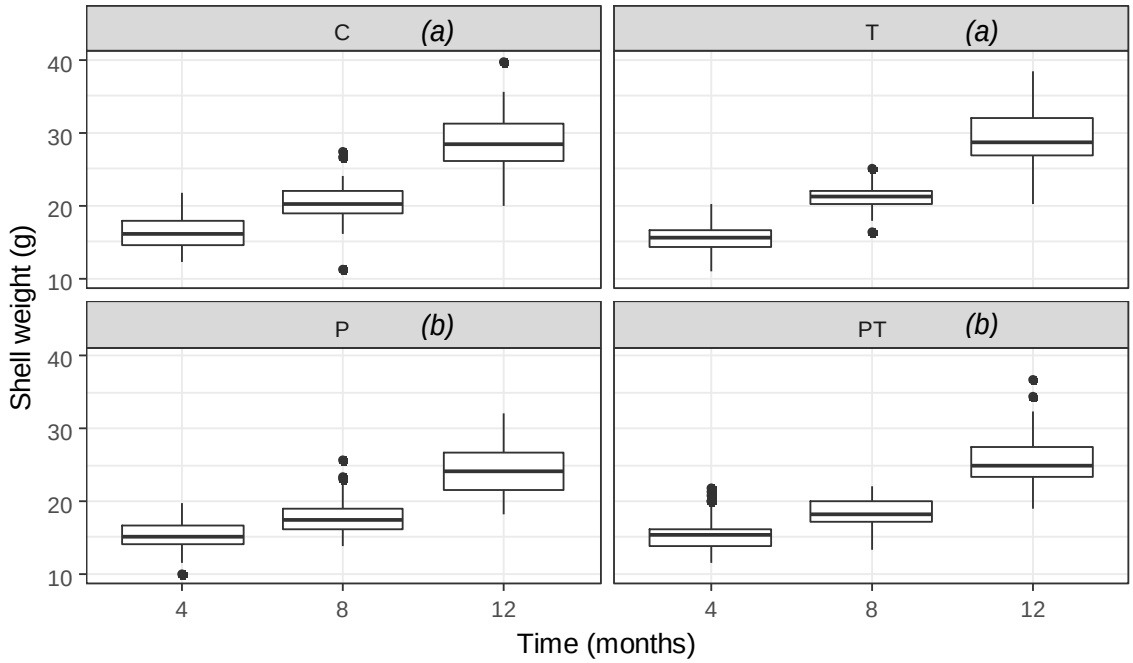

Figure 4.3.1. Boxplots of the shell weights (± standard deviation) of abalone, *H. midae*, exposed to four treatments (C=control, T=temperature, P=pH, PT=pH x temperature) over a 12-month experimental period in a flow-through seawater system. Each treatment group contains repeated measurements at 0-, 4-, 8-, and 12-month sampling times. Same letters in italics between treatments denotes no statistical difference between treatments (alpha = 0.05).

Table 4.3.1. Pairwise differences of abalone shell weights between four treatments (C=control, T=temperature, P=pH, PT=pH x temperature) using the Tukey method to compare family estimates. Significant values are taken at the 5% level and shaded in grey.

Contrast Treatments	Comparison (g)	Comparison (%)	Degrees of Freedom	t-ratio	p-value
C - T	-0.84	-2.9%	16	-0.175	1.00
C - P	4.30	16.4%	16	6.061	<0.01
C - PT	3.17	11.8%	16	4.442	<0.01
T - P	5.1	19.3%	16	6.236	<0.01
T - PT	4.01	14.7%	16	4.617	<0.01
P - PT	-1.13	-4.6%	16	-1.619	0.40

Treatment had a significant effect on abalone shell length over the course of the study (df=16, F=7.80, p<0.01). Shells from the control treatment (83.50±3.73 mm) and temperature treatment (84.34±3.85 mm) were significantly longer than shells from the pH treatment (81.31±3.85 mm) after 12 months (Table 4.3.2). There was no significant difference in length between shells from the pH x temperature treatment (82.15±4.01 g) and the control and temperature treatments or between shells from the pH and pH x temperature treatments after 12 months (Table 4.3.2).

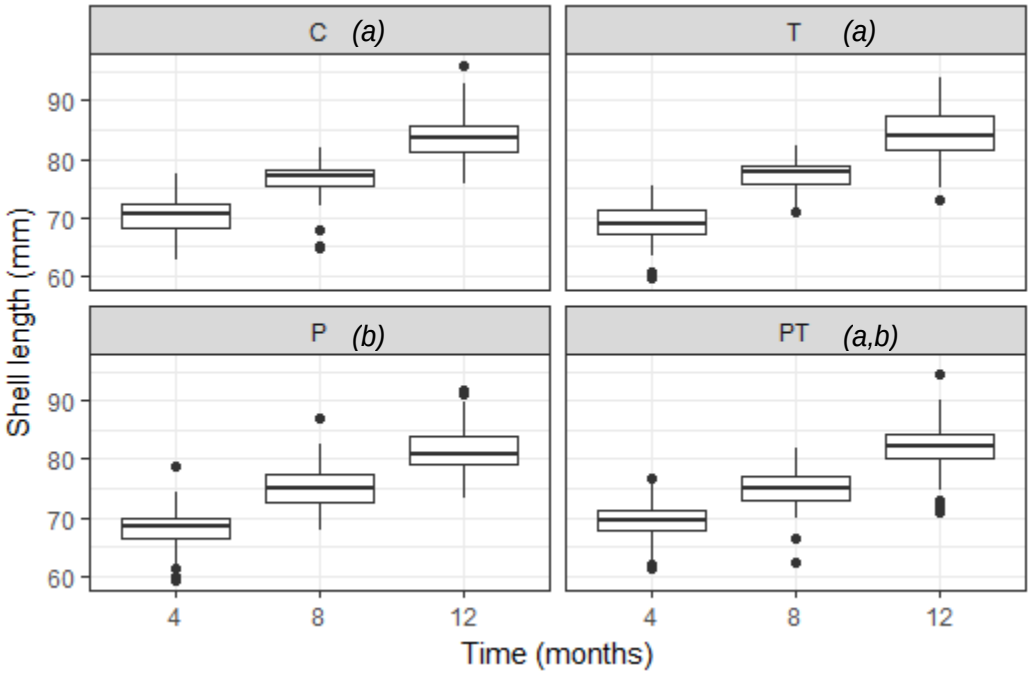

Figure 4.3.2. Boxplots of the shell lengths (± standard deviation) of abalone, *H. midae*, exposed to four treatments (C=control, T=temperature, P=pH, PT=pH x temperature) over a 12-month experimental period in a flow-through seawater system. Each treatment group contains repeated measurements at 0-, 4-, 8-, and 12-month sampling times. Same letters in italics between treatments denotes no statistical difference between treatments (alpha = 0.05)

Table 4.3.2. Pairwise differences of abalone shell lengths between four treatments (C=control, T=temperature, P=pH, PT=pH x temperature) using the Tukey method to compare family estimates. Significant values are taken at the 5% level and shaded in grey.

Contrast Treatments	Comparison (mm)	Comparison (%)	Degrees of Freedom	t-ratio	p-value
C - T	-0.85	-2.9%	16	0.044	1.00
C - P	2.19	8.3%	16	4.122	<0.01
C - PT	1.35	5.0%	16	2.307	0.14
T - P	3.0	11.4%	16	4.078	<0.01
T - PT	2.19	8.0%	16	2.263	0.15
P - PT	-0.84	-3.4%	16	-1.815	0.30

Treatment had a significant effect on abalone shell width over the course of the study (df=16, F=9.90, p<0.01). Shells from the control treatment (57.53±2.96 mm) and temperature treatment (57.70±3.17 mm) were significantly wider than shells from the pH treatment (55.67±2.97 mm) after 12 months (Table 4.3.3). Shells from the control treatment were significantly wider than shells from the pH x temperature treatment (56.14±2.84 mm). There were no significant differences in shell width between abalone from the control and temperature treatments, temperature and pH x temperature treatments, or between abalone from the pH and pH x temperature treatments (Table 4.3.3).

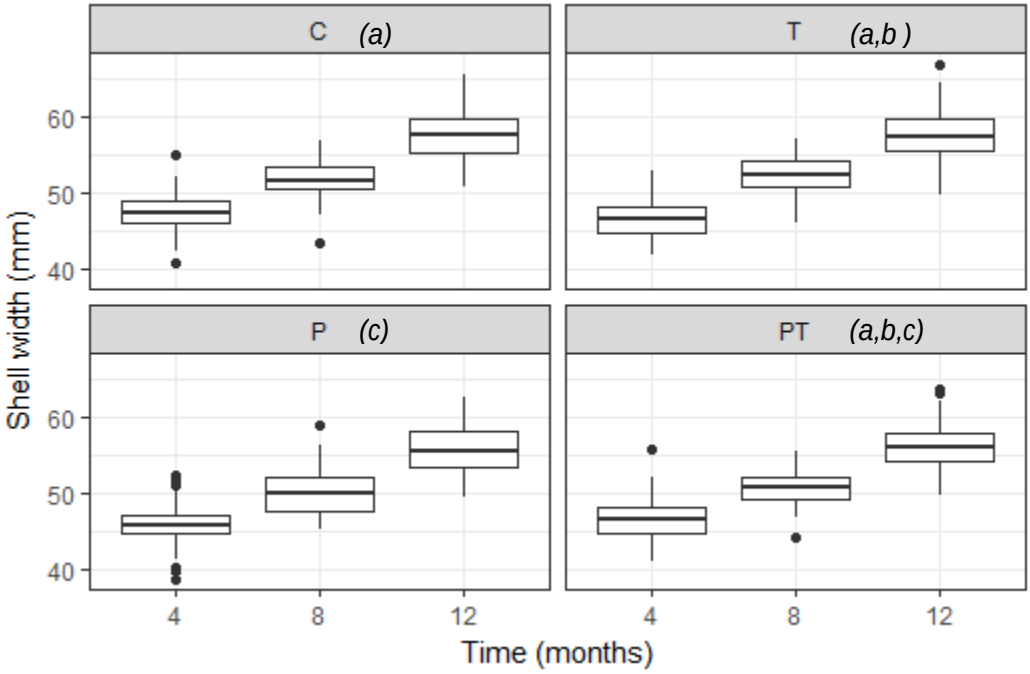

Figure 4.3.3. Boxplots of the shell width (± standard deviation) of abalone, *H. midae*, exposed to four treatments (C=control, T=temperature, P=pH, PT=pH x temperature) over a 12-month experimental period in a flow-through seawater system. Each treatment group contains repeated measurements at 0-, 4-, 8-, and 12-month sampling times. Same letters in italics between treatments denotes no statistical difference between treatments (alpha = 0.05).

Table 4.3.3. Pairwise differences of abalone shell widths between four treatments (C=control, T=temperature, P=pH, PT=pH *x* temperature) using the Tukey method to compare family estimates. Significant values are taken at the 5% level and shaded in grey.

Contrast Treatments	Comparison (mm)	Comparison (%)	Degrees of Freedom	t-ratio	p-value
C - T	-0.17	-0.3%	16	0.385	0.98
C - P	1.86	3.3%	16	4.691	<0.01
C - PT	1.39	2.4%	16	2.998	0.04
T - P	2.0	3.6%	16	4.307	<0.01
T - PT	1.56	2.7%	16	2.614	0.08
P - PT	-0.47	-0.8%	16	-1.693	0.36

Treatment had a significant effect on shape (length:width) over the course of the study (df=2.3, χ^2=0.049, p<0.01). Abalone from the control treatment had a significantly different shape in comparison to all other treatments (Table 4.3.4). Shell shape in ambient conditions was fairly stable for 8 months, with a shift to wider shape thereafter (Figure 4.3.5). The response in abalone shell shape to temperature and pH x temperature treatments was a linear, gradual change in shape towards a wider, shorter shell over the course of the experiment (Figure 4.3.5). The response in abalone shell shape to the pH treatment was a shift towards longer shells between 4 to 8 months of exposure to treatment conditions, with a change to wider shells thereafter (Figure 4.3.5).

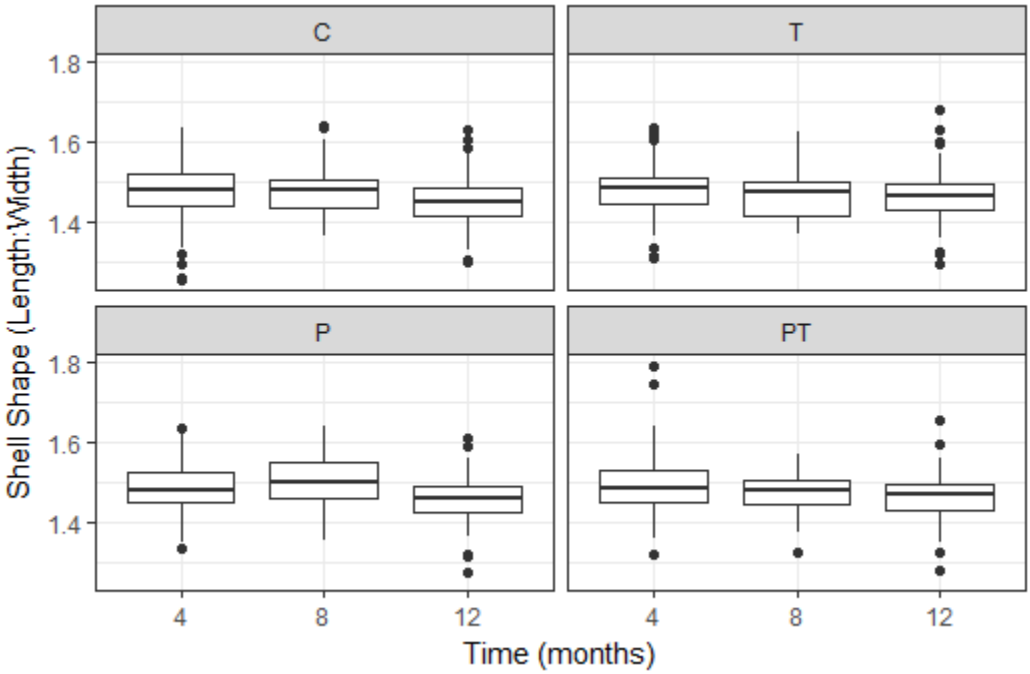

Figure 4.3.4. Boxplots of the shell shape (length:width, ± standard deviation) of abalone, *H. midae*, exposed to four treatments (C=control, T=temperature, P=pH, PT=pH *x* temperature) over a 12-month experimental period in a flow-through seawater system. Each treatment group contains repeated measurements at 0-, 4-, 8-, and 12-month sampling times.

Table 4.3.4. Ordered factor contrasts of smoothing terms for abalone shell shape (length:width) over the 12 month study. Significant values are taken at the 5% level and shaded in grey.

Contrast Treatments	Comparison (ratio)	Comparison (%)	Estimated Degrees of Freedom	F-value	p-value
C - T	-64.09	-1.3%	1.00	4.085	0.04
C - P	275.81	5.9%	1.85	6.041	<0.01
C - PT	190.63	4.0%	1.00	10.754	<0.01

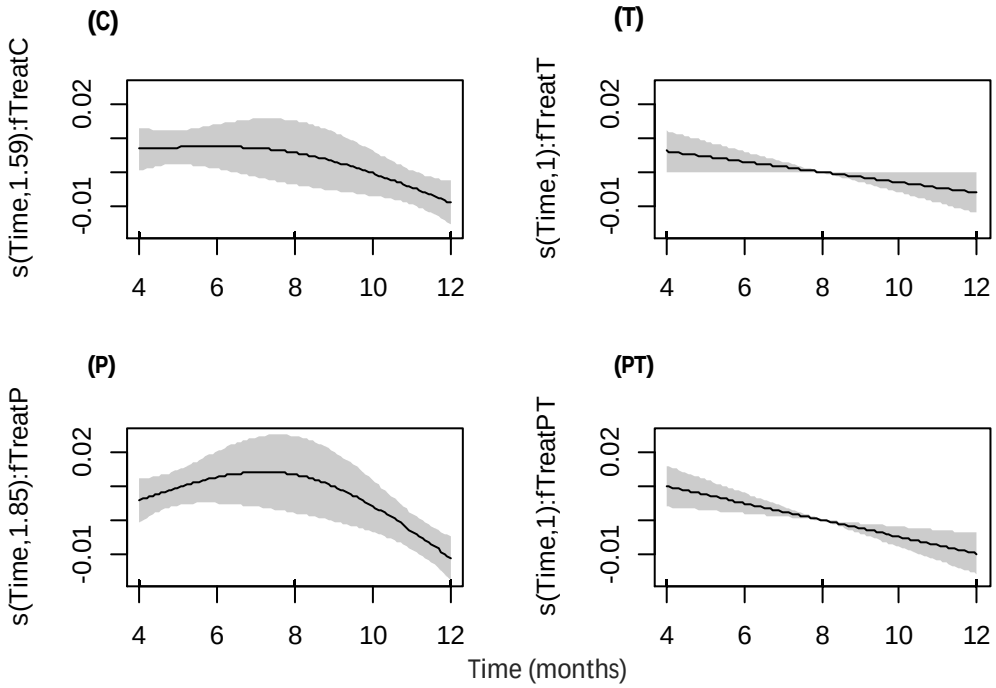

Figure 4.3.5. Smoothing function (log transformed) of abalone shell shape (length:width) response to four treatments: (C) Control, (T) Temperature, (P) pH, and (PT) pH *x* temperature, over a 12 month experimental period in the optimal generalized additive mixed model. The estimated degrees of freedom (EDF) for each treatment are listed on the y-axis for each treatment.

Treatment had a significant effect on abalone shell area over the course of the study (df=16, F=9.00, p<0.01). Shells from the control treatment (4810.23±420.07 mm^2) and temperature treatment (4874.32±443.40 mm^2) were significantly larger in area than shells from the pH treatment (4534.42±422.51 mm^2) after 12 months (Table 4.3.5). There were no significant differences in shell area between abalone from the control and temperature treatments; temperature, control and pH x temperature (4619.60±424.60 mm^2) treatments, or between abalone from the pH and pH x temperature treatments (Table 4.3.5).

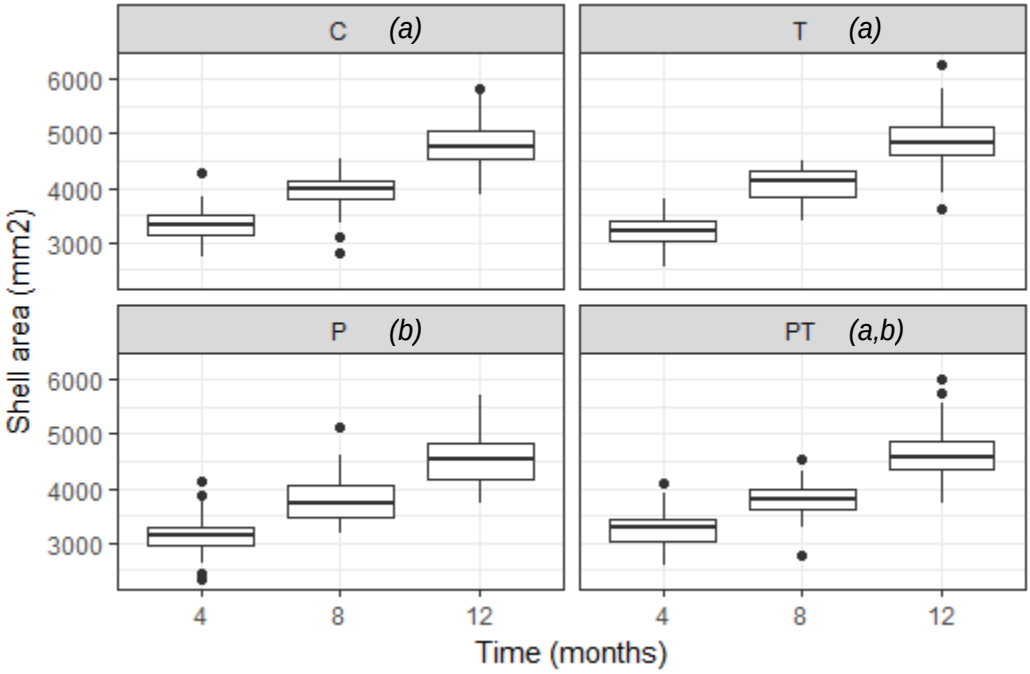

Figure 4.3.6. Boxplots of the shell area (± standard deviation) of abalone, *H. midae*, exposed to four treatments (C=control, T=temperature, P=pH, PT=pH x temperature) over a 12-month experimental period in a flow-through seawater system. Each treatment group contains repeated measurements at 0-, 4-, 8-, and 12-month sampling times. Same letters in italics between treatments denotes no statistical difference between treatments (alpha = 0.05).

Table 4.3.5. Pairwise differences of abalone shell area between four treatments (C=control, T=temperature, P=pH, PT=pH x temperature) using the Tukey method to compare family estimates. Significant values are taken at the 5% level and shaded in grey.

Contrast Treatments	Comparison (mm)	Comparison (%)	Degrees of Freedom	t-ratio	p-value
C - T	-64.09	-1.3%	16	0.4	0.98
C - P	275.81	5.9%	16	4.544	<0.01
C - PT	190.63	4.0%	16	2.646	0.08
T - P	339.89	7.2%	16	4.144	<0.01
T - PT	254.72	5.4%	16	2.245	0.15
P - PT	-85.18	-1.9%	16	-1.899	0.27

4.3.2. Shell Compression

Treatment had a significant effect on the maximum force/load (MF) that each shell could endure during compression (Figure 4.3.7) over the course of the study (df=1.9, χ^2=1.606, p<0.01). Abalone shells from the control treatment could sustain the most compressive force after 12 months (551.15 ± 145.08 N). Abalone shells from the control treatment had a significantly different MF over time in comparison to all other treatments (Table 4.3.6); shell MF increased exponentially over time (Figure 4.3.8). The response in abalone shell MF to the pH (475.15 ± 117.22 N) and pH x temperature (502.13 ± 141.97 N) treatments was similar to the control, with the exception of a slight decrease in

strength at the 8 month sampling period and weaker shells overall (Figure 4.3.8). The response in abalone shell MF to the temperature treatment (547.61 ± 129.39 N) was a linear (edf=1.00), gradual increase in strength for the duration of the study (Figure 4.3.8).

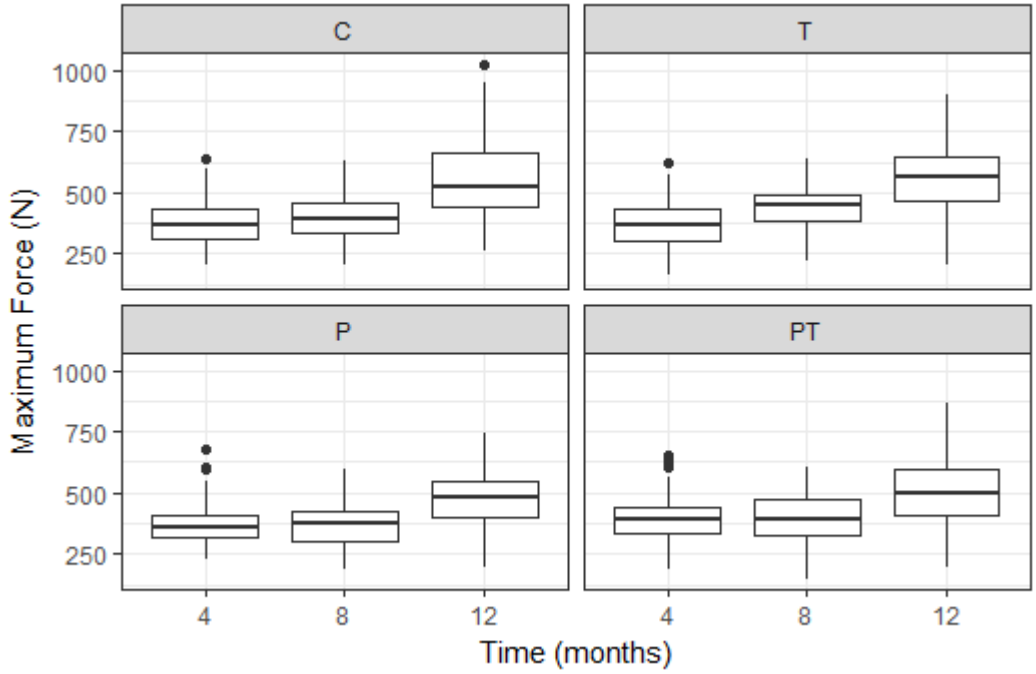

Figure 4.3.7. Boxplots of the maximum compressive force (± standard deviation) of abalone, *H. midae*, shells exposed to four treatments (C=control, T=temperature, P=pH, PT=pH x temperature) over a 12-month experimental period in a flow-through seawater system. Each treatment group contains repeated measurements at 0-, 4-, 8-, and 12-month sampling times.

Table 4.3.6. Ordered factor contrasts of smoothing terms for abalone shell maximum compressive force between treatments (C=control, T=temperature, P=pH, PT=pH x temperature) over the 12-month study. Significant values are taken at the 5% level and shaded in grey.

Contrast Treatments	Comparison (N)	Comparison (%)	Estimated Degrees of Freedom	F-value	p-value
C - T	3.54	0.6%	1.00	16.963	<0.01
C - P	-76.00	-14.8%	1.99	7.453	<0.01
C - PT	-49.02	-9.3%	1.99	6.882	<0.01

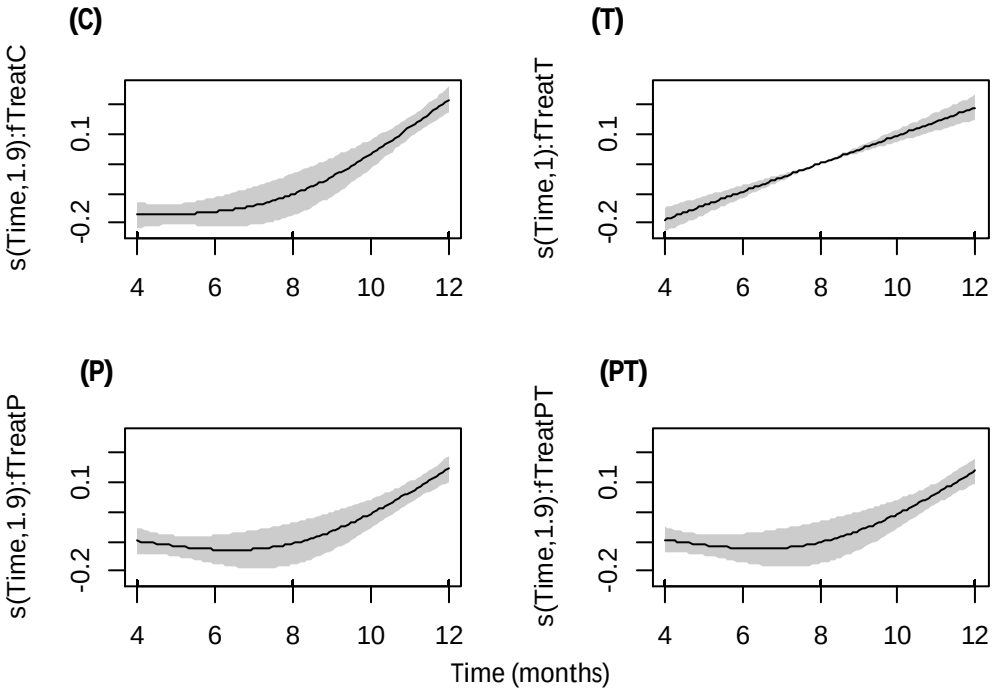

Figure 4.3.8. Smoothing function (log transformed) of abalone shell maximum compressive force response to four treatments (C=control, T=temperature, P=pH, PT=pH x temperature) over a 12 month experimental period in the optimal generalized additive mixed model. The estimated degrees of freedom (EDF) for each treatment are listed on the y-axis for each treatment

4.3.3 Shell Mineralogy

The mineralogical study of abalone shells was represented by percentage weight of aragonite (Figure 4.3.9), and average diameter of aragonite (Figure 4.3.10) and calcite (Figure 4.3.11) crystals in the shells of abalone exposed to experimental conditions for 12 months.

Treatment did not have a significant effect on the percentage weight of aragonite in abalone shells after 12 months of exposure to experimental conditions (df=16, F=0.130, p=0.9412; Table 4.3.7).

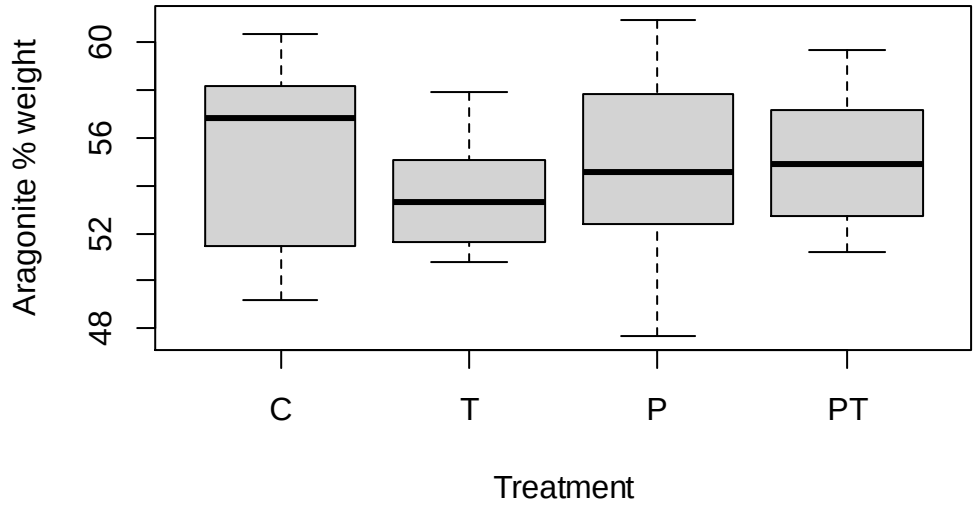

Figure 4.3.9. Percentage weight of aragonite crystals (± standard deviation) in abalone shells, *Haliotis midae*, exposed to four seawater treatments (C=control, T=temperature, P=pH, PT=pH x temperature) after a 12-month experimental period in a flow-through seawater system.

Table 4.3.7. Pairwise differences of the percentage weight of aragonite in abalone shells between four treatments (C=control, T=temperature, P=pH, PT=pH x temperature) using the Tukey method to compare family estimates. Significant values are taken at the 5% level and shaded in grey.

Contrast Treatments	Comparison (%)	Degrees of Freedom	t-ratio	p-value
C - T	1.65	16	1.2	0.64
C - P	0.42	16	0.260	0.99
C - PT	0.10	16	0.102	1.00
T - P	-1.2	16	-0.94	0.78
T - PT	-1.6	16	-1.099	0.69
P - PT	-0.32	16	-0.159	1.00

Treatment did not have a significant effect on the diameter of aragonite crystals in abalone shells after 12 months of exposure to experimental conditions (df=16, F=0.825, p=0.49; Table 4.3.8).

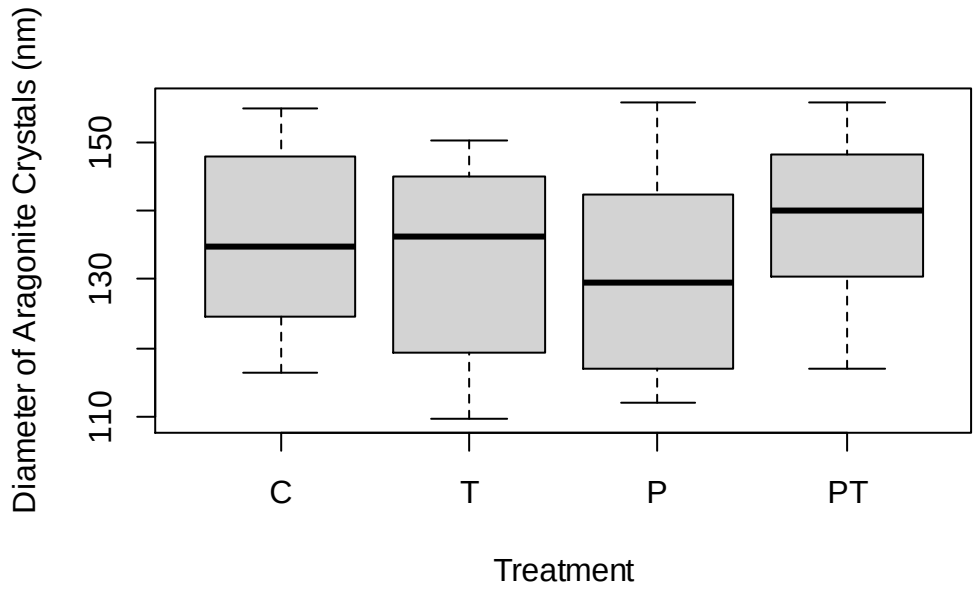

Figure 4.3.10. Average diameter of aragonite crystals (± standard deviation) in abalone shells, *Haliotis midae*, exposed to four seawater treatments (C=control, T=temperature, P=pH, PT=pH x temperature) after a 12-month experimental period in a flow-through seawater system.

Table 4.3.8. Pairwise differences of the average diameter of aragonite crystals in abalone shells between four treatments (C=control, T=temperature, P=pH, PT=pH x temperature) using the Tukey method to compare family estimates. Significant values are taken at the 5% level and shaded in grey.

Contrast Treatments	Comparison (nm)	Comparison (%)	Degrees of Freedom	t-ratio	p-value
C - T	3.73	2.8%	16	0.864	0.82
C - P	5.34	4.0%	16	0.535	0.95
C - PT	-2.38	-1.7%	16	-0.598	0.93
T - P	1.61	1.2%	16	-0.285	0.99
T - PT	-6.11	-4.5%	16	-1.472	0.46
P - PT	-7.71	-5.7%	16	-1.11	0.68

Treatment did not have a significant effect on the diameter of calcite crystals in abalone shells after 12 months of exposure to experimental conditions (df=16, F=2.256, p=0.12; Table 4.3.9).

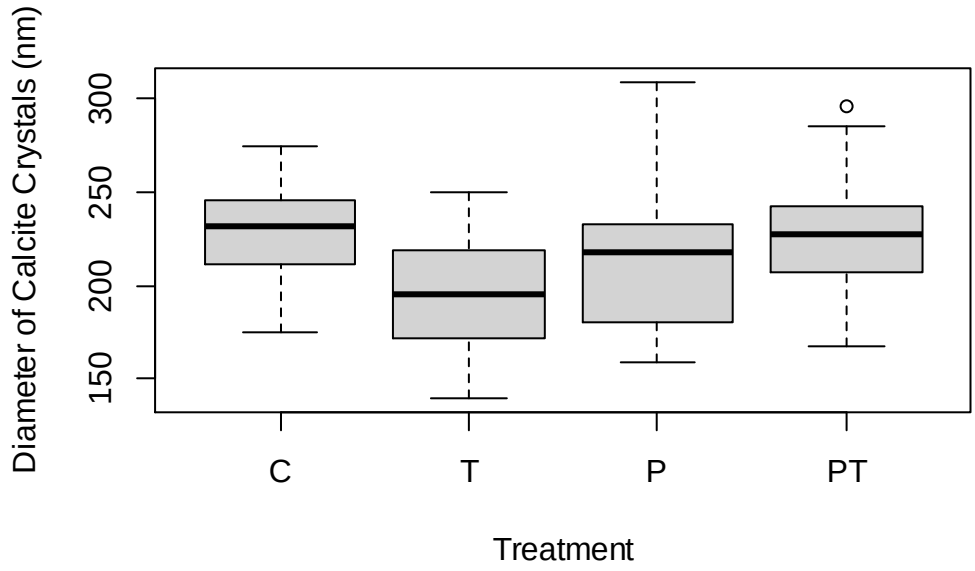

Figure 4.3.11. Average diameter of calcite crystals (± standard deviation) in abalone shells, *Haliotis midae*, exposed to four seawater treatments (C=control, T=temperature, P=pH, PT=pH x temperature) after a 12-month experimental period in a flow-through seawater system.

Table 4.3.9. Pairwise differences of the average diameter of calcite crystals in abalone shells between four treatments (C=control, T=temperature, P=pH, PT=pH x temperature) using the Tukey method to compare family estimates. Significant values are taken at the 5% level and shaded in grey.

Contrast Treatments	Comparison (mm)	Comparison (%)	Degrees of Freedom	t-ratio	p-value
C - T	34.24	16.1%	16	2.396	0.12
C - P	16.79	7.6%	16	1.196	0.64
C - PT	4.86	2.1%	16	0.369	0.98
T - P	-17.5	-8.3%	16	-1.2	0.63
T - PT	-29.39	-13.9%	16	-2.026	0.22
P - PT	-11.94	-5.4%	16	-0.827	0.84

4.4 Discussion

This study provides the first evidence that decreased pH negatively effects *H. midae* shell growth and strength and changes the shape of the shell. It presents the first experimental findings of the effects of variably warmed– and lowered pH seawater on *H. midae* shell morphology, strength and mineralogy. This study aimed to determine the impact of lowered pH, warming and a combination of these two factors on adult abalone shells by maintaining the natural variability of the seawater parameters in a land-based aquaculture facility over the course of 12 months. To the author's knowledge, this is the first study that will assess the effects of these treatments on adult *H. midae* shell growth, morphology, strength and mineralogy.

Table 4.4.1. Summary of results reported as mean ± standard deviation for *H. midae* exposed to four treatments (C=control, T=temperature, P=pH, PT=pH x temperature) for 12 months. Means followed by the same letter(s) within a column are not significantly different ($p<0.05$).

Treatment	Weight (g)	Length (mm)	Width (mm)	Shape (length: width)	Area (mm^2)	Force (N)	Aragonite (% weight)	Aragonite Diameter (nm)	Calcite Diameter (nm)
C	28.43 ± 3.74^{a}	83.50 ± 3.73^{a}	57.53 ± 2.96^{a}	1.453 ± 0.059^{a}	4810.23 ± 420.07^{a}	551.15 ± 145.08^{a}	55.09 ± 3.86^{a}	136.36 ± 12.17^{a}	230.34 ± 27.44^{a}
T	29.27 ± 4.04^{a}	84.34 ± 3.85^{a}	57.70 ± 3.17^{ac}	1.464 ± 0.063^{b}	4874.32 ± 443.40^{a}	547.61 ± 129.39^{b}	53.44 ± 2.14^{a}	132.64 ± 14.43^{a}	196.09 ± 33.49^{a}
P	24.13 ± 3.34^{b}	81.31 ± 3.85^{b}	55.67 ± 2.97^{b}	1.462 ± 0.057^{b}	4534.42 ± 422.51^{b}	475.15 ± 117.22^{b}	54.67 ± 4.15^{a}	131.03 ± 15.55^{a}	213.54 ± 41.14^{a}
PT	25.26 ± 3.24^{b}	82.15 ± 4.01^{ab}	56.14 ± 2.84^{bc}	1.465 ± 0.057^{b}	4619.60 ± 424.60^{ab}	502.13 ± 141.97^{b}	54.99 ± 2.59^{a}	138.74 ± 12.23^{a}	225.47 ± 38.42^{a}

Reduced pH seawater had the most pronounced effect on *H. midae* shell parameters (Table 4.4.1). Abalone shells grown in variable, reduced pH conditions weighed 16.4 % less than shells grown in ambient conditions after 12 months. Reduced pH conditions affected shell morphology in comparison to shells grown in ambient conditions by reducing the length (-8.3 %) and width (-3.3 %) of shells, resulting in longer-shaped shells with a 5.9% smaller area and weaker (-14.8 %) structure.

These findings concur with previous research on other abalone species. Adult *H. tuberculata* exposed to a reduced, constant seawater pH of 7.7 for 5 months displayed a reduction in shell growth (in terms of length) and strength in comparison to abalone cultured in an ambient, constant seawater pH of 8.0 (Avignon et. al. 2020). Contrary to the findings of the current study, *H. tuberculata* shell weight was not affected by reduced seawater pH (Avignon et. al. 2020). However, Auzoux-Bordenhave et. al. (2020) noted a reduction in shell length, weight, and strength of 6-month-old *H. tuberculata* after 3 months of exposure to reduced, constant seawater pH of 7.6 (control: pH 8.1). Avignon et. al. (2020) hypothesised that the reduction in shell compressive force may indicate that lowered seawater pH altered the biomineral architecture leading to a more fragile shell based on their evidence of differences in the texture and organization of outer and inner surface layers. Abalone larvae from a range of *Haliotis* species also exhibited reduced shell growth under hypercapnic conditions, but to a greater extent than *H. midae* adults, as calcification rates are higher in juvenile stages (Li et. al. 2018, Onitsuka et. al. 2018, Wessels et. al. 2018, Guo et. al. 2015, Kim et. al. 2013, Byrne et. al. 2011b, Crim et. al. 2011, Kimura et. al. 2011).

A substantial decrease in the strength of *H. midae* (and *H. tuberculata*) shells could increase the risk of shell damage in aquaculture operations and susceptibility of abalone to predators in nature. A lot of uncertainty arises when scaling ocean acidification responses in controlled environments to

natural communities and predator-prey interactions, as a common response to predation in calcifying animals is an increase in shell production (Kroeker et. al. 2014). Lord et. al. (2017) exposed several intertidal species (crab: *Pachygrapus crassipes*, whelks: *Nucella ostrina*, mussels: *Mytilus galloprovincialis*, and abalone: *Haliotis rufescens*) to variable, reduced seawater pH (-0.3) and warming (+2 °C) conditions for 10 weeks and assessed predator-prey interactions. Elevated CO_2 significantly reduced juvenile *H. rufescens* shell weight by 40 % (Lord et. al. 2017). Abalone produced larger amounts of shell relative to tissue in the presence of crabs, but still had a lower shell to tissue ratio under elevated CO_2 conditions in comparison to ambient conditions (Lord et. al. 2017). Responses to ocean acidification and predation can vary between species, as is seen in a recent study by Barclay et. al. (2019). Two intertidal gastropods (*Tugela funebralis* and *Nucella ostrina*) were exposed to variable, reduced pH seawater (- 0.5; controlled by HCl and $NaHCO_3$) and predation cues for 6 months. Predation cues had no effect on shell strength in either *T. funebralis* or *N. ostrina. T. funebralis* shell growth was reduced by 83 % in reduced pH conditions, and 50 % weaker, and growth was reduced by 63 % under predation cues (Barclay et. al. 2019). *N. ostrina* shell growth was not affected by reduced pH conditions; however shells were 10 % weaker (Barclay et. al. 2019). The reductions in shell growth and strength reported by Barclay et. al. (2019) for *T. funebralis* are extreme, especially for an intertidal species that is more accustomed to large variations in seawater temperature and pH. This increased vulnerability to acidification may be due to the slow-growing nature of this species (Frank 1975) and an inability to repair/maintain shell growth within the 6 month experimental period, or this exaggeration may be due to experimental techniques. Whilst it is now standard that ocean acidification experiments manipulate pH only by CO_2 diffusion and not the use of acids, these findings concur with the findings of Lord et. al. (2017) where *N. ostrina* exposed to variable, elevated CO_2 conditions for 10 weeks displayed no change in shell growth.

Lowered seawater pH did not have a significant effect on the shell mineralogy of *H. midae*. These findings concur with the multi-species analysis by Ries (2011) which noted no significant changes in calcite/aragonite ratios in monomineralic species. Although the calcite/aragonite ratios within the shells was not affected, future studies may want to assess the effects of acidification and warming on *H. midae* calcification rates as the decrease in shells weights due to exposure to reduced pH seawater is indicative of a decline in shell calcification.

Increased seawater temperature did not have any significant effects on shell weight, strength or mineralogy (Table 4.4.1) potentially because the increase in temperature was within the thermal optimum range of *H. midae* (Vosloo & Vosloo 2010, Britz et. al. 1997, Tarr 1995). An increase in seawater temperature (+ 2 °C above ambient including natural variability) also had no effect on juvenile *H. rufescens* shell weight after 10 weeks of exposure to experimental conditions (Lord et. al. 2017). Conflicting results were reported by Vilchis et. al. (2005) in an examination of the effects of warmed seawater (+ 2.5 °C above ambient including natural variability) on the shell growth (length) of adult *H. rufescens* and *Haliotis fulgens* after 49 weeks of experimental cultivation. *H. fulgens* shell growth was robust to warmed seawater and *H. rufescens* shell growth was significantly reduced in warmed seawater (Vilchis et. al. 2005). Thus variable, warmed seawater can have differing results on *H. rufescens*, and potentially *H. midae*, shell growth depending on the age of the abalone and local

environmental temperatures and variability that the abalone are cultivated in (See Chapter 6 for further discussion). Variation in seawater temperatures at local scales has been shown to affect the biological responses of juvenile *H. fulgens* (Boch et. al. 2018). *H. fulgens* displayed the largest shell growth in abalone that were placed in warmer sites, approximately 2.5 km apart and ~ 200 m separation offshore (Boch et. al. 2018). The findings by Boch et. al. (2018) indicate that climate change experiments, aimed at informing management practices, need to include local variability and environmental conditions.

Warmed conditions had a significant effect on the change in *H. midae* shell strength over time. Abalone shell strength increased constantly over time when exposed to warmed seawater as opposed to those in ambient conditions which showed a period of invariance in shell strength between June 2015 and October 2015 (summer months) before shell strength exponentially increased. Despite this difference, shells grown in ambient seawater were 0.8 % stronger than those grown in warmed conditions. These findings do not concur with the response of the mussel *Mytilus edulis* to 4 °C warming (Mackenzie et. al. 2014). Warming significantly reduced the shell strength of *Mytilus edulis* by approximately 60 % after 6 months of experimental cultivation (Mackenzie et. al. 2014). Shell strength can be attributed to shell weight (Auzoux-Bordenhave et. al. 2020), with stronger shells being larger or thicker. Shell thickness was not assessed in this study, however future studies may want to assess the effects on temperature on shell strength in combination with shell thickness calcification as warmed seawater has been shown to affect *H. tuberculata* calcification. Calcification in *H. tuberculata* shells has been shown to increase with an increase in seasonal temperatures from 10.5 °C in winter in contrast to 18.3 °C in summer (Chapperon et. al. 2019). This effect is likely to be species-specific; in the meta-analysis of 228 studies on the biological responses of calcifying organisms to ocean acidification and warming, Kroeker et. al. (2013) noted that elevated temperature had no clear effect on calcification estimates across taxa.

The attribution of *H. tuberculata* shell weight to shell strength (Auzoux-Bordenhave et. al. 2020) concurs with the current findings as shell weight and strength were not affected by warmer seawater after 12 months (Table 4.4.1), however seawater temperature did have an effect on the change in shell shape of *H. midae* during experimental cultivation. *H. midae* shells from the temperature treatment displayed a linear change in shell shape, similar to a linear change in shell strength, towards a wider shell in comparison to abalone from the ambient treatment which displayed a period of growth in length before expanding the width of the shell. These findings suggest that the preferred directional growth of the shells during periods of warming is towards a wider shape, which impacts the strength of the shell. At present, studies on temperature-related changes in *H. midae* calcification and comparable studies on *H. midae* shell directional growth are lacking and it is unclear as to what affected a change in shell shape and more research will need to be conducted. Although this study did not look at the shape of the pedal muscle, future studies should focus on whether the change in shell shape correlates with a change in pedal muscle shape, and assess the economic impact that a possible change in shape of the pedal muscle, due to a change in shape of the shell, might have on the abalone industry.

H. midae mineralogy was robust to changes in seawater temperature, which does not concur with the response of bivalve mineralogy to increased seawater temperatures. A multi-species analysis of

bivalve mineralogical response to temperature by Lowenstam (1954a, 1954b, 1964) indicates an inverse relationship between the percentage calcite in the shell and the mean temperature of the local environment. Lowenstam (1954a, 1954b, 1964) also noted that the same factors operated for some species of gastropods, but *Haliotis* species were not included in any of the analyses. Kennedy et. al. (1969) and Dodd (1963) also noted that while aragonite and calcite ratios should be temperature dependant, the difference in ratios of calcite and aragonite in whole shells will tend to diminish as shells increase in size above 12mm in length. This could explain why there was no significant difference in aragonite percentage weight between treatments in this study, as all shell lengths greatly exceeded 12mm. Future research should investigate changes in shell mineralogy, particularly percentage changes in calcite and aragonite, of juvenile *H. midae* within the first 5 months of age, as cultivated abalone exceed 12mm in length within 5 months.

The combination of reduced pH and increased temperature had similar effects on abalone shell weight, and strength as the lowered pH treatment. However, the additional factor of temperature did affect a difference in shell morphology, in particular shell length (Table 4.4.1). Thus the shell length and width of abalone from the multi-factor treatment were comparable with abalone from the control, raised temperature and lowered pH treatments, despite abalone in the latter treatment having significantly shorter shells than abalone in the control and temperature treatments. Unfortunately, the change in shell growth due to the combination of warming and acidification is novel and, to date, there are no studies on the combined effects of warming and acidification on adult abalone shell morphology. Extrapolation of results from studies on the effects of warming and acidification on abalone larval stages would be questionable due to the different life history stage, and the increased sensitivity of mollusc larvae to changing seawater parameters (Kroeker et. al. 2013).

In conclusion, it appears that under near-future climate change conditions, ocean acidification will pose a greater risk to shell growth, morphology and integrity in the commercial species *H. midae* than warming, in the main growing area of South Africa. Reduced pH seawater had negative effects on shell growth, size, and strength. Warming did not negate the adverse effects of ocean acidification on shell weight or strength; however the length and width of the shells were moderately increased. It appears that warming has an indirect effect on shell strength via a widening in shell shape, although this did not increase shell strength. *H. midae* shell mineralogy was robust to both reduced pH and warming. These effects are of particular concern in this economically and ecologically important abalone species. Cultivated abalone shells will be more susceptible to damage during handling with a reduction in weight due to a reduction in shell size. This will have economic impacts on abalone aquaculture practices due to an increase in cultivation time to reach market-size and reduction in quality of abalone if the shells are more easily damaged. The decrease in shell strength due to reduced seawater pH might reduce the protection offered by shells against natural predators in naturally-occurring, over-fished *H. midae* populations.

CHAPTER 5:
Going Green: The Use of *Ulva* to Mitigate Seawater Acidification by Photosynthetic Carbon Uptake in Abalone Aquaculture

5.1. Introduction

As anthropogenic CO_2 accumulates in the atmosphere and is absorbed by the oceans, we face a situation that requires mitigation of excess CO_2, not only for local ecosystems, but for industries that utilize the ocean for food production (Narita et. al. 2012, Stewart-Sinclair et. al. 2020). Photosynthesizing organisms such as kelps and seaweeds are promising mitigation tools due to their uptake of dissolved inorganic carbon (bicarbonate and CO_2) for use as a carbon source during photosynthesis (van Ginneken 2019, Murie & Bourdeau 2020). *Ulva* (Chlorophyta) is the most promising mitigation tool for use in abalone aquaculture systems because it is easy to grow in large volumes, provides a nitrogen-rich food source, can be utilised as a biofuel and photobioreactor, is an effective tool for bioremediation of excess nutrients in Integrated Multi-Trophic Aquaculture (IMTA), and is used in partial recirculation systems (Bolton et. al. 2016).

Green seaweed cultivation is the third highest producing aquacultural product in Southern Africa, representing 15.4 % of total aquacultural product by weight, and 8.3 % of global green seaweed production (FAO 2018). *Ulva* is the most commonly cultivated green seaweed in abalone aquaculture systems, with an estimated production of 2000 tonnes of fresh weight per year (Bolton et. al. 2016, Rothman et. al. 2020). *Ulva* has been successfully cultivated in these abalone aquaculture systems since 2002, primarily as a food source and, to a lesser extent, to enable partial recirculation (Troell et. al. 2006, Bolton et. al. 2009, Neveux et. al. 2018). *Ulva rigida* is the predominantly aquacultured *Ulva* sp. in South African abalone aquaculture systems, although many studies have specified the use of *Ulva lactuca* in these systems prior to determination by molecular evidence (Robertson-Andersson et. al. 2003, Robertson-Andersson et. al. 2006, Shuuluka et. al. 2013). Species level taxonomy is particularly confusing for *Ulva* due to the lack of agreement between traditional morphologically-based taxonomy nomenclature and molecular clades (Bolton et. al. 2016, Bolton 2019). *U. rigida* (as *U. lactuca*) grown in oval raceways on abalone aquaculture facilities has been shown to be a more effective food source for abalone when grown in recirculated abalone effluent because of its higher nitrogen concentration (26 % protein vs 20 % protein) and resulting higher weight gain in abalone that were fed a diet of effluent-grown *Ulva* (Robertson-Andersson et. al. 2011).

Ulva is also a high-value, edible aquaculture product in South East Asian countries for consumption by marine animals and humans (Carl et. al. 2014). *Ulva spp*. are commonly used in seaweed biorefinery systems: the fractionation of seaweed to co-produce multiple products such as minerals, salts, starch, lipids, ulvan (a water-soluble polysaccharide obtained from the cell walls of *Ulva*; Kidgell et. al. 2019), proteins, and cellulose, for use in animal feeds, chemicals, cosmetics, nutritional supplements and biofuels (Bolton et. al. 2016, Rothman et. al. 2020; Table 5.1). Synthesis of Mn_2ZnO_4 from *Ulva linza*, *Ulva flexuosa (as Ulva tubulosa*), *Ulva fasciata*, *U. rigida*, and *Ulva reticulata* has shown strong antimicrobial activity against gram positive and gram negative bacteria, comparable to commercially available antibiotics (Sivaprakash et. al. 2019). The production potential of land-based *U. rigida* (as *U. lactuca*) cultivation in the Northern hemisphere was determined to be

2 to 20 times the production potential of conventional terrestrial energy crops (Bruhn et. al. 2011). Although these same volumes have not been produced in South Africa or Europe, it is a very promising solution to terrestrial energy crops and the reduction of carbon footprints in abalone aquaculture (Nobre et al. 2010).

Ulva is also a promising biofuel owing to its high carbohydrate content that can be converted by microbes to biomethane or bioethanol (Bikker et. al. 2016, Chemodanov 2017a,b, Osman et. al. 2020, Polikovsky et. al. 2020). Ethanol production from various *Ulva spp*. biomass has the potential to produce of 229.5 - 1735 g ethanol.m^{-2}.y^{-1}, with an energy density of 5.74 - 43.5 MJ.m^{-2}.y^{-1} and a power density of 0.18 - 1.36 W.m^{-2} (Bikker et. al. 2016, Chemodanov et. al. 2017b). *Ulva compressa* and *U. rigida* have been shown to successfully produce maximum energy rates ranging from 0.029 – 0.081 Wh.L^{-1}.d-1 as photobioreactors (Chemodanov et. al. 2017a) and *U. intestinalis* was able to produce a biodiesel recovery of 32.3 mg.g^{-1} of dry weight (Osman et. al. 2020). Although cultivation of a biorefinery feedstock can be unpredictable and affected by environmental factors including epiphytic bacteria, much progress has been made to improve consistency using microbiome engineering (Osman et. al. 2020). Progress in biofuel production is imperative due to limited fossil fuels and increasing anthropogenic CO_2 emissions. There is a need for alternative energy sources and *Ulva* has the potential to mitigate CO_2 emissions, in terms of avoided CO_2 emissions by fossil fuels, by approximately 1500 t.km^{-2}.y^{-1} (Duarte et. al 2017).

Despite the many uses and potential uses of *Ulva*, the most pertinent to marine aquaculture in a high CO_2 world is its functionality as a bioremediation medium. *Ulva* uses inorganic carbon and other nutrients in seawater for growth and photosynthesis; thus reducing nutrients that are harmful to abalone , such as ammonia, in recirculation systems (Robertson-Andersson 2008, Nobre et. al. 2010, Yokoyama & Ishihi 2010, Bolton et. al. 2016,). Carbon uptake by *Ulva* is able to reduce seawater CO_2 concentrations and in turn increase seawater pH, but is dependent on the uptake potential of the cultivated *Ulva* (Dreschler & Beer 1991, Young & Gobler 2018). Young and Gobler (2018) applied a mitigation system using *Ulva* in a constant, ocean acidification scenario (pCO_2 ~ 1700 µatm) and assessed the growth of several bivalve species (*Mercenaria mercenaria*, *Crassostrea virginica*, *Argopecten irradians*, *Mytilus edulis*) over a period of two weeks. Although *Ulva* did not fully mitigate the effect of reduced growth caused by elevated CO_2, the addition of *Ulva* into the system caused a significant increase in growth of *M. mercenaria* in terms of shell length, shell weight and tissue weight; a significant increase in shell length of *C. virginica* and juvenile *A. irradians; and* a significant increase in shell length, and tissue weight of adult *A. irradians. M. edulis* did not display a reduction in growth in response to elevated CO_2, but did show a significant increase in growth in response to *Ulva* bioremediation (Young and Gobler 2018). Young and Gobler (2018) noted no significant difference in the pH of seaweed-treated seawater, but did note a significant increase in seawater Ω_{cal} and Ω_{arg} after bioremediation by *Ulva,* as well as a significant correlation between the growth of bivalves and the saturation states of seawater.

To date, no further research has been conducted on the mitigation potential of *Ulva* in a high-CO_2 environment or the effects that seaweed-treated seawater has on abalone.

Table 5.1. *Ulva* (Chlorophyta)-based macroalgae biorefinery (MAB) studies carried out for production of various products (adapted from Prabhu et. al. 2020).

Algae species	Biorefinery products	Technologies/Methods	Reference
U. lactuca	Protein and carbohydrates	Osmotic shock, enzymatic hydrolysis, pulsed electric field, and high shear homogenization	Postma et. al. 2017
U. lactuca	Animal feed, acetone, butanol, ethanol, and 1,2-propanediol	Thermal and enzymatic hydrolysis, fermentation	Bikker et. al. 2016
Chaetomorpha linum	Bioethanol and biogas	Thermochemical hydrolysis, enzymatic hydrolysis, fermentation	Ben Yahmed et. al. 2016
Ulva fasciata	Mineral-rich liquid extract (MRLE),lipid, ulvan, and cellulose	Mechanical grinding, thermal and chemical extraction, fermentation	Trivedi et. al. 2016
Ulva ohnoi and *Ulva tepida*	Mainly salt (demonstrating the use of leftover biomass for protein, fertilizer, animal feed and fuel)	Aqueous washing and drying	Magnusson et. al. 2016
U. lactuca	Mineral extract, lipid, ulvan, protein, cellulose	Mechanical pressing and crushing, heat treatment, organic solvent extraction, alkali extraction, chemical extraction	Gajaria et al.2017
U. lactuca	ABE (acetone, butanol, ethanol)	Pre-treatment, enzymatic saccharification, fermentation	van der Wal et. al.2013
Ulva rigida	Liquid stream with carbohydrate and salt; a remaining stream with concentrated protein	Ionic liquid deconstruction	Pezoa-Conte et. al. 2015
Ulva ohnoi	Salt, ulvan, pigment, and protein	Aqueous, thermal, and chemical extraction	Glasson et. al. 2017
U. lactuca	Sap, ulvan, protein, methane	Aqueous, thermal, chemical extraction, and anaerobic fermentation	Mhatre et. al. 2018
Ulva ohnoi	Protein, salt, ulvan	Aqueous washing and drying	Magnusson et. al. 2019
Ulva ohnoi	Salts, starch, lipids, ulvan, proteins, cellulose	Aqueous washing, ethanol extraction, oxalate salt extraction, alkaline treatment	Prabhu et. al. 2020

5.1.1 Aims and Objectives

The aims of this study were to investigate the potential use of *Ulva* (Chlorophyta) as a mitigational tool to ameliorate reduced pH (-0.4 from ambient) seawater, by photosynthetic carbon uptake, in a flow-through abalone aquaculture system on a South African abalone aquaculture facility. This study will assess the affects that seaweed-treated seawater will have on abalone growth, spawning patterns, acid-base regulation, shell growth, morphology, shell strength and mineralogy over 12 months in comparison to ambient and acidified seawater. Ambient seawater retained natural pH and temperature variability and acidified seawater was offset to natural pH variability using CO_2/O_2 diffusion and a data-logger-relay system to incorporate local-scale variability of seawater in the abalone aquaculture facility, where this experiment was based. The experimental tanks were built outside, without shelter, alongside commercial abalone tanks to provide environmental realism and realistic feedback for commercial abalone aquaculture production. Experimental abalone tanks were smaller than those used in commercial aquaculture production, but were stocked in accordance with

the facility's commercial stocking density per tank. Food and feeding regimes were maintained in accordance with the facility's regimes.

This study also aims to assess whether the incorporation of an *Ulva*-bioremediation tank into a flow-through system in an abalone aquaculture facility will be sufficient to mitigate the negative effects of predicted acidified seawater pH on *H. midae* (see Chapter 3 and 4). This will provide valuable information on a possible mitigation strategy for South African abalone aquaculture facilities facing negative economic effects due to predicted ocean acidification.

This multi-parameter study will determine the effects of ambient and reduced pH seaweed-treated seawater on abalone growth (body- , meat- , and shell- mass), acid-base regulation, shell growth and morphology, shell strength and shell mineralogy using repeated measures of wet weight, condition factor (CF), muscle mass, haemolymph samples, shell weight, shell morphometrics, and shell strength, collected every 4 months when the abalone were size-graded and tanks were re-stocked, in keeping with commercial aquacultural timeframes for size-grading. GBI and shell mineralogy was analysed once, after 12 months of exposure to experimental conditions when all abalone were able to be harvested.

It is hypothesised that *H. midae* exposed to ambient, seaweed-treated seawater will display an increase in shell and tissue growth, similar to the response of *M. mercenaria* and *A. irradians* in seaweed-treated seawater due to an increased aragonite saturation state and warming of the seawater by *Ulva* (Young and Gobler 2018). *Ulva* has enhanced light-absorbing properties, due to its growth form and pigment complex, and absorbs incoming solar radiation converting it to heat energy (Figueroa & Niell 1989, Robertson-Andersson 2003, Bolton et. al. 2008). It is hypothesized that abalone acid-base regulation, condition factor and shell mineralogy will be similar to those in ambient conditions. Shell strength is hypothesised to be similar, if not weaker, than those in ambient conditions, and GBI is hypothesised to be lower than those in ambient conditions due to warmer water (See Chapter 4) in the *Ulva* flow-through systems (Table 5.3.4).

If flow-through *Ulva*-bioremediation is able to ameliorate acidified seawater, by carbon uptake, to comparable levels with ambient seawater, it is hypothesised that *H. midae* growth, acid-base regulation, shell morphology, strength and mineralogy will be similar to those in ambient conditions. If not, it is hypothesised that *H. midae* growth, acid-base regulation, shell morphology, strength and mineralogy will be similar to those in reduced pH conditions.

5.2 Methods

See Chapter 2 for experimental design, animal husbandry and general methods. The control and lowered pH treatments are presented in this chapter for comparison.

5.2.1 *Ulva* sp. culture

Farmed *Ulva rigida* was provided by Abagold Ltd. (Hermanus, South Africa) for use in this experiment as a mitigation tool to increase pH by removing CO_2 from seawater via photosynthesis. An *Ulva* mitigational system was not applied to the pHxtemperature treated seawater due to physical space limitation on the abalone farm. I elected to use the *Ulva* mitigational system on reduced pH seawater instead of the combination of pH and temperature because reduced pH was shown to have the most significant impact on *H. midae* weight reduction in a commercial system (Yearsley 2007, Naylor et. al. 2011). The seaweed was contained in two 480L tanks (1 m x 1 m x 0.48 m; *l* x *b* x *h*) with a water depth of 0.45 m and an incoming seawater flow rate of 6.7L.min^{-1}, an equivalent of 20 volume exchanges every 24 hours. The seaweed was rotated vertically in the tank using continuously pumped air (Figure 5.2.1). Two cool-white fluorescent tubes (one light fixture) were mounted 0.5 m above each seaweed tank and connected to a daylight sensor which switched the lights on in low light. In this way, the seaweed tanks were constantly exposed to a minimum of 149 µmol m^{-2} s^{-1}of light in order to reduce the nocturnal increase in CO_2 concentrations caused by respiration of the seaweed. Removable black plastic covers were placed over the tanks at night so that nearby commercial and experimental abalone tanks were not exposed to or influenced by nocturnal illumination. Robertson-Andersson (2003) determined that a stocking density of 3 kg.m^{-2} of *Ulva* provided maximum nutrient removal, but this density resulted in a non-significant difference in pH in her later thesis (Robertson-Andersson 2006); therefore in an attempt to increase CO_2 uptake in the tanks, each seaweed tank in this study was stocked with 4 kg of seaweed, an equivalent of 4 kg.m^{-2} and was harvested/restocked once a week to maintain stocking density. A 480L tank, separate from the experimental system and identical to the experimental seaweed tanks, supplied with seawater from the same commercial source was stocked with 6 kg of *Ulva rigida* at the start of the experiment. This tank was used to cultivate *U. rigida* to restock both experimental seaweed tanks when necessary with the same culture of seaweed. The restocking tank was designed in an identical fashion to the experimental seaweed tanks, but did not contain an alternative light source. The restocking tank was fertilised with 250 ml of ammonium phosphate every 7 days. During fertilization, valves supplying influent water were closed at 16:00 directly prior to the addition of fertilizer and were reopened at 08:00 the next morning. Air supply was not altered during this process and the seaweed continued to rotate in the tank overnight.

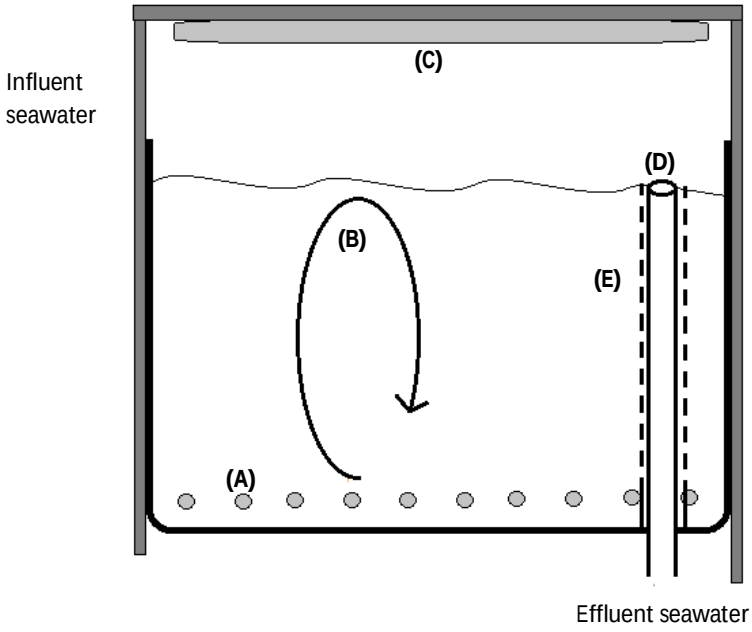

Figure 5.2.1. Schematic diagram of an experimental seaweed tank (1 m x 1 m x 0.48 m; *l* x *b* x *h)* containing *Ulva rigida*, with a water depth of 0.45 m. Influent seawater enters the tank from the experimental header tank. Seawater is aerated via (A) air holes that continuously release pumped air. The pumped air (B) circulates the seaweed vertically exposing the seaweed to sunlight during the day or light from (C) two cool-white fluorescent tubes above the tank during the night. Water exits the tank via (D) an overflow pipe surrounded by (E) 2mm oyster-mesh which prevents pieces of seaweed from entering the experimental abalone tanks. Figure is not to scale.

5.2.2 *Ulva* sp. yield

Seaweed yield averaged 0.11±0.17 kg.week^{-1} in ambient seawater and 0.07±0.17 kg.week^{-1} in acidified seawater over the 12-month experimental period (Table 5.2.1, Figure 5.2.2). The highest yield was achieved June and December 2015, but showed a decline in growth in January and February during peak summer months, possibly as a result of photoinhibition (Cabello-Pasinia et. al. 2000).

Table 5.2.1. Mean (±SD) seaweed yield for the control - (CM) and pH- mitigation (PM) treatments during the experimental period from February 2015 to February 2016. Values are displayed as average grams per week ± standard deviation.

	12 months	Feb-Jun '15	Jun-Oct '15	Oct '15-Feb '16
Control mitigation (CM)	111.3±170.0 g	113.5±163.8 g	166.8±153.4 g	53.0±184.2 g
pH mitigation (PM)	73.7±169.1 g	76.8±246.5 g	96.0±22.9 g	49.4±145.0 g

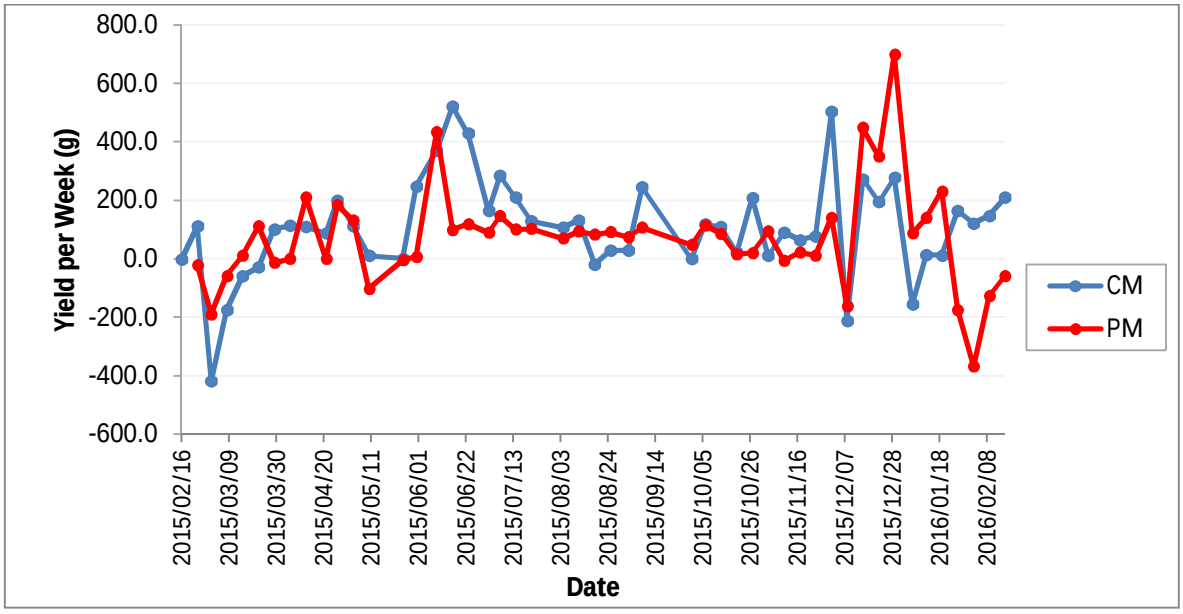

Figure 5.2.2. Weekly *Ulva* yield for the two experimental seaweed tanks with ambient (CM) and acidified (PM) influent seawater for the experimental period from 16 February 2015 to 16 February 2016.

5.2.3 Influence on seawater pH

Seawater pH was monitored daily at the outflow of each experimental abalone tank between 09:00 and 10:00 every morning and in the afternoon between 15:00 and16:00 (Table 2.2). Samples were taken in the morning between 09:00 and 10:00 in order to achieve the most reliable estimate of daily means (Yearsley 2008) and in the evening to increase water quality monitoring (see Chapter 2). *Ulva* increased ambient seawater pH by an average of 0.31±0.09 for the entire experimental period and by 0.35±0.004, 0.40±0.004 and 0.19±0.01 during the day from February-June 2015, June-October 2015 and October 2015-February 2016 respectively (Figure 5.2.3). Nocturnal pH was not measured during this experiment, although it is likely that there would have been a larger range of values had this been incorporated. An example of seawater pH variation between sampling times is provided in Figure 5.2.4.

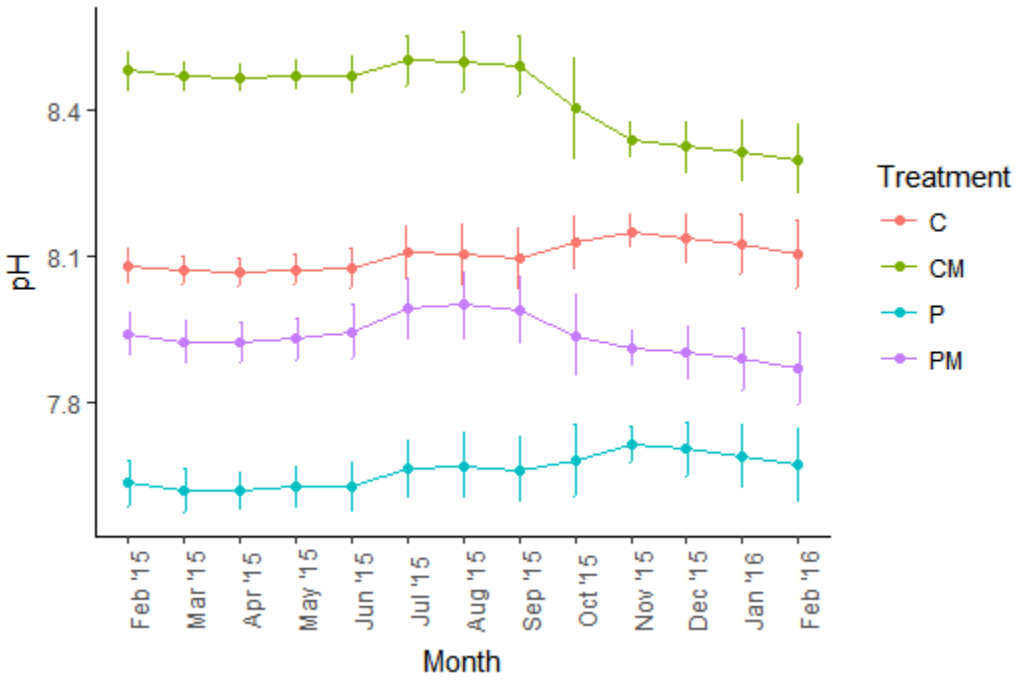

Figure 5.2.3. Mean seawater pH (with error bars for standard deviation) of four experimental treatment groups, control (C), pH (P), control mitigation (CM) and pH mitigation (PM), measured twice daily (09:00 over the course of the experiment from 16 February 2015 to 16 February 2016.

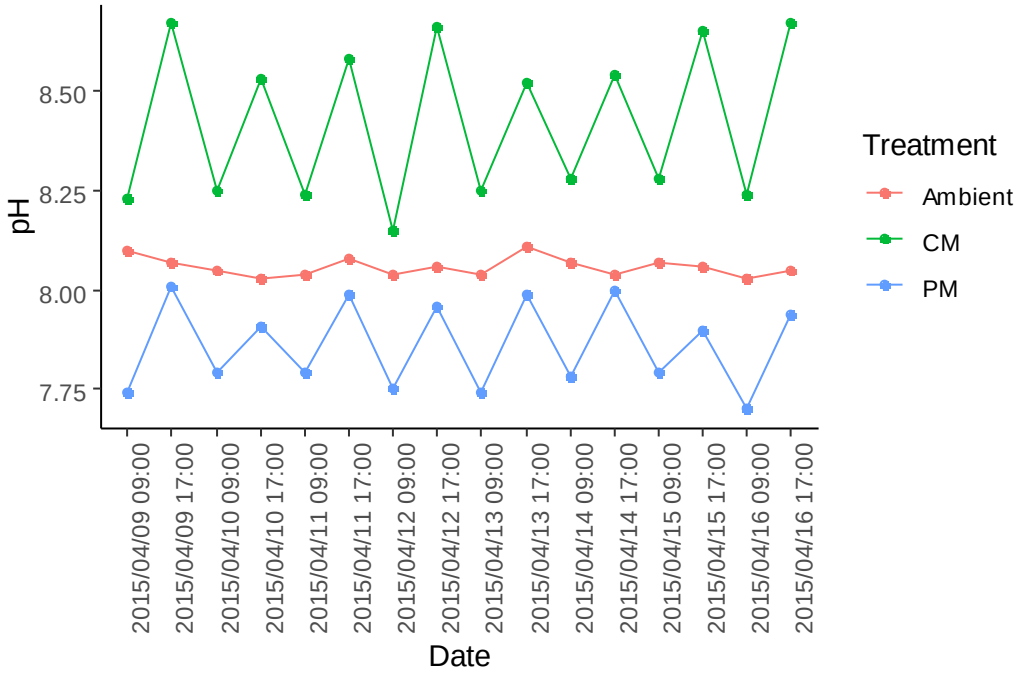

Figure 5.2.4. Seawater pH sampled from tanks in the ambient, control mitigation (CM), and pH mitigation treatments (PM) between 9th April 2015 – 16th April 2015.

5.2.4 Influence on seawater temperature

Seawater temperature was monitored daily at the outflow of each experimental abalone tank between 09:00 and 10:00 every morning and in the evenings between 15:00 and 16:00 (Table 2.2). Samples were taken in the morning between 09:00 and 10:00 in order to achieve the most reliable estimate of daily means (Yearsley 2007) and in the evening to increase water quality monitoring (see Chapter 2). *Ulva* increased ambient seawater temperature by an average of 0.96±0.16 °C for the entire experimental period and by 1.58±0.25 °C, 0.86±0.01 °C and 0.57±0.01 °C during the day from February-June 2015, June-October 2015 and October 2015-February 2016 respectively (Figure 5.2.5).

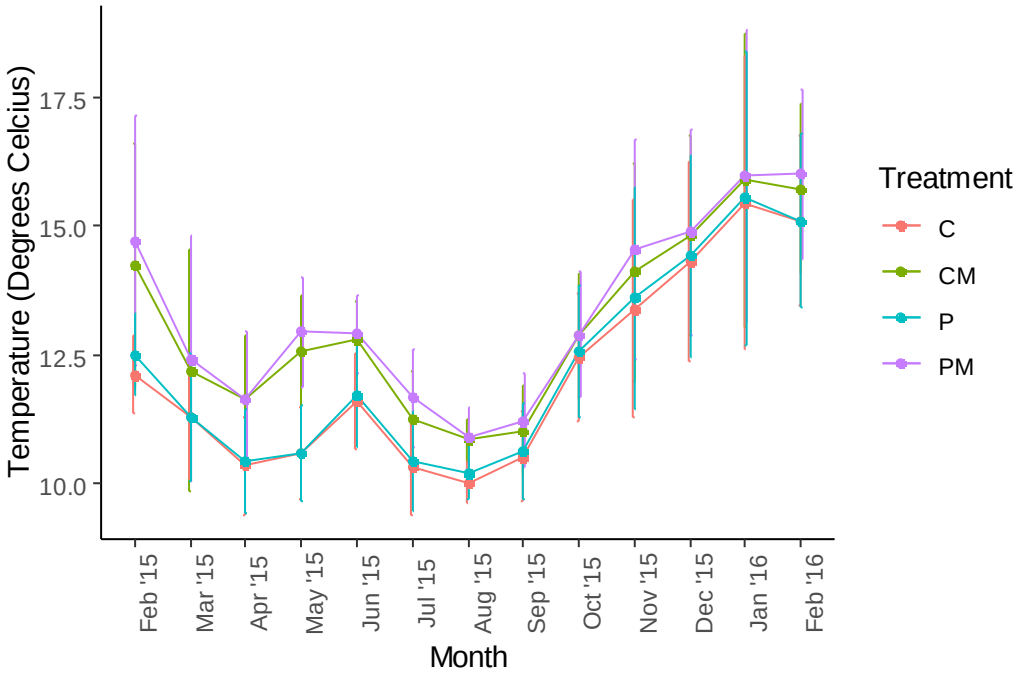

Figure 5.2.5. Mean seawater temperature (with standard deviation) of four experimental treatment (C=control, P=pH, CM=control mitigation, PM=pH mitigation) measured twice daily over the course of the experiment from 16 February 2015 to 16 February 2016.

5.2.5 Biological Measurements

Size-grading procedure and methods used for measurements obtained during size-grading for wet weight and condition factor (CF) are explained in Chapter 3 (Section 3.2.1).

Factory processing procedure and methods used for measurements obtained during factory processing for muscle mass, proportion meat to body mass (PMB), shell weight, shell length, shell width, shell area and shell shape are explained in Chapter 3 (Section 3.2.2) and Chapter 4 (Section 4.2.1). Procedures for obtaining measurements of abalone Gonadal Bulk Indices (GBI) are explained in Chapter 3 (Section 3.2.3).

Procedures for obtaining measurements of abalone haemolymph pH, bicarbonate concentration and total CO_2 are explained in Chapter 3 (Section 3.2.4). Environmental conditions at the time of haemolymph extraction were recorded (Table 5.2.2). Chapter 4 explains the procedures used to obtain measurements of shell strength (Section 4.2.2), percentage weight of aragonite, and crystal diameters of aragonite and calcite (Section 4.2.3).

Table 5.2.2. Environmental conditions (± standard deviation) of experimental tanks from four treatments (C=control, P=pH, CM=control mitigation, PM=pH mitigation) at time of haemolymph sampling.

Sample date	Treatment	Tank pH	Tank temperature
June '15	C	8.07 ± 0.00	11.19 ± 0.01
	P	7.63 ± 0.00	11.23 ± 0.02
	CM	8.47 ± 0.01	11.51 ± 0.00
	PM	7.97 ± 0.01	11.53 ± 0.01
Oct '15	C	8.15 ± 0.00	12.76 ± 0.01
	P	7.73 ± 0.00	12.76 ± 0.01
	CM	8.45 ± 0.01	13.06 ± 0.01
	PM	8.26 ± 0.00	13.06 ± 0.01
Feb '16	C	8.09 ± 0.01	8.07 ± 0.01
	P	7.65 ± 0.02	8.10 ± 0.01
	CM	8.28 ± 0.01	8.52 ± 0.01
	PM	7.85 ± 0.01	8.53 ± 0.01

5.2.6 Statistical Analysis

To determine whether whole wet weight, muscle mass, GBI, shell weight, shell length, shell width, shell area, percentage weight of aragonite, and diameter of aragonite and calcite crystals changed as a function of time within individual treatment groups, the *lme* function from the *nlme* package (Pinheiro et. al. 2016) in R (The R Core Team, 2012) was used to create linear mixed effects models. The response variable was transformed in the case of non-normal data distribution (Table 5.2.3). Residual spread and homogeneity of variances was tested by applying a Bartlett test to each model (Table 5.2.3). Temporal autocorrelation was determined by means of autocorrelation function (ACF) plots (Table 5.2.3). Model selection was determined using AIC values for each response variable (Table 5.2.4).

Table 5.2.3. Transformations and model assumption tests for linear mixed effects models.

Response Variable	Data Transformation	Bartlett Test	Variance structure	Autocorrelation Structure	Rho
Whole wet weight	Log	K^2=3.658, df=3, p=0.30	None	AR1	0.33
Muscle mass	None	K^2=46.656, df=3, p<0.01	*VarIdent*	None	0.06
GBI	Square Root	K^2=1.332, df=3, p=0.72	None	N/A	N/A
Shell Weight	None	K^2=5.720, df=3, p=0.13	None	None	0.002
Shell Length	None	K^2=0.661, df=3, p=0.88	None	None	0.03
Shell Width	None	K^2=4.458, df=3, p=0.22	None	None	0.06
Shell Area	None	K^2=0.8712, df=3, p=0.843	None	None	0.05
Percentage weight of aragonite	None	K^2=0.593, df=3, p=0.90	None	N/A	N/A
Diameter of aragonite crystals	None	K^2=0.814, df=3, p=0.85	None	N/A	N/A
Diameter of calcite crystals	None	K^2=0.814, df=3, p=0.85	None	N/A	N/A

Table 5.2.4. Linear mixed effects models used to determine the effect of treatment over time for *H. midae* exposed to four treatments over a 12 month period.

Response Variable	Formula	Random Effect	AIC
Whole wet weight	y ~ Treatment * Time	1+Time|Tank	2037.27
Muscle mass	y ~ Treatment * Time	1+Time|Tank	6791.93
GBI	y ~ Treatment	1|Tank	152.76
Shell Weight	y ~ Treatment * Time	0+Time|Tank	4740.69
Shell Length	y ~ Treatment + Time	0+Time|Tank	5160.08
Shell Width	y ~ Treatment + Time	1|Tank	4757.06
Shell Area	y ~ Treatment * Time	0+Time|Tank	13998.83
Percentage weight of aragonite	y ~ Treatment	1|Tank	324.05
Diameter of aragonite crystals	y ~ Treatment	1|Tank	441.17
Diameter of calcite crystals	y ~ Treatment	1|Tank	569.23

To determine whether non-linear data such as: abalone PMB, condition factor, haemolymph pH, haemolymph bicarbonate, shell shape, and compressive force changed as a function of time within individual treatment groups, the *gam* function from the *mgcv* package (Wood 2003, Wood 2011, Wood et. al. 2016) in R (The R Core Team, 2012) was used to create a generalized additive mixed effects models. The response variable was transformed in the case of non-normal data distribution (Table 5.2.5). Residual spread and homogeneity of variances was determined by residual plots of the response and fitted values of the model (Table 5.2.5). Model selection was based on model fit (R^2-values) and the generalized cross-validation statistic (GCV) of GAM models (Table 5.2.6). An AR1 structure was applied to each model. The general formula used for each response variable was:

$$y \sim Treatment + s(Time, by=Treatment, k=3) + s(Tank, Time, bs="re")$$

with the exception of CF (the number of knots (k) was extended to 4).

Table 5.2.5. Transformations and model assumption tests for generalized additive mixed effects models.

Response Variable	Transformation	Residual Plot
PMB	Logit transformation and scale distributed	Homogenous
CF	None	Homogenous
Haemolymph pH	Logit transformation and scale distributed	Homogenous
Haemolymph bicarbonate	None	Homogenous
Shell Shape	None	Homogenous
Compressive Force	Log Transformation	Homogenous

Table 5.2.6. Model fit statistics for generalized additive mixed effects models.

Response Variable	GCV	R 2
PMB	0.0012187	0.206
CF	0.010923	0.12
Haemolymph pH	0.0064792	0.753
Haemolymph bicarbonate	0.13994	0.325
Shell Shape	0.0044918	0.0522
Compressive Force	0.012302	0.279

5.3 Results

5.3.1 Seawater Parameters

Mean seawater carbonate chemistry parameters are presented in Chapter 2. Ambient seawater temperature was 15.64±2.16 °C for the duration of the experiment and followed natural environmental variations. Average ambient seaweed-treated seawater temperature was 16.60±2.18 °C for the duration of the experiment and followed natural environmental variations. Average acidified, seaweed-treated seawater temperature was 16.62±2.18 °C for the duration of the experiment and followed natural environmental variations.

Average ambient seawater pH was 8.10±0.06 for the duration of the experiment and followed natural environmental variations. Average CO_2-diffused seawater pH was 7.66±0.07 in the pH treatment tanks offset to natural environmental pH variations. Average ambient seaweed-treated seawater pH was 8.43±0.09 for the duration of the experiment and followed natural environmental variations. Average acidified and seaweed-treated seawater pH was 7.94±0.07 for the duration of the experiment and followed natural environmental variations. Salinity was 35.5±0.03 in all experimental tanks and remained fairly stable for the duration of the experiment.

5.3.2 Abalone Growth

Abalone growth was measured in terms of wet weight (Figure 5.3.1). Treatment had a significant effect on abalone wet weight over the course of the study ($df=16$, $F=8.4$, $p<0.01$). There was no significant difference between abalone from the control treatment (112.2±14.3 g) and control mitigation treatment (109.0±12.8 g). Abalone from the control treatment and control mitigation treatment were significantly heavier than those from the pH treatment (102.6±14.7 g) after 12 months (Table 5.3.1). There was no significant difference between abalone from the control mitigation treatment and the pH mitigation treatment after 12 months (Table 5.3.1).

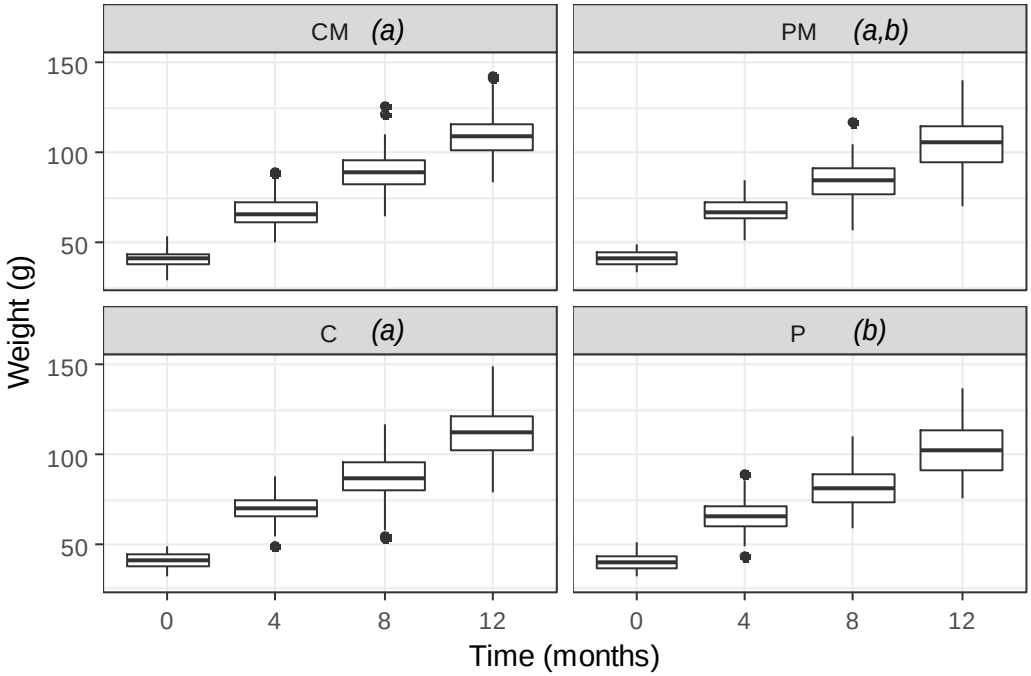

Figure 5.3.1 Boxplots of the wet weights (± standard deviation) of abalone, *H. midae*, exposed to four treatments (CM=control mitigation, PM=pH mitigation, C=ambient control, P=pH) over a 12 month experimental period in a flow-through seawater system. Each treatment group contains repeated measurements at 0-, 4-, 8-, and 12-month sampling times. Same letters in italics between treatments denotes no statistical difference between treatments (alpha = 0.05).

Table 5.3.1. Pairwise differences of abalone wet weights between treatments (C=control, P=pH, CM=control mitigation, PM=pH mitigation) using the Tukey method to compare family estimates. Significant values are taken at the 5% level and shaded in grey.

Contrast Treatments	Comparison (g)	Comparison (%)	Degrees of Freedom	t-ratio	p-value
C - CM	37.15	39.7%	16	0.988	0.76
C - P	41.19	45.0%	16	4.731	<0.01
C - PM	39.09	42.2%	16	2.357	0.13
CM - P	4.04	5.5%	16	3.743	0.01
CM - PM	1.94	2.6%	16	1.369	0.54
P - PM	-2.09	-2.9%	16	-2.374	0.12

5.3.3 Abalone Muscle Mass

Abalone muscle tissue growth was represented by abalone muscle mass (Figure 5.4.2). Treatment had a significant effect on abalone muscle mass over the course of the study (df=16, F=21.710, p<0.01). Abalone from the control treatment (66.14±9.64 g) had significantly heavier muscle mass than abalone from the mitigation control (55.71±9.17), pH mitigation (55.84±9.20 g), and pH (59.97±10.15 g) treatments after 12 months (Table 5.3.2). There was no significant difference between the muscle mass of abalone from the pH treatment and pH mitigation treatment or

between abalone from the control mitigation treatment and the pH and pH mitigation treatments after 12 months (Table 5.3.2).

Abalone muscle mass increased significantly over time for all treatments except the two mitigation treatments (Table 5.4.3). Abalone muscle mass did not increase significantly for abalone in the mitigation treatments between October 2015 and February 2016 (Table 5.3.3). The average muscle mass of abalone from the control mitigation treatment was 1.9 % (2.04 g) non-significantly (df=16, t=1.070, p=0.99) heavier than abalone from the control treatment in October 2015. The average muscle mass of abalone from the pH mitigation treatment was 1.0 % (0.98 g) non-significantly (df=16, t=0.517, p=1.00) heavier than abalone from the control treatment in October 2015

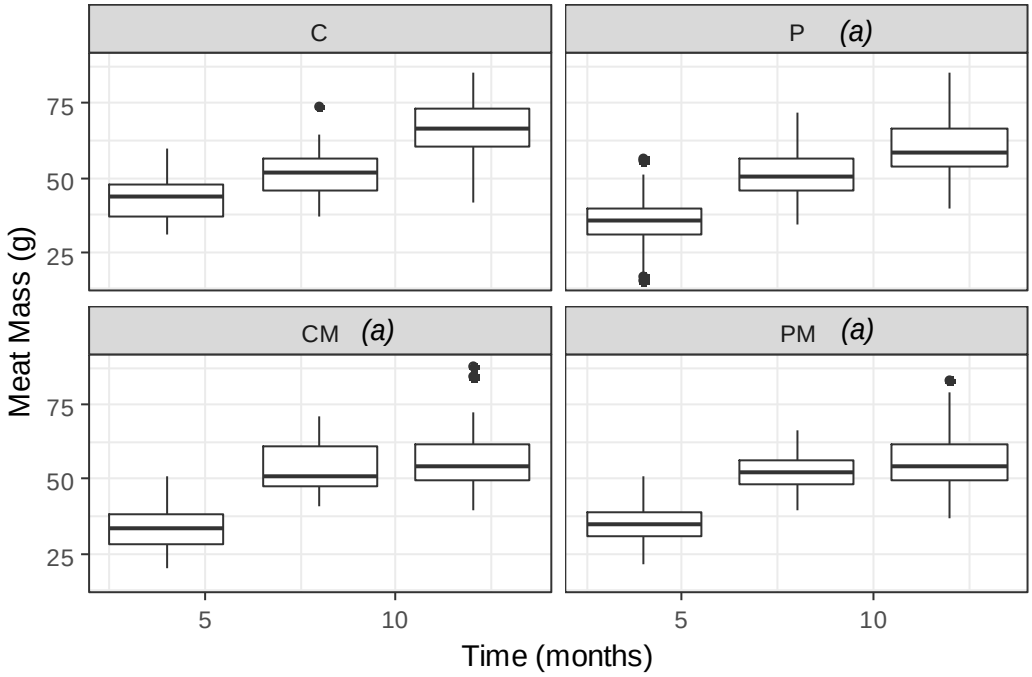

Figure 5.3.2 Muscle mass (± standard deviation) of abalone, *Haliotis midae*, exposed to four seawater treatments (C=control, P=pH, CM=control mitigation, PM=pH mitigation) over a 12 month experimental period in a flow-through seawater system. Each treatment group contains repeated measurements at 4-, 8-, and 12-month sampling times. Same letters in italics between treatments denotes no statistical difference between treatments (alpha = 0.05).

Table 5.3.2. Pairwise differences of abalone muscle mass between treatments (C=control, P=pH, CM=control mitigation, PM=pH mitigation) using the Tukey method to compare family estimates. Significant values are taken at the 5% level and shaded in grey.

Contrast Treatments	Comparison (g)	Comparison (%)	Degrees of Freedom	t-ratio	p-value
C - CM	20.07	35.8%	16	7.143	<0.01
C - P	18.32	32.2%	16	5.487	<0.01
C - PM	19.63	34.8%	16	6.689	<0.01
CM - P	-1.75	-3.7%	16	-1.655	0.38

CM - PM	-0.45	-1.0%	16	-0.453	0.97
P - PM	1.30	2.8%	16	1.202	0.63

Table 5.3.3. Pairwise differences between abalone muscle mass within treatments (C=control, P=pH, CM=control mitigation, PM=pH mitigation) between sampling times using the Tukey method to compare family estimates. Significant values are taken at the 5% level and shaded in grey.

Treatment	Contrast times	Comparison (g)	Comparison (%)	Degrees of Freedom	t-ratio	p-value
Control Mitigation	4-8	20.01	59.8%	932	-12.801	<0.01
	8-12	2.23	4.2%	932	-1.311	0.98
pH Mitigation	4-8	17.05	48.8%	932	-10.908	<0.01
	8-12	3.83	7.4%	932	-2.242	0.52
Control	4-8	8.64	20.2%	932	-5.53	<0.01
	8-12	14.70	28.6%	932	-8.634	<0.01
pH	4-8	16.67	48.5%	932	-10.668	<0.01
	8-12	8.93	17.5%	932	-5.243	<0.01

5.3.3. Proportion muscle to whole body mass (PMB)

The proportion of meat to whole body mass was represented as PMB (Figure 5.3.3). Treatment had a significant effect on abalone PMB over the course of the study (df=2.3, χ^2=0.09, p<0.01). Abalone from the control treatment had a significantly different PMB from all other treatments (Table 5.3.4). Abalone from the control treatment displayed a continual decrease in PMB over time (Figure 5.3.3); whereas abalone from the control mitigation, pH mitigation and pH treatments displayed a peak PMB in October 2015 in comparison to lower PMB in June 2015 and February 2016 (Figure 5.3.5).

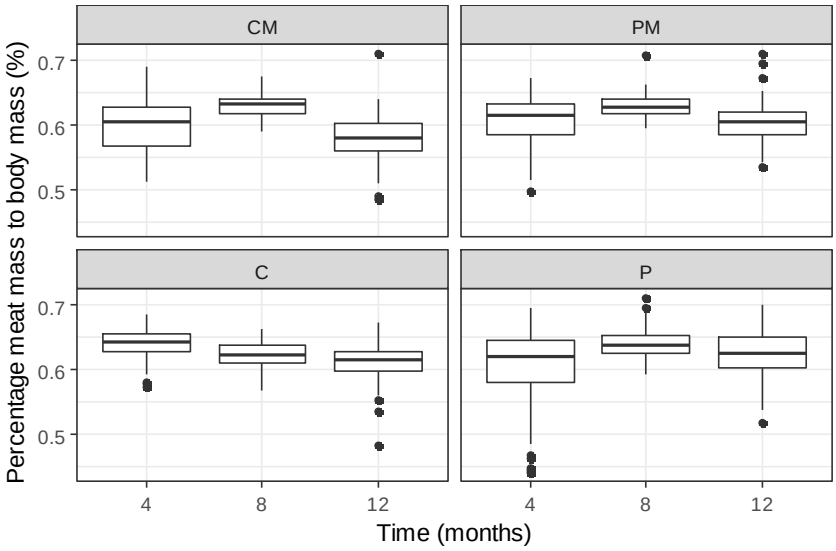

Figure 5.3.3. PMB (± standard deviation) of abalone, *Haliotis midae*, exposed to four seawater treatments (C=control, P=pH, CM=control mitigation, PM=pH mitigation) over a 12 month experimental period in a flow-through seawater system. Each treatment group contains repeated measurements at 4-, 8-, and 12-month sampling times.

Table 5.3.4. Ordered factor contrasts of smoothing terms for abalone PMB between four treatments (C=control, P=pH, CM=control mitigation, PM=pH mitigation) over the 12 month study. Significant values are taken at the 5% level and shaded in grey.

Contrast Treatments	Estimated Degrees of Freedom	F-value	p-value
C - P	1.954	13.589	<0.01
C - CM	1.972	20.549	<0.01
C - PM	1.932	6.771	<0.01

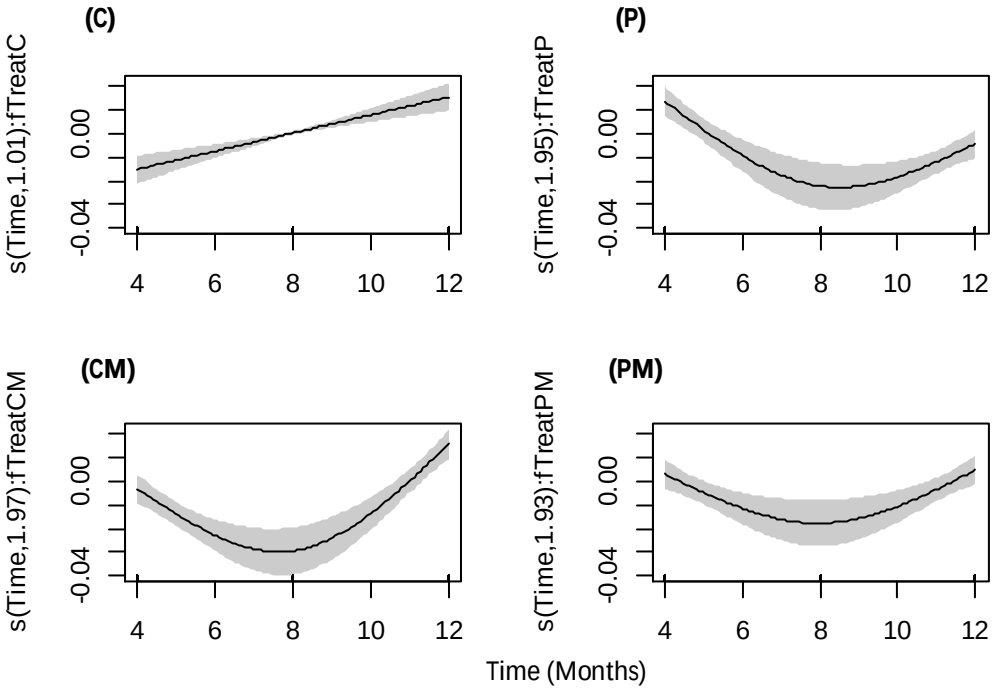

Figure 5.3.4. Smoothing function with fitted values of abalone proportion of muscle to whole body mass (PMB) response to four treatments (C) ambient control, (P) pH, (CM) control mitigation, and (PM) pH mitigation, over a 12 month experimental period in the optimal generalized additive model. Estimated degrees of freedom for each smoothing term are listed on the y-axis labels. Results are depicted after logit transformation and scale distribution.

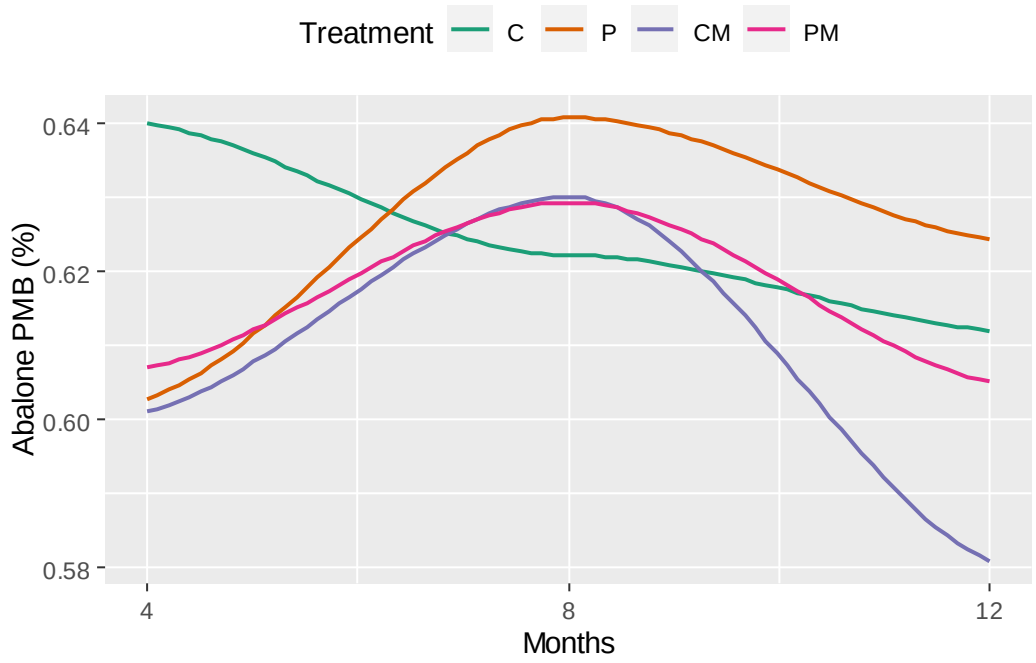

Figure 5.3.5. Abalone PMB response to four treatments (C=control, P=pH, CM=control mitigation, PM=pH mitigation) over a 12-month experimental period using LOESS smoothers. Each treatment group contains repeated measurements at 4-, 8-, and 12-month sampling times.

5.3.4 Condition Factor

Abalone from all treatments had a condition factor (CF) greater than 1, indicating that all abalone were in good condition during the experimental period. Treatment had a significant effect (df=4.3, χ^2=1.739, p<0.01) on abalone condition factor (CF) the course of the study (Figure 5.3.6). Abalone in ambient conditions had a significantly different response in CF over 12 months in comparison to the other treatments (Table 5.3.5). Abalone from the control treatment displayed a peak in CF in June 2015 and a trough in CF in November 2015 (Figure 5.3.7). Abalone from the control mitigation and pH mitigation treatments displayed a peak in CF in October 2015 with a slight decline thereafter (Figure 5.3.7). Abalone from the pH treatment displayed a peak in CF in July 2015 with a gradual decline thereafter (Figure 5.3.7).

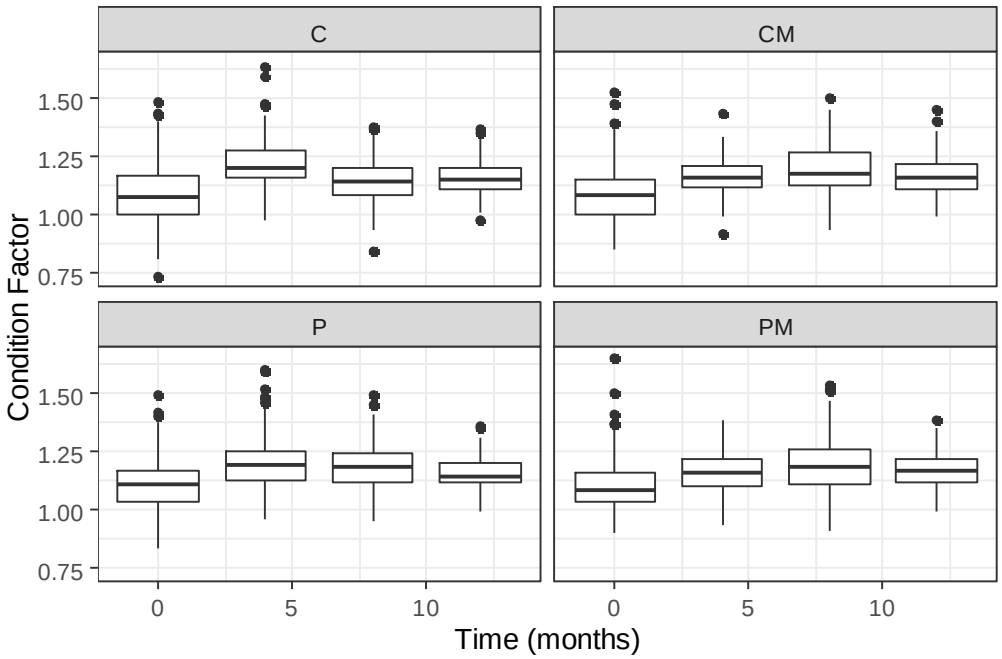

Figure 5.3.6. Condition factor (± standard deviation) of abalone, *Haliotis midae*, exposed to four seawater treatments (C=control, P=pH, CM=control mitigation, PM=pH mitigation) over a 12-month experimental period in a flow-through seawater system. Each treatment group contains repeated measurements at 4-, 8-, and 12-month sampling times.

Table 5.3.5. Ordered factor contrasts of smoothing terms for abalone condition factor between treatments (C=control, P=pH, CM=control mitigation, PM=pH mitigation) over a 12-month experimental period. Significant values are taken at the 5% level and shaded in grey.

Contrast Treatments	Estimated Degrees of Freedom	F-value	p-value
C - P	2.606	19.324	<0.01
C - CM	2.804	18.339	<0.01
C - PM	2.356	10.685	<0.01

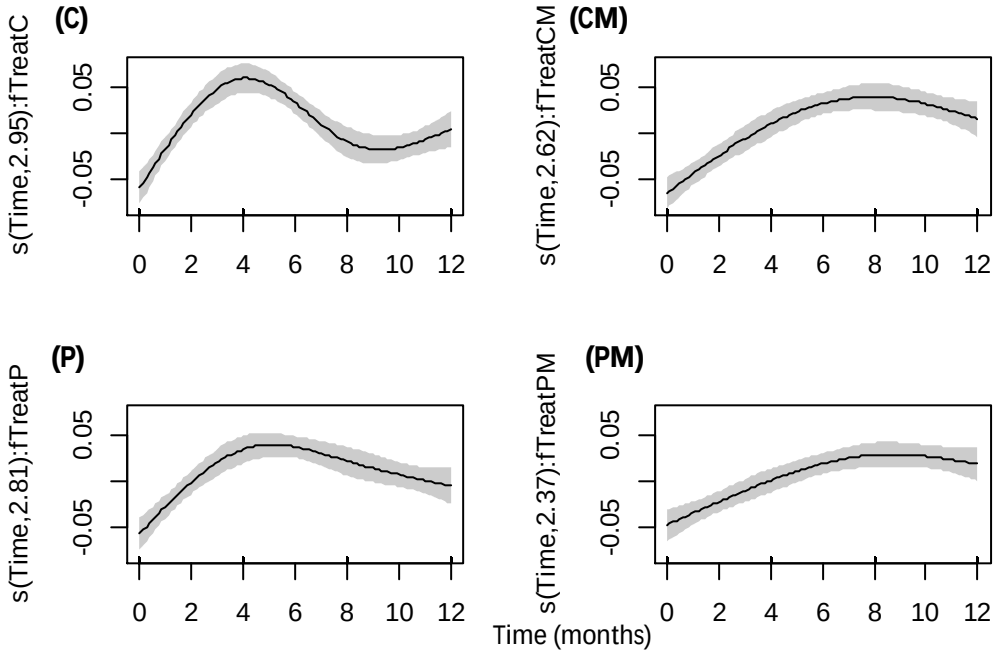

Figure 5.3.7. Smoothing function of abalone condition factor (CF) response to four treatments (C=control, P=pH, CM=control mitigation, PM=pH mitigation) over a 12 month experimental period in the optimal generalized additive model. The estimated degrees of freedom (EDF) for each treatment are listed on the y-axis for each treatment.

5.3.3 Gonad development

Abalone gonadal bulk index (GBI) differed significantly (df=3, F=1.739, p<0.01) between treatments after 12 months of exposure to experimental conditions (Figure 5.3.8). Abalone from the low pH treatment (0.551±0.196 g.mm^{-1}) had significantly smaller GBIs than those from the ambient (0.833±0.285 g.mm^{-1}), mitigation control (0.898±0.297 g.mm^{-1}), and pH mitigation (0.736±0.266 g.mm^{-1}) treatments (Table 5.3.6).

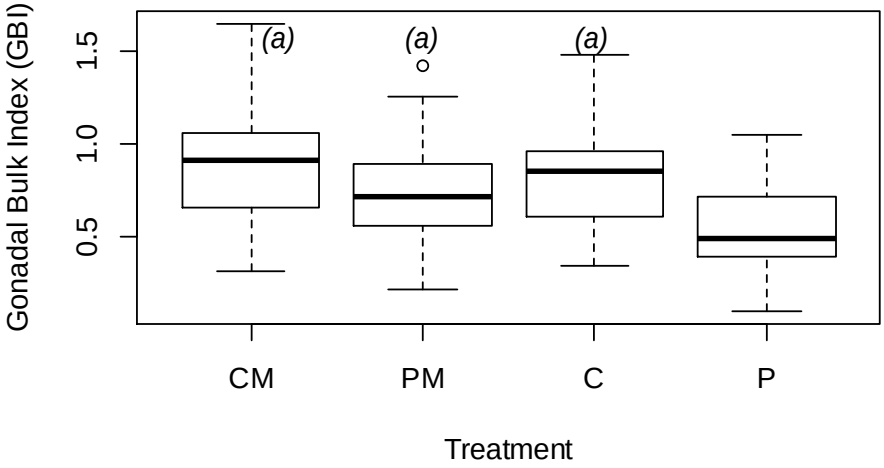

Figure 5.3.8. Gonadal bulk index (GBI, ± standard deviation) of abalone, *Haliotis midae*, exposed to four seawater treatments (C=control, P=pH, CM=control mitigation, PM=pH mitigation) for a 12-month experimental period in a flow-through seawater system. Same letters in italics between treatments denotes no statistical difference between treatments (alpha = 0.05).

Table 5.3.6. Pairwise differences between abalone gonadal body indices (GBI) between treatments (C=control, P=pH, CM=control mitigation, PM=pH mitigation) using the Tukey method to compare family estimates. Significant values are taken at the 5% level and shaded in grey.

Contrast Treatments	Comparison (mm3.g-1)	Comparison (%)	Degrees of Freedom	t-ratio	p-value
C - CM	-0.06	-7.5%	16	0.917	0.80
CM - PM	0.16	20.6%	16	2.379	0.12
C - PM	0.10	12.3%	16	1.463	0.48
P - PM	-0.19	-29.1%	16	3.001	0.04
P - CM	-0.35	-48.2%	16	5.372	<0.01
C - P	0.28	41.1%	16	4.459	<0.01

5.3.4 Haemolymph pH and bicarbonate

In vivo haemolymph parameters of *H. midae* are presented in Table 5.3.7. Haemolymph pH and bicarbonate concentration were analysed for statistical differences and patterns over time.

Table 5.3.7. *In vivo* haemolymph parameters (± standard deviation) of *H. midae* exposed to four seawater treatments (C=control, P=pH, CM=control mitigation, PM=pH mitigation) for 12 months (Feb 2015 - Feb 2016), sampled every 4 months.

Sample date	Treatment	pH	cCO_2 (mM)	pCO_2 (Torr)	pCO_2 (kPa)	$[HCO_3^-]$ ($mmol^{-1}$)
June '15	CM	7.30±0.04	2.19±0.43	2.33±0.42	0.31±0.06	2.08±0.42
	PM	7.35±0.05	2.28±0.5	2.21±0.61	0.29±0.08	2.18±0.47
	C	7.24±0.06	1.96±0.32	2.41±0.36	0.32±0.05	1.85±0.31
	P	7.28±0.07	2.19±0.47	2.45±0.6	0.33±0.08	2.08±0.45
Oct '15	CM	7.47±0.08	2.80±0.45	2.09±0.52	0.28±0.07	2.71±0.43
	PM	7.26±0.08	2.43±0.44	2.83±0.54	0.38±0.07	2.30±0.43
	C	7.42±0.05	2.83±0.26	2.33±0.32	0.31±0.04	2.73±0.25
	P	7.29±0.05	2.83±0.3	3.14±0.36	0.42±0.05	2.69±0.29
Feb '16	CM	7.27±0.16	2.36±0.24	2.91±1.32	0.39±0.18	2.23±0.20
	PM	7.02±0.05	2.33±0.42	4.63±1.09	0.62±0.15	2.12±0.38
	C	7.15±0.08	2.38±0.26	3.63±0.65	0.48±0.09	2.22±0.24
	P	7.02±0.06	2.33±0.2	4.68±0.67	0.62±0.09	2.12±0.19

There was a significant difference (df=8.2, χ^2=1.360, p<0.01) in the response of abalone haemolymph pH to the treatments over time (Figure 5.3.9). Abalone in ambient conditions displayed a significantly different response in haemolymph pH to the other treatments (Table 5.3.8). Haemolymph pH in ambient conditions peaked after 8 months (October 2015) then declined until the end of the experimental period (Figure 5.3.10). Abalone from the pH and pH mitigation treatments did not follow the same response as abalone in ambient conditions; both treatments remained fairly stable for 8 months of exposure to experimental conditions and declined thereafter

(Figure 5.3.10). Abalone from the pH and pH mitigation treatment had the lowest haemolymph pH at the end of the experimental period (Table 5.3.8). Abalone from the ambient mitigation treatment had a similar response in haemolymph pH as those from the control treatment, but had a larger variance in pH at the end of the experimental period (Figure 5.3.10).

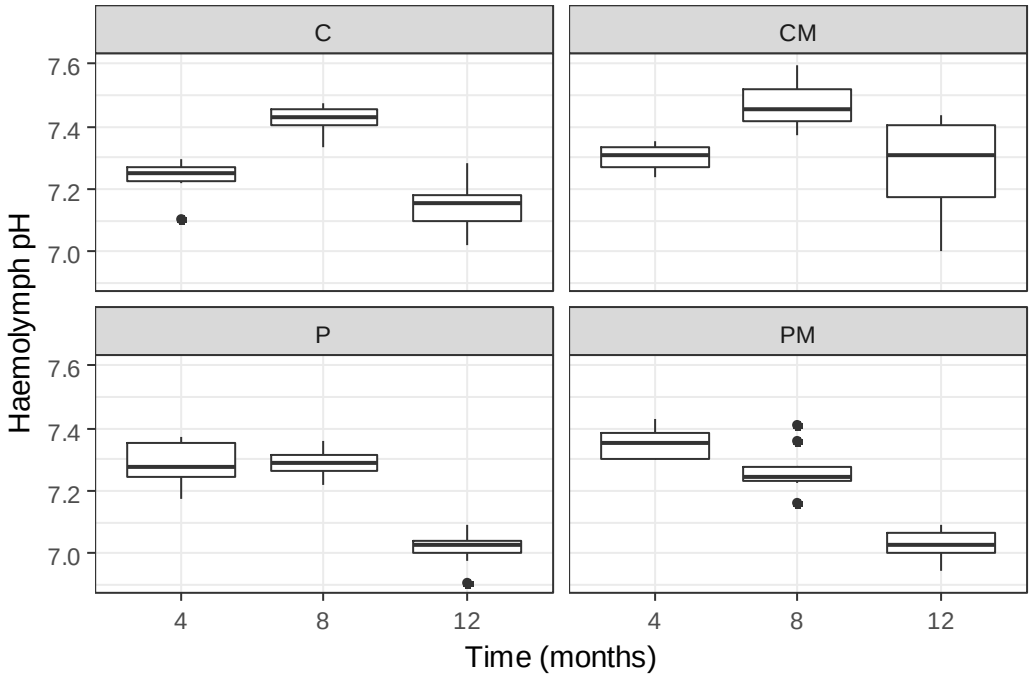

Figure 5.3.9. Haemolymph pH (± standard deviation) of abalone, *Haliotis midae*, exposed to four seawater treatments (C=control, P=pH, CM=control mitigation, PM=pH mitigation) over a 12-month experimental period in a flow-through seawater system. Each treatment group contains repeated measurements at 4-, 8-, and 12-month sampling times.

Table 5.3.8. Ordered factor contrasts of smoothing terms for abalone haemolymph pH between four treatments (C=control, P=pH, CM=control mitigation, PM=pH mitigation) over the 12-month study. Significant values are taken at the 5% level and shaded in grey.

Contrast Treatments	Estimated Degrees of Freedom	F-value	p-value
C - P	1.911	19.580	<0.01
C - CM	1.950	9.660	<0.01
C - PM	1.708	23.300	<0.01

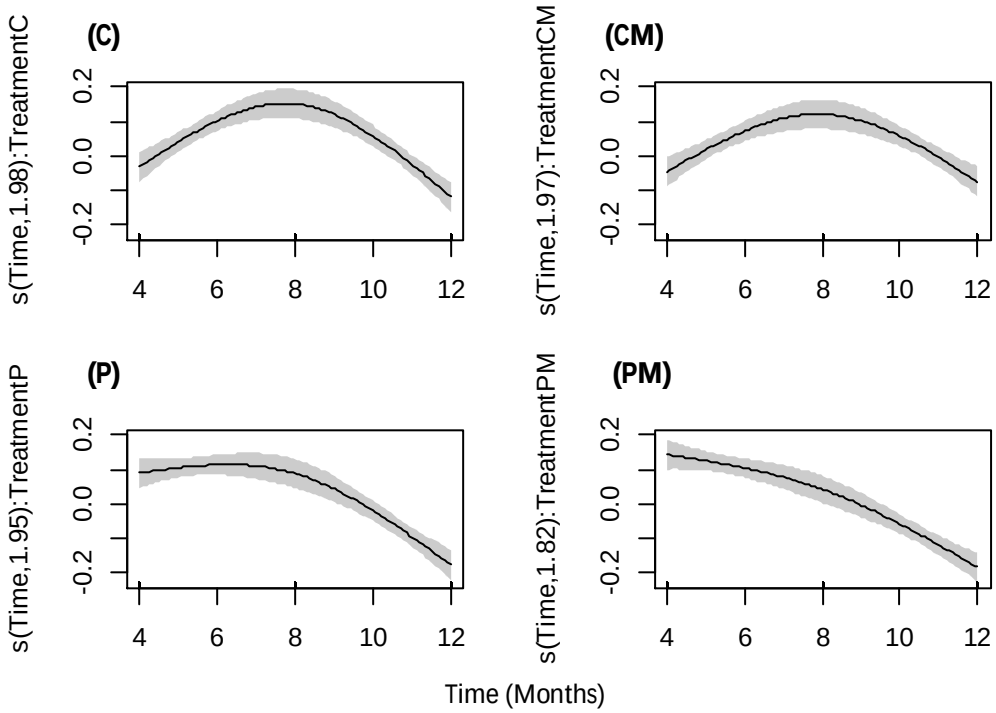

Figure 5.3.10. Smoothing function of abalone haemolymph pH response to four treatments (C=control, P=pH, CM=control mitigation, PM=pH mitigation) over a 12-month experimental period in the optimal generalized additive model. The estimated degrees of freedom (EDF) for each treatment are listed on the y-axis for each treatment.

Treatment had a significant effect (df=7.1, χ^2=6.647, p<0.01) on the response of haemolymph bicarbonate concentrations [HCO_3^-] over the course of the study (Figure 5.3.11). Abalone in ambient conditions displayed a significantly different response in haemolymph [HCO_3^-] to the low pH and pH mitigation treatments over the course of the study (Table 5.3.9). Haemolymph [HCO_3^-] in ambient conditions peaked after 8 months (October 2015) then declined until the end of the experimental period. Abalone from the low pH treatment displayed a similar response in haemolymph pH, but had a lower [HCO_3^-] after 12 months in comparison to the control (Table 5.3.9). Abalone from the pH mitigation treatment displayed a linear (edf=1.00), fairly stable haemolymph [HCO_3^-] over the course of the study (Figure 5.3.12). There was no significant difference in the response of haemolymph [HCO_3^-]to ambient and ambient mitigation treatments over the course of the study (Table 5.3.9).

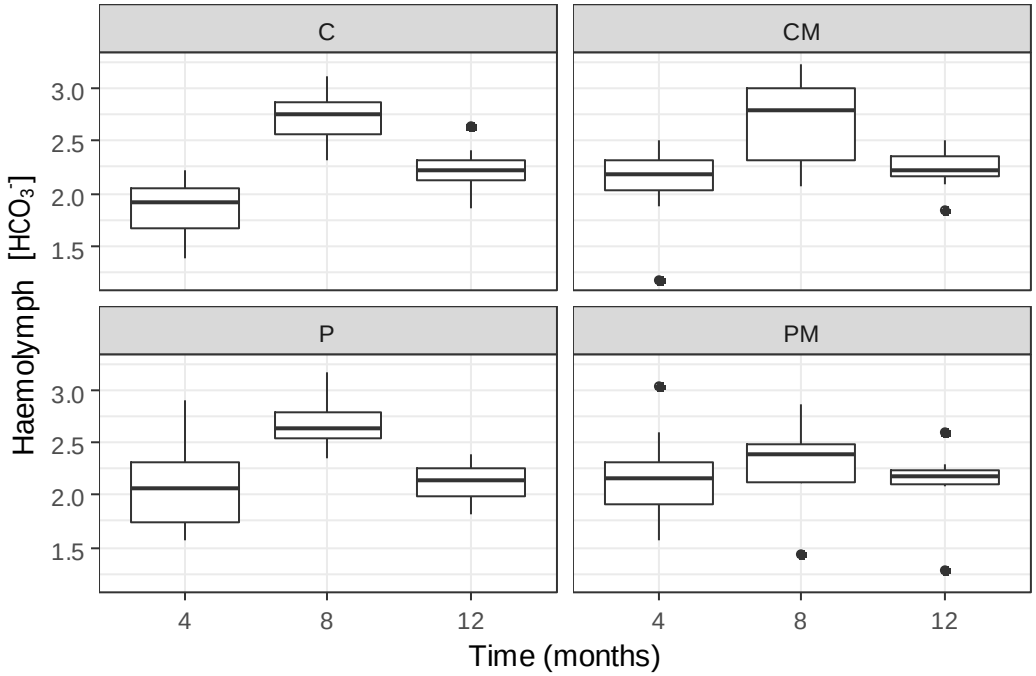

Figure 5.3.11. Haemolymph bicarbonate concentrations (± standard deviation) of abalone, *Haliotis midae*, exposed to four seawater treatments (C=control, P=pH, CM=control mitigation, PM=pH mitigation) over a 12 month experimental period in a flow-through seawater system. Each treatment group contains repeated measurements at 4-, 8-, and 12-month sampling times.

Table 5.3.9. Ordered factor contrasts of smoothing terms for abalone haemolymph bicarbonate concentrations between treatments (C=control, P=pH, CM=control mitigation, PM=pH mitigation) over the 12-month study. Significant values are taken at the 5% level and shaded in grey.

Contrast Treatments	Estimated Degrees of Freedom	F-value	p-value
C - P	1.916	0.094	0.76
C - CM	1.903	4.129	0.03
C - PM	1.000	5.068	0.01

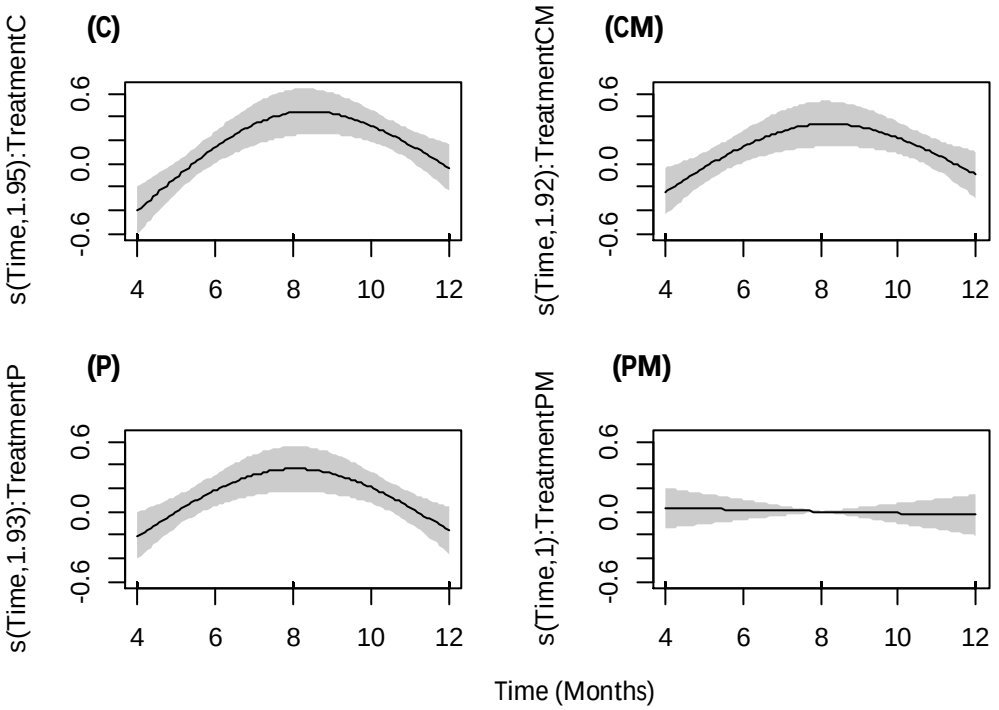

Figure 5.3.12. Smoothing function of abalone haemolymph bicarbonate concentration response to four treatments (C=control, P=pH, CM=control mitigation, PM=pH mitigation) over a 12-month experimental period in the optimal generalized additive model. The estimated degrees of freedom (EDF) for each treatment are listed on the y-axis for each treatment.

Abalone haemolymph from the control treatment ranged in pH from 7.15-7.42, in [HCO_3^- + CO_3^{2-}] from 1.85-2.73 mM, and in pCO_2 from 1.96-2.83 Torr over the course of the study. The Henderson-Hasselbalch diagram displayed a similar status of [HCO_3^- + CO_3^{2-}], pCO_2 and pH for all treatments in comparison to the control treatment after 4 months of exposure to experimental conditions. Contrasting treatments had slightly higher haemolymph pH and [HCO_3^- + CO_3^{2-}] in comparison to the control treatment (Figure 3.3.15 A).

The Henderson-Hasselbalch diagram of the pH mitigation treatment showed similar movement in [HCO_3^- + CO_3^{2-}], pCO_2 and pH compared with that of the control treatment (Figure 5.4.12 A, B; Table 5.4.7), with the exception of the final sampling period (Fig. 5.3.13 C). Haemolymph pH from the control mitigation treatment was 0.13 units (1.7 %) more than the control treatment after 12 months (Figure 5.3.13 B), and haemolymph pCO_2 from abalone in the control mitigation treatment was 0.723 Torr (22.1 %) less than the control treatment after 12 months (Figure 5.3.13 B).

The Henderson-Hasselbalch diagram of the pH mitigation treatment showed similar movement in [HCO_3^- + CO_3^{2-}], pCO_2 and pH compared with the pH treatment over 12 months, with one exception (Figure 5.3.13 B). After 8 months of exposure to experimental conditions, abalone from the pH mitigation treatment had lower pCO_2 (0.31 Torr, 10.4%) and [HCO_3^- + CO_3^{2-}] (0.39 mM, 15.6%) in comparison to the pH treatment, indicating respiratory compensation in the pH mitigation treatment; however by the end of the experimental period abalone from both treatments shared a similar acid-base status.

After 12 months, there was a distinct difference in acid-base status between abalone from the control treatment, control mitigation treatment, and the pH and pH mitigation treatments. Haemolymph [HCO_3^- + CO_3^{2-}] from the pH mitigation treatment was 0.43 mM (17.0 %) less than the control treatment, and 0.406 mM (16.2 %) less than the control mitigation treatment during this period. Abalone from the pH mitigation treatment had a similar [HCO_3^- + CO_3^{2-}] to the pH treatment; however the pH was 0.12 units (1.8 %) more alkaline than the control treatment and 0.25 units (3.5 %) more alkaline than the control mitigation treatment (Figure 5.3.13 C). Haemolymph pCO_2 of abalone from the pH mitigation treatment was 1.00 Torr (24.1 %) more than the control treatment and 1.72 Torr (45.7 %) more than the control mitigation treatment (Figure 5.3.13 C).

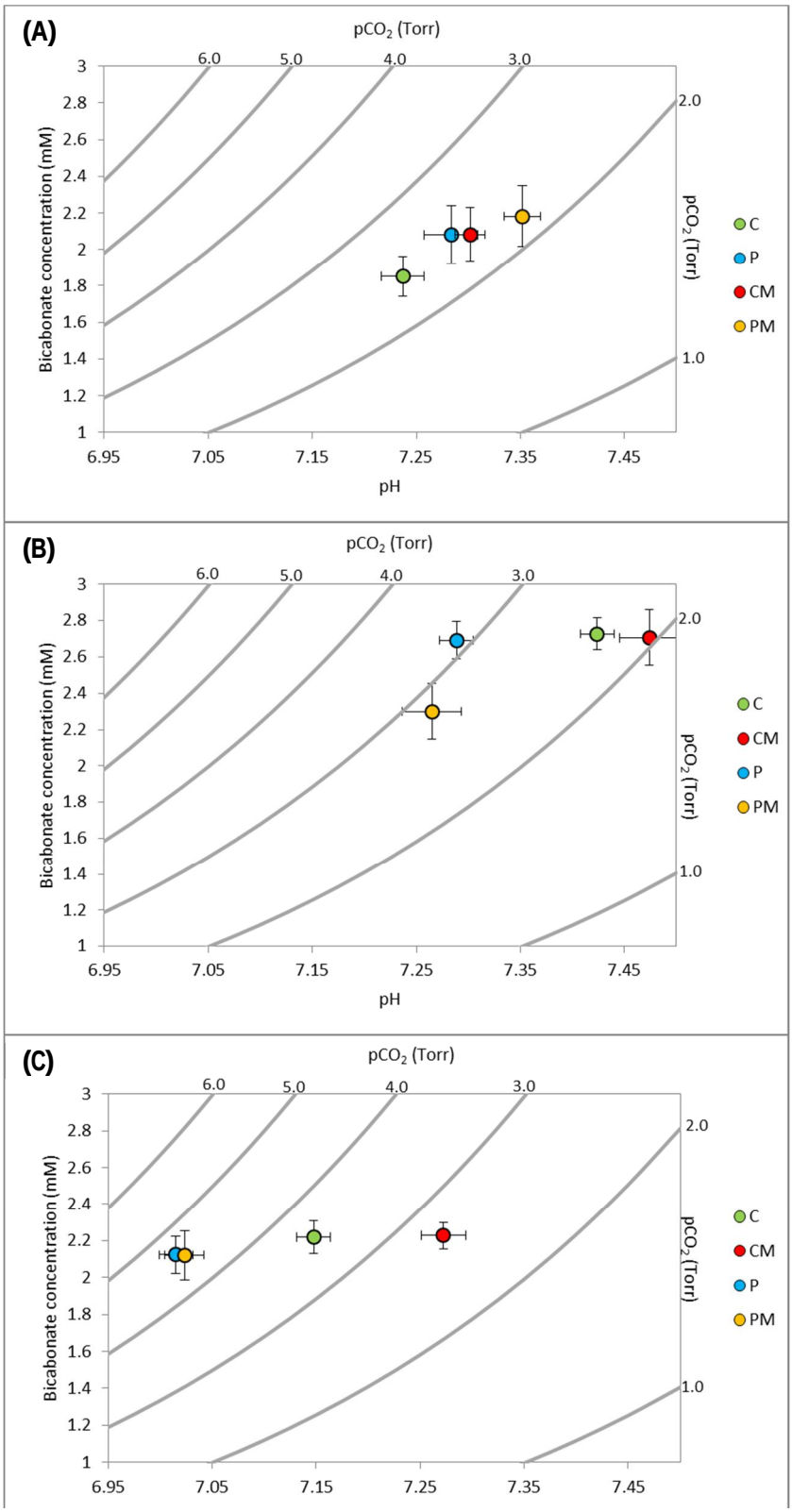

Figure 5.3.13. Davenport diagrams for haemolymph samples from adult *H. midae*, exposed to four seawater treatments (C=control, P=pH, CM=control mitigation, PM=pH mitigation) for **(A)** 4-, **(B)** 8- , and **(C)** 12-months in a flow-through seawater system. The pCO_2 isopleths (grey lines) were derived from the Henderson–Hasselbalch equation. Appropriate values for the first dissociation constant (pK'1) and solubility coefficient (α) were derived from Truchot (1976). Values are means ± S.E. (1 Torr = 0.133 kPa).

5.3.5. Shell Growth and Morphology

Abalone shell morphology was represented by abalone shell weight (Figure 5.3.14), length (Figure 5.3.15), width (Figure 5.3.16), shape (Figure 5.3.17), and area (Figure 5.3.19).

Treatment had a significant effect on abalone shell weight over the course of the study (df=16, F=16.316, p<0.01). Shell from the control (28.43±3.74 g) and control mitigation (27.31±3.35 g) treatments were significantly heavier than those from the pH (24.13±3.34 g) and pH mitigation (25.15±3.19 g) treatments after 12 months (Table 5.3.10). There was no significant difference between shells from the pH mitigation treatment and the pH treatment or between those from the control and control mitigation treatments (Table 5.4.10).

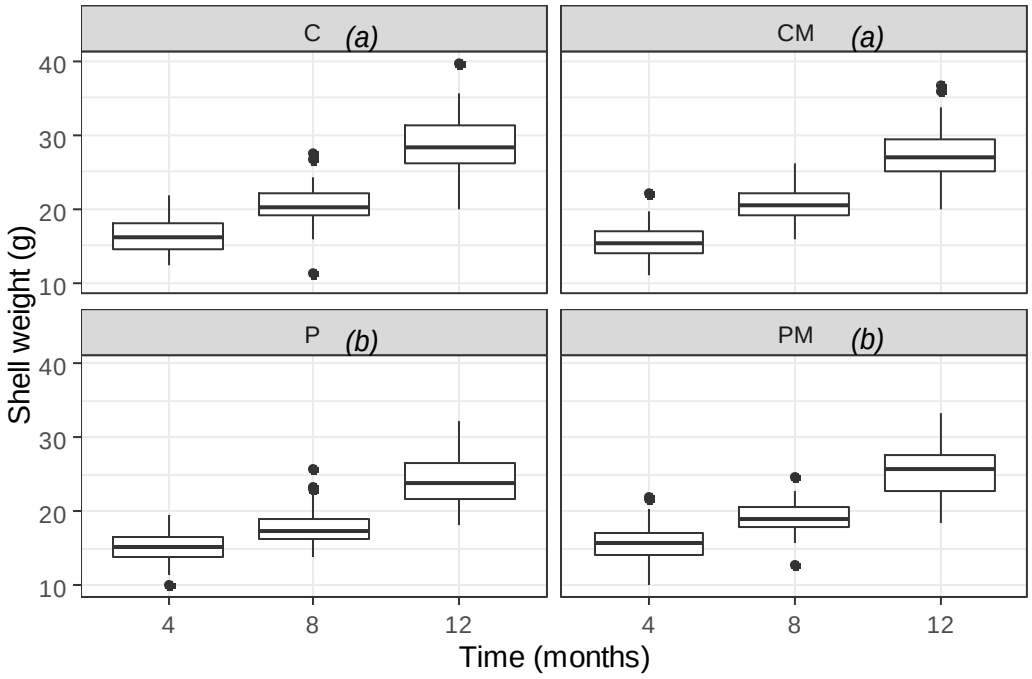

Figure 5.3.14. Shell weights (± standard deviation) of abalone, *Haliotis midae*, exposed to four seawater treatments (C=control, P=pH, CM=control mitigation, PM=pH mitigation) over a 12-month experimental period in a flow-through seawater system. Each treatment group contains repeated measurements at 4-, 8-, and 12-month sampling times. Same letters in italics between treatments denotes no statistical difference between treatments (alpha = 0.05).

Table 5.3.10. Pairwise differences of abalone shell weights between treatments (C=control, P=pH, CM=control mitigation, PM=pH mitigation) using the Tukey method to compare family estimates. Significant values are taken at the 5% level and shaded in grey.

Contrast Treatments	Comparison (g)	Comparison (%)	Degrees of Freedom	t-ratio	p-value
C - CM	1.12	4.0%	16	2.170	0.17
C - P	4.30	16.4%	16	7.790	<0.01
C - PM	3.29	12.3%	16	5.062	<0.02
CM - P	3.18	12.4%	16	5.620	<0.03
CM - PM	2.16	8.2%	16	2.891	0.047
P - PM	-1.02	-4.1%	16	-2.728	0.06

Treatment had a significant effect on abalone shell length over the course of the study (df=16, F=8.66, p<0.01). Shells from the control (83.50±3.73 mm) and control mitigation (82.78±3.81 mm) treatments were significantly longer than those from the pH treatment (81.31±3.85 mm) after 12 months (Table 5.3.11). There was no significant difference in length between shells from the pH mitigation treatment (81.74±3.84 mm) and the pH treatment, or between shells from control, pH mitigation and control mitigation treatments after 12 months (Table 5.3.11).

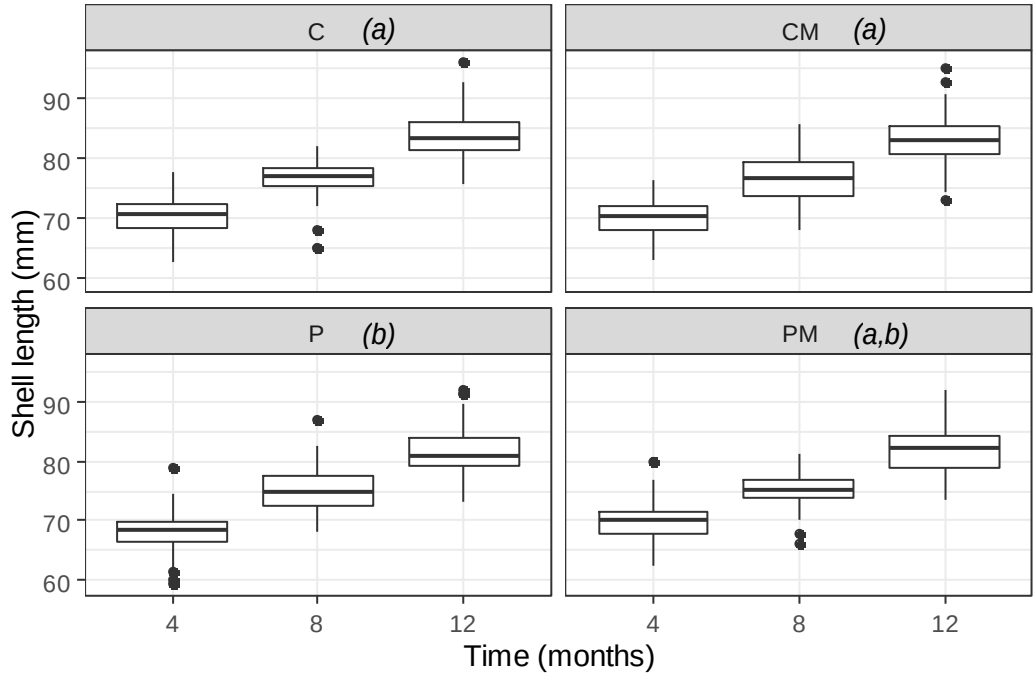

Figure 5.3.15. Shell lengths (± standard deviation) of abalone, *Haliotis midae*, exposed to four seawater treatments (C=control, P=pH, CM=control mitigation, PM=pH mitigation) over a 12-month experimental period in a flow-through seawater system. Each treatment group contains repeated measurements at 4-, 8-, and 12-month sampling times. Same letters in italics between treatments denotes no statistical difference between treatments (alpha = 0.05).

Table 5.3.11. Pairwise differences of abalone shell lengths between treatments (C=control, P=pH, CM=control mitigation, PM=pH mitigation) using the Tukey method to compare family estimates. Significant values are taken at the 5% level and shaded in grey.

Contrast Treatments	Comparison (mm)	Comparison (%)	Degrees of Freedom	t-ratio	p-value
C - CM	0.72	0.9%	16	0.970	0.77
C - P	2.19	2.7%	16	4.804	<0.01
C - PM	1.76	2.1%	16	2.269	0.15
CM - P	1.47	1.8%	16	3.834	<0.01
CM - PM	1.04	1.3%	16	1.299	0.576
P - PM	-0.43	-0.5%	16	-2.535	0.09

Treatment had a significant effect on abalone shell width over the course of the study (df=16, F=16.6, p<0.01). Shells from the control (57.53±2.96 mm) and control mitigation treatments (56.81±2.81 mm) were significantly wider than those from the pH treatment (55.67±2.97 mm) after 12 months (Table 5.3.12). There were no significant differences in shell width between abalone from the pH mitigation treatment (55.80±3.07 mm) and low pH treatment or between shells from the control, pH mitigation and control mitigation treatments after 12 months (Table 5.3.12).

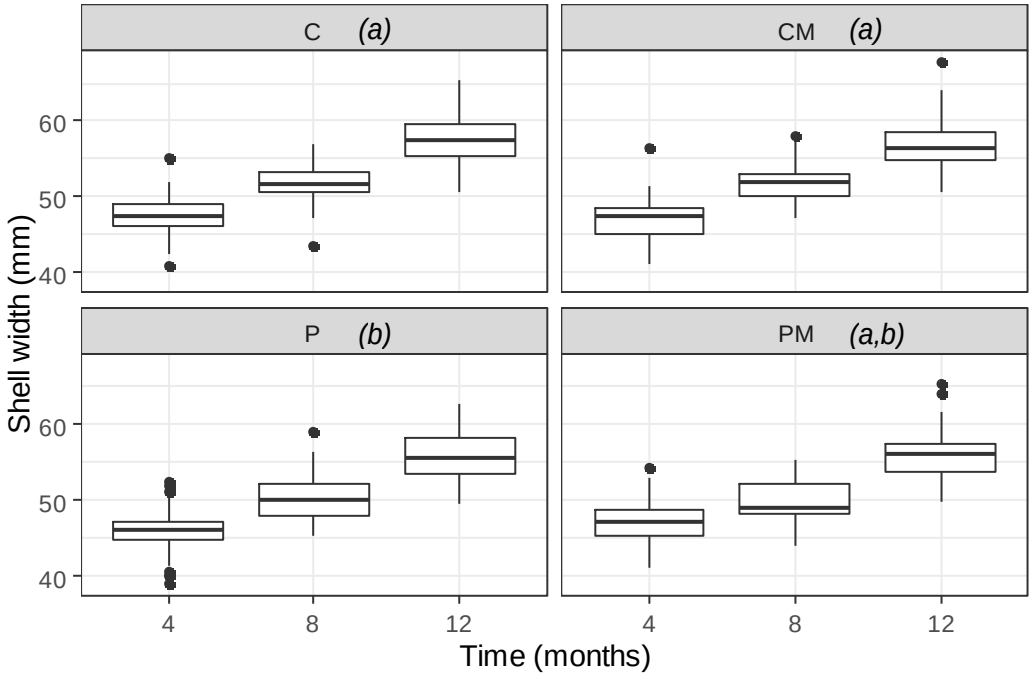

Figure 5.3.16. Shell widths (± standard deviation) of abalone, *Haliotis midae*, exposed to four seawater treatments (C=control, P=pH, CM=control mitigation, PM=pH mitigation) over a 12-month experimental period in a flow-through seawater system. Each treatment group contains repeated measurements at 4-, 8-, and 12-month sampling times. Same letters in italics between treatments denotes no statistical difference between treatments (alpha = 0.05).

Table 5.3.12. Pairwise differences of abalone shell widths between treatments (C=control, P=pH, CM=control mitigation, PM=pH mitigation) using the Tukey method to compare family estimates. Significant values are taken at the 5% level and shaded in grey.

Contrast Treatments	Comparison (mm)	Comparison (%)	Degrees of Freedom	t-ratio	p-value
C - CM	0.72	1.3%	16	1.658	0.38
C - P	1.86	3.3%	16	6.515	<0.01
C - PM	1.73	3.0%	16	4.366	<0.01
CM - P	1.14	2.0%	16	4.857	<0.01
CM - PM	1.01	1.8%	16	2.701	0.07
P - PM	-0.13	-0.2%	16	-2.149	0.18

Treatment had a significant effect on abalone shell shape the course of the study (df=7.2, χ^2=0.187, p<0.01). Abalone from the control treatment had a significantly different shape in comparison to all other treatments (Table 5.3.13). Shell shape in ambient conditions was fairly stable for 8 months, with a shift to wider shape thereafter (Figure 5.3.18). The response in abalone shell shape to the control mitigation treatment was a linear (edf=1.00), gradual change in shape towards a wider, shorter shell over the course of the experiment (Figure 5.3.18). The response in abalone shell shape to the pH and pH mitigation treatments was a shift towards longer shells between 4 to 8 months of exposure to treatment conditions, with a change to wider shells thereafter (Figure 5.3.18).

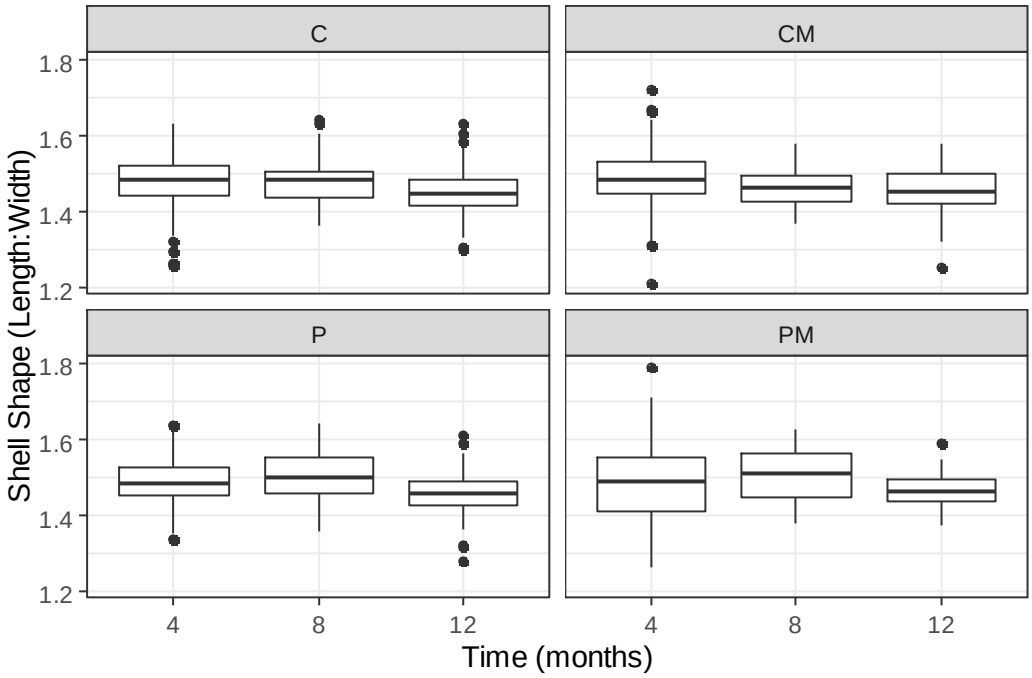

Figure 5.3.17. Shell shape (± standard deviation) of abalone, *Haliotis midae*, exposed to four seawater treatments (C=control, P=pH, CM=control mitigation, PM=pH mitigation) over a 12-month experimental period in a flow-through seawater system. Each treatment group contains repeated measurements at 4-, 8-, and 12-month sampling times.

Table 5.3.13. Ordered factor contrasts of smoothing terms for abalone shell shape between treatments (C=control, P=pH, CM=control mitigation, PM=pH mitigation) over the 12-month study. Significant values are taken at the 5% level and shaded in grey.

Contrast Treatments	Estimated Degrees of Freedom	F-value	p-value
C - P	1.83	5.311	<0.01
C - CM	1.00	9.218	<0.01
C - PM	1.87	4.845	0.01

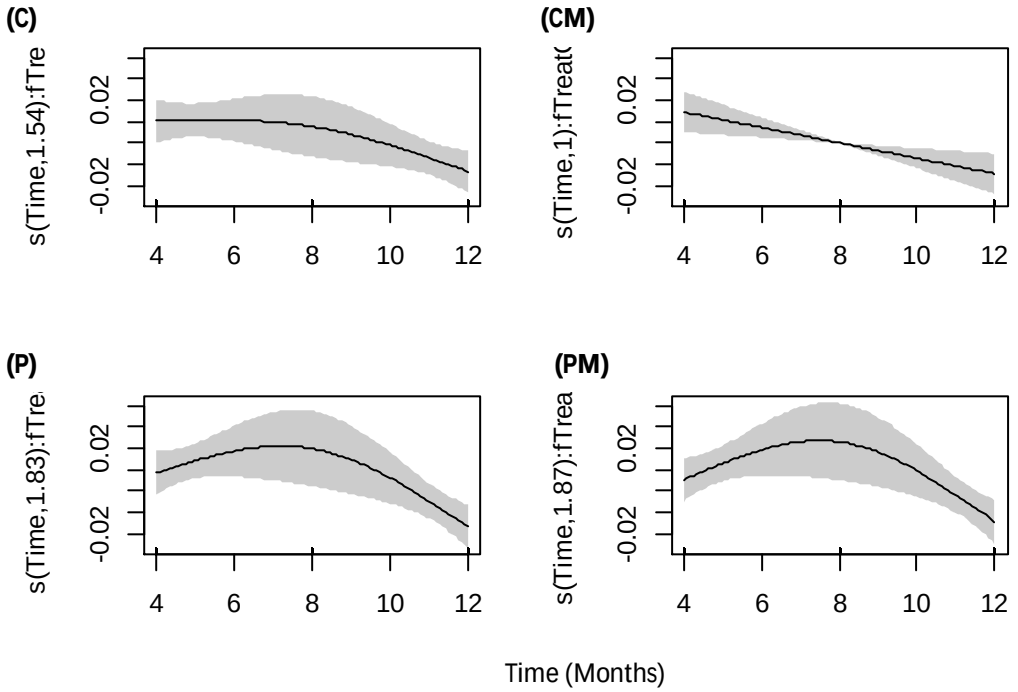

Figure 5.3.18. Smoothing function with fitted values of abalone shell shape (length:width) response to four treatments (C=control, P=pH, CM=control mitigation, PM=pH mitigation) over a 12-month experimental period in the optimal generalized additive model. Degrees of freedom for each smoothing term are listed on the y-axis labels.

Treatment had a significant effect on abalone shell area over the course of the study (df=16, F=13.08, p<0.01). Shells from the control (4810.23±420.07 mm^2) and control mitigation (4709.76±413.79 mm^2) treatment were significantly larger than those from the pH treatment (4534.42±422.51 mm^2). Shells from the control treatment were significantly larger than those from the pH mitigation (4570±449.06 mm^2) treatment (Table 5.3.14). There were no significant differences in shell area between abalone from the control and control mitigation treatments, or between shells from the control mitigation treatment and pH mitigation treatment (Table 5.3.14). There was no significant difference in shell widths between the pH mitigation treatment and the pH treatment (Table 5.3.14).

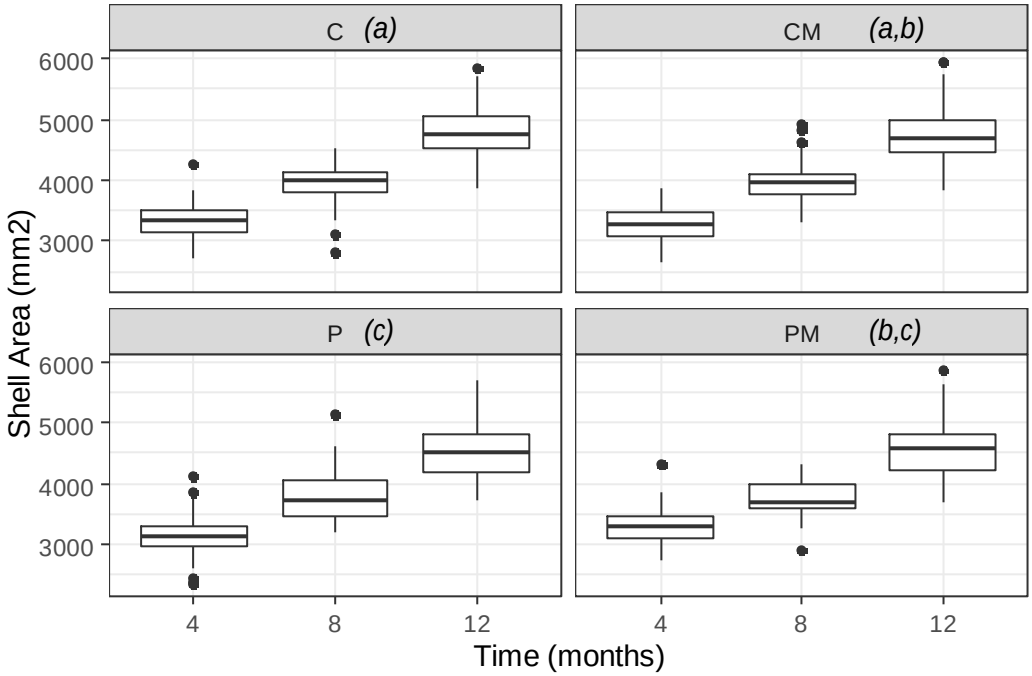

Figure 5.3.19. Shell area (± standard deviation) of abalone, *Haliotis midae*, exposed to four seawater treatments (C=control, P=pH, CM=control mitigation, PM=pH mitigation) over a 12-month experimental period in a flow-through seawater system. Each treatment group contains repeated measurements at 4-, 8-, and 12-month sampling times. Same letters in italics between treatments denotes no statistical difference between treatments (alpha = 0.05).

Table 5.3.14. Pairwise differences of abalone shell area between treatments (C=control, P=pH, CM=control mitigation, PM=pH mitigation) using the Tukey method to compare family estimates. Significant values are taken at the 5% level and shaded in grey.

Contrast Treatments	Comparison (mm^2)	Comparison (%)	Degrees of Freedom	t-ratio	p-value
C - CM	100.47	2.1%	16	1.479	0.47
C - P	275.80	5.9%	16	5.931	<0.01
C - PM	239.35	5.1%	16	3.838	0.01
CM - P	175.34	3.8%	16	4.452	<0.01
CM - PM	138.88	3.0%	16	2.359	0.13
P - PM	-36.46	-0.8%	16	-2.093	0.20

5.3.6. Shell Compression

Treatment had a significant effect on the maximum force/load (MF) that each shell could endure during compression (Figure 5.3.20) over the course of the study (df=2.26, χ^2=0.135, p<0.01). Abalone shells from the control treatment could sustain the most compressive force after 12 months (551.15 ± 145.08 N). Abalone shells from the control treatment had a significantly different MF over time in comparison to all other treatments (Table 5.3.15); shell MF increased exponentially over time (Figure 5.3.21). The response in abalone shell MF to the control mitigation (536.64±137.04 N) and pH mitigation (497.34±118.87 N) treatments was a linear (edf=1.00), gradual increase in strength for the duration of the study (Figure 5.3.21). The response in abalone shell MF to the pH treatment (475.15 ± 117.22 N) was similar to the control, with the exception of a slight decrease in strength at the 8 month sampling period and weaker shells overall (Figure 5.3.21)

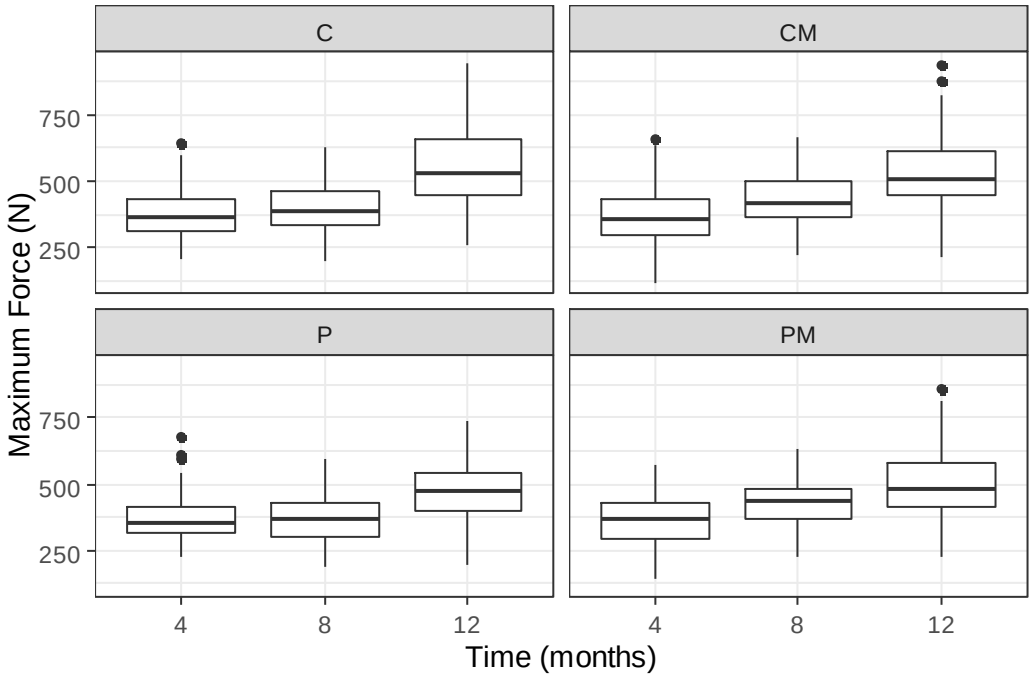

Figure 5.3.20. Maximum force (± standard deviation), in Newtons (N), that each abalone, *Haliotis midae*, shell could endure during compression tests after exposure to four seawater treatments (C=control, P=pH, CM=control mitigation, PM=pH mitigation) over a 12 month experimental period in a flow-through seawater system. Each treatment group contains repeated measurements at 4-, 8-, and 12-month sampling times.

Table 5.3.15. Ordered factor contrasts of smoothing terms for abalone shell maximum compressive force between treatments (C=control, P=pH, CM=control mitigation, PM=pH mitigation) over the 12-month study. Significant values are taken at the 5% level and shaded in grey.

Contrast Treatments	Comparison (N)	Comparison (%)	Estimated Degrees of Freedom	F-value	p-value
C - P	76.00	14.81	1.904	7.815	<0.01
C - CM	14.51	2.67	1.00	17.152	<0.01
C - PM	53.81	10.26	1.00	11.782	<0.01

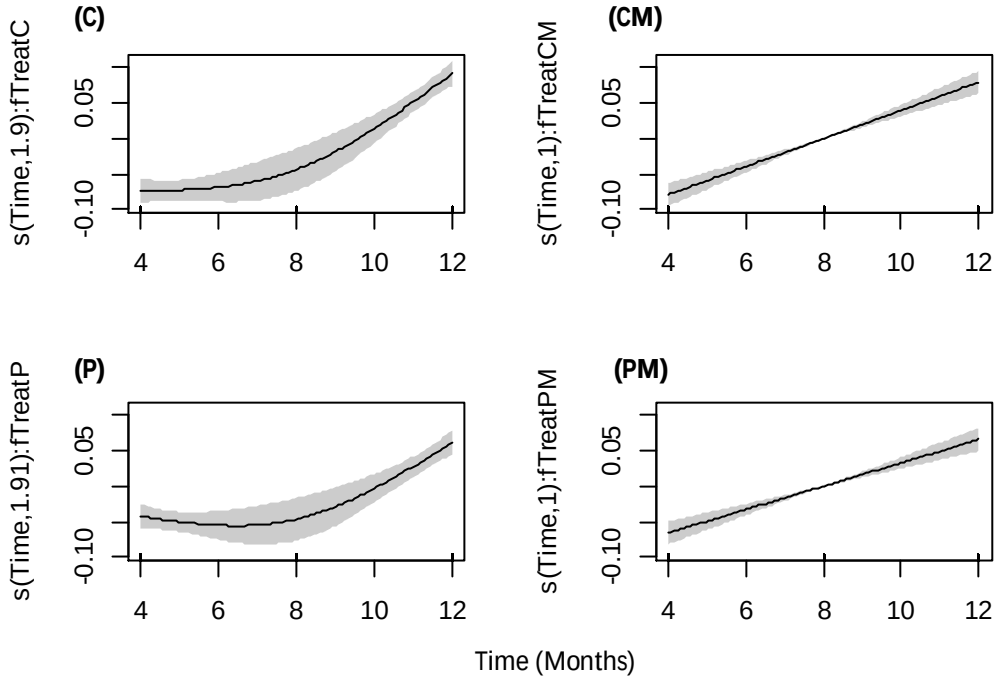

Figure 5.3.21. Smoothing function with fitted values of shell compressive force response (logarithmic scale) to four treatments (C=control, P=pH, CM=control mitigation, PM=pH mitigation), over a 12-month experimental period in the optimal generalized additive model. Degrees of freedom for each smoothing term are listed on the y-axis labels.

5.3.7 Shell Mineralogy

The mineralogical study of abalone shells was represented by percentage weight of aragonite (Figure 5.3.22), and average diameter of aragonite (Figure 5.3.23) and calcite (Figure 5.3.24) crystals in the shells of abalone exposed to experimental conditions for 12 months.

Treatment did not have a significant effect on the percentage weight of aragonite in abalone shells after 12 months of exposure to experimental conditions (df=16, F=0.130, p=0.9412; Table 5.3.16).

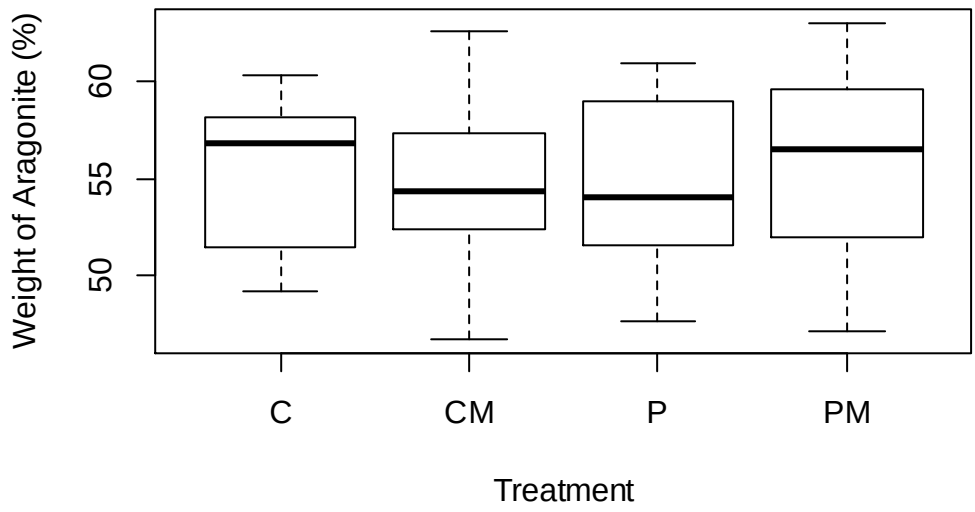

Figure 5.3.22. Percentage weight of aragonite (± standard deviation) of abalone shells, *Haliotis midae*, exposed to four seawater treatments (C=control, P=pH, CM=control mitigation, PM=pH mitigation) for a 12-month experimental period in a flow-through seawater system.

Table 5.3.16. Pairwise differences of the percentage weight of aragonite in abalone shells between four treatments (C=control, P=pH, CM=control mitigation, PM=pH mitigation) using the Tukey method to compare family estimates. Significant values are taken at the 5% level and shaded in grey.

Contrast Treatments	Comparison (%)	Degrees of Freedom	t-ratio	p-value
C - CM	37.86	16	0.232	1.00
C - P	-39.11	16	-0.226	1.00
C - PM	49.48	16	0.303	0.99
CM - P	1.25	16	0.007	1.00
CM - PM	-87.33	16	-0.544	0.95
P - PM	-88.58	16	-0.521	0.95

Treatment did not have a significant effect on the diameter of aragonite crystals in abalone shells after 12 months of exposure to experimental conditions (df=16, F=0.177, p=0.9105; Table 5.3.17).

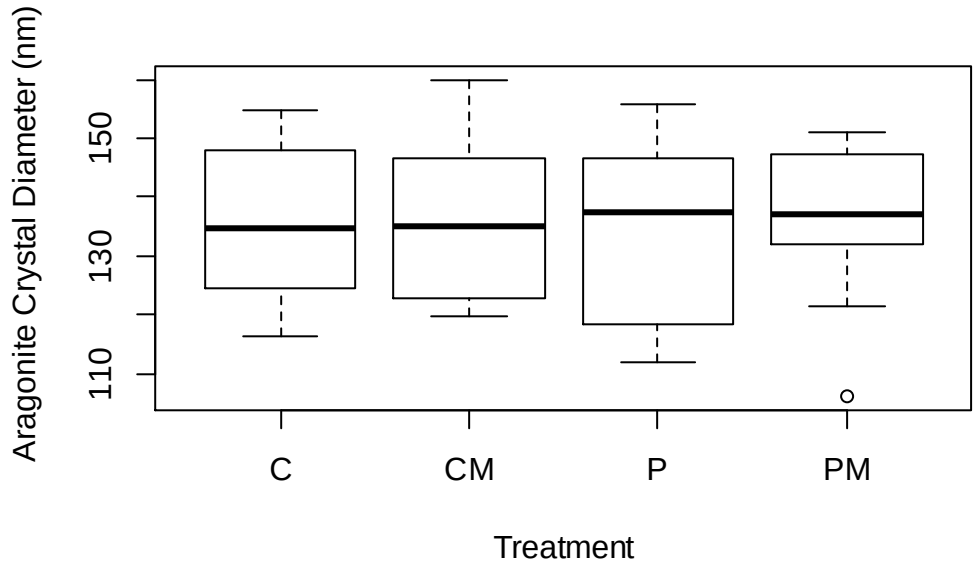

Figure 5.3.23. Aragonite crystal diameter (± standard deviation) of abalone shells, *Haliotis midae*, exposed to four seawater treatments (C=control, P=pH, CM=control mitigation, PM=pH mitigation) for a 12-month experimental period in a flow-through seawater system.

Table 5.3.17. Pairwise differences of the average diameter of aragonite crystals in abalone shells between four treatments (C=control, P=pH, CM=control mitigation, PM=pH mitigation) using the Tukey method to compare family estimates. Significant values are taken at the 5% level and shaded in grey.

Contrast Treatments	Comparison (nm)	Comparison (%)	Degrees of Freedom	t-ratio	p-value
C - CM	0.59	0.43	16	0.117	1.00
C - P	-2.88	-2.14	16	-0.540	0.95
C - PM	0.82	0.60	16	0.162	1.00
CM - P	2.29	1.70	16	0.436	0.97
CM - PM	-1.41	-1.03	16	-0.284	0.99
P - PM	-3.70	-2.73	16	-0.704	0.89

Treatment did not have a significant effect on the diameter of calcite crystals in abalone shells after 12 months of exposure to experimental conditions (df=16, F=0.332, p=0.80; Table 5.3.18).

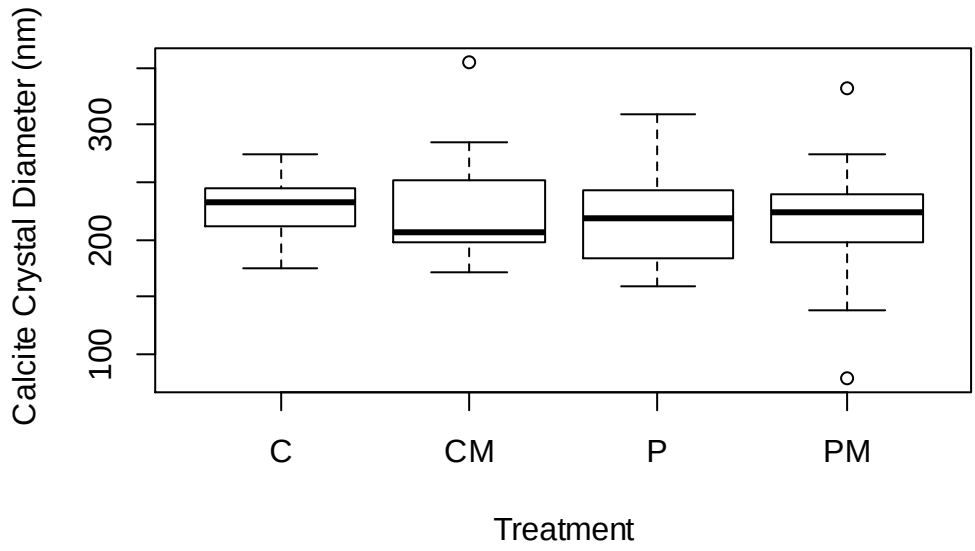

Figure 5.3.24. Calcite crystal diameter (± standard deviation) of abalone shells, *Haliotis midae*, exposed to four seawater treatments (C=control, P=pH, CM=control mitigation, PM=pH mitigation) for a 12-month experimental period in a flow-through seawater system.

Table 5.3.18. Pairwise differences of the average diameter of calcite crystals in abalone shells between four treatments (C=control, P=pH, CM=control mitigation, PM=pH mitigation) using the Tukey method to compare family estimates. Significant values are taken at the 5% level and shaded in grey.

Contrast Treatments	Comparison (nm)	Comparison (%)	Degrees of Freedom	t-ratio	p-value
C - CM	2.98	1.30	16	0.173	1.00
C - P	-13.83	-6.19	16	-0.757	0.87
C - PM	-13.66	-6.11	16	-0.792	0.86
CM - P	10.85	4.89	16	0.604	0.93
CM - PM	10.68	4.81	16	0.630	0.92
P - PM	-0.17	-0.08	16	-0.010	1.00

5.4 Discussion

This experiment exposed South African abalone, *H. midae*, to four variable conditions: ambient, lowered pH (0.4 below ambient), ambient seaweed-treated and acidified seaweed-treated seawater for 12 months. *Ulva rigida* was used in the seaweed-treated seawater treatments prior to flow-through into abalone tanks. Experimentally manipulated seawater pH was achieved by CO_2/O_2 diffusion in header tanks and applied to the natural variability within ambient seawater. This experiment was conducted on an abalone aquaculture facility to provide realistic feedback on a possible mitigation strategy for the South African abalone aquaculture industry in the face of climate change. To the author's knowledge, this is the first study that will assess the effects of these treatments on *H. midae* growth, spawning pattern, acid-base regulation, shell morphology, shell strength and mineralogy (Table 5.4.1).

The *Ulva*-mitigation system was not able to ameliorate acidified seawater (-0.4 below ambient), by carbon uptake, to comparable levels with ambient seawater. Ambient mean seawater pH was 8.1±0.06 and seaweed-treated mean seawater pH was 7.94±0.07 over the duration of the study. The *Ulva*-mitigation system was able to increase acidified seawater pH (-0.4 below ambient) by an average of ~0.28 over 12 months in comparison to acidified seawater (7.66±0.07). The average yield of *Ulva* grown in the acidified system (73.7±169.1 $g.week^{-1}$) was 40 % less than the average yield of *Ulva* grown in the ambient system (111.3±170.0 $g.week^{-1}$) and indicates a decrease in *Ulva* yield when cultivated in reduced pH seawater, although this was not intended to be assessed or included in the experimental design. It is likely that photosynthesis was inhibited in reduced pH seawater resulting in reduced carbon uptake and growth, as pH alters the balance between CO_2, bicarbonate and carbonate in seawater (Hurd et. al. 2020). The equilibrium reaction for CO_2 is illustrated below:

$$H_20 + CO_2 \leftrightarrow H_2C0_3 \leftrightarrow H^+ + HC0_3^- \leftrightarrow 2H^+ + C0_3^-$$

Reactions shift to the left as pH declines (Robertson-Andersson 2003, Hurd et. al. 2020).

In a recent study by Figueroa et. al. (2021), *Ulva rigida* was cultured in elevated CO_2 conditions (700 ppm vs. 380 ppm) under solar radiation for 6 days and exhibited a decrease in photosynthetic production and a decrease in photoprotective capacity in comparison to *Ulva* cultured in ambient conditions and *Ulva* cultured in elevated CO_2 conditions under artificial lighting. Figueroa et. al. (2021) also noted that, when cultured under solar radiation as opposed to artificial lighting, *U. rigida* exhibited photoinhibition at noon during peak light availability. It is therefore plausible that the design of the *Ulva*-mitigation tanks in the current study can be improved by shading the *Ulva* tanks during the day to prevent photoinhibition and promote photosynthetic production. This was trialled by Robertson-Andersson (2003) and it was concluded that a maximum benefit in specific growth rate occurred when *Ulva* tanks were shaded with 50 % shade cloth between September and February.

The findings of Figueroa et. al. (2021) exemplify the need for realistic experimental conditions that include environmental factors, such as solar radiation (saturating light), to better predict species responses to climate change scenarios and better inform policy makers. For example, Rautenberger et. al. (2015) cultivated *Ulva rigida* under artificial lighting in reduced pH conditions (7.59 vs 7.97) for 7 days and noted that saturating light rather than reduced pH increased *U. rigida* photosynthesis and growth, which is contradictory to the findings of Figueroa et. al. (2021) where *U. rigida* was

Table 5.4.1. Summary of results reported as mean ± standard deviation for *H. midae* exposed to four treatments (C=control, P=pH, CM=control mitigation, PM=pH mitigation) for 12 months. Means followed by the same letter(s) within a column are not significantly different ($p<0.05$).

Treatment	Wet Weight (g)	Muscle Mass (g)	PMB (%)	CF ($g.mm^{-1}$)	GBI ($g.mm^{-1}$)	pH	HCO_3^- ($mmol^{-1}$)	Shell Weight (g)	Shell Length (mm)	Width (mm)	Shell Shape	Shell Area (mm^2)	Shell Strength (N)	Arago-nite (%wt)	Aragonite Diameter (nm)	Calcite Diameter (nm)
CM	109.0 ± 12.8^{a}	55.71 ± 9.17^{a}	0.581 ± 0.033^{b}	1.17 ± 0.09^{b}	0.898 ± 0.297^{a}	7.27 ± 0.16^{b}	2.23 ± 0.20^{b}	27.31 ± 3.35^{a}	82.78 ± 3.81^{a}	56.81 ± 2.81^{a}	1.458 ± 0.055^{b}	4709.76 ± 413.79^{ab}	536.64 ± 137.04^{b}	54.71 ± 4.37^{a}	135.77 ± 13.94^{a}	227.36 ± 49.91^{a}
PM	104.9 ± 14.1^{ab}	55.84 ± 9.20^{a}	0.605 ± 0.029^{b}	1.17 ± 0.08^{b}	0.736 ± 0.266^{a}	7.02 ± 0.05^{b}	2.12 ± 0.38^{b}	25.15 ± 3.19^{a}	81.74 ± 3.84^{ab}	55.80 ± 3.07^{ab}	1.466 ± 0.042^{b}	4570.88 ± 449.06^{bc}	497.34 ± 118.87^{b}	55.58 ± 4.77^{a}	137.18 ± 12.72^{a}	216.68 ± 57.91^{a}
C	112.2 ± 14.3^{a}	66.14 ± 9.64^{a}	0.612 ± 0.028^{a}	1.12 ± 0.08^{a}	0.833 ± 0.285^{a}	7.15 ± 0.08^{b}	2.22 ± 0.24^{a}	28.43 ± 3.74^{b}	83.50 ± 3.73^{a}	57.53 ± 2.96^{a}	1.453 ± 0.059^{a}	4810.23 ± 420.07^{a}	551.15 ± 145.08^{a}	55.09 ± 3.86^{a}	136.36 ± 12.17^{a}	230.34 ± 27.44^{a}
P	102.6 ± 14.7^{b}	59.97 ± 10.15^{a}	0.624 ± 0.035^{b}	1.12 ± 0.07^{b}	0.551 ± 0.196^{b}	7.02 ± 0.06^{b}	2.12 ± 0.19^{a}	24.13 ± 3.34^{b}	81.31 ± 3.85^{b}	55.67 ± 2.97^{b}	1.462 ± 0.057^{b}	4534.42 ± 422.51^{c}	475.15 ± 117.22^{b}	54.67 ± 4.15^{a}	131.03 ± 15.55^{a}	213.54 ± 41.14^{a}

cultivated outside, under solar radiation, where *Ulva* was light saturated. Other previous studies also found *Ulva* can experience enhanced growth when grown under elevated CO_2 concentrations under artificial lighting (Olischläger et al., 2013, Young and Gobler 2016, Young and Gobler 2017, Young and Gobler 2018) and caution should be applied when using these findings for aquacultural or natural applications. Reductions in photosynthetic ability have also been shown in *U. lactuca* when cultivated in reduced pH conditions. *Ulva lactuca* exhibited a decrease in chlorophyll-*a* content and decrease in photosynthetic yield when cultured in constant, acidified seawater (pH: 7.4) in comparison to ambient (pH: 8.2) conditions for 7 days (Sousa et. al. 2021). Although the ocean acidification conditions used in their study were far more excessive than those predicted for the year 2100 (Hoegh-Guldberg et. al. 2014), Sousa et. al. (2021) determined that *U. lactuca* was able to tolerate short-term (7 days) reduced pH conditions by inducing non-photochemical quenching, changing pigment contents (decreasing chlorophyll-*a* and increasing carotenoids), and increasing antioxidant enzymes, as seen in tidal rock pools (See Chapter 6, section 6.2.2).

The pH mitigation strategy, by carbon uptake in *Ulva*-mitigation tanks, succeeded in increasing abalone wet weight to comparable levels with abalone grown in ambient conditions alone. However, despite an increase in wet weight, abalone from the pH-mitigation treatment were still not significantly heavier than abalone grown in low pH conditions (Table 5.4.1). The reduction in muscle mass was reflected in abalone proportion of muscle to body mass (PMB). Abalone PMB naturally decreases with age as the shell area and weight increases, as seen in the ambient conditions. Abalone exposed to acidified- and ambient-seaweed-treated seawater had 1.0 % and 1.9 % heavier muscle tissue, respectively, than abalone in ambient conditions after 8 months (October), resulting in a larger PMB in comparison to ambient conditions, however muscle tissue did not increase significantly after October. This resulted in significantly lower PMB in abalone exposed to ambient and acidified seaweed-treated seawater in comparison to those in ambient conditions, and comparable muscle mass to abalone grown in acidified seawater alone. Abalone cultivated in ambient seaweed-treated seawater also displayed similar changes in muscle mass to abalone in the pH-mitigation treatment and wet weight was not significantly different from those grown in ambient conditions. These findings concur with literature on the same species using partial (25%) recirculation with *Ulva rigida (*as *Ulva lactuca)*. Robertson-Andersson (2006) noted no significant difference in growth in terms of whole weight of *H. midae* grown in a flow-through system and a 25% recirculation system which incorporated *Ulva* as a biofilter. Robertson-Andersson (2006) also noted that abalone grown in the *Ulva*-incorporated, partial recirculation system had significantly higher growth rates in October and November, but abalone grown in an ambient flow-through system grew better in summer months resulting in an ultimate non-significant difference in weight or length by February. A decline in muscle growth and a decline in *Ulva* yield both occurred from October 2015 – February 2016 (Table 5.3.1), possibly as a result of an increase in solar radiation during summer months. Without comparative literature on this novel research, it is hard to definitively pinpoint the cause for such a change in muscle growth. Research on Integrated-Multi-Trophic Aquaculture (IMTA) has focused solely on the use of seaweeds as a biofilter for nutrient removal rather than pH control (Robertson-Andersson et. al. 2006, Robertson-Andersson et. al. 2008, Barrington et. al. 2009, Abreu et. al. 2011, MacDonald et. al. 2011, Marinho et. al. 2013, Ben-Ari et. al. 2014, Holdt & Edwards 2014, Fang et. al. 2016, Shpigel et. al. 2017, Laramore et. al. 2018, Shpigel et. al. 2018a, Shpigel et. al. 2018b). *Ulva* (not identified to species level) was assessed as a

mitigational tool to ameliorate the effects of invariable, acidified seawater (pH: 7.37 vs ambient 7.98) on several bivalve species (*Mercenaria mercenaria*, *Crassostrea virginica*, *Argopecten irradians*, *Mytilus edulis*) in a laboratory-based study for 2 weeks (Young and Gobler 2018). The study by Young and Gobler (2018) used a decline in pH that was more excessive than predicted by the end of the century (Hoegh-Guldberg et. al. 2014) and *Ulva* was grown under artificial lighting and *Ulva* was cultivated in the same culture tanks as the bivalves. Reactions to seaweed-treated seawater were species-specific (Young and Gobler 2018). *M. mercenaria*, *C. virginica* and *A. irradians* exhibited a decrease in tissue growth when cultivated in acidified seawater (Young and Gobler 2018). *M. mercenaria*, *C. virginica* and adult *A. irradians* exhibited a significant increase in tissue growth when cultivated in ambient, seaweed-treated seawater in comparison to ambient conditions and exhibited a significant increase in tissue growth when cultivated in acidified, seaweed-treated seawater in comparison to acidified conditions (Young and Gobler 2018). Juvenile *A. irradians* tissue growth was not significantly affected by the presence of *Ulva* in acidified or ambient conditions (Young and Gobler 2018). *M. edulis* tissue growth was not significantly affected by acidified seawater; however *M. edulis* did have significantly increased tissue growth when cultivated in ambient, seaweed-treated seawater in comparison to ambient conditions and exhibited a significant increase in tissue growth when cultivated in acidified, seaweed-treated seawater in comparison to acidified conditions (Young and Gobler 2018). Young and Gobler (2018) suggest that natural/aquacultured collections of *Ulva* may provide a refuge for bivalves in acidified environments (See Chapter 6, section 6.2.2); although this will need to be established by increasing the duration of the exposure period and including the effects of seasonal solar radiation on *Ulva*. The reduction in tissue growth caused by acidified seawater on these bivalve species (not including *M. edulis*) are similar to the findings on abalone in acidified seawater; however seaweed-treated seawater did not increase abalone growth as seen in bivalves (Young and Gobler 2018). Another theory that might explain the negative impacts of seaweed-treated seawater on abalone is the production of secondary metabolites by *Ulva*. *Ulva lactuca* has been shown to increase the production of extracellular dimethylsulphoniopropionate (DMSP) when cultured in elevated CO_2 conditions (1514 µatm) in comparison to ambient conditions (432 µatm) for 7 days (Kerrison et. al. 2012). DMSP breaks down into dimethyl sulphide (DMS) and DMS accumulation in *H. midae* fed an *Ulva*-based diet has been found to produce a repellent taste and odour in abalone processed for canning (Smit et. al. 2007), but the effects of DMSP from non-dietary sources, released by *Ulva*, on abalone have not been studied. If DMSP is released by *Ulva* under stressful conditions, such as acidification and photoinhibition, it is plausible that the release of DMSP, an activated defence system against herbivory (Van Alstyne et. al. 2001), may have reduced abalone feeding, resulting in decreased muscle mass. Further research is needed on this topic to provide valuable information on the interaction between *Ulva* and abalone in stressor scenarios.

From an aquaculture production perspective, the non-significant difference in whole abalone weight between abalone grown in ambient conditions and abalone grown in acidified, seaweed-treated seawater indicates no change for the production and sale of live abalone; however the production of abalone for canning and drying would be negatively affected if abalone were harvested in summer months due to lower meat mass of the abalone.

The decline in meat mass and PMB may be linked to an increase in physiological stress. Abalone grown in ambient, seaweed-treated seawater displayed a change in acid-base regulation after 8

months (October), before which there had been no discernible difference to abalone cultured in ambient seawater. After October, abalone grown in ambient, seaweed-treated seawater displayed a more alkaline haemolymph pH and lowered pCO_2, which is an indication of uncompensated respiratory alkalosis, a condition where increased respiration elevates haemolymph pH beyond the normal range. This reflects a similar acid-base status to that of abalone cultivated in the elevated temperature treatment, which also displayed reduced pCO_2 and elevated pH with similar bicarbonate concentrations to abalone grown in ambient conditions (See Chapter 3). The addition of *Ulva* into the ambient seawater cultivation system increased seawater temperatures by 0.96 °C over the course of this study, although this temperature differential is still within the optimal cultivation temperature for *H. midae*. Abalone grown in acidified, seaweed-treated seawater followed similar changes in acid-base regulation over time in comparison to abalone from the reduced pH treatment (See Chapter 3 for discussion), resulting in lower intercellular pH and increased pCO_2, an indication of partially compensated respiratory acidosis. This suggests that the respiratory and metabolic stress involved in acid-base regulation left limited energy for other metabolic demands such as muscle tissue growth (Sokolova 2013).

Abalone from all treatments had a healthy condition factor (CF >1) and abalone exposed to ambient conditions show a reduction in CF (Table 5.4.1), indicative of a spawning event (Wood & Buxton 1996), in November. This corresponds to the spawning period of *H. midae* during October-December estimated by Newman (1967). Abalone exposed to ambient-seaweed-treated and acidified-seaweed-treated seawater displayed an absence of a spawning event as shown by the absence of a steep decline in CF during the experimental period. Despite this, abalone in seaweed-treated seawater had comparable GBI's to those in ambient conditions. Acidified seawater alone had the largest impact on abalone GBI over the course of the study (Table 5.4.1). Prolonged metabolic stress and reduced growth may have resulted in reduced GBI after 12 months of exposure to low pH conditions. It is highly plausible that energy may have been diverted from gonad development and growth towards homeostasis. Aalto et. al. (2020) noted that *H. fulgens* fecundity scaled with abalone size, revealing that a decrease in growth rate or maximum size due to environmental stressors, such as ocean acidification, had disproportionate effects on larval production in adult *H. fulgens* populations. However, *H. midae* grown in acidified, seaweed-treated seawater exhibited similar metabolic stress to abalone grown in reduced pH conditions alone, if not to a greater extent. Abalone size may have affected GBI as abalone grown in acidified, seaweed-treated seawater had non-significantly longer and wider shells than abalone grown in acidified seawater, but were comparable to abalone grown in ambient and ambient, seaweed-treated seawater. Gonad maturation and spawning of *H. midae* (Newman 1967, Wood & Buxton 1996) and other abalone species (Litaay & De Silva 2003, Awaji & Hamano 2004, Grubert & Ritar 2004) has been shown to be largely influenced by seawater temperature. The mitigational effects of *Ulva* on abalone GBI correspond with the robustness of abalone GBI to the pH x temperature treatment in Chapter 3. *Ulva*-mitigation tanks increased seawater temperature by an average of 0.96±0.16 °C over the 12-month experimental period. This suggests that perhaps the temperature increase of the seaweed-treated seawater may have indirectly mitigated the effects of lowered GBI caused by reduced seawater pH.

Acidified seawater had the most pronounced effect on *H. midae* shell growth, with significant reductions in weight, length, width and area, including growth of the shell towards a wider shape than ambient conditions (Chapter 4). Young and Gobler (2018) found similar reductions in shell weight and length when *M. mercenaria*, *C. virginica* and *A. irradians* were exposed to higher elevations in seawater CO_2. *Ulva*-mitigation of acidified seawater increased shell length and width to comparable levels with ambient and ambient, seaweed-treated seawater, however shells were still non-significantly longer and wider than those from acidified conditions (Table 5.4.1). *Ulva*-mitigation of acidified seawater increased shell area to comparable levels with ambient, seaweed-treated seawater, however shells were still non-significantly larger than those from acidified conditions Ambient, seaweed-treated seawater had no significant effect on shell growth, but the shape of the shell over time was significantly affected; with shells changing more gradually over time towards a wider shape in comparison to ambient conditions where shells retained a fairly stable shape for the first 8 months of the experiment before growing into a wider shape. These findings different from those of Young and Gobler (2018). *Ulva*-mitigation of acidified seawater resulted in a significant increase in shell weight and length of *M. mercenaria* and *M. edulis* in comparison to those grown in acidified seawater after 2 weeks of exposure to experimental conditions (Young and Gobler 2018). *A. irradians* shell length was significantly longer when cultivated in acidified, seaweed-treated seawater in comparison to acidified conditions, but shell weight was unaffected (Young and Gobler 2018). Ambient, seaweed-treated seawater caused a significant increase in shell weight and length in *M. mercenaria* and *M. edulis*, and a significant increase in shell length in *A. irradians* in comparison to ambient conditions (Young and Gobler 2018). Shell weight and length of *C. virginica* was not significantly affected by ambient and seaweed-treated seawater (Young and Gobler 2018). The effects of seaweed-treated seawater on bivalve growth varied between species (Young and Gobler 2018), which may account for the incongruence in findings between the current study and the study by Young and Grobler (2018) although seawater parameters and techniques used in experimental cultivation of *Ulva* were also dissimilar. Macroalgae are able to affect carbonate systems, ultimately increasing aragonite and calcite saturation states of seawater, as seen by Young and Gobler (2018), creating a more favourable environment for shell formation in calcifying organisms (Byrne 2011, Byrne et. al. 2011b, Gazeau et al. 2013; Kroeker et al. 2013, Pzreslawski et. al. 2015, Fassbender et al. 2016), although no significant increase in seawater pH was noted by Young & Gobler (2018). It seems that, due to possible photoinhibition and the inability to ameliorate seawater pH to ambient pH levels, the *Ulva*-mitigation system used in this study was not able to provide sufficiently favourable conditions in this experimentally-acidified scenario, which resulted in reduced abalone shell growth in comparison to ambient conditions.

Acidified seawater significantly reduced shell strength by 14.8 % in comparison to those in ambient conditions (Chapter 4, Table 5.4.1). Uptake of carbon from acidified seawater by *Ulva* increased the strength of abalone shells by 4.6 % in comparison to those in acidified conditions. The strength of abalone shells was not significantly affected by ambient, seaweed-treated seawater after 12 months. Acidified and ambient seaweed-treated seawater did impact the change in shell strength over time in in comparison to ambient conditions. Abalone shell strength increases exponentially with time as the size of the shell increases, as seen by abalone grown in ambient conditions. Abalone grown in seaweed-treated seawater displayed a gradual, linear increase in shell strength over time, which resulted in 9.0 % and 6.5 % stronger shells in ambient and acidified seaweed-treated conditions, respectively, in comparison to those grown in ambient conditions after 8 months

(October). After October, shells in ambient conditions increased exponentially in strength and were ultimately stronger than shells grown in both *Ulva*-mitigation treatments. The influence of *Ulva* on shell strength in molluscs has not been previously studied and further research is needed to assess the interactive effects of *Ulv*a on abalone shell growth in stressor conditions.

H. midae shells were comprised of ~55 % aragonite (by weight, Table 5.4.1). *H. midae* shell mineralogy was robust to reduced seawater pH (Chapter 4), and both seaweed-treated seawater conditions. These findings concur with the multi-species analysis by Ries (2011) which noted no significant changes in calcite/aragonite ratios in monomineralic species (species that produce a predominant proportion of one calcium carbonate polymorph in comparison to another) exposed to elevated CO_2 conditions.

In conclusion, bio-mitigation of acidified seawater by *Ulva rigida* increased abalone wet weight, GBI, shell length, shell width and shell area in comparison to acidified conditions. Abalone gonad development is strongly influenced by temperature and it is suggested that warming caused by *Ulva* cultivation promoted abalone GBI. However, *Ulva*-mitigation of ambient and acidified seawater caused a significant reduction in abalone muscle mass during summer months in comparison to abalone grown in ambient seawater. This decrease in muscle mass occurred concurrently with a decline in *Ulva* yield, suggesting an interactive effect of *Ulva* (under stressor conditions due to photoinhibition) and abalone which needs to be studied further. The findings of this study are useful in the development of a mitigational strategy for abalone aquaculture in the face of climate change. The most pertinent improvement to the current mitigational strategy is shading of the *Ulva* tanks during months with strong solar radiation (October – March) to prevent photoinhibition, followed by an increased frequency of fertilization during these months. Without a mitigational strategy in place, abalone aquaculture facilities can expect a reduction in abalone growth and abalone quality with weaker, more easily damaged shells due to ocean acidification. Research needs to be directed towards mitigations strategies for aquaculture facilities, which include local-scale variability and local environmental conditions to provide realistic guidance on management decisions.

CHAPTER 6:
General Discussion

Ocean acidification (OA), more so than ocean warming, is likely to pose several challenges to South African abalone aquaculture. With predicted declines in ocean surface pH by 0.4 units and warming of 1.5 °C by the year 2100, abalone farms are likely to start seeing increasing changes in abalone production and quality. It is pertinent that aquaculture facilities invest in mitigational strategies to adapt to changing environmental conditions (Baragé et. al. 2018, Ahmed et. al. 2019, Galappaththi et. al. 2020).

This study had three main objectives:

1) Assess the impacts of ocean acidification and warming, alone and in combination, on *Haliotis midae* growth, meat yield, spawning patterns and physiology.

2) Assess the impacts of ocean acidification and warming, alone and in combination, on *H. midae* shell growth, morphology, strength and mineralogy.

3) Determine whether the incorporation of *Ulva*-mitigation tanks into a flow through aquaculture system will mitigate the negative effects of ocean acidification on *H. midae*.

This study aimed to provide the aquaculture industry and government with environmentally realistic information on the likely impact of climate change on abalone aquaculture by incorporating natural seawater variability from a high-production area in an aquaculture setting.

The findings of this thesis conclude the following:

Ocean acidification has the potential to:

- Reduce abalone growth by 8.9 % and reduce meat yield by 9.8 %, thereby reducing the proportion of meat to whole body mass by 6.2 % in comparison to current conditions.
- Reduce abalone GBI by 40.8 % and halt/delay natural abalone spawning events in October-December.
- Cause an imbalance in acid-base regulation of abalone, resulting in metabolic acidosis and increased metabolic stress, making abalone more susceptible to disease and parasitic infection (Cheng et. al. 2004).
- Reduce abalone shell weight by 16.4 %, shell length by 8.3 %, and shell width by 3.3 %, resulting in longer-shaped shells with 5.9 % less area and a 14.8 % weaker structure.

Ocean warming has the potential to:

- Affect a change in proportion meat to body mass (PMB) over time, with maximum abalone PMB recorded in October. This indicates that abalone farms will need to adjust harvesting times accordingly to maximize meat yield for canning and drying.

- Reduce abalone GBI in comparison to ambient conditions without affecting spawning pattern
- Increase haemolymph pH and bicarbonate concentrations (indicative of metabolic alkalosis)
- Change the shape of the shell over time through a gradual shift towards a wider shell in comparison to ambient conditions, which displayed a period of growth in length before expanding the width of the shell
- Affect shell strength over time through a gradual, linear increase in strength as opposed to ambient conditions, which showed a period of invariance in shell strength between June 2015 and October 2015 (summer months) before shell strength exponentially increased.

The combination of warming and acidification has the potential to:

- Have similar negative effects on abalone growth, shell weight, and shell strength as acidification conditions in comparison to ambient conditions.
- Cause a more severe acid-base imbalance (metabolic acidosis) in abalone than ocean acidification would alone, potentially increasing the risk of disease (Cheng et. al. 2004).
- Increase shell length and width in comparison to abalone in acidification conditions.

Ulva-treated seawater:

- Raised the pH of acidified seawater by an average of 0.28 units over 12 months, but proved unable to raise it to the equivalent of ambient seawater.
- When used as a mitigatory tool for acidified seawater, increased abalone wet weight (during winter months), GBI, shell length, width and area in comparison to abalone grown in acidified seawater
- Using ambient and acidified seawater input increased the strength of shells by 9.0 % and 6.5 % respectively, in comparison to abalone grown in ambient and acidified seawater respectively.
- Increased abalone muscle mass after 8 months (October) in comparison to ambient conditions but caused a decline in abalone muscle mass between October and February (summer months). This may be a result of a negative interactive effect between *Ulva*-treated seawater and abalone due to a release of DMSP by *Ulva* under stressful conditions (acidification and photoinhibition), or a result of metabolic stress in the abalone.
- Using ambient seawater input resulted in a more alkaline haemolymph pH and lowered pCO_2 in abalone, which is an indication of respiratory alkalosis. Acidified, *Ulva*-mitigated seawater had similar effects on abalone as those in acidified conditions.

Abalone mineralogy was robust to changes in environmental conditions and was unaltered by acidification, warming or *Ulva*-treated seawater, or their combinations.

6.1. Is OA a threat to mollusc aquaculture and abalone aquaculture specifically?

At present, over 400 aquatic species are farmed globally, of which 42 species are marine calcifying molluscs (FAO 2018b, Galappaththi et. al. 2020). Previous research assessing the impacts of climate change on aquaculture has focused primarily on the indirect impacts of climate change on aquaculture such as: changing patterns of precipitation, salinity, frequency and severity of extreme

weather events, changes in primary productivity, harmful algal blooms and incidence and spread of disease (Karvonen et. al. 2010, Frost et. al. 2012, Brugère & De Young 2015, FAO 2018c, Stewart-Sinclaire et. al. 2020). Very little research has incorporated the direct effects of ocean acidification into climate change assessment models in aquaculture (Hughes et. al. 2012, Froehlich et. al. 2018, Stewart-Sinclaire et. al. 2020). Climate change vulnerability assessments of fisheries and aquaculture are routinely applied to fisheries and fin-fish aquaculture, whilst the vulnerability of broad scale aquaculture to climate change has only recently been investigated (Handisyde et. al. 2017, Froehlich et. al. 2018, Galappaththi et. al. 2020, Stewart-Sinclaire et. al. 2020). Hughes et. al. (2012) and Froehlich et. al. (2018) have identified mollusc aquaculture as being particularly susceptible to the combined effects of OA and climate change. Froehlich et. al. (2018) used species-specific growth limits to map potential cultivation sites and incorporated global ensemble model predictions for sea surface temperature (SST), primary productivity and OA for the year 2100 into their model and reported potential reductions in productivity potentials in most suitable bivalve growing areas over time. Stewart-Sinclaire et. al. (2020) reported that mollusc aquaculture in several countries was particularly vulnerable to climate change, but noted that predicting sensitivity is challenging due to missing data and sparse research on species-specific responses to all climate change aspects, and varying species-specific responses through life-history stages.

Vulnerability of mollusc aquaculture to climate change, and specifically OA, is dependent on the geographic location of the farm, species cultivated, and economic ability of the farm and region to adapt to changing environmental conditions (Brugère & De Young 2015, FAO 2018c, Froehlich et. al. 2018, Ahmed et. al. 2019, Galappaththi et. al. 2020, Stewart-Sinclaire et. al. 2020, Tan & Zheng 2020). OA impacts biological and biogeochemical processes at their most fundamental level, but the impacts are very dependent on widely varying CO_2 tolerances of different species and taxonomic groups. (Fabry et. al. 2008, Doney et. al. 2009, Ries et. al. 2009, Kroeker et. al. 2010, Byrne et. al. 2011a, Kroeker et. al. 2013, Przeslawski et. al. 2015, Pfister et. al. 2016, Barage et. al. 2018, Cattano et. al. 2018). In general, without adaptation to OA, mollusc aquaculture is particularly susceptible to the effects of OA due to increased sensitivity at larval and juvenile stages (Pörtner et. al. 2004, Orr et. al. 2005, Gazeau et. al. 2007, Doney et. al. 2009, Fabry et. al. 2009, Feely et. al. 2009, Hendricks et. al. 2009, Ries et. al. 2009, Auzoux-Bordanave et. al. 2010, Kroeker et. al. 2010, Byrne et. al. 2011, Byrne et. al. 2011b, Crim et. al. 2011, Kimura et. al. 2011, Byrne & Przeslawski et. al. 2013, Kroeker et. al. 2013, Guo et. al. 2015, Pacifici et. al. 2015, Przeslawski et. al. 2015, Waldbusser et. al. 2015, Boch et. al. 2018, Campanati et. al. 2018, Li et. al. 2018, Onitsuka et. al. 2018, Wessel et. al. 2018, Auzoux-Bordanave et. al. 2020). Mollusc larvae have accelerated calcification rates, higher energetic costs, and a larger, exposed surface area in comparison to adults, making them far more susceptible to the impacts of OA (Waldbusser et. al. 2015). Although, the larvae of some species, such as the rock oyster (*Saccostrea cucullata*) and Olympia oyster (*Ostrea lurida*), have demonstrated a resistance to constant, reduced pH seawater (Waldbusser et. al. 2016, Companati et. al. 2018). Most mollusc aquaculture facilities can expect mass mortalities of larvae and juveniles and reduced calcification and growth (Byrne & Przeslawski 2013, Przeslawski et. al. 2015, Tan & Zheng 2020). Various other impacts include reduced embryonic growth (Kurihara et. al. 2007, Gazeau et. al. 2010), growth and developmental anomalies (Watson et al. 2009, Byrne et. al. 2011b), shell strength reductions (Mackenzie et. al. 2014), and weakening of mussel byssus attachment (Zhao et al. 2017, O'Donnell et al. 2013). Climate change and OA may also increase the risks for animal

health, due to an increase in metabolic stress and by changing the occurrence of pathogens and susceptibility of organisms to infections, pathogens and parasites (Barange et. al. 2018).

.

Declines in surface ocean pH by 0.3-0.45 are predicted for the year 2100 (Hoegh-Guldber et. al. 2014); however the impacts of ocean acidification have already affected oyster hatcheries in Northern Oregon, USA. In 2006, an oyster hatchery (*Crassostrea gigas*) in Northern Oregon, Whiskey Creek Hatchery, experience an 80 % decline in larval production. Larval mortality rates continued at 75 % until 2008 (Kelly et. al. 2014). It was then determined that increased larval mortalities coincided with periods of strong coastal upwelling. The oceans are the largest active carbon sinks on Earth, absorbing more than a quarter of anthropogenic CO_2 in the last 20 years (Mikaloff-Fletcher et. al. 2006, Hartmann et. al. 2013, Wanninkhof et. al. 2013, Le Quére et. al. 2014, Schmitt 2018). Excess atmospheric CO_2 is transferred to the deep ocean by ocean circulation and biological pumps where it is temporarily stored and removed from the surface (Feely et. al. 2008, Hugh-Guldberg et. al. 2014). During upwelling events this deep, CO_2-enriched seawater is brought back to the surface. Coastal environments that experience upwelling also experience elevated CO_2 conditions during upwelling events (Feely et. al. 2008, Barton et. al. 2012, Branch et. al. 2013). The upwelling events that resulted in Whiskey Creek Hatchery's larval mortalities in 2006 had brought CO_2-enriched seawater to the surface that had been locked in the deep ocean since the 1960's (Feely et. al. 2008, Branch et. al. 2013). Unfortunately due to the exponential increase in atmospheric CO_2 over time, aquaculture facilities can expect CO_2 concentrations in upwelling events to reflect these higher CO_2 concentrations (Branch et. al. 2013). Thus, mollusc aquaculture facilities, particularly those in upwelling regions, need to formulate mitigation strategies to prevent production losses before they occur. Each mollusc aquaculture facility is subject to unique circumstances and environmental conditions, thus climate change research and adaptations need to be guided by a strong understanding of the relevant aquaculture system and local environment to make a reliable assessment of potential climate change risks (Baragé et. al. 2018).

Abalone aquaculture is also threatened by the combination of gradual OA and upwelling events. Abalone farms are reliant on coastal seawater input and are directly affected by environmental variability and change. OA has been shown to impact abalone by reducing larval survival, increasing the number of malformed larvae, reducing growth and calcification, reducing shell strength and weight, and eroding shells (Table 6.1). Hatcheries will be most at risk to reductions in lowered seawater pH due to increased sensitivity of larvae to OA (Morash & Alter 2015). The majority of South African abalone farms are situated in upwelling environments (Santana-Casiano et. al. 2009, Goschen et. al. 2012, Smit et. al. 2013) and most farms receive seawater water in close proximity to kelp beds. These farms will experience elevated CO_2 seawater during upwelling events, superimposed by natural diurnal fluctuations in pH, with CO_2 uptake by the kelp and consequent higher pH during the day (due to photosynthesis) and CO_2 release and lower pH at night (respiration). Although larval die-offs have not been experienced to the same degree as seen in the Whiskey Creek Hatchery, abalone farms can expect upwelling conditions to impact larval survival in the near-future as the concentration of CO_2 in upwelled seawater increases (Branch et. al. 2013). In this case, the location of abalone farms and their ability to adapt to changing environmental

conditions will affect their vulnerability to OA. This study used abalone from a specific group of broodstock in an aquacultural setting, which may have a limiting effect on the scope of adaptation for *H. midae*. Wild-caught *H. midae* may have different responses due to increased genetic variation in the population.

Local seawater temperatures will also determine the severity of OA on cultivated abalone. The current findings show that warmer seawater in conjunction with acidified seawater non-significantly increased abalone growth and muscle mass in comparison to acidified conditions alone. Data collected from Smit et. al. (2013) show seawater monthly mean temperatures to range between 11-14 °C on the west coast, 14-16 °C in Hermanus, and approximately 18-20+ °C near Haga Haga (Figure 6.1). This could mean that abalone farms on the west coast and, less so, southwest coast may benefit from an increase in temperature as these temperatures would be within *H. midae's* optimum thermal range of 12 °C to 20 °C (Britz et. al. 1997, Vosloo & Vosloo 2010), however farms on the east coast with currently warmer temperatures may see a decline in abalone growth due to increased metabolic stress in warmer seawater outside of their optimum range (Sokolova et. al. 2012). Further research is needed to determine the effects of OA and warming on *H. midae* larvae; however it is expected that the impacts would be similar to those seen in other *Haliotis* spp. which includes: reduced growth and calcification, larval malformation, and an increase in larval mortalities (Table 6.1).

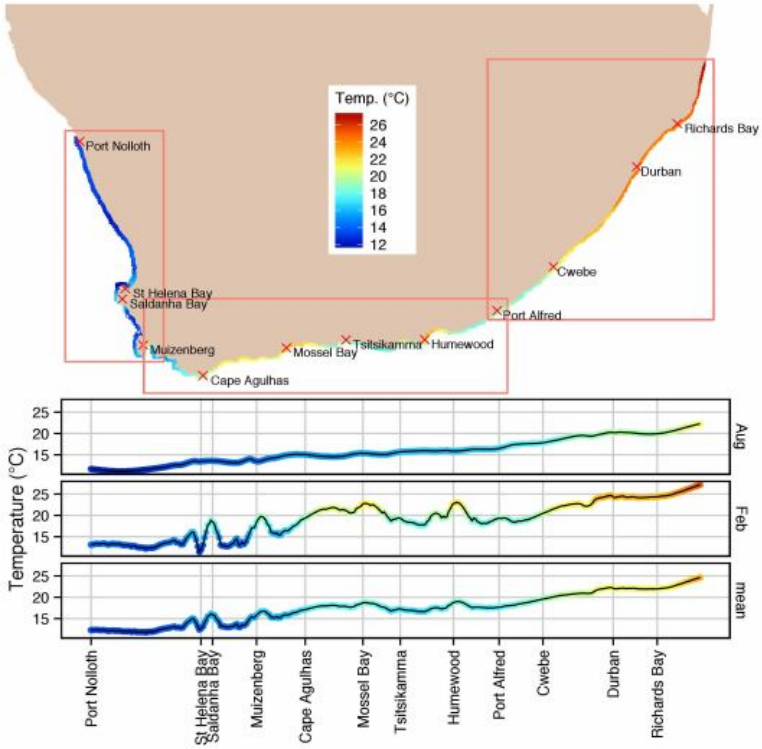

Figure 6.1. Interpolated summertime inshore in situ temperature data for the entire coast between measurement sites from Port Nolloth to Sodwana Bay. These same data are also plotted in the lower panel (b) to further highlight the alongshore gradients. The middle and upper panels in (b) show the seasonal mean monthly in situ temperature for August and February respectively representing winter and summer (Smit et. al. 2013).

Table 6.1. Studies on the response of *Haliotis* spp. to ocean acidification conditions.

Species	Experimental OA conditions (pH/CO2)	Duration	Response to OA conditions	Reference
Haliotis rufescens (larvae)	7.87	6 days	Reduced thermal tolerance	Zippay & Hoffman 2010
Haliotis rufescens (juveniles)	7.5	2 x 24 hours over 15 days	Reduced shell growth	Kim et. al. 2011
Haliotis rufescens (juveniles)	7.62	1 month	Reduced body and tissue weight, pale shells	White 2011
Haliotis rufescens (juveniles)	-0.3 from ambient	3 months	Reduced shell weight and shell:tissue ratio	Lord et. al. 2017
Haliotis coccoradiata (larvae)	7.8, 7.6	21 hours	Reduced calcification and abnormal larval development	Byrne et. al. 2011b
Haliotis kamtschatkana (larvae)	800 ppm	8 days	Reduced shell growth. Shell abnormalities and absence of shell	Crim et. al. 2011
Haliotis discus hannai (larvae)	1650 µatm	75 hours	Reduced shell length, fertilization rate, and hatching rate. Increased malformation and survival of larvae.	Kimura et. al. 2011
Haliotis discus hannai (juveniles)	7.9, 7.7	3 months	Reduced body weight, exposed nacreous layer	Li et. al. 2018
Haliotis diversicolor (larvae)	1500 µatm, 2000µatm, 3000µatm	24 hours	Reduced shell length, hatching rate, fertilization rate, and development	Guo et. al. 2015
Haliotis discus hannai (larvae)	1200µatm	3 days	Increased larval malformation and mortalities. Decreased shell length	Onitsuka et. al. 2018
Haliotis discus hannai (juveniles)	7.8, 7.5	9 days	Corroded aragonite plates and structures	Zheng et. al. 2020
Haliotis tuberculata (larvae)	7.8,7.7	5 days	Reduced larval shell growth and survival. Increased developmental abnormalities	Wessel et. al. 2018
Haliotis tuberculata (juveniles)	7.8, 7.7, 7.6	3 months	Reduced shell length, weight and strength	Auzoux-Bordenave et. al. 2020
Haliotis tuberculata (adults)	7.7	5 months	Reduced shell length and strength. Eroded shells	Avignon et. al. 2020

6.2. How can abalone aquaculture adapt to OA?

Mitigation strategies are necessary for adaptation to OA and abalone farms need to start trialling various strategies before OA causes mass larval mortalities or affects production. Various strategies have been used in mollusc aquaculture to mitigate the impacts of OA, but their suitability in abalone aquaculture is highly dependent on economic flexibility and each farm's unique circumstances.

1. Monitor seawater pH and change farm operations

Whiskey Creek Hatchery implemented complex monitoring systems to track seawater pH, CO_2 concentrations, and aragonite saturations states (Barton et. al. 2012, Branch et. al. 2013, Kelly et. al. 2014). This provided more information on local seawater variability over time, which helped the hatchery determine a correlation between aragonite saturation states at the time of spawning and oyster growth rates (Barton et. al. 2012). Full understanding of the local environment in crucial in implementing a mitigation strategy as a blanket solution for all farms is not always possible (Barage et. al. 2018). Using these monitoring systems, farms adapted their operational procedures by avoiding any tank-filling operations in the early morning when CO_2 concentrations were elevated (Barton et. al. 2012). During upwelling events, seawater was only taken from the ocean in the afternoon during the diurnal low-point in CO_2 concentrations (Branch et. al. 2013). As most facilities use flow-through systems, they would only be able to use this strategy if the farm had access to large-volume seawater storage tanks. Tank cleaning would need to be accomplished in the late morning or afternoon to avoid filling tanks with high-CO_2 seawater and tank cleaning would need to be avoided during upwelling events. Another alternative would be to place seawater inlet pipes as close as possible to surrounding kelp beds or planting new kelp beds near the inlet, strategically selecting seawater from the kelp canopy. Murie & Bourdeau (2020) determined that seawater pH in the kelp canopy was 0.16 units more than at the benthos, with 12 % less pCO_2. Seawater pH at the kelp bed edge is only slightly more (0.05 units) than in the kelp bed interior, reaching a maximum pH of 8.38 units during the day (Murie & Bourdeau 2020).

2. Switch cultivation sites

Goose Point Oysters, Oregon, opened a hatchery in Hawaii to produce oyster larvae, where seawater CO_2 concentrations were more favourable (Branch et. al. 2013). Larvae were grown in the Hawaii hatchery for 1-2 weeks before being flown back to their original facility in Oregon for the rest of the cultivation period. This is a rather extreme solution and, depending on the new site, may not be a permanent solution as ocean acidification intensifies. There would be economic and transportation challenges involved with this strategy; however if there is a sheltered site for the hatchery that is not in an upwelling region and is easily accessible from the grow-out facility it may be viable option.

3. Genetic Breeding

Animals with shorter generational times (weeks to months) have a better chance at adapting to OA naturally via beneficial genetic mutations than animals with longer generational times (years), such as abalone (Miller et. al. 2009, Tan & Zheng 2020). High genetic diversity in parents and/or multiple generations are required to obtain resilience and beneficial genetic mutations in offspring (Griffith & Gobler 2017, Swezey et. al. 2020). Swezey et. al. (2020) looked at increasing genetic diversity by sourcing red abalone*, Haliotis rufescens*, from strong upwelling systems and comparing their OA-tolerance to cultivated abalone from weaker upwelling systems. *H. rufescens* that were sourced from strong upwelling regions were more tolerant of OA conditions than cultivated abalone from weaker upwelling systems, which had a lower survival rate (Swezey et. al. 2020).They also found that

the offspring of abalone from strong upwelling systems were more tolerant of OA conditions due to population-specific provisioning of lipids to offspring (Swezey et. al. 2020). The variation in larval lipid consumption ratios between paternal crosses was a necessary phenotype for survival under OA conditions (Swezey et. al. 2020). Without increasing genetic diversity, multigenerational studies are required. Griffith and Gobler (2017) noted no transgenerational acclimation to OA in *Mercenaria mercenaria* and *Argopecten irradians* after a single generation, but did find an increased sensitivity in offspring from OA-cultivated animals than those from ambient conditions. In nature, this sensitivity could carry-over into multiple generations before a beneficial mutation or natural selections occurs (Sultan 2007, Tan & Zheng 2020), which is why it is so necessary to start a breeding program for OA-tolerance in abalone.

Genetic breeding programmes are currently in place through a collaboration between 5 abalone farms in South African to select for faster growing abalone; however these programmes can be adapted for genetic breeding of abalone resilient to future ocean acidification conditions. The first step to this program would be the identification of phenotypic traits that convey resilience to OA. A genetic programme would be a long-term solution, but highly beneficial for abalone farms or cooperative organisations that can afford to put in the time and effort needed.

4. Addition of Chemicals and Recirculation Systems

Whiskey Creek Hatchery added calcium chloride ($CaCl_2$) and sodium carbonate (Na_2CO_3) to natural seawater to increase aragonite saturation levels, which improved hatchery production during upwelling events (Branch et. al. 2013). This method could be applied to abalone hatcheries in their current state, however a dosing and monitoring system would need to be installed. Another alternative, as shown by Vivanco-Aranda et. al. (2011) and Naylor et. al. (2013) would be to redesign the farm and hatchery systems from a flow-through system into a chemically-dosed recirculation system. Vivanco-Aranda et. al. (2011) used sodium bicarbonate ($NaHCO_3$) to maintain alkalinity above 100 $ml.L^{-1}$ $CaCO_3$ within the recirculation system. *Haliotis rufescens* was cultivated in a dosed recirculation system and an un-dosed flow-through system for 18 weeks (~4 months). *H. rufescens* growth rate and survival were significantly better in the recirculation system, in comparison to the un-dosed flow through system (Vivanco-Aranda et. al. 2011). Naylor et. al. (2013) compared the growth of *H. midae* in a dosed a serial-use raceway with sodium hydroxide ($NaOH^-$) to an ambient serial-use raceway, but noted no significant difference in growth between the serial-use raceways. Naylor et. al. (2013) concluded that this method may be more feasible in a recirculation system.

Recirculation systems allow abalone farms to provide seawater to every cultivation tank without needing to draw seawater from the ocean during upwelling events provided there is a high level of recirculation (50+ %). Installation of recirculation systems also allows abalone farms to integrate seaweed into the system as a biofilter for nutrient waste removal (Robertson-Andersson et. al. 2006, Robertson-Andersson et. al. 2007, Robertson-Andersson et. al. 2008, Bolton et. al. 2009, Nobre et. al. 2010, Robertson-Andersson et. al. 2011, Neveux et. al. 2018, Rothman et. al. 2020). Integrated Multi-Trophic Aquaculture (IMTA) partial recirculation systems using *Ulva* has been incorporated into three South African abalone farms (Buffeljags, Diamond Coast Abalone, and I&J). These partial recirculation systems range between 50 % partial-recirculation (Buffeljags and Diamond Coast Abalone) and 25 % partial-recirculation (I&J, Robertson-Andersson 2003). The latter system was

discontinued due to potential biosecurity risks associated with recirculation, although this system ran for a number of years. IMTA's provide many benefits (See Bolton et. al. 2009 for a full review), such as:

-The removal of nutrients from seawater (ammonia, ammonium, nitrate, nitrite, phosphate), with the removal of ammonia being critical to abalone health due to its toxicity at farm concentrations (Reddy-Lopata et. al. 2006). Neori et. al. (2003) developed a 3-stage Ulva tank system to remove additional ammonia from the system.

-Reduction in CO_2 by photosynthesis and increase in seawater pH during the day,

-Increase in dissolved oxygen during the day.

- Seaweed can be used to supplement the diet of abalone (Naidoo et. al. 2006, Dlaza et. al. 2008).

- Increase seawater temperature in conjunction with a seaweed-supplemented diet can promote faster growth of abalone (Nobre et. al. 2010, Neveux et. al. 2018).

- Allow farms to recirculate water during unfavourable ocean conditions by avoiding ocean input. Recirculation level can be increased to 100 % over short periods to avoid conditions such as harmful algal blooms and upwelling; however additional *Ulva* raceway capacity is required for this eventuality (Neveux et. al. 2018).

- Increased farm profits in comparison to monoculture (Bolton et. al. 2009, Nobre et. al. 2010).

Despite the multitude of benefits provided by IMTA's, some abalone farms are still cautious of incorporating *Ulva* into abalone systems due to fears of potential biosecurity risks in spite of the lack of direct evidence for IMTA's increasing or spreading disease (Neveux et. al. 2018). Urhtermore, investigations still need to be conducted on the impacts of DMSP-release by *Ulva* (under stressful conditions such as acidification and photoinhibition) on abalone growth and physiology, however unfavourable/stressful conditions can be monitored and prevented by shading and alkali chemical addition.

In the cases where redesign of a flow-through system into a recirculation system is not possible, the incorporation of flow-through *Ulva*-cultivation systems may be a viable alternative mitigation strategy.

6.2. Can seaweed mitigate OA effects?

6.2.1. Aquaculture

Although the use of seaweeds to mitigate ocean acidification in an aquaculture scenario has been discussed in literature (Clements & Chopin 2016, Froehlich et. al. 2018, Ahmed et. al. 2019, Galappaththi et. al. 2020, Stewart-Sinclaire et. al. 2020, Tan & Zheng 2020), only a few other studies exist at present that examine the efficacy of seaweeds in mitigating the impacts of ocean acidification on cultivated calcifying organisms (Young and Gobler 2018). Brown algae, *Fucus vesiculosus*, and seagrass, *Zostera marina*, have demonstrated the ability to increase seawater pH by 0.3 units relative to macrophyte-free seawater (Wahl et. al. 2017). This resulted in a significant

increase in calcification of the blue mussel, *Mytilus edulis*, and a shift in the calcifying activity of the mussel to daylight hours (Wahl et. al. 2017). In a 24-hour experiment, brown seaweed, *Sargassum hemiphyllum,* was shown to be able to absorb more CO_2 than was respired by the Portuguese oyster, *Magallana angulata*. The current study showed an improvement in abalone growth with the incorporation of a seaweed cultivation tank into a flow through system in comparison to those grown in acidified seawater despite incomplete amelioration of seawater pH to ambient conditions. This current design could be improved by an increase in fertilization rate of the *Ulva* tanks between November and March, as Robertson-Andersson (2003) noted an increase in ammonium and phosphate uptake by cultivated *Ulva* during summer months in unshaded conditions. An additional improvement is to cultivate *Ulva* in a larger tank/race-way. Robertson-Andersson (2003) cultivated *Ulva* in large tanks (5x1m with 0.6m depth) and was able to achieve a seawater pH above 9 during the day. Seawater pH was similar to ambient pH from 14:00-21:00 Robertson-Andersson (2003). At present abalone farms grow *Ulva* in large (~ 30 m long) paddle-raceways with no reliable pH information to date. Young and Gobler (2018) noted a significant increase in juvenile *M. mercenaria* and *A. irradians* growth in *Ulva*-treated (cultivated under artificial lighting) seawater compared to ambient seawater. *Ulva rigida* and *Gracilaria gracilis* (Wild Coast Abalone) are both successfully cultivated in South Africa, although *Ulva* is easier to cultivate and maintain (Bolton et. al. 2009, Bolton et. al. 2016) than *Gracilaria* in land-based systems as Gracilaria becomes epiphytised with diatoms and filamentous algae and the seedstock needs to be manually cleaned (J.J. Bolton *pers. comm*).

Another important factor to consider is the extent to which cultivated seaweeds might be impacted by OA. The response of seaweed productivity to elevated CO_2 concentrations will depend largely on the inorganic carbon acquisition kinetics of each species (Chung et. al 2017). Seaweeds that have active carbon concentrating mechanisms (CCM) are generally less affected by elevated CO_2 than species with little or no CM activity, thus responding with an increase in photosynthetic rate (Johnston et. al. 1992, Holbrook et. al. 1998, Kübler et. al. 1999, Giordano et. al. 2005, Johnson et. al. 2013, Chung et. al. 2017). *Gracilaria lemaneiformis* (now *Gracilariopsis lemaneiformis*) and *Gracilaria changii* (now *Crassiphycus changii*) have both demonstrated increased growth under elevated CO_2 conditions (Zou & Gou 2009, Lee et. al. 2019). *Ulva lactuca* and *Ulva rigida* also exhibited increased photosynthetic rates under elevated CO_2 conditions; however both species were also rendered more susceptible to photoinhibition (Zou et. al. 2007, Figueroa et. al. 2021). In situ cultivation of *Gracilaria* and *Ulva* (unidentified) also displayed an increase in photosynthetic rates under elevated CO_2 conditions; however *Ulva* photosynthetic rates were also closely linked to nutrient supply (Young & Gobler 2016). Thus, abalone farms will need to monitor and carefully maintain seawater nutrients in seaweed tanks and will need to have a separate cultivation tank which can be used to restock the flow-through seaweed tank in the event of a collapse in the stock. The ideal design for a flow-through seaweed system would be a dual flow-through tank system, whereby one tank experiences natural photoperiods and the second tanks receives the opposite photoperiod. In this way, abalone farms would be able to alternate the water supply from each tank to avoid nocturnal declines in pH, caused by respiration. This design was not able to be used in the current study due to space restrictions on the abalone farm.

Another obstacle to consider is seawater temperature. Cultivated seaweeds have an optimal thermal range, which when exceeded can result in metabolic changes and lead to a decline in growth (Steneck et. al. 2002, Israel et. al. 2010, Chung et. al. 2017, Liu et. al. 2019). Thus it is imperative that

the cultivator has a good understanding of local temperatures and the optimal thermal tolerance of the cultivated species, keeping in mind predicted land/sea surface temperature increases as well as temperature increases that arise from the cultivation of seaweed (Hoegh-Guldberg et. al. 2014, Barage et. al. 2018). For example, Robertson-Andersson (2003) noted a 5 °C temperature increase caused by cultivated *Ulva* and in the current study we noted an average temperature differential of 1.56 °C. In regions where the water temperature is already warm (eg. Haga Haga), these temperature differentials may influence the cultivator in the choice of a more appropriate, heat-tolerant species.

6.2.2. Nature

Global seaweed communities are estimated to absorb 1.5 Pg.C.year-1 via their net production (Krause-Jensen & Duarte 2016, Duarte et. al. 2017). In nature, seaweed communities may provide vital refugia (areas where localized environmental conditions protect species from unfavourable conditions) by influencing the diel pH variability through shifts in photosynthesis and respiration (Hendriks et. al. 2014, Kapsenberg & Hoffman 2016, Kapsenberg & Cyronak 2019).

At the smallest spatial scale, seawater chemistry may be modified by an organism's diffusion boundary layer (DBL), and the physical properties that determine the size of the boundary layer (Hurd et. al. 2011, Noisette & Hurd 2018, Kapsenberg & Cyronak 2019, Johnson et.al. 2020). For example, the DBL of the brown alga, *Fucus serratus,* created a refugia for epibionts, *Balanus improvius* and *Electra pilosa*, under OA conditions (pH: 7.7 vs ambient: 8.1); however under fluctuating pH conditions growth of the epibionts were inhibited (Johnson et. al. 2020).

On a larger scale, adaptive refugia such as rock pools provide relief from unfavourable conditions through their macroalgal assemblages (Bracken et. al. 2018). Macroalgal photosynthetic activity in rock pool assemblages has been shown to be robust to predicted increases in seawater CO_2 and temperature, providing the possibility of refugia for calcifying organisms under climate change conditions (Legrand et. al. 2018). CO_2 was added to 10 macrophyte-dominated tidal pools in California, USA, to assess macroalgae's efficiency in removing CO_2 under ocean acidification conditions (Bracken et. al. 2018). It was determined that photosynthetic activity of macroalgal communities in the rock pools significantly reduced seawater CO_2 and increased pH, fully mitigating the effects of additional CO_2 (Bracken et. al. 2018). In Greenland, tidal macroalgae in rock pools have been shown to absorb CO_2 during the day in summer, raising the pH from 8.14 to 8.69 (Duarte & Krause-Jensen 2018). This absorption of CO_2 and increase in aragonite saturation state was positively correlated with an increase in calcification of calcifying organisms and net ecosystem productivity rates (Duarte & Krause-Jensen 2018), which has the ability to increase growth in calcifying organisms.

Seagrass meadows can increase seawater pH during the day on a scale from millimetres to hundreds of meters (Semesi et. al. 2009, Guilini et al. 2017, Hendriks et al. 2014, Manzello et al. 2012, Cyronak et. al. 2018, Koweek et. al. 2018, Vizzini et. al. 2019). However the mitigation potential is highly dependent on the tidal phasing, water depth and geo-physical parameters of the seagrass meadow (Koweek et. al. 2018). As mentioned previously, kelp beds also have the capacity to increase seawater pH and decrease pCO_2 over large spatial scales during the day and the positioning within kelp beds (e.g. canopy vs. benthos) can affect the degree of carbonate-system change by photosynthesis (Murie & Bourdeau 2020).

The problem with macroalgae providing refugia to calcifying organisms under OA conditions is that periods of net photosynthesis are accompanied by periods of net respiration, which can intensify the negative effects of OA (Kapsenberg & Cyronak 2019). Thus unfavourable conditions can be temporarily avoided in these refugia, but they can also play a role in enhancing the adaptive capacity of organisms (Koweek et. al. 2018, Kapsenberg & Cyronak 2019).

6.3. Environmental realism vs. laboratory control?

Including natural variability and external environmental conditions (i.e. exposure to weather conditions) into climate change studies is an incorporation of environmental realism. There is often a trade-off between fully controlled laboratory approaches and the inclusion of environmental realism in climate change studies.

A fully controlled, experimental approach in laboratory settings provides feedback on the relationship between drivers (e.g. OA) and the physiological, ecosystem or evolutionary response in the target organism (Riebessel & Gattuso 2015, Boyd et. al. 2018, Baumann 2019). This allows researchers to obtain basal information on species responses and clarify mechanisms for the observed responses (Baumann 2019). However this approach lacks environmental realism as the response of the study organism may vary in nature due to indirect effects from the environment (Boyd et. al. 2018, Baumann 2019). Inclusion of environmental realism includes indirect environmental effects which can ultimately determine ecosystem responses (Boyd et. al. 2018, Baumann 2019). Studies which are designed to provide feedback to an industry, such as aquaculture, require both approaches to determine mechanistic effects as well as realistic responses of the study organism to changing environmental conditions in an aquaculture environment (Reid et. al. 2019).

Laboratory-controlled experiments have the benefit of allowing a higher degree of replication and better statistical power from the data collected. The incorporation of environmental realism into this study was logistically challenging. A higher degree of replication would have called for a larger set of data-logger-relay systems, CO_2 and temperature controls as well as more header tanks for each treatment. Because this study was based on an abalone farm, there was a set amount of physical space allotted to the experiment next to commercial abalone tanks. This experiment abutted against commercial tanks and a roadway with barely enough space for vehicles to drive past. The inclusion of additional header tank systems and power sources were not an option. Monitoring of each element within the system was also challenging due to the multiple parameters that were constantly analysed. The experiment was exposed to sea air and each electrical component needed to be assessed and maintained daily to avoid corrosion of electrical wires and circuits. Exposure of the system to the elements posed further difficulties in winter when a storm blew off the lids of the header tanks and destroyed the pH meters inside of them. Maintaining a pH controller system was especially difficult when exposed to the weather as calibration of the probes required a sheltered area free from rain for 2 hours at a time. This was resolved through the use of plastic sheeting and a staple gun. Another point that is mentioned by Boyd et. al. (2018) and Baumann (2019) is that of cost. The design and maintenance of a system that incorporates environmental realism can exceed those of laboratory-controlled experiments due to weathering of equipment, and the inclusion of relay systems for multiple drivers (Boyd et. al. 2018, Baumann 2019).

However, despite the challenges that this experiment imposed, it has provided beneficial information for the abalone aquaculture industry. A prominent finding from this experiment, in comparison to controlled experiments on *H. midae*, is the response of abalone to increased temperatures. Previous thermal research on *H. midae* growth used constant conditions (Britz et. al. 1997, Vosloo & Vosloo 2010) and reflected inflated growth increases with an increase in temperature in comparison to abalone grown in a variable system.

Lastly, it should be acknowledged that highly artificial and controlled experiments conducted over short time periods do not allow for extrapolation to longer time scales (Boyd et. al. 2018). This removes the possibility of adaptation (individual or generational) or acclimation of the organism to the environmental conditions, especially if the organism is slow-growing (Browman et. al. 2016, McElhany 2017). Even the current study could be expanded over a longer time period to incorporate the complete life cycle of the abalone; however in an aquaculture setting this period can be as lengthly as 5-6 years. To the author's knowledge no other climate change study on calcifier response to OA and warming has exceeded the length of current study.

REFERENCES

Aalto E.A., Barry J.P., Boch C.A., Litvin S.Y., Micheli F., Woodson C.B. &G.A. De Leo (2020) Abalone populations are most sensitive to environmental stress effects on adult individuals. Marine Ecology Progress Series 643: 75–85.

Abreu M.H., Pereira R., Yarish C., Buschmann A.H. & I. Sousa-Pinto (2011) IMTA with *Gracilaria vermiculophylla*: Productivity and nutrient removal performance of the seaweed in a land-based pilot scale system. Aquaculture 312(1-4): 77-87.

Adkins J.F., Naviaux J.D., Subhas A.V., Dong S. & W.M. Berelson (2021) The dissolution rate of $CaCo_3$ in the ocean. Annual Review of Marine Science 13(1): 57-80.

Ahmed N., Thompson S. & M. Glaser (2019) Global aquaculture productivity, environmental sustainability, and climate change adaptability. Environmental Management 63: 159–172.

Alfaro A.C., Young T. & K. Bowden (2014) Neurophysiological control of swimming behaviour, attachment and metamorphosis in black-footed abalone (*Haliotis iris*) larvae. New Zealand Journal of Marine and Freshwater Research 48(3): 314-334.

Anderson R.J., Levitt J.G. & A. Share (1996) Experimental investigations for the mariculture of *Gracilaria* in Saldanha bay, South Africa. Journal of Applied Phycology 8: 421–430.

Andersson A.J. & D. Gledhill (2013) Ocean acidification and coral reefs: effects on breakdown, dissolution, and net ecosystem calcification. Annual Review of Marine Science 5: 321-348.

Arnone V., González-Dávila M. & J.M. Santana-Casiano (2017) CO_2 fluxes in the South African coastal region. Marine Chemistry 195: 41-49.

Atkinson A., Siegel V., Pakhomov E. & P. Rothery (2004) Long-term decline in krill stock and increase in salps within the Southern Ocean. Nature 432, 100-103.

Auzoux-Bordenave S., Badou A., Gaume B., Berland S., Helléouet M-N., Milet C. & S. Huchette (2010) Ultrastructure, chemistry and mineralogy of the growing shell of the European abalone *Haliotis tuberculata*. Journal of Structural Biology 171: 277–290.

Auzoux-Bordenave S., Wessel N., Badou A., Martin S., M'Zoudi S., Avignon S., Roussel S., Huchette S. & P. Dubois (2020) Ocean acidification impacts growth and shell mineralization in juvenile abalone (*Haliotis tuberculata*). Marine Biology 167:11.

Avignon S., Auzoux-Bordenave S., Martin S., Dubois P., Badou A., Coheleach M. , Richard N., Di Giglio S., Malet L., Servili A., Gaillard F., Huchette S. & S. Rousse (2020) An integrated investigation of the effects of ocean acidification on adult abalone (*Haliotis tuberculata*). ICES Journal of Marine Science, doi:10.1093/icesjms/fsz257

Awaji M. & K. Hamano (2004) Gonad formation, sex differentiation and gonad maturation processes in artificially produced juveniles of the abalone, *Haliotis discus hannai*. Aquaculture 239: 397-411.

Bakun A. (1990) Global climate change and intensification of coastal ocean upwelling. Science 247: 198-201.

Baragé M., Moussa B. & J. Comby (2018) "Climate change perception and adaptation strategy associated with farming techniques in Tamou district wester Niger farmers. African Journal of Agricultural Research 13(30): 1496-1507.

Barange M. & R.I. Perry (2009) Physical and ecological impacts of climate change relevant to marine and inland capture fisheries and aquaculture. In K. Cochrane, C. De Young, D. Soto and T. Bahri (eds). Climate change implications for fisheries and aquaculture: overview of current scientific knowledge. FAO Fisheries and Aquaculture Technical Paper. No. 530. Rome, FAO. pp. 7–106.

Barbraud C., Weimerskirch H., Bost C-A., Forcada J., Trathan P. & D Ainley (2008) Are king penguin populations threatened by Southern Ocean warming? Proceedings of the National Academy of Science of the United States of America 105(26): E38.

Barclay K.M., Gaylord B., Jellison B.M., Shukla P., Sanford E. & L.R. Leighton (2019) Variation in the effects of ocean acidification on shell growth and strength in two intertidal gastropods. Marine Ecology Progress Series 626: 109–121.

Barkai R. & C.L. Griffiths (1986) Diet of the South African abalone, *Haliotis midae*. South African Journal of Marine Science 4(1): 37-44. DOI: 10.2989/025776186784461891.

Barrington K., Chopin T. & S. Robinson (2009) Integrated multi-trophic aquaculture (IMTA) in marine temperate waters. FAO Fisheries and Aquaculture Technical Paper 529: 7-46.

Barton A., Hales B., Waldbusser G.G., Langdon C. & R.A. Feely (2012) The Pacific oyster, Crassostrea gigas, shows negative correlation to naturally elevated carbon dioxide levels: Implications for near-term ocean acidification effects. Limnology Oceanography 57 (3):698-710.

Baumann H. (2019) Experimental assessments of marine species sensitivities to ocean acidification and co-stressors: how far have we come? Canadian Journal of Zoology 97: 399–408.

Béguinot J. (2014) Covarying shell growth parameters and the regulation of shell shape in marine bivalves: a case study on *Tellinoidea*. Journal of Marine Biology, Article ID 519510, 10 pages.

Behrenfeld M. J., O'Malley R.T., Siegel D.A., McClain C.R., Sarmiento J.L., Feldman G.C., Milligan P.G., Letelier R.M. & E.S. Boss (2006) Climate driven trends in contemporary ocean productivity. Nature 444:752-755.

Belkin I.M. (2009) Rapid warming of large marine ecosystems. Progress in Oceanography, 81(1-4): 207-213.

Ben-Ari T., Neori A., Ben-Ezra D., Shauli L., Odintsov V. & M. Shpigel (2014) Management of *Ulva lactuca* as a biofilter of mariculture effluents in IMTA system. Aquaculture 434: 493-498.

Ben-Horin T., Lenihan H.S. & K.D. Lafferty (2013) Varibale intertidal temperature explains why disease endangers black abalone. Ecological Sociey of America 94(1): 161-168.

Ben-Yahmed N., Jmel M.A., Ben Alaya M., Bouallagui H., Marzouki M.N. & I. Smaali (2016) A biorefinery concept using the green macroalgae *Chaetomorpha linum* for the coproduction of bioethanol and biogas. Energy and Conversion Management 119: 257–265.

Bikker P., van Krimpen M.M., van Wikselaar P., Houweling-Tan B., Scaccia N., van Hal J.W., Huijgen W.J.J., Cone J.W. & A.M. López-Contreras (2016) Biorefinery of the green seaweed *Ulva lactuca* to produce animal feed, chemicals and biofuels. Journal of Applied Phycology 28: 3511-3525.

Blamey L.K., Branch G.M. & K. Reaugh-Flower (2010) Temporal changes in kelp forest benthic communities following an invasion by the rock lobster Jasus lalandii. African Journal of Marine Science 32(3):481-490.

Blamey L.K., Plagányi É.E. & G.M.Branch (2013) Modeling a regime shift in a kelp forest ecosystem caused by a lobster range expansion. Bulletin of Marine Science 89(1): 347-375.

Boch C.A., Micheli F., AlNajjar M., Monismith S.G., Beers J.M., Bonilla J. C., Espinoza A.M., Vazquez-Vera L. & C.B. Woodson (2018) Local oceanographic variability influences the performance of juvenile abalone under climate change. Scientific Report, Nature 8: 5501. DOI:10.1038/s41598-018-23746-z

Bolton J.J., Robertson-Andersson D.V., Shuulaka D. & L. Kandjengo (2009) Growing *Ulva* (Chlorophyta) in integrated systems as a commercial crop for abalone feed in South Africa: a SWOT analysis. Journal of Applied Phycology 21(5): 575-583.

Bolton J.J., Davies-Coleman M. & Coyne V.E. (2013). Innovative processes and products involving marine organisms. African Journal Marine Science 35: 449–464.

Bolton J.J., Cyrus M.D., Brand M.J., Joubert M. & B.M. Macey (2016). Why grow Ulva? Its potential in the future of seaweed aquaculture. Perspectives in Phycology 3: 113–120.

Bolton J.J. (2019) The problem of naming commercial seaweeds. Journal of Applied Phycology 32(2): 751-758.

Bothes L., Smit A.J. & P.A. Cook (2003) The potential threat of algal blooms to the abalone (*Haliotis midae*) mariculture industry situated around the South African coast. Harmful algae 2(4): 247-259.

Boyd P.W., Collins S., Dupont S., Fabricius K., Gattuso J.P., Havenhand J., Hutchins D.A., Riebesell U., Rintoul M.S., Vichi M., Biswas H., Ciotti A., Gao K., Gehlen M., Hurd C.L., Kurihara H., McGraw C.M., Navarro J.M., Nilsson G.E., Passow U. & H.O. Pörtner (2018) Experimental strategies to assess the biological ramifications of multiple drivers of global ocean change — a review. Global Change Biology 24: 2239–2261. doi:10.1111/gcb.14102.

Bracken M.E.S., Silbiger N.J., Bernatchez G. & C.J.B. Sorte (2018) Primary producers may ameliorate impacts of daytime CO2 addition in a coastal marine ecosystem. PeerJ 6: e4739.

Branch T.A., De Joseph B.M., Ray L.J. & C.A. Wagner (2013) Impacts of ocean acidification on marine seafood. Trends in Ecology & Evolution 28(3): 178-186.

Breitburg D.L., Salisbury J., Bernhard J.M., Cai W.-J., Dupont S., Doney S.C., Kroeker K.J., Levin L., Long W.C., Milke L.M., Miller S.H., Phelan B., Passow U., Seibel B.A., Todgham A.E. & A.M. Tarrant (2015) And on top of all that… Coping with ocean acidification in the midst of many stressors. Oceanography 28: 48–61. doi:10.5670/oceanog.2015.31.

Breitburg D.L., Levin L.A., Oschlies A., Grégoire M., Chavez F.P., Conley D.J., Garçon V., Gilbert D., Gutiérrez D. & K. Isensee (2018) Declining oxygen in the global ocean and coastal waters. Science 359(6371): eaam7240. doi:10.1126/science.aam7240. PMID:29301986.

Britz P.J., Hecht T. & S. Mangold (1997) Effect of temperature on growth, feed consumption and nutritional indices of *Haliotis midae* fed a formulated diet. Aquaculture 152: 191-203.

Browman H.I. (2016) Applying organized scepticism to ocean acidification research. ICES Journal of Marine Science 73(3): 529–536.

Brugère C. & C. De Young (2015) Assessing climate change vulnerability in fisheries and aquaculture: Available methodologies and their relevance for the sector. FAO Fisheries and Aquaculture Technical Paper. Rome, Italy: FAO.

Bruhn A., Dahl J., Nielsen H.B., Nikolaisen L., Rasmussen M.B., Markager S., Olesen B., Arias C. & P.D. Jensen (2011) Bioenergy potential of *Ulva lactuca*: biomass yield, methane production and combustion. Bioresource Technology 102:2595–2604.

Bürgener M. (2010) The CITES Appendix III Listing of Abalone (*Haliotis midae*) - Impact on Illegal Harvest and Trade, TRAFFIC Bulletin, 23. TRAFFIC International, Cambridge, United Kingdom.

Burton E.A. & L.M. Walter (1987) Relative precipitation rates of aragonite and Mg calcite from seawater: temperature or carbonate ion control? Geology 15(2): 111-114.

Busenberg E. & N.L. Plummer (1986). A comparative study of the dissolution and crystal growth kinetics of calcite and aragonite. U.S. Geological Surveys Bulletin 1578: 139-168.

Byrne M. (2011) Impact of ocean warming and acidification on marine invertebrate life history stages: Vulnerabilities and potential for persistence in changing ocean. Oceanography and Marine Biology: An Annual Review 49:1-42.

Byrne M., Selvakumaraswmay P., Ho M.A., Woolsey E. H.D. Nguyen (2011a) Sea urchin development in a global change hotspot, potential for southerly migration of thermotolerant propagules. Deep Sea Research Part II: Topical Studies in Oceanography 58(5): 712-719.

Byrne M., Ho M., Wong E., Soars N.A., Selvakumaraswamy P., Shepard-Brennand H., Dworjanyn S.A. & A.R. Davis (2011b) Unshelled abalone and corrupt urchins: Development of marine calcifiers in a changing ocean. Proceedings of the Royal Society B. 278(1716): 2376-2383.

Byrne M. & R. Przeslawski (2013) Multistressor impacts of warming and acidification of the ocean on marine invertebrates' life histories. Integrative and Comparative Biology 53(4): 582–596. doi:10.1093/icb/ict049. PMID:23697893.

Cabello-Pasinia A., Aguirre-von-Wobeser E. & F.L. Figueroa (2000) Photoinhibition of photosynthesis in *Macrocystis pyrifera* (Phaeophyceae), *Chondrus crispus* (Rhodophyceae) and *Ulva lactuca* (Chlorophyceae) in outdoor culture systems. Journal of Photochemistry and Photobiology B: Biology 57(2-3): 169-178.

Cameron, J.N. (1971) Rapid method for determination of total carbon dioxide in small blood samples. Journal of Applied Physiology 31(4): 632-634.

Cameron J.N. (1986) Carbon dioxide measurement. *In*: Principles of physiological measurement. Academic Press. Inc., Florida, U.S.A. pp 87-101.

CamillaCampanati C., Dupont S., Williams G.A. & V. Thiyagarajan (2018) Differential sensitivity of larvae to ocean acidification in two interacting mollusc species. Marine Environmental Research 141: 66-74.

Carl C., de Nys R. & N.A. Paul (2014) The seeding and cultivation of a tropical species of filamentous Ulva for algal biomass production. PLoS One 9:e98700

Cattano C., Claudet J., Domenici P. & M. Milazzo (2018) Living in a high CO_2 world: a global meta-analysis shows multiple trait-mediated fish responses to ocean acidification. Ecological Monographs 88(3): 320-335.

Chapperon C., Clavier C., Dugué C., Amice E., Le Goff M. & S. Roussel (2019) Seasonal and diurnal variability in carbon respiration, calcification and excretion rates of the abalone *Haliotis tuberculata L*. Journal of the Marine Biological Association of the United Kingdom 99(2): 393-402.

Chemodanov A., Robin A., & A. Golberg (2017a) Design of marine macroalgae photobioreactor integrated into building to support seagriculture for biorefinery and bioeconomy. Bioresource Technology 241: 1084–1093.

Chemodanov A., Jinjikhashvily G., Habiby O., Liberzon A., Israel A., Yakhini Z. & A. Golberg (2017b) Net primary productivity, biofuel production and CO_2 emissions reduction potential of *Ulva* sp. (Chlorophyta) biomass in a coastal area of the Eastern Mediterranean. Energy Conversion Management 148:497–1507.

Chemodanov A., Robin A., Jinjikhashvily G., Yitzhak D., Liberzon A. & Israel A., A. Golberg (2019) Feasibility study of *Ulva* sp. (Chlorophyta) intensive cultivation in a coastal area of the Eastern Mediterranean Sea. Biofuel, Bioproducts and Biorefining 13(4): 864-877.

Cheng W., Hsiao I-S., Hsu C-H. & J.C. Chen (2004) Change in water temperature on the immune response of Taiwan abalone *Haliotis diversicolor supertexta* and its susceptibility to *Vibrio parahaemolyticus*. Fish & Shellfish Immunity 17(3): 235-243.

Chopin T., Buschmann A.H., Halling C., Troell M., Kautsky N., Neori A., Kraemer G.P., Zertuche-González J.A., Yarish C. & C. Neefus (2001) Integrating seaweeds into marine aquaculture systems: a key toward sustainability. Journal of Phycology 37(6): 975-986.

Christensen J.H., Hewitson B., Busuioc A., Chen A., Gao X., Held I., Jones R., Kolli R.K., Kwon W.-T., Laprise R., Magaña Rueda V.,. Mearns L, Menéndez C.G., Räisänen J., Rinke A., Sarr A. & P. Whetton (2007) Regional climate projections. In: Climate Change 2007: The Physical Science Basis. Contribution of Working Group I to the Fourth Assessment Report of the Intergovernmental Panel on Climate Change [Solomon, S., D. Qin, M. Manning, Z. Chen, M. Marquis, K.B. Averyt, M. Tignor, and H.L. Miller (eds.)]. Cambridge University Press, Cambridge, UK and New York, NY, USA, pp. 847-940.

Ciais P., Sabine C., Bala G., Bopp L., Brovkin V., Canadell J., Chhabra A., DeFries R., Galloway J., Heimann M., Jones C., Le Quéré C., Myneni R.B., Piao S. & Thornton P. (2013) Carbon and Other Biogeochemical Cycles. In: Climate Change 2013: The Physical Science Basis. Contribution of Working Group I to the Fifth Assessment Report of the Intergovernmental Panel on Climate Change [Stocker, T.F., D. Qin, G.-K. Plattner, M. Tignor, S.K. Allen, J. Boschung, A. Nauels, Y. Xia, V. Bex and P.M. Midgley (eds.)]. Cambridge University Press, Cambridge, United Kingdom and New York, NY, USA.

Chung I.K., Sondak C.F.A. & J. Beardall (2017) The future of seaweed aquaculture in a rapidly changing world. European Journal of Phycology 52(4): 495-505.

Clements J.C. & T. Chopin (2018) Ocean acidification and marine aquaculture in North America: potential impacts and mitigation strategies.Reviews in Aquaculture 9(4): 326-341.

Cockcroft A.C., van Zyl D. & L. Hutchings (2008) Large-scale changes in the spatial distribution of South African West Coast rock lobsters: an overview. African Journal of Marine Science 30:149-159.

Collins M., Knutti R., Arblaster J., Dufresne J.-L., Fichefet T., Friedlingstein P., Gao X., Gutowski W.J., Johns T., Krinner G., Shongwe M., Tebaldi C., Weaver and M. & Wehner A.J. (2013) Long-term Climate Change: Projections, Commitments and Irreversibility. In: Climate Change 2013: The Physical Science Basis. Contribution of Working Group I to the Fifth Assessment Report of the Intergovernmental Panel on Climate Change [Stocker, T.F., D. Qin, G.-K. Plattner, M. Tignor, S.K. Allen, J. Boschung, A. Nauels, Y. Xia, V. Bex and P.M. Midgley (eds.)]. Cambridge University Press, Cambridge, United Kingdom and New York, NY, USA.

Cook P.A. (2016) Recent trends in worldwide abalone production. Journal of Shellfish Research, 35: 581–583.

Cornwall C.E. & C.L. Hurd (2016) Experimental design in ocean acidification research: problems and solutions. ICES Journal of Marine Science 73(3): 572-581.

Cornwall C.E., Comeau S., DeCarlo T.M., Moore B., D'Alexis Q. & M.T. McCulloch (2018) Resistance of corals and coralline algae to ocean acidification: physiological control of calcification under natural pH variability. Proceedings of the Royal Society B 285: 1884.

Crawford R.J.M., Cockroft A.C., Dyer B.M. & L. Upfold (2008) Divergent trends in bank cormorants *Phalacrocorax neglectus* breeding in South Africa's Western Cape consistent with a distributional shift of rock lobsters *Jasus lalandii*. African Journal of Marine Science 30(1): 161-166.

Crim R.N., Sunday J.M. & C.D.G. Harley (2011) Elevated seawater CO_2 concentrations impair larval development and reduce larval survival in endangered northern abalone (*Haliotis kamtschatkana*). Journal of Experimental Marine Biology and Ecology 400(1-2): 272-277.

Cripps I.L., Munday P.L., McCormick M.I. (2011) Ocean acidification affects prey detection by a predatory reef fish. PLoS ONE 6(7): e22736. https://doi.org/10.1371/journal.pone.0022736

Cubasch U., Wuebbles D., Chen D., Facchini M.C., Frame D., Mahowald N., & J.-G. Winther (2013) Introduction. In: Climate Change 2013: The Physical Science Basis. Contribution of Working Group I to the Fifth Assessment Report of the Intergovernmental Panel on Climate Change [Stocker, T.F., D. Qin, G.-K. Plattner, M. Tignor, S.K. Allen, J. Boschung, A. Nauels, Y. Xia, V. Bex and P.M. Midgley (eds.)]. Cambridge University Press, Cambridge, United Kingdom and New York, NY, USA.

Cummings V.J., Smith A.M., Marriott P.M., Peebles B.A. & N.J. Halliday (2019) Effect of reduced pH on physiology and shell integrity of juvenile *Haliotis iris* (pāua) from New Zealand. PeerJ 7:e7670 https://doi.org/10.7717/peerj.7670

Cyronak T., Andersson A.J., D'Angelo S., Bresnahan P., Davidson C., Griffin A., Kindeberg T., Pennise J., Takeshita Y. & M. White (2018) Short-term spatial and temporal carbonate chemistry variability in two contrasting seagrass meadows: Implications for pH buffering capacities. Estuaries and Coasts 41: 1282–1296.

Davies T.T. & Hooper P.R. (1963) The determination of the calcite:aragonite ratio in mollusc shells by X-ray diffraction. Mineralogical Magazine 33(262):608-612.

Day E. (1998) Ecological interactions between abalone (*Haliotis midae*) juveniles and sea urchins (*Parechinus angulosus*), off the South-west coast of South Africa. Dissertation. University of Cape Town, Cape Town, South Africa.

Day E. & G. M. Branch (2000) Field evidence for an association between juveniles of the South African abalone *Haliotis midae* and the sea urchin *Parechinus angulosus*. South African Journal of Marine Science 22:137–144.

Day E. & G.M. Branch (2002) Effects of sea urchins (*Parechinus angulosus*) on recruits and juveniles of abalone (*Haliotis midae*). Ecological Monographs 72(1): 133-149.

Davison I.R. & G.A. Pearson (1996) Stress tolerance in intertidal seaweeds. Journal of Phycology 32: 197–211.

DEAT (2003) Policy for the Allocation of Commercial Fishing Rights in the Abalone Fishery. Department of Environmental Affairs and Tourism, Pretoria, South Africa (2003)

DEAT (2007) Marine Living Resources Act (Act No.18 of 1998) Draft regulations for the protection of abalone (*Haliotis*) (Wild) government Gazette No. 30542, Notice, R.1141, Department of Environmental Affairs and Tourism, Pretoria, South Africa

Demarcq, H., 2009: Trends in primary production, sea surface temperature and wind in upwelling systems (1998-2007). Progress in Oceanography, 83(1), 376-385.

Dhir B. (2015) Status of Aquatic Macrophytes in Changing Climate: A Perspective. Journal of Environmental Science and Technology 8 (4): 139-148.

Díaz F., del Río-Portîlla M.A., Sierra E., Aguilar M. & A.D. Re-Araujo (2000) Preferred temperature and critical thermal maxima of red abalone *Haliotis rufescens*. Journal of Thermal Biology 25(3): 25-261.

Diaz-Almela E., Nuria M. & C.M. Duarte (2007) Consequences of Mediterranean warming events in seagrass (*Posidonia oceanica*) flowering records. Global Change Biology 13: 224–235.

Dixson D.L., Munday P.L. & G.P. Jones (2010) Ocean acidification disrupts the ability of fish to detect predator olfactory cues. Ecology Letters 13: 68-75. doi: 10.1111/j.1461-0248.2009.01400.x.

Dlaza T.S., Maneveldt G.W. & C. Viljoen (2008) Growth of post-weaning abalone fed commercially available formulated feeds supplemented with fresh wild seaweed. African Journal of Marine Science 30(1): 199-203.

Doney S., Fabry V., Feely R. & J. Kleypas (2009) Ocean acidification: The other CO_2 problem. Annual Review of Marine Science 1:169-192.

Dove S., Kline D.I., Pantos O., Angly F.E., Tyson G.W. & O. Hoegh-Guldberg (2013) Future reef decalcification under a business-as-usual CO_2 emission scenario. Proceedings of the National Academy of Sciences of the United States of America, 110(38): 15342-15347.

Drechsler Z. & S. Beer (1992). Utilization of Inorganic Carbon by *Ulva lactuca*. Plant Physiology 98(4): 1439-1444.

Duarte C.M., Hendriks I.E., Moore T.S., Olsen Y.S., Steckbauer A., Ramajo L., Carstensen J., Trotter J.A. & M. McCulloch (2013) Is ocean acidification an open-ocean syndrome? Understanding anthropogenic impacts on seawater pH. Estuaries Coasts 36: 221-236.

Duarte C.M., Wu J., Xiao X., Bruhn A. & D. Krause-Jensen (2017) Can Seaweed Farming Play a Role in Climate Change Mitigation and Adaptation? Frontiers in Marine Science 4:100.

Duarte C.M. & D. Krause-Jensen (2018) Greenland tidal pools as hot spots for ecosystem metabolism and calcification. Estuaries and Coasts 41: 1314–1321.

Durant J., Hjermann D., Ottersen G., Stenseth N. (2007) Climate and the match or mismatch between predator requirements and resource availability. Climate Research 33: 271-283.

Eggert A. (2012) Seaweed responses to temperature. In: Bischof, CWaK (ed.). Seaweed Biology. Springer-Verlag, Berlin Heidelberg. pp. 47–66.

Espinosa H.D., Juster A.L., Latourte F.J., Loh O.Y., Gregoire D. & P.D. Zavattieri (2011) Tablet-level origin of toughening in abalone shells and translation to synthetic composite materials. Nature Communications 2:173

Fabricius K.E., Langdon C., Uthicke S., Humphrey C., Noonan S., De'ath G., Okazaki R., Muehllehner N., Glas M.S. & J.M. Lough (2011) Losers and winners in coral reefs acclimatized to elevated carbon dioxide concentrations. Nature Climate Change 1(3): 165-169.

Fabry V.J., Seibel B.A. Feely R.A. & J.C. Orr (2008) Impacts of ocean acidification on marine fauna and ecosystem processes. ICES Journal of Marine Science 65(3): 414-432.

Fang J., Zhang J., Xiao T., Huang D. & S. Liu (2016) Integrated multi-trophic aquaculture (IMTA) in Sanggou Bay, China. Aquaculture Environment Interactions 8: 201-205.

FAO (2018a) Top ten species groups in global aquaculture 2018 (1950-2018; Released March 2020). Food and Agriculture Organization of the United Nations. Available at www.fao.org/fishery/statistics/software/fishstatj/en.

FAO (2018b) Fishery and Aquaculture Statistics (Released October 2020). Food and Agriculture Organization of the United Nations. Available at: http://www.fao.org/fishery/static/Yearbook/YB2018_USBcard/root/capture/yearbook_capture.pdf

FAO (2018c) The State of World Fisheries and Aquaculture 2018–Meeting the Sustainable Development Goals. FAO, Rome.

Fassbender A.J., Sabine C.L. & K.M. Feifel (2016) Consideration of coastal carbonate chemistry in understanding biological calcification. Geophysical Research Letters 43: 4467–4476.

Feely, R.A. & C.T.A. Chen (1982) The effect of excess CO_2 on the calculated calcite and aragonite saturation horizons in the northeast Pacific. Geophysical Research Letters 9(11): 1294–1297.

Feely, R.A., Sabine C.L., Lee K., Millero F.J., Lamb M.F., Greeley D., Bullister J.L., Key R.M., Peng T-.H., Kozyr A., Ono T. & C.S. Wong (2002) In situ calcium carbonate dissolution in the Pacific Ocean. Global Biogeochemical Cycles 16(4): 1144.

Feely R.A., Sabine C.L., Lee K., Berelson W., Kleypas J., Fabry V.J. & F.J. Millero (2004) Impact of anthropogenic CO_2 on the $CaCO_3$ system in the oceans. Science 305:362-366.

Feely R.A., Doney S.C. & S.R. Cooley (2009) Ocean acidification present conditions and future changes in a high CO_2 world. Oceanography 22(4): 36-47.

Fernández C. (2011) The retreat of large brown seaweeds on the north coast of Spain: the case of Saccorhiza polyschides. European Journal of Phycology 46: 352–360.

Figueroa F.L., Bonomi-Barufi J., Celis-Plá P.S.M., Nitschke U., Arenas F., Connan S., Abreu M.H., Malta E-J., Conde-Álvarez R., Chow F., Mata M.T., Meyerhoff O., Robledo D. & D.B. Stengel (2021) Short-term effects of increased CO_2, nitrate and temperature on photosynthetic activity in *Ulva rigida* (Chlorophyta) estimated by different pulse amplitude modulated fluorometers and oxygen evolution. Journal of Experimental Biology 72(2): 491-509.

Fitzmaurice G.N., Laird N.M. & Ware J. (2004) Applied Longitudinal Analysis, Wiley-IEEE.

Foden W. B., Butchart S.H.M., Stuart S.N., Vié J-C., Akçakaya H.R., Angulo A., DeVantier L.M., Gutsche A., Turak E., Cao L., Donner S.D., Katariya V., Bernard R., Holland R.A., Hughes A.F., O'Hanlon S.E., Garnett S.T., Şekercioğlu Ç.H. & G.M. Mace (2013) Identifying the world's most climate change vulnerable species: a systematic trait-based assessment of all birds, amphibians and corals. PLoS One 8: e65427.

Food and Agricultural Organization (FAO) of the United Nations (2017a) World abalone production at high levels, yet prices remain steady. Market report (02/01/2017) http://www.fao.org/in-action/globefish/market-reports/resource-detail/en/c/902588

Food and Agricultural Organization (FAO) of the United Nations (2017b) Abalone production continues to grow, coupled with continuing demand, prices high and stable. Market report (03/07/2017) http://www.fao.org/in-action/globefish/market-reports/resource-detail/en/c/902597/

Forster G.R. (1967) The growth of *Haliotis tuberculata*: results of tagging experiments in Guernsey 1963–65. Journal of the Marine Biological Association of the United Kingdom 47(2): 287-300.

Frank P.W. (1975) Latitudinal variation in the life history features of the black turban snail *Tegula funebralis* (Prosobranchia: Trochidae). Marine Biology 31: 181–192.

Frieder C.A., Nam S.H., Martz T.R. & L.A. Levin (2012) High temporal and spatial variability of dissolved oxygen and pH in a nearshore Californian kelp forest. Biogeosciences 9: 3917-3930.

Froehlich H.E., Gentry R.R. & B.S. Halpern (2018) Global change in marine aquaculture production potential under climate change. Nature, Ecology & Evolution 2(11): 1745.

Frost M., Baxter J.M., Buckley P.J., Cox M., Dye S.R. & N.W. Harvey (2012) Impacts of climate change on fish, fisheries and aquaculture. Aquatic Conservation: Marine and Freshwater Ecosystems 22(3): 331–336.

Fu G., Valiyaveettil S., Wopenka B. & D. E. Morse (2005) $CaCO_3$ Biomineralization: Acidic 8-kDa proteins isolated from aragonitic abalone shell nacre can specifically modify calcite crystal morphology. Biomacromolecules 6: 1289-1298.

Galappaththi E.K., Ichien S.T., Hyman A.A., Aubrac C.J. & J.D. Ford (2020) Climate change adaptation in aquaculture. Reviews in aquaculture 12(4): 2160-2176.

Gallardo W.G., Bautista-Teruel M.N., Fermin A.C. & C.L. Marte (2003) Shell marking by artificial feeding of the tropical abalone *Haliotis asinina* Linne juveniles for sea ranching and stock enhancement. Aquaculture Research 34(10): 839-842.

Gao K.S., Ji Y. & Y. Aruga (1999) Relationship of CO_2 concentrations to photosynthesis of intertidal macroalgae during emersion. Hydrobiologia 399: 355–359.

Gajaria T.K., Suthar P., Baghel R.S., Balar N.B., Sharnagat P., Mantri V.A. & C.R.K. Reddy (2017) Integration of protein extraction with a stream of byproducts from marine macroalgae: a model forms the basis for marine bioeconomy. Bioresources and Technologies 243: 867–873.

García-Esquivel Z., Montes-Magallón S. & M.A. González-Gómez (2007) Effect of temperature and photoperiod on the growth, feed consumption, and biochemical content of juvenile green abalone, *Haliotis fulgens*, fed on a balanced diet. Aquaculture 262: 129-141.

Garrett R. & C. Grisham (2010) Biochemistry, Brooks. (4th ed., pp. 511–812). Belmont, CA: Brooks Cole, Cengage Learning.

Gazeau F., Quiblier C., Jansen J.M., Gattuso J.P., Middelburg J.J. & C.H.R. Heip (2007) The impact of elevated CO_2 on shellfish calcification. Geophysical Research Letters 34: LO7603.

Gazeau F., Gattuso J.P., Dawber C., Pronker A.E., Peene F., Peene J., Heip C.H.R. & J.J. Middelburg (2010) Effect of ocean acidification on the early life stages of the blue mussel *Mytilus edulis*. Biogeosciences 7: 2051–2060.

Gazeau F., Parker L.M., Comeau S., Gattuso J-P., O'Connnor W.A., Martin S., Pörtner H-O. & P.M. Ross (2013) Impacts of ocean acidification on marine shelled molluscs. Marine Biology 160(8):2207-2245.

Geiger D.L. (1999) Distribution and biogeography of the recent Haliotidae (Gastropoda: Vetigastropoda) world-wide. Bollettino Malacologico XXXV: 57-120.

Geiger D.L. & B. Owen (2012) Abalone: Worldwide Haliotidae. ConchBooks, Hackenhein, Germany, 361pp.

Genade A.B., Hirst A. L. & C. J. Smit (1988) Observations on the spawning, development and rearing of the South African abalone *Haliotis midae* Linn. South African Journal of Marine Science, 6(1):3-12. DOI: 10.2989/025776188784480465

Giordano M., Beardall J. & Raven J.A. (2005) CO_2 concentrating mechanisms in algae: mechanisms, environmental modulation and evolution. Annual Review of Plant Biology 56: 99–131.

Glasson C.R.K., Sims I.M., Carnachan S.M., de Nys R. & M. Magnusson (2017) A cascading biorefinery process targeting sulfated polysaccharides(ulvan) from *Ulva ohnoi*. Algal Research 27: 383–391.

Gleckler P.J., Santer B., Domingues C., Pierce D., Barnett T., Church J., Taylor K., Achuta R.K., Boyer T., & M. Ishii (2012) Human-induced global ocean warming on multi-decadal timescales. Nature Climate Change 2: 524-529.

Gordon H.R. (2000). World abalone supply, markets and pricing: historical, current and future prospectives. Opening Speech: 4th International Abalone Symposium, Cape Town, South Africa. University of Cape Town, February 6–11 2000.

Goschen W.S., Schumann E.H., Bernard K.S., Bailey S.E. & S.H.P. Deyzel (2012) Upwelling and ocean structures off Algoa Bay and the south-east coast of South Africa. African Journal of Marine Science 34(4): 525-536.

Gradinger R. (2009) Sea-ice algae: Major contributors to primary production and algal biomass in the Chukchiand Beauford seas in May/June 2002. Deep Sea Research II 56: 1201-1212.

Gray B.E. & A.M. Smith (2004) Mineralogical variation in shells of the blackfoot abalone, *Haliotis iris* (Mollusca: Gastropoda: Haliotidae), in southern New Zealand. Pacific Science 58(1):47-64.

Greenwood P.J. & T. Bennett (1981) Some effects of temperature-salinity combinations on the early development of the sea urchin *Parechinus angulosus* (Leske) fertilization. Journal of Experimental Marine Biology and Ecology 51(2-3): 119-131.

Gregg W., Conkright M., Ginoux P., O'Reilly J. & N. Casey (2003) Ocean primary production and decadal trends. Geophysical Research Letters 30(15):2909. DOI:10.1029/2003GL016889.

Griffith A. & C.J. Gobler (2017) Transgenerational exposure of North Atlantic bivalves to ocean acidification renders offspring more vulnerable to low pH and additional stressors. Scientific Reports 7: 11394.

Grubert M.A. & A.J. Ritar (2004) Temperature effects on the dynamics of gonad and oocyte development in captive wild-caught blacklip (*Haliotis rubra*) and greenlip (*Haliotis laevigata*) abalone. Invertebrate Reproduction and Development 45: 185-196.

Guilini K., Weber M., de Beer D., Schneider, M., Molari M., Lott C., Bodnar W., Mascart T., De Troch M. & A. Vanreusel (2017) Response of *Posidonia oceanica* seagrass and its epibiont communities to ocean acidification. PLoS ONE 12: e0181531.

Guo X., Huang M., Pu F., You W. & C. Ke (2015) Effects of ocean acidification caused by rising CO_2 on the early development of three mollusks. Aquatic Biology 3: 147-157.

Hahn K.O. (1988) Artificial induction of spawning and fertilisation. In: Handbook of culture of abalone and other marine gastropods. Boca Raton: CRC Press, pp. 53-70.

Hall-Spencer J.M., Rodolfo-Metalpa R., Martin S., Ransome E., Fine M., Turner S.M., Rowley S.J., Tedesco D. & M-C. Buia (2008) Volcanic carbon dioxide vents show ecosystem effects of ocean acidification. Nature 454: 96–99.

Handisyde N., Telfer T.C. & L.G. Ross (2017) Vulnerability of aquaculture-related livelihoods to changing climate at the global scale. Fish and Fisheries 18(3): 466–488.

Hansen J., Sato M., Ruedy R., Lo K., Lea D.W. & M. Medina-Elizade (2006) Global temperature change. PNAS 103(39):14288-14293.

Hansen, J., Ruedy R., Sato M. & K. Lo (2010) Global surface temperature change. Reviews of Geophysics, 48: RG4004.

Harley C.D.G., Anderson K.M., Demes K.W., Jorve J.P., Kordas R.L., Coyle T.A. & M.H. Graham (2012) Effects of climate change on global seaweed communities. Journal of Phycology 48: 1064–1078.

Hartmann, D.L., A.M.G. Klein Tank, M. Rusticucci, L.V. Alexander, S. Brönnimann, Y. Charabi, F.J. Dentener, E.J. Dlugokencky, D.R. Easterling, A. Kaplan, B.J. Soden, P.W. Thorne, M. Wild and P.M. Zhai, (2013) Observations: Atmosphere and Surface. In: AR5 Climate Change 2013: The Physical Science Basis. Contribution of Working Group I to the Fifth Assessment Report of the Intergovernmental Panel on Climate Change [Stocker, T.F., D. Qin, G.-K. Plattner, M. Tignor, S.K. Allen, J. Boschung, A. Nauels, Y. Xia, V. Bex and P.M. Midgley (eds.)]. Cambridge University Press, Cambridge, United Kingdom and New York, NY, USA.

Harvey B.P., Gwynn-Jones D. & P.J. Moore (2013) Meta-analysis reveals complex marine biological responses to the interactive effects of ocean acidification and warming. Ecology and Evolution 3(4): 1016–1030. doi:10.1002/ece3.516. PMID: 23610641.

Hauck M. & N.A. Sweijd, (1999) A case study of abalone poaching in South Africa and its impact on fisheries management. ICES Journal of Marine Sciences 56: 1024-1032.

Haupt T.M., Novak T., Naylor M. & L. Auerswald (unpublished) The thermal response of adult abalone, *Haliotis midae*, following exposure to chronic hypercapnia. In preparation.

Hauri C., Gruber N., Plattner G., Alin S., Feely R.A., Hales B. & P.A. Wheeler (2009) Ocean acidification in the California Current system. Oceanography 22(4):60-71.

Hawkins S.J. (1981) The influence of Patella grazing on the fucoidan barnacle mosaic on moderately exposed rocky shores. Kieler Meeresforsch 5: 537–544.

Hecht T. (1994) Behavioural thermoregulation of the abalone, *Haliotis midae*, and the implications for intensive culture. Aquaculture 126(1-2): 171-181.

Hendriks I.E., Duarte C.M. & M. Alvarez (2009) Vulnerability of marine biodiversity to ocean acidification: A meta-analysis. Estuarine, Coastal and Shelf Science 86(2): 157-164.

Hendriks I.E., Olsen Y.S., Ramajo L., Basso L., Steckbauer A., Moore T.S., Howard J. & C.M. Duarte (2014) Photosynthetic activity buffers ocean acidification in seagrass meadows. Biogeosciences 11: 333–346.

Hepburn C.D., Pritchard D.W., Cornwall C.E., McLeod R.J., Beardall J., Rave J.A. & C.L. Hurd (2011) Diversity of carbon use strategies in a kelp forest community: implications for a high CO_2 ocean. Global Change Biology 17: 2488–2497.

Heuer R.M. & M. Grosell (2014) Physiological impacts of elevated carbon dioxide and ocean acidification on fish. American Journal of Physiology – Regulatory, Integrative and Comprehensive 307: R1061-R1084.

Hoang T.H., Qin J.G., Stone D.A.J, Harris J.O., Duong D.N. & M.S. Bansemer (2016) Colour changes of greenlip abalone (*Haliotis laevigata* Donovan) fed fresh macroalgae and dried algal supplement. Aquaculture 456: 16-23.

Hoang T.H., Stone D.A.J., Duong D.N., Bansemer M.S., Harris J.O. & J.G. Qin (2017) Colour change of greenlip abalone (*Haliotis laevigata* Donovan) fed formulated diets containing graded levels of dried macroalgae meal. Aquaculture 468(1): 278-285.

Hochachka P. & G. Somero (2002) Biochemical Adaptation: Mechanism and Process in Physiological Evolution. International Union of Biochemistry and Molecular Biology Inc., Oxford University Press, New York, 480 pp.

Hoegh-Guldberg O., Mumby P.J., Hooten A.J., Steneck R.S., Greenfield P., Gomez E., Harvell C.D., Sale P.F., Edwards A.J., Caldeira K., Knowlton N., Eaking C.M., Iglesias-Prieto R., Muthiga N., Bradbury R.H., Dubi A. & M.E. Hatziolos (2007) Coral reefs under rapid climate change and ocean acidification. Science 318, 1737-1742.

Hoegh-Guldberg O. & J.F. Bruno (2010) The impact of climate change on the World's marine ecosystems. Science 328(5985):1523-1528. DOI: 10.1126/science.1189930.

Hoegh-Guldberg, O., Cai R., Poloczanska E.S., Brewer P.G., Sundby S., Hilmi K., Fabry V.J., & S. Jung (2014) The Ocean. In: Climate Change 2014: Impacts, Adaptation, and Vulnerability. Part B: Regional Aspects. Contribution of Working Group II to the Fifth Assessment Report of the Intergovernmental Panel on Climate Change [Barros, V.R., C.B. Field, D.J. Dokken, M.D. Mastrandrea, K.J. Mach, T.E. Bilir, M. Chatterjee, K.L. Ebi, Y.O. Estrada, R.C. Genova, B. Girma, E.S. Kissel, A.N. Levy, S. MacCracken, P.R. Mastrandrea, and L.L. White (eds.)]. Cambridge University Press, Cambridge, United Kingdom and New York, NY, USA, pp. 1655-1731.

Hoffman G.E., Smith J.E., Johnson K.S., Send U., Levin L.A., Micheli F., Paytan A., Price N.N., Peterson B., Takeshita Y., Matson P.G., Crook E.D., Kroeker K.J., Gambi M.C., Rivest E.B., Frieder C.A., Yu P.C. & T.R. Martz (2011) High frequency dynamics of ocean pH: A multi-ecosystem comparison. PLoS ONE 6(12): e28983.

Holbrook G.P., Beer S., Spencer W.E., Reiskind J.B., Davis J.S. & G. Bowes (1988) Photosynthesis in marine macroalgae: evidence for carbon limitation. Canadian Journal of Botany 66: 577–582.

Holdt S.L. & M.D. Edwards (2014) Cost-effective IMTA: a comparison of the production efficiencies of mussels and seaweed. Journal of Applied Phycology 26: 933–945.

Hoque M.E., Shehryar M. & Islam K.N. (2013) Processing and characterization of cockle shell calcium carbonate ($CaCO_3$) bioceramic for potential application in bone tissue engineering. Materials Science & Engineering. 2(4):132.

Hughes S., Yau A., Max L., Petrovic N., Davenport F., Marshall M., McClanahan T.R., Allison E.H. & J.E. Cinner (2012) A framework to assess national level vulnerability from the perspective of food security: The case of coral reef fisheries. Environmental Science & Policy, 23: 95–108.

Hunter C. M., Caswell H., Runge M.C., Regehr E.V., Amstrup S.C. & I. Stirling (2010) Climate change threatens polar bear populations: a stochastic demographic analysis. Ecology 91: 2883–2897.

Hurd C.L., Cornwall C.E., Currie K., Hepburn C.D., Mcgraw C.M., Hunter K.A. & P.W. Boyd (2011). Metabolically induced pH fluctuations by some coastal calcifiers exceed projected 22nd century ocean acidification: A mechanism for differential susceptibility? Global Change Biology 17:3254-3262.

Hurd C.L., Beardall J., Comeau S., Cornwall C.E., Havenhand J.N., Munday P.L., Parker L.M., Raven J.A. & C.M. McGraw (2019) Ocean acidification as a multiple driver: how interactions between changing seawater carbonate parameters affect marine life. Marine and Freshwater Research 71(3): 263-274.

Hurlbert S. H. (1984) Pseudoreplication and the design of ecological field experiments. Ecological Monographs 54: 187-211.

Hutchings, L., van der Lingen C.D., Shannon L.J., M. Crawford R.J., Verheye H.M.S., Bartholomae C.H., van der Plaas A.K., Louw D., Kreiner A., Ostrowski M., Fidel Q., Barlow R.G., Lamont T., Coetzee J., Shillington F., Veitch J., Currie J.C. & P.M.S. Monteiro (2009) The Benguela Current: an ecosystem of four components. Progress in Oceanography, 83(1-4): 15-32.

Jackson D.J., McDougall C., Green K., Simpson F., Wörheide G. & B.M. Degnan (2006) A rapidly evolving secretome builds and patterns a sea shell. BMC Biology 4: 40.

James R. & R. Washington (2013) Changes in African temperature and precipitation associated with degrees of global warming. Climatic Change, 117(4): 859-872.

Jardillier E., Rousseau M., Gendron-Badou A., Fröhlich F., Smith D.C., Martin M., Helléouet M.-N., Huchette S., Doumenc D. & S. Auzoux-Bordenave (2008) A morphological and structural study of the larval shell from the abalone *Haliotis tuberculata*. Marine Biology 154: 735-744.

Johnson V.R., Brownlee C., Rickaby R.E.M., Graziano M., Milazzo M. & J.M. Hall-Spencer (2013) Responses of marine benthic microalgae to elevated CO_2. Marine Biology 160: 1813-1824.

Johnson M.J., Hennigs L.M., Sawall Y., Pansch C. & M. Wall (2020) Growth response of calcifying marine epibionts to biogenic pH fluctuations and global ocean acidification scenarios. Limnology and Oceanography 9999: 1-14.

Johnston A.M., Maberly S.C. & J.A. Raven (1992) The acquisition of inorganic carbon by four red macroalgae. Oecologia 92: 317–326.

Jones P. D., Lister D. H., Osborn T. J., Harpham C., Salmon M. & C. P. Morice (2012) Hemispheric and large-scale land-surface air temperature variations: An extensive revision and an update to 2010. Journal of Geophysical Research: Atmospheres 117: D05127.

Joshi M., Hawkins E., Sutton R., Lowe J. & D. Frame (2011) Projections of when temperature change will exceed 2°C above pre-industrial levels. Nature Climate Change 1(8): 407-412.

Kapsenberg L. & G.E. Hofmann (2016) Ocean pH time-series and drivers of variability along the northern Channel Islands, California, USA. Limnology and Oceanography 61: 953–968.

Kapsenberg L. & T. Cyronak (2019) Ocean acidification refugia in variable environments. Global Change Biology 25(10): 3201-3214.

Karl T.R. & K.E. Trenberth (2003) Modern global climate change. Science 302(5651):1719-1723. DOI: 10.1126/science.1090228

Karvonen A., Rintamäki P., Jokela J. & E.T. Valtonen (2010) Increasing water temperature and disease risks in aquatic systems: Climate change increases the risk of some, but not all, diseases. International Journal for Parasitology 40(13): 1483–1488.

Katti K.S., Mohanty B. & D. R. Katti (2006) Nanomechanical properties of nacre. Journal of Materials Research 21: 1237-1242.

Keeling, C., Bacastow R., Bainbridge A., Ekdahl C., Guenther P., Waterman L. & J. Chin (1976a) Atmospheric Carbon-Dioxide Variations at Mauna-Loa Observatory, Hawaii. Tellus, 28: 538–551.

Keeling, C. D., Adams J.A. & C. A. Ekdahl (1976b) Atmospheric carbon dioxide variations at South Pole. Tellus 28**:** 553–564.

Keller C., Brunner D., S. Henne, Vollmer M., O'Doherty S. & S. Reimann (2011) Evidence for under-reported western European emissions of the potent greenhouse gas HFC-23. Geophysical Research Letters 38: L15808.

Kelly R.P, Cooley S.R. & T. Klinger (2014) Narratives Can Motivate Environmental Action: The Whiskey Creek Ocean Acidification Story. Ambio 43(5): 592-599.

Kennedy J.J., Rayner N.A., Smith R.O., Parker D.E. & M. Saunby (2011) Reassessing biases and other uncertainties in sea surface temperature observations measured in situ since 1850: 2. Biases and homogenization. Journal of Geophysical Research: Atmospheres 116: D14104.

Kerrison P., Suggett D.J., Hepburn L.J. & M. Steinke (2012) Effect of elevated pCO_2 on the production of dimethylsulphoniopropionate (DMSP) and dimethylsulphide (DMS) in two species of *Ulva* (Chlorophyceae). Biogeochemistry 110: 5-16.

Kidgell J.T., Magnusson M., de Nys R. & C.R.K. Glasson (2019) Ulvan: A systematic review of extraction, composition and function. Algal Research 39: 101422.

Kim T.W., Barry J.P. & F. Micheli (2013) The effects of intermittent exposure to low-pH and low-oxygen conditions on survival and growth of juvenile red abalone. Biogeosciences 10: 7255-7262.

Kimura R., Takami H., Ono T., Onitsuka T. & Y. Nojiri (2011) Effects of elevated pCO_2 on the early development of the commercially important gastropod, Ezo abalone *Haliotis discus hannai*. Fisheries Oceanography 20**:** 357–366.

Kleypas, J.A., Buddemeier R.W., Archer D., Gattuso J.P., Langdon C. & B.N. Opdyke (1999) Geochemical consequences of increased atmospheric carbon dioxide on coral reefs. Science 284: 118–120.

Knapp J.L., Bridges C.R., Krohn J., Hoffman L.C. & L. Auerswald (2015) Acid–base balance and changes in haemolymph properties of the South African rock lobsters, *Jasus lalandii*, a palinurid decapod, during chronic hypercapnia. Biochemical and Biophysical Research Communications 461(3): 475-480.

Kocot K.M., Aguilera F., McDougall C., Jackson D.J. & B.M. Degnan (2016) Sea shell diversity and rapidly evolving secretomes: insights into the evolution of biomineralization. Frontiers in Zoology 13: 23-27

Koweek D.A., Zimmerman R.C., Hewett K.M., Gaylord B., Giddings S.N., Nickols K.J., Ruesink J.L., Stachowicz J.J., Takeshita Y. & K. Caldeira (2018) Expected limits on the ocean acidification buffering potential of a temperate seagrass meadow. Ecological Applications 28(7): 1694-1714.

Krause-Jensen D. & C.M. Duarte (2016) Substantial role of macroalgae in marine carbon sequestration. Nature Geoscience 9: 737-742.

Kroeker K.J., Kordas R.L., Crim R. & G.S. Singh (2010) Meta-analysis reveals negative yet variable effects of ocean acidification on marine organisms. Ecology Letters 13:1419-1434.

Kroeker K.J., Kordas R.L., Crim R., Hendriks I.E., Ramajo L., Duarte C.M. & J-P. Gattuso (2013) Impacts of ocean acidification on marine organisms: quantifying sensitivities and interactions with warming. Global Change Biology 19(6): 1884-1896.

Kroeker K.J., Sanford E., Jellison B.M. & B. Gaylord (2014) Predicting the effects of ocean acidification on predator-prey interactions: a conceptual framework based on coastal molluscs. The Biological Bulletin 226: 211–222.

Kübler J.E., Johnston A.M. & J.A. Raven (1999) The effects of reduced and elevated CO_2 and O_2 on the seaweed *Lomentaria articulata*. Plant Cell and Environment 22: 1303–1310.

Kurihara H. & Y. Shirayama (2004) Effects of increased atmospheric CO_2 on sea urchin early development. Marine Ecology Progress Series 274: 161–169.

Kurihara H., Kato S. & A. Ishimatsu (2007) Effects of increased seawater pCO_2 on early development of the oyster *Crassostrea gigas*. Aquaculture Biology 1: 91–98.

Laramore S., Baptiste R., Wills P.S. & M.D. Hanisak (2018) Utilization of IMTA-produced *Ulva lactuca* to supplement or partially replace pelleted diets in shrimp (*Litopenaeus vannamei*) reared in a clear water production system. Journal of Applied Phycology 30: 3606-3610.

Lawrimore J. H., Menne M. J., Gleason B. E., Williams C. N., Wuertz D. B., Vose R. S. & J. Rennie (2011) An overview of the Global Historical Climatology Network monthly mean temperature data set, version 3. Journal of Geophysical Research: Atmospheres, 116: D19121.

Leduc G., Herbert C.T., Blanz T., Martinez P. & R. Schneider (2010) Contrasting evolution of sea surface temperature in the Benguela upwelling system under natural and anthropogenic climate forcings. Geophysical Research Letters, 37(20): L20705, doi:10.1029/2010GL044353.

Lee S. (2004) Utilization of dietary protein, lipid, and carbohydrate by abalone *Haliotis discus hannai*: A review. Journal of Shellfisheries Research 23: 1027-1030.

Lee W.K., Lim Y-Y. & C-L. Ho (2019) pH affects growth, physiology and agar properties of agarophyte *Gracilaria changii* (Rhodophyta) under low light intensity from Morib, Malaysia. Regional Studies in Marine Science 30: 100738.

Legrand E., Riera P., Bohner O., Coudret J., Schlicklin F., Derrien M. & S. Martin (2018) Impact of ocean acidification and warming on the productivity of a rock pool community. Marine Environmental Research 136: 78-88.

Leighton D.L., Byhower M.J., Kelly J.C., Hooker G.N. & D.E. Morse (1981) Acceleration of development and growth in young green abalone (*Haliotis fulgens*) using warm effluent seawater. Journal of the World Aquaculture Society 12(1): 170-180.

Lenth R. (2018). *emmeans*: Estimated Marginal Means, aka Least-Squares Means. R package version 1.1. https://CRAN.R-project.org/package=emmeans.

Lester N. (2012) Ocean acidification from an aquacultural and ecological perspective: threats facing South African abalone, *Haliotis midae*, and the Cape sea urchin, *Parechinus angulosus*. Unpublished BSc (Honour's) dissertation. University of Cape Town, South Africa.

Leung J.Y. S., Connell S.D., Nagelkerken I. & B.D. Russell (2017) Impacts of Near-Future Ocean Acidification and Warming on the Shell Mechanical and Geochemical Properties of Gastropods from Intertidal to Subtidal Zones. Environmental Science and Technology 51(21): 12097–12103.

Le Quéré C., Peters G.P., Andres R.J., Andrew R.M., Boden T.A., Ciais P., Friedlingstein P., Houghton R.A., Marland G., Moriarty R., Sitch S.,Tans P., Arneth A., Arvanitis A., Bakker D.C.E., Bopp L., Canadell J.G., Chini L.P., Doney S.C., Harper A., Harris I., House J.I., Jain A.K., Jones S.D., Kato E., Keeling R.F., Klein Goldewijk I., Körtzinger A.,Koven C., Lefèvre N., Maignan F., Omar A., Ono T., Park G.-H., Pfeil B., Poulter B., Raupach M.R., Regnier P., Rödenbeck C., Saito S., Schwinger J., Segschneider J., Stocker B.D., Takahashi T., Tilbrook B., van Heuven S., Viovy N., Wanninkhof R., Wiltshire A. & S. Zaehle (2014) Global carbon budget 2013, Earth System Science Data 6(1):235–263. DOI:10.5194/essd-6-235-2014.

Li J., Mao Y., Jiang Z., Zhang J., Fang J. & D. Bian (2018) The detrimental effects of CO_2-driven chronic acidification on juvenile Pacific abalone (*Haliotis discus hannai*). Hydrobiologia 809:297–308.

Lima F.P., Ribeiro P.A., Queiroz N., Hawkins S.J. & A.M. Santos (2007) Do distributional shifts of northern and southern species of algae match the warming pattern? Global Change Biology 13: 2592–2604.

Linnaeus C. (1758) Systema Naturae per regna tria naturae, secundum classes, ordines, genera, species, cum characteribus, differentiis, synonymis, locis. *Editio decima, reformata. Laurentius Salvius: Holmiae.* ii, 824 pp.

Lischka S., Büdenbender J., Boxhammer T. & U. Riebesell (2011) Impact of ocean acidification and elevated temperatures on early juveniles of the polar shelled pteropod *Limacina helicina*: mortality, shell degradation, and shell growth. Biogeosciences 8:919-932.

Litaay M. & S.S. De Silva (2003) Spawning season, fecundity and proximate composition of the gonads of wild-caught blacklip abalone (*Haliotis rubra*) from Port Fairy waters, south eastern Australia. Aquatic Living Resources 16: 353-361.

López-Urrutia A., San Martin E., Harris R. P. & X. Irigoien (2006) Scaling the metabolic balance of the oceans. Proceedings of the National Academy of Science of the United States of America 103:8739-8744.

Lopičić Z.R., Stojanović M.D., Marković S.B., Milojković J.V., Mihajlović M.L., Radoičić T.S.K. & M.L. Kijevčanin (2019) Effects of different mechanical treatments on structural changes of lignocellulosic waste biomass and subsequent Cu (II) removal kinetics. Arabian Journal of Chemistry 12(8): 4091-4103.

Lord J., Barry J.P. & D. Graves (2017) Impact of climate change on direct and indirect species interactions. Marine Ecology Progress Series 571: 1–11.

Lowenstam H.A. (1954) Factors affecting the aragonite: calcite ratios in carbonate-secreting marine organisms. The Journal of Geology 62(3): 284-32.

Lowenstam H.A. & S Wiener (1983) Mineralization by organisms and the evolution of biomineralisation. Biomineralization and Biological Metal Accumulation 191-203.

Lowenstam H.A. & S Wiener (1989) Chapter 6: Mollusca. *In*: On Biomineralization. Oxford University Press, New York, USA. 336 pp.

Lyon R.G. (1996) Aspects of the physiology of the South African abalone, *Haliotis midae* L., and implications for intensive abalone culture. M.Sc. Thesis, Rhodes University, Grahamstown, 85 pp.

MacDonald B.A., Robinson S.M.C. & K.A. Barrington (2011) Feeding activity of mussels (*Mytilus edulis*) held in the field at an integrated multi-trophic aquaculture (IMTA) site (Salmo salar) and exposed to fish food in the laboratory. Aquaculture 314(1-4): 244-251.

Mackenzie C.L., Ormondroyd G.A., Curling S.F., Ball R.J., Whiteley N.M., Malham S.K. (2014) Ocean warming, more than acidification, reduces shell strength in a commercial shellfish species during food limitation. PLoS ONE 9(1): e86764. https://doi.org/10.1371/journal.pone.0086764.

Mackey K., Morris J., Morel F. & S. Kranz (2015) Response of Photosynthesis to Ocean Acidification. Oceanography, 28(2), 74-91.

Magnusson M., Carl C., Mata L., de Nys R. & N.A. Paul (2016) Seaweed salt from *Ulva*: a novel first step in a cascading biorefinery model. Algal Research 16:308–316.

Magnusson M., Glasson C.R.K., Vucko M.J., Angell A.,Neoh T.L. & R. de Nys (2019) Enrichment processes for the production of high-protein feed from the green seaweed *Ulva ohnoi*. Algal Research 41: 101555.

Manzello D.P., Kleypas J.A., Budd D.A., Eakin C.M., Glynn P.W. & C. Langdon (2008) Poorly cemented coral reefs of the eastern tropical Pacific: possible insights into reef development in a high-CO_2 world. Proceedings of the National Academy of Sciences of the United States of America 105(30): 10450-10455.

Manzello D.P., Enochs I.C., Melo N., Gledhill D.K. & E.M. Johns (2012) Ocean acidification refugia of the Florida Reef Tract. PLoS ONE 7: e41715.

Marchais V., Jolivet A., Hervé S., Roussel S., Schöne B.R., Grall J., Chauvaud L. & J. Clavier (2017) New tool to elucidate the diet of the former *Haliotis tuberculata* (L.): Digital shell color analysis. Marine Biology 164: 71.

Marie B., Marie A., Jackson D.J., Dubost L., Degnan B.M., Milet C. & F. Marin (2010) Proteomic analysis of the organic matrix of the abalone *Haliotis asinina* calcified shell. Proteome Science 8(54). https://doi.org/10.1186/1477-5956-8-54

Marinho G., Nunes C., Sousa-Pinto I., Pereira R., Rema P. & L.M.P. Valente (2013) The IMTA-cultivated Chlorophyta *Ulva* spp. as a sustainable ingredient in Nile tilapia (*Oreochromis niloticus*) diets. Journal of Applied Phycology 25: 1359–1367.

Mariotti L., Coppola E., Sylla M.B., Giorgi F. & C. Piani (2011) Regional climate model simulation of projected 21st century climate change over an all-Africa domain: comparison analysis of nested and driving model results. Journal of Geophysical Research D: Atmospheres, 116(D15): D15111, doi:10.1029/2010JD015068.

Martínez B., Viejo R.M., Carreño F. & S.C. Aranda (2012) Habitat distribution models for intertidal seaweeds: responses to climatic and non-climatic drivers. Journal of Biogeography 39: 1877–1890.

Marubini F., Ferrier-Pages C. & J.P. Cuif (2003). Suppression of skeletal growth in scleractinian corals by decreasing ambient carbonate-ion concentration: a cross-family comparison. Proceedings of the Royal Society of London B 270: 179–184.

Masson-Delmotte V., Schulz M., Abe-Ouchi A., Beer J., Ganopolski A., González Rouco J.F., Jansen E., Lambeck K., Luterbacher J., Naish T., Osborn T., Otto-Bliesner B., Quinn T., Ramesh R., Rojas M., Shao X.

& A. Timmermann (2013) Information from Paleoclimate Archives. In: Climate Change 2013: The Physical Science Basis. Contribution of Working Group I to the Fifth Assessment Report of the Intergovernmental Panel on Climate Change [Stocker, T.F., D. Qin, G.-K. Plattner, M. Tignor, S.K. Allen, J. Boschung, A. Nauels, Y. Xia, V. Bex and P.M. Midgley (eds.)]. Cambridge University Press, Cambridge, United Kingdom and New York, NY, USA.

Matthews I & P.A. Cook (1995) Diatom diet of abalone post-larvae (*Haliotis midae*) and the effect of pre-grazing the diatom overstorey. Marine and Freshwater Research 46(3): 545-548.

Mayfield S. & G.M. Branch (2000) Interrelations among rock lobsters, sea urchins, and juvenile abalone: implications for community management. Canadian Journal of Fisheries and Aquatic Sciences 57(11):2175-2185.

McElhany P. (2017) CO_2 sensitivity experiments are not sufficient to show an effect of ocean acidification. ICES Journal of Marine Science 74(4): 926–928.

McInerney F. A. & S. L.Wing (2011). The Paleocene-Eocene thermal maximum: A perturbation of carbon cycle, climate, and biosphere with implications for the future. Annual Review of Earth and Planetary Sciences 39(1): 489–516.

Meehl G.A., Stocker T.F., Collins W.D., Friedlingstein P., Gaye J.M., Gregory A.T., Kitoh A., Knutti R., Murphy J.M., Noda A., Raper S.C.B., Watterson I.G., Weaver A.J. & Z.-C. Zhao (2007) Global Climate Projections. In: Climate Change 2007: The Physical Science Basis. Contribution of Working Group I to the Fourth Assessment Report of the Intergovernmental Panel on Climate Change [Solomon, S., D. Qin, M. Manning, Z. Chen, M. Marquis, K.B. Averyt, M. Tignor and H.L. Miller (eds.)]. Cambridge University Press, Cambridge, United Kingdom and New York, NY, USA.

Melatunan S., Calosi P., Rundle S.D., Widdicombe S. & A.J. Moody (2013) Effects of ocean acidification and elevated temperature on shell plasticity and its energetic basis in an intertidal gastropod. Marine Ecology Progress Series 472: 155-168.

Menig R., Meyers M.H., Meyers M.A. & K.S. Vecchio (2000) Quasi-static and dynamic mechanical response of *Haliotis rufescens* (abalone) shells. Acta Materialia 48(9): 2383-2398.

Meyer D., Dimitriadou E., Hornik K., Weingessel A. & F. Leisch (2020). *e1071:* Misc functions of the department of statistics. Probability Theory Group (Formerly: E1071), TU Wien. R package version 1.7-4. https://CRAN.R-project.org/package=e1071

Meyers M.A., Lin A.Y-M., Chen P-Y. & J. Muyco (2008) Mechanical strength of abalone nacre: Role of the soft organic layer. Journal of the Mechanical Behaviour of Biomedical Materials 1(1): 76-85.

Mhatre A., Gore S., Mhatre A., Trivedi N., Sharma M., Pandit R., Anil A. & A. Lali (2018) Effect of multiple product extractions on bio-methane potential of marine macrophytic green alga *Ulva lactuca*. Renewable Energy 132: 742–751.

Michaelidis B., Ouzounis C., Paleras A. & H.O. Pörtner (2005). Effects of long-term moderate hypercapnia on acid–base balance and growth rate in marine mussels *Mytilus galloprovincialis*. Marine Ecology Progress Series 293: 109–118.

Mikaloff-Fletcher S.E., Gruber N. Jacobson A.R.J., Doney S.C., Dutkiewitcz S., Gerber M., Follows M., Joos F., Lindsay K., Menemenlis D., Mouchet A., Müller S.A. & J.L.Sarmiento (2006) Inverse estimates of anthropogenic CO_2 uptake, transport, and storage by the ocean. Global Biogeochemical Cycles 20: GB2002. DOI:10.1029/2005GB002530.

Miller A.W., Reynolds A.C., Sobrino C. & G.F. Riedel (2009) Shellfish face uncertain future in high CO_2 world: Influence of acidification on oyster larvae calcification and growth in estuaries. PLoS One 4. e5661.

Mohring M.B., Wernberg T., Kendrick G.A. & M.J. Rule (2013) Reproductive synchrony in a habitat-forming kelp and its relationship with environmental conditions. Marine Biology 160: 119–126.

Moore S. E. & H. P. Huntington (2008) Arctic marine mammals and climate change: Impacts and resilience. Ecological Applications 18(2):S157-165.

Morash A.J. & K. Alter (2015) Effects of environmental and farm stress on abalone physiology: perspectives for abalone aquaculture in the face of global climate change. Reviews in Aquaculture 7: 1-27.

Muller S. (1986) Taxonomy of the genus *Haliotis* in South Africa. Transactions of the Royal Society of South Africa 46: 69–77.

Munday P.L., Dixson D.L., Donelson J.M., Jones G.P., Pratchett M.S., Devitsina G.V. & K.B. Døving (2009) Ocean acidification impairs olfactory discrimination and homing ability of a marine fish. Proceedings of the national Academy of Sciences of the Unites States of America 106(6): 1848-1852.

Murie K.A. & P.E. Bourdeau (2020) Fragmented kelp forest canopies retain their ability to alter local seawater chemistry. Scientific Reports 10: 11939.

Naidoo K., Maneveldt G., Ruck K. & J.J. Bolton (2006) A comparison of various seaweed-based diets and formulated feed on growth rate of abalone in a land-based aquaculture system. Journal of Applied Phycology 18: 437–443.

Narita D., Rehdanz K. & R.S.J. Tol (2012) Economic costs of ocean acidification: a look into the impacts on global shellfish production. Climatic Change 113: 1049-1063.

Naylor M.A., Kaiser H. & C.L.W. Jones (2011) Water quality in a serial-use raceway and its effect on the growth of South African abalone, *Haliotis midae* Linneaeus, 1785. Aquaculture research 42: 918-930.

Neori A., Msuya F.E., Shauli L., Schuenhoff A., Kopel F. & M. Shpigel (2003) A novel three-stage seaweed (*Ulva lactuca*) biofilter design for integrated mariculture. Journal of Applied Phycology 15: 543–553.

Neveux N., Bolton J.J., Bruhn A., Roberts D.A. & M. Ras (2018) The bioremediation potential of seaweeds: recycling nitrogen, phosphorus, and other waste products. Blue Biotechnology: Production and Use of Marine Molecules 217–41.

Newman G.G. (1964) Abalone (perlemoen) research and its application to an industry. Commercial Industries 23: 76-78.

Newman G.G. (1967) Reproduction of the South African abalone *Haliotis midae*. Investigational Report for the Division of Sea Fisheries, South Africa 64: 24 pp.

Newman G.G. (1968) Growth of the South African abalone, *Haliotis midae*. Investigational Report for the Division of Sea Fisheries, South Africa 67: 24 pp.

Newman G.G. (1969) Distribution of the abalone (*Haliotis midae*) and the effect of temperature on productivity. Investigational Report of the Division of Sea Fisheries, South Africa 74: 1-7.

Niang I., Ruppel O.C., Abdrabo M.A., Essel A., Lennard C., Padgham J. & P. Urquhart (2014) Africa. In: Climate Change 2014: Impacts, Adaptation, and Vulnerability. Part B: Regional Aspects. Contribution of Working Group II to the Fifth Assessment Report of the Intergovernmental Panel on Climate Change [Barros, V.R., C.B. Field, D.J. Dokken, M.D. Mastrandrea, K.J. Mach, T.E. Bilir, M. Chatterjee, K.L. Ebi, Y.O. Estrada, R.C. Genova, B. Girma, E.S. Kissel, A.N. Levy, S. MacCracken, P.R. Mastrandrea, and L.L. White (eds.)]. Cambridge University Press, Cambridge, United Kingdom and New York, NY, USA, pp. 1199-1265.

NOAA (Accessed on 10 January 2021) Global Monitoring Laboratory, Earth system research laboratories. Available at: https://www.esrl.noaa.gov/gmd/ccgg/trends/

Nobre A.M., Robertson-Andersson D., Neori A. & K. Sankar (2010) Ecological–economic assessment of aquaculture options: Comparison between abalone monoculture and integrated multi-trophic aquaculture of abalone and seaweeds. Aquaculture 306: 116-126.

Noisette F. & C. Hurd (2018). Abiotic and biotic interactions in the diffusive boundary layer of kelp blades create a potential refuge from ocean acidification. Functional Ecology 32: 1329–1342.

Novak T. (2012) Einfluss der ozeanversauerung auf die Südafrikanische abalone, *Haliotis midae*. MSc thesis, Heinrich-Heine-Universität Düsseldorf, Germany.

O'Connor M. I., Bruno J.F., Gaines S.D., Halpern B.S., Lester S.E., Kinlan B.P. & J.M. Weiss(2007) Temperature control of larval dispersal and the implications for marine ecology, evolution, and conservation. Proceeding of the National Academy of Science of the United States of America 104:1266-1271.

O'Donnell M.J., George M.N. & E. Carrington (2013). Mussel byssus attachment weakened by ocean acidification. Nature Climate Change 3(6): 587–590.

Olischläger M., Bartsch I., Gutow L. & C. Wiencke (2013) Effects of ocean acidification on growth and physiology of *Ulva lactuca* (Chlorophyta) in a rockpool-scenario. Phycological Research 61: 180–190.

Onitsuka T., Takami H., Muraoka D., Matsumoto Y., Nakatsubo A., Kimura R., Ono T. & Y. Nojiri (2018) Effects of ocean acidification with pCO_2 diurnal fluctuations on survival and larval shell formation of Ezo abalone, *Haliotis discus hannai*. Marine Environmental Research 134: 28-36.

Orlowsky B. & S.I. Seneviratne (2012) Global changes in extreme events: regional and seasonal dimension. Climatic Change, 110(3-4): 669-696.

Orr J.C., Fabry V.J., Aumont O., Bopp L., Doney S.C., Feely R.A., Gnanadesikan A., Gruber N., Ishida A, Joos F., Key R.M., Lindsay K., Maier-Reimer A., Matear R., Monfray P., Mouchet A., Najjar R.G., Plattner G-K., Rodgers K.B., Sabine C.L., Sarmiento J.L., Schlitzer R., Slater R.D., Totterdell I.J., Weirig M-F., Yamanaka Y. & A. Yool (2005). Anthropogenic ocean acidification over the twenty-first century and its impact on calcifying organisms. Nature 437: 681–686.

Osman M.E.H., Abo-Shady A.M., Elshobary M.E., El-Ghafar M.O.A. & F. Abomohra (2020) Screening of seaweeds for sustainable biofuel recovery through sequential biodiesel and bioethanol production. Environmental Science and Pollution Research 27: 32481–32493.

Pacifici M., Foden W.B., Visconti P., Watson J.E.M., Butchart S.H.M., Kovacs K.M., Scheffers B.R., Hole D.G., Martin T.G., Akçakaya H.R., Corlett R.T., Huntley B., Bickfort D., Carr J.A., Hoffman A.A., Midgley G.F., Pearce-Kelly P., Pearson R.G., Williams S.E., Willis S.G., Young B. & C. Rondinini (2015) Assessing species vulnerability to climate change. Nature Climate Change 5:215-224.

Palacios S.L. & R.C. Zimmerman (2007) Response of eelgrass *Zostera marina* to CO_2 enrichment: possible impacts of climate change and potential for remediation of coastal habitats. Marine Ecology Progress Series 344: 1–13.

Pandolfi J.M., Connolly S.R., Marshall D.J. & A. Cohen (2011) Projecting coral reef futures under global warming and ocean acidification. Science 333(6041):418-422. DOI: 10.1126/science.1204794

Parliamentary Monitoring Group (2020) Commercial Fishing organisations: Fish SA; WWF & AquaCulture. Meeting Report: 16 July 2020. Available at: https://pmg.org.za/committee-meeting/30478/#:~:text=Abalone%20was%20the%20most%20valuable,which%20were%20worth%20R1%20billion.

Petit J.R., Jouzel J., Raynaud D., Barkov N.I., Barnola J.-M., Basile I., Bender M., Chappellaz J., Davis M., Delaygue G., Delmotte M., Kotlyakov V.M., Legrand M., Lipenkov V.Y., Lorius C., Épin L.P., Ritz C., Satlzman E. & M. Stievenard (1999) Climate and Atmospheric history of the past 420,000 years from the Vostok ice core, Antarctica. Nature 399:429-436.

Pezoa-Conte R., Leyton A., Anugwom I., Von Schoultz S., Paranko J.,Mäki-Arvela P., Willför S., Muszyński M., Nowicki J., Lienqueo M.E. & J.P. Mikkola (2015) Deconstruction of the green alga *Ulva rigida* in ionic liquids: closing the mass balance. Algal Research 12: 262–273.

Pfister C.A., Esbaugh A.J., Frieder C.A., Baumann H., Bockmon E.E., White M.M., Carter B.R., Benway H.M., Blanchette C.A., Carrington E., McClintock J.B., McCorkle D.C., McGillis W.R., Mooney T.A. & P.

Ziveri (2014) Detecting the unexpected: a research framework for ocean acidification. Environmental Science and Technology 48: 9982–9994. doi:10.1021/es501936p.

Pierce D.W., Gleckler P.J., Barnett T.P., Santer B.D. & P.J. Durack (2012) The fingerprint of human-induced changes in the ocean's salinity and temperature fields. Geophysical Research Letters 39(21): L21704, doi:10.1029/2012GL053389.

Pinheiro J., Bates D., DebRoy S., Sarkar D. & R Core Team (2016). _nlme: Linear and Nonlinear Mixed Effects Models_. R package version 3.1-125, <URL: http://CRAN.R-project.org/package=nlme>.

Pitcher G.C. & T.A.Probyn (2010) Red tides and anoxia: an example from the southern Benguela current system. In: P. Pagou, G. Hallegraeff (Eds.) Fourth International Conference on Harmful Algae and Intergovernmental Oceanographic Commission of UNESCO, pp. 198-201.

Plagányi É.E. & D.S. Butterworth (2010) A spatial-and age-structured assessment model to estimate the impact of illegal fishing and ecosystem change on the South African abalone *Haliotis midae* resource. African Journal of Marine Science 32: 207-236.

Plagányi É.E., Butterworth D.S. & M. Burgener (2011) Illegal and unreported fishing on abalone—Quantifying the extent using a fully integrated assessment model. Fisheries Research 107(1-3): 221-232.

Polikovsky M., Califano G., Dunger N., Wichard T. & A. Golberg (2020) Engineering bacteria-seaweed symbioses for modulating the photosynthate content of *Ulva* (Chlorophyta): Significant for the feedstock of bioethanol production. Algal Research 49: 101945.

Poloczanska E.S., Brown C.J., Sydeman W.J., Kiessling W., Schoeman D.S., Moore P.J., Brander K., Bruno J.F., Buckley L.B., Burrows M.T., Duarte C.M., Halpern B.S., Holding J., Kappel C.V., O'Connor M.I., Pandolfi J.M., Parmesan C., Schwing F., Thompson S.A. & A.J. Richardson (2013) Global impact of climate change on marine life. Nature Climate Change 3:919-925.

Polovina J., Howell E. & M. Abecassis (2008) Oceans least productive waters are expanding. Geophysical Research Letters 35: L03618.

Polovina J.J., Dunne J.P., Woodworth P.A. & E.A. Howell (2011) Projected expansion of the subtropical biome and contraction of the temperate and equatorial upwelling biomes in the North Pacific under global warming. ICES Journal of Marine Science 68(6):986-995.

Pörtner H.O., Langenbuch M. & A. Reipschlager (2004). Biological impact of elevated ocean CO_2 concentrations: lessons from animal physiology and earth history. Journal of Oceanography 60: 705–718.

Pörtner H.O. & A.P. Farrell (2008) Physiology and climate change. Science 322(5902): 690-692.

Postma P.R., Cerezo-Chinarro O., Akkerman R.J., Olivieri G., Wijffels R.H., Brandenburg W.A. & M.H.M. Eppink (2018) Biorefinery of the macroalgae *Ulva lactuca*: extraction of proteins and carbohydrates by mild disintegration. Journal of Applied Phycology 30:1281–1293.

Prabhu M.S., Israel A., Palatnik R.R., Zilberman D. & A. Golberg (2020) Integrated biorefinery process for sustainable fractionation of *Ulva ohnoi* (Chlorophyta): process optimization and revenue analysis. Journal of Applied Biology 32: 2271–2282.

Przeslawski R., Byrne M. & C. Mellin (2015) A review and meta-analysis of the effects of multiple abiotic stressors on marine embryos and larvae. Global Change Biology 21(6): 2122–2140. doi:10.1111/gcb.12833.

Proudfoot L., Kaehler S. & C.D. McQuaid (2008) Using growth band autoflourescence to investigate large-scale variation in growth of the abalone *Haliotis midae*. Marine Biology 153(5): 789-796.

Qi Z.H., Liu H.M., Li B., Mao Y.Z., Jiang Z.J., Zhang J.H. & J.G. Fang (2010) Suitability of two seaweeds, *Gracilaria lemaneiformis* and *Sargassum pallidum*, as feed for the abalone *Haliotis discus hannai* Ino. Aquaculture 300: 189–193.

R Core Team (2016). R: A language and environment for statistical computing. R Foundation for Statistical Computing, Vienna, Austria. URL https://www.R-project.org/.

Raemaekers S. J.-P. N. & P. Britz (2009) Profile of the illegal abalone fishery (Haliotis midae) in the Eastern Cape Province, South Africa: Organised pillage and management failure. Fisheries Research 97: 183–195.

Raemaekers S., Hauck M., Bürgener M., Mackenzie A., Maharaj G., Plegányi E.E. & P.J. Britz (2011) Review of the causes of the rise of the illegal abalone fishery and consequent closure of the rights-based fishery. Ocean and Coastal Management 54:433-445.

Rautenberger R., Fernandez P.A., Strittmatter M., Heesch S., Cornwall C.E., Hurd C.L. & M.Y. Roleda (2015) Saturating light and not increased carbon dioxide under ocean acidification drives photosynthesis and growth in *Ulva rigida* (Chlorophyta). Ecology and Evolution 5(4): 874-888.

Raven, J., Caldeira K., Elderfield H., Hoegh-Guldberg O., Liss P., Riebesell U., Shepherd J., Turley C. & A. Watson (2005) Ocean acidification due to increasing atmospheric carbon dioxide. The Royal Society, The Clyvedon Press Ltd, Cardiff, UK , 59 pp.

Rayner N. A., Brohan P., Parker D.E., Folland C.K., Kennedy J.J., Vanicek M., Ansell T.J. & S.F.B. Tett (2006) Improved analyses of changes and uncertainties in sea surface temperature measured in situ since the mid-nineteenth century: The HadSST2 dataset. Journal of Climatology 19:446–469.

Réaumur R. A. (1716) Eclaircissemens de quelques difficultés sur la formation et l'accroissement des coquilles. Histoire de l'Académie Royale des Sciences Avec les Mémoires de Mathematique et Physique 384–394.

Reddy-Lopata K., Auerswald L. & Cook P.A. (2006) Ammonia toxicity and its effect on the growth of the South African abalone *Haliotis midae* Linnaeus. Aquaculture 261(2):678-687. doi: 10.1016/j.aquaculture.2006.06.020.

Rhein, M., Rintoul S.R., Aoki S., Campos E., Chambers D., Feely R.A., Gulev S., Johnson G.C., Josey S.A., Kostianoy A., Mauritzen C., Roemmich D.,. Talley L.D & F. Wang (2013) Observations: Ocean. In: Climate Change 2013: The Physical Science Basis. Contribution of Working Group I to the Fifth Assessment Report of the Intergovernmental Panel on Climate Change [Stocker, T.F., D. Qin, G.-K. Plattner, M. Tignor, S.K. Allen, J. Boschung, A. Nauels, Y. Xia, V. Bex and P.M. Midgley (eds.)]. Cambridge University Press, Cambridge, United Kingdom and New York, NY, USA.

Rhode C., Bester-van der Merwe A.E. & R. Roodt-Wilding (2017) An assessment of spatio-temporal genetic variation in the South African abalone (*Haliotis midae*), using SNPs: implications for conservation management. Conservation Genetics 18:17–31.

Richter, I., Behera S.K., Masumoto Y., Taguchi B., Komori N. & T. Yamagata (2010) On the triggering of Benguela Niños: remote equatorial versus local influences. Geophysical Research Letters, 37(20), L20604, doi:10.1029/2010GL044461.

Riebesell U., Zondervan I., Rost B., Tortell P.D., Zeebe R.E. & F.M.M. Morel (2000). Reduced calcification of marine plankton in response to increased atmospheric CO_2. Nature 407: 364–367.

Riebesell U., Körtzinger A. & A. Oschlies (2009) Sensitivities of marine carbon fluxes to ocean change. Proceedings of the National Academy of Sciences of the United States of America 106(49): 20602-20609.

Riebesell U. & J.P. Gattuso (2015) Lessons learned from ocean acidification research. Nature Climate Change 5: 12–14.

Ries J.B., Cohen A.L. & D.C. McCorkle (2009) Marine calcifiers exhibit mixed responses to CO_2-induced ocean acidification. Geology 37(12): 1131-1134.

Robertson-Andersson D.V. (2003) The cultivation of *Ulva lactuca* (Chlorophyta) in an integrated aquaculture system, for the production of abalone feed and the bioremediation of aquaculture effluent. Master's thesis. University of Cape Town, Cape Town.

Robertson-Andersson D.V. (2006) Biological and economical feasibility studies of using seaweeds *Ulva lactuca* (Chlorophyta) in recirculation systems in abalone farming. PhD Thesis, University of Cape Town, Cape Town.

Robertson-Andersson D.V., Potgieter M., Hansen J., Bolton J.J., Troell M., Anderson R.J., Halling C. & T. Probyn (2008) Integrated seaweed cultivation on an abalone farm in South Africa. Journal of Applied Phycology 20: 579–595.

Robertson-Andersson D.V., Maneveldt G.W. & K. Naidoo (2011) Effects of wild and farm-grown macroalgae on the growth of juvenile South African abalone *Haliotis midae* Linnaeus. African Journal of Aquatic Science 36(3): 331–337.

Rodolfo-Metalpa R., Martin S., Ferrier-Pages C. & J. P Gattuso (2010) Response of Mediterranean corals to ocean acidification. Biogeosciences Discussions 6: 7103–7131.

Rogers-Bennett L., Dondanville R.F., Moore J.D. & I. Vilchis (2010) Response of red abalone reproduction to warm water, starvation and disease stressors: Implications of ocean warming. Journal of Shellfish Research 29(3): 599-611.

Rohde R., Nuller R.A., Jacobsen R., Muller E., Perlmutter S., Rosenfeld A., Wurtele J., Groom D. & C. Wickham (2013) A new estimate of the average Earth surface land temperature spanning 1753 to 2011. Geoinformatics & Geostatistics: An Overview, 1, doi:10.4172/ gigs.1000101.

Rothman M.D., Anderson R.J., Kandjengo L. & J.J. Bolton (2020) Trends in seaweed resource use and aquaculture in South Africa and Namibia over the last 30 years. Botanica Marina 63(4): 315-325.

Rouault M., Pohl B., & P. Penven (2010) Coastal oceanic climate change and variability from 1982 to 2009 around South Africa. African Journal of Marine Science, 32(2): 237-246.

Roy C., van der Lingen C.D., Coetzee J.C. & J.R.E. Lutjeharms (2007) Abrupt environmental shift associated with changes in the distribution of Cape anchovy, *Engraulis encrasicolus* spawners in the southern Benguela. American Journal of Marine Science 29(3): 309-319.

Sabine, C.L., Key R.M., Feely R.A. & D. Greeley (2002) Inorganic carbon in the Indian Ocean: Distribution and dissolution processes. Global Biogeochemical Cycles, 16(4):1067. DOI:10.1029/2002GB001869.

Sabine C.L., Feely R.A., Gruber N., Key R.M., Lee K., Bullister J.L., Wanninkhof R., Wong C.S., Wallace D.W.R., Tilbrook B., Millero F.J., Peng T-S., Kozyr A., Ono T. & A.F. Rios (2004) The oceanic sink for anthropogenic CO_2. Science 305(5682):367–371.

Sales J. & P.J. Britz (2001) Research on abalone (*Haliotis midae* L.) cultivation in South Africa. Aquaculture research 32(11): 863-874.

Salway J.G. (2004) Metabolism at a glance. Guildford, UK: Wiley Blackwell.

Sanderson M.G., Hemming D.L. & R.A. Betts (2011) Regional temperature and precipitation changes under warming. Philosophical Transactions of the Royal Society A, 369(1934): 85-98.

Santana-Casiano J.M., González-Dávila M. & I.R. Ucha (2009) Carbon dioxide fluxes in the Benguela upwelling system during winter and spring: a comparison between 2005 and 2006. Deep-Sea Research Part II: Topical Studies in Oceanography 56(8-10): 533-541.

Sarazin G., Michard G. & Prevot F.M. (1999) A rapid and accurate spectroscopic method for alkalinity measurements in sea water samples. Water Research 33(1): 290-294.

Sarma V.V.S.S., Ono T. & T. Saino (2002) Increase of total alkalinity due to shoaling of aragonite saturation horizon in the Pacific and Indian Oceans: Influence of anthropogenic carbon inputs. Geophysical Research Letters, 29(20): 1971, DOI:10.1029/2002GL015135.

Schlegel R.W. & A.J. Smit (2016) Climate change in coastal waters: Time series properties affecting trend estimation. Journal of Climate 29:9113-9124.

Schmitt R. (2018) The Ocean's Role in Climate. Oceanography 31(2): 32-40.

Shirayama Y. & H. Thornton (2005) Effect of increased atmospheric CO_2 on shallow water marine benthos. Journal of Geophysical Research 110: C09S08.

Shuuluka D., Bolton J.J. & R.J. Anderson (2013) Protein content, amino acid composition and nitrogen-to-protein conversion factors of *Ulva rigida* and *Ulva capensis* from natural populations and *Ulva lactuca* from an aquaculture system, in South Africa. Journal of Applied Phycology 25: 677–685.

Shpigel M.,Guttman L., Shauli L., Odintsov V., D. Ben-Ezra & S. Harpaz (2017) *Ulva lactuca* from an Integrated Multi-Trophic Aquaculture (IMTA) biofilter system as a protein supplement in gilthead seabream (*Sparus aurata*) diet. Aquaculture 481: 112-118.

Shpigel M., Shauli L., Odintsov V., D. Ben-Ezra, Neori A. & L. Guttman (2018a) The sea urchin, *Paracentrotus lividus*, in an Integrated Multi-Trophic Aquaculture (IMTA) system with fish (*Sparus aurata*) and seaweed (*Ulva lactuca*): Nitrogen partitioning and proportional configurations. Aquaculture 490: 260-269.

Shpigel M., Shauli L., Odintsov V., Ashkenazi N. & D. Ben-Ezra (2018b) *Ulva lactuca* biofilter from a land-based integrated multi trophic aquaculture (IMTA) system as a sole food source for the tropical sea urchin *Tripneustes gratilla elatensis*. Aquaculture 496: 221-231.

Siikavuopio S.I., Mortensen A., Dale T. & A. Foss (2007). Effects of carbon dioxide exposure on feed intake and gonad growth in green sea urchin, *Strongylocentrotus droebachiensis*. Aquaculture 266: 97–101.

Sillmann J. & E. Roeckner (2008) Indices for extreme events in projections of anthropogenic climate change. Climatic Change, 86(1-2): 83-104.

Simon C.A., Ludford A. & S. Wynn (2006) Spionid polychaetes infesting cultured abalone *Haliotis midae* in South Africa. African Journal of Marine Science 28(1): 167-171.

Sivaprakash G., Mohanrasu K., Ananthi V., Jothibasu M., Nguyen D.D., Ravindran B., Chang S.W., Nguyen-Tri P., Tran N.H., Sudhakar M., Gurunathan K., Arokiyaraj S. & A. Arun (2019) Biodiesel production from *Ulva linza*, *Ulva tubulosa*, *Ulva fasciata*, *Ulva rigida*, *Ulva reticulate* by using Mn_2ZnO_4 heterogenous nanocatalysts. Fuel 255: 115744.

Smale D. & T. Wernberg (2013) Extreme climatic event drives range contraction of a habitat-forming species. Proceedings of the Royal Society B 280: 2012–2829.

Smit A.J., Robertson-Andersson D.V., Peall S. & J.J. Bolton (2007) Dimethylsulfoniopropionate (DMSP) accumulation in abalone *Haliotis midae* (Mollusca: Prosobranchia) after consumption of various diets, and consequences for aquaculture. Aquaculture 269: 377-389.

Smith S.V. & G.S. Key (1975) Carbon dioxide and metabolism in marine environments. Limnology and Oceanography 20: 493–495.

Smith A.M., Key M.M., Henderson Z.E., Davis V.C. & Winter D.J. (2016) Pretreatment for removal of organic material is not necessary for X-Ray-diffraction determination of mineralogy in temperate skeletal carbonate. Journal of Sedimentary Research 86(12):1425-1433. DOI: https://doi.org/10.2110/jsr.2016.86.

Sokal R.R. & Rohlf F.J. (1995) Biometry. Third edition. Freeman, New York, 887p.

Sokolova I.M., Frederich M., Bagwe R., Lannig G. & A.A. Sukhotin (2012) Energy homeostasis as an integrative tool for assessing limits of environmental stress tolerance in aquatic invertebrates. Marine Environmental Research 79: 1–15.

Sousa G.T., Neto M.C.L., Choueri R.B. & Í.B. Castro (2021) Photoprotection and antioxidative metabolism in *Ulva lactuca* exposed to coastal oceanic acidification scenarios in the presence of Irgarol. Aquatic Toxicology 230: 105717.

Stæhr, P.A. & T. Wernberg (2009) Physiological responses of *Ecklonia radiata* (Laminariales) to a latitudinal gradient in ocean temperature. Journal of Phycology 45: 91–99.

Steinberg J. (2005) The illicit abalone trade in South Africa. Institute for Security Studies Paper No. 105. 16 pp.

Stewart-Sinclair P.J., Last K.S., Payne B.L. & T.A. Wilding (2020) A global assessment of the vulnerability of shellfish aquaculture to climate change and ocean acidification. Ecology and Evolution 10(7): 3518-3534.

Strotz L.C., Saupe E.E., Kimmig J. & B.S. Lieberman (2018) Metabolic rates, climate and macroevolution: a case study using Neogene molluscs. Proceedings of the Royal Society B. 285: 20181292.

Sultan S.E. (2007) Development in context: the timely emergence of eco-devo. Trends in Ecology and Evolion 22: 575–58.

Swezey D.S., Boles S.E., AquilinoK.M., Stott H.K., Bush D., Whitehead A., Rogers-Bennett L., Hill T.M. & E. Sanford (2020) Evolved differences in energy metabolism and growth dictate the impacts of ocean acidification on abalone aquaculture. PNAS 17(42): 26513-26519.

Takeshita Y., Frieder C.A., Martz T.R., Ballard J.R., Feely R.A., Kram S., Nam S., Navarro M.O., Price N.N. & J.E. Smith (2015) Including high-frequency variability in coastal ocean acidification projections, Biogeosciences 12: 5853–5870.

Tan K. & H. Zheng (2020) Ocean acidification and adaptive bivalve farming. Science of the Total Environment 701: 134794.

Tanaka K., Taino S., Haraguchi H., Prendergast G. & M. Hiraoka (2012) Warming off southwestern Japan linked to distributional shifts of subtidal canopy-forming seaweeds. Ecology and Evolution n/a-n/a.

Tarr R.J.Q. (1993) Stock assessment, and aspects of the biology of the South African abalone, *Haliotis midae*. M.Sc. thesis, University of Cape Town, Cape Town, South Africa 156 pp.

Tarr R.J.Q. (1995) Growth and movement of the South African abalone ***Haliotis midae***: a reassessment. Marine and Freshwater Research 46: 583–590.

Tarr R.J.Q., Williams P.V.G. & A.J. Mackenzie (1996) Abalone, sea urchins and rock lobster: a possible ecological shift may affect traditional fisheries. South African Journal of Marine Science 17:311-315.

Tarr R.J.Q. (2000) The South African abalone (*Haliotis midae*) fishery; a decade of challenges and change. Canadian Special Publication: Fisheries and Aquatic Science 130: 32–40.

Teniswood C.M.H., Roberts D., Howard W.R. & J.E. Bradby (2013) A quantitative assessment of the mechanical strength of the polar pteropod ***Limacina helicina antarctica s***hell. ICES Journal of Marine Science, 70:1499-1505.

Thomson A.M., Calvin K.V., Smith S.J., Kyle G.P., Volke A., Patel P., Delgado-Arias S., Bond-Lamberty B., Wise M.A., Clarke L.E. & J.A. Edmonds (2011) RCP4.5: a pathway for stabilization of radiative forcing by 2100. Climatic Change 109:77-94, DOI:10.1007/s10584-011-0151-4.

Thompson D. W. (1942) On Growth and Form. Cambridge University Press, London, UK.

Thomsen L., Aguzzi J., De Loe F., Ogston A. & A. Purser (2017) The Oceanic biological bump: Rapid carbon transfer to depth at Continental Margins during winter. Scientific Reports 7:10763.

Tortell P.D., Payne C., Gueguen C., Strzepek R.F., Boyd P. & B. Rost (2008) Inorganic carbon uptake by Southern Ocean phytoplankton. Limnology and Oceanography 53(4): 1266-1278.

Trimborn S., Brenneis T., Sweet E. & B. Rost (2013) Sensitivity of Antarctic phytoplankton species to ocean acidification: Growth, carbon acquisition and species interaction. Limnology Oceanography 58(3): 997-1007.

Trivedi N., Baghel R.S., Bothwell J., Gupta V., Reddy C.R.K., Lali A.M. & B. Jha (2016) An integrated process for the extraction of fuel and chemicals from marine macroalgal biomass. Scientific Reports 6: 30728.

Troell M., Robertson-Andersson D., Anderson R.J., Bolton J.J., Maneveldt G., Halling C. & T. Probyn (2006) Abalone farming in South Africa: An overview with perspectives on kelp resources, abalone feed, potential for on-farm seaweed production and socio-economic importance. Aquaculture 257(1-4): 266-281.

Truchot J.-P. (1976) Carbon dioxide combining properties of the blood of the shore crab, *Carcinus maenas* (L.): Carbon dioxide solubility coefficient and carbonic acid dissociation constants. Journal of Experimental Biology64: 45-67.

Tutschulte T.C. & J.H. Connell (1988) Feeding behavior and algal food of three species of abalones (Haliotis) in southern California. Marine Ecology Progress Series 49: 57-64.

Van Alstyne K.L., Wolfe G.V., Freidenburg T.S., Neill A. & C. Hicken (2001) Activated defense systems in marine macroalgae: evidence for an ecological role for DMSP cleavage. Marine Ecology Progress Series 213: 53-65.

Van Ginneken (2019) The Application of the Seaweeds in Neutralizing the "Ocean Acidification" as a Long-Term Multifaceted Challenge. Journal of Geoscience and Environment Protection 7(12): 126-138.

Van der Merwe E. (2009) Toward best management practices for the growth of the abalone *Haliotis midae* Linnaeus on a commercial South African abalone farm. Unpublished Master's dissertation, University of the Western Cape, South Africa.

Van der Wal H., Sperber B.L.H.M., Houweling-Tan B., Bakker R.C., Brandenburg W. & A.M. López-Contreras (2013) Production of acetone, butanol, and ethanol from biomass of the green seaweed *Ulva lactuca*. Bioresources and Technologies 128: 431–437.

Vargas C.A., Lagos N.A., Lardies M.A., Duarte C., Manríquez P.H., Aguilera V.M., Broitman B., Widdicombe S. & S. Dupont (2017) Species-specific responses to ocean acidification should account for local adaptation and adaptive plasticity. Nature Ecology & Evolution 1: 0084.

Vázquez-Domínguez E., Vaqué D. & J.M. Gasol (2007) Ocean warming enhances respiration and carbon demand of coastal microbial plankton. Global Change Biology 13(7):1327-1334.

Venter L., Loots D.T., Mienie L.J., van Rensburg P.J.J., Mason S., Vosloo A. & J. Z. Lindeque (2018) Uncovering the metabolic response of abalone (*Haliotis midae*) to environmental hypoxia through metabolomics. Metabolomics 14: 49.

Vilchis L.I., Tegner M.J., Moore J.D., Friedman C.S., Riser K.L., Robbins T.T. & P.K. Dayton (2005) Ocean warming effects on growth, reproduction, and survivorship of Southern California abalone. Ecological Applications 15(2): 469–480.

Vivanco-Aranda M., Gallardo-Escarate C.J., & M.A. Del Rio-Portilla (2011) Low-density culture of red abalone juveniles, *Haliotis rufescens* Swainson 1822, in recirculating aquaculture system and flow-through system. Aquaculture Research 42: 161–168.

Vizzini S., Apostolaki E.T., Ricevuto E., Polymenakou P. & A. Mazzola (2019) Plant and sediment properties in seagrass meadows from two Mediterranean CO_2 vents: Implications for carbon storage capacity of acidified oceans. Marine Environmental Research 146: 101-108.

Vosloo A, Laas A. & Vosloo D. (2013) Differential responses of juvenile and adult South African abalone (Haliotis midae Linnaeus) to low and high oxygen levels. Comparative biochemistry and physiology. Part A, molecular and integrative physiology, 164(1):192-9. doi: 10.1016/j.cbpa.2012.09.002.

Wahl M., Covachã S.S., Saderne V., Hiebenthal C., Müller J.D., Pansch C. & Y. Sawall (2017) Macroalgae may mitigate ocean acidification effects on mussel calcification by increasing pH and its fluctuations. Limnology and Oceanography 63(1): 3-21.

Waldbusser G.G., Hales B., Langdon C.J., Haley B.A., Schrader P., Brunner E.L., Gray M.W., Miller C.A. & I. Gimenez (2015) Saturation state sensitivity of marine bivalve larvae to ocean acidification. Nature Climate Change 5: 273-280.

Waldbusser G.G., Gray M.W., Hales B., Langdon C.J., Haley B.A., Gimenez I., Smith S.R., Brunner E.L. & G. Hutchinson (2016) Slow shell building, a possible trait for resistance to the effects of acute ocean acidification. Limnology and Oceanography 61(6): 1969–1983.

Wanninkhof R., Park G.-H., Takahashi T., Sweeney C., Feely R., Nojiri Y., Gruber N., Doney S.C., McKinley G.A., Lenton A., Le Quéré C., Heinze C., SchwingerJ., Graven H. & S. Khatiwala (2013) Global ocean carbon uptake: Magnitude, variability and trends. Biogeosciences 10: 1983–2000. DOI:10.5194/bg-10-1983-2013.

Watson S.-A., Southgate P.C., Tyler P.A. & L.S. Peck (2009) Early larval development of the Sydney rock oyster *Saccostrea glomerata* under near-future predictions ofCO_2-driven ocean acidification. Journal of Shellfish Research 28: 431–437.

Watterson I.G. (2009) Components of precipitation and temperature anomalies and change associated with modes of the Southern Hemisphere. International Journal of Climatology, 29(6): 809-826.

Waycott M., Collier C., McMahon K., Ralph P., McKenzie L., Udy J. & A. Grech (2007) Vulnerability of seagrasses in the Great Barrier Reef to climate change. In: Johnson J.E. & P.A. Marshall (eds.). Climate Change and the Great Barrier Reef. Great Barrier Reef Marine Park. Authority and Australian Greenhouse Office Australia. pp. 193–299

Weiner S. & P.M. Dove (2003) An overview of biomineralization processes and the problem of the vital effect. Reviews in Mineralogy and Geochemistry 54(1): 1–29.

Welladsen H.M., Southgate P.C. & K. Heimann (2010) The effects of exposure to near-future levels of ocean acidification on shell characteristics of *Pinctada fucata* (Bivalvia: Pteriidae). Molluscan Research 30(3): 125-130.

Wernberg T., Russell B.D., Moore P.J., Ling S.D., Smale D.A., Campbell A., Coleman M.A., Steinberg P.D., Kendrick G.A. & S.D. Connell (2011) Impacts of climate change in a global hotspot for temperate marine biodiversity and ocean warming. Journal of Experimental Marine Biology and Ecology 400(1-2): 7-16.

Wernberg T., Arenas F., Olabarria C., Thomsen M.S. & M.B. Mohring (2016) Threats to ecosystem engineering macrophytes: climate change. In: Marine macrophytes as foundation species (ed: Ólafsson E.); Science Publisher/CRC Press, Boca Raton, USA. pp 201–225.

Wessel N., Martin S., Badou A., Dubois P., Huchette S., Julia V., Nunes F., Harney E., Paillard C. & S. Auzoux-Bordenave (2018) Effect of CO_2–induced ocean acidification on the early development and shell mineralization of the European abalone (*Haliotis tuberculata*). Journal of Experimental Marine Biology and Ecology 508: 52-63.

White L. (2011) The effects of ocean acidification and upwelling conditions on the growth and calcification of the red abalone (*Haliotis rufescens*). Unpublished Master's Dissertation. California State University, San Marcos

Wiltshire K.H. & B.F.J. Manly (2004) The warming trend at Helgoland Roads, North Sea: phytoplankton response. Helgoland Marine Research 58:269.

Wolf-Gladrow DA, Riebesell U, Burkhardt S, Bijma J (1999) Direct effects of CO_2concentration on growth and isotopic composition of marine plankton. Tellus B 51(2):461–476.

Wolf-Gladrow D.A., Zeebe R.E., Klaas C., Körtzinger A. & A.G. Dickson (2007) Total alkalinity: The explicit conservative expression and its application to biogeochemical processes. Marine Chemistry, doi:10.1016/j.marchem.2007.01.006

Wolf-Gladrow D.A. & B. Rost (2014) Ocean acidification and oceanic carbon cycling. In: Freedman B. (eds) Global Environmental Change. Handbook of Global Environmental Pollution, vol 1. Springer, Dordrecht.

Wood A.D. & C.D. Buxton (1996) Aspects of the biology of the abalone *Haliotis midae* (Linn, 1758) on the east coast of South Africa. 2. Reproduction. South African Journal of Marine Science 17(1): 69-78. DOI: 10.2989/025776196784158356

Wood S.N. (2003) Thin-plate regression splines. Journal of the Royal Statistical Society (B) 65(1): 95-114.

Wood S.N. (2011) Fast stable restricted maximum likelihood and marginal likelihood estimation of semip arametric generalized linear models. Journal of the Royal Statistical Society (B) 73(1):3-36.

Wood S.N., Pya N. & B. Saefken (2016) Smoothing parameter and model selection for general smooth models (with discussion). Journal of the American Statistical Association 111:1548-1575.

Yearsley R. (2007) Water quality, abalone growth and the potential for integrated mariculture on a South African abalone, *Haliotis midae* L., farm. Unpublished Master's dissertation. Rhodes University, South Africa.

Yokoyama H. & Y. Ishihi (2010) Bioindicator and biofilter function of Ulva spp. (Chlorophyta) for dissolved inorganic nitrogen discharged from a coastal fish farm — potential role in integrated multi-trophic aquaculture. Aquaculture 310: 74-83.

Young C.S. & C.J. Gobler (2016) Ocean acidification accelerates the growth of two bloom-forming, estuarine macroalgae. PLoS ONE 11: e0155152.

Young C.S. & C.J. Gobler (2017) The organizing effects of elevated CO_2 on competition among estuarine primary producers. Scientific Reports-UK 7: 7667.

Young C.S. & C.J. Gobler (2018) The ability of macroalgae to mitigate the negative effects of ocean acidification on four species of North Atlantic bivalve. Biogeosciences 15: 6167–6183.

Zar J.H. (1999) Biostatistical analysis. Fourth edition. Prentice-Hall, Upper Saddle River, USA.

Zhao X., Guo C., Han Y., Che Z., Wang Y., Wang X., Chai X., Wu H. & G. Liu (2017) Ocean acidification decreases mussel byssal attachment strength and induces molecular byssal responses. Marine Ecology Progress Series 565: 67–77.

Zheng X., Lei S., Zhao S., Ye G., Ma R., Liu L., Xie Y., Shi X. & J. Chen (2020) Temperature elevation and acidification damage microstructure of abalone via expression change of crystal induction genes. Marine Environmental Research 162: 105114.

Ziervogel G., New M., van Garderen E.A., Midgley G., Taylor A., Hamann R., Stuart-Hill S., Myers J. & M. Warburton (2014) Climate change in South Africa, WIREs Climate Change 5:605-620. DOI: 10.1002/wcc.295.

Zippay M.L. & G.E. Hofmann (2010) Effect of pH on gene expression and thermal tolerance of early life history stages of red abalone (*Haliotis rufescens*). Journal of Shellfish Research 29:429–439.

Zimmerman R.C., Kohrs D.G., Steller D.L. & R.S. Alberte (1997) Effects of CO_2 enrichment on productivity and light requirements of eelgrass. Plant Physiology 15: 599–607.

Zou D. & K. Gao (2002) Effects of desiccation and CO_2 concentrations on emersed photosynthesis in *Porphyra haitanensis* (Bangiales, Rhodophyta), a species farmed in China. European Journal of Phycology 37: 587–592.

Zou D.H., Gao K.S. & Z.X. Ruan (2007) Daily timing of emersion and elevated atmospheric CO_2 concentration affect photosynthetic performance of the intertidal macroalga *Ulva lactuca* (Chlorophyta) in sunlight. Botanica Marina 50: 275–279.

Zou D. & K. Gao (2009). Effects of elevated CO_2 on the red seaweed *Gracilaria lemaneiformis* (Gigartinales, Rhodophyta) grown at different irradiance levels. Phycologia 48: 510–517.

Zuur A.F., Ieno E.N., Walker N.J. & Smith G.M. (2012) Mixed Effects Models and Extensions in Ecology with R, Statistics for Biology and Health, DOI 10.1007/978-0-387-87458-6_1, Springer Science + Business Media, LLC 2009.